FLOODING EXPERIMENTS WITH STEAM/WATER AND AIR/WATER AT ELEVATED PRESSURE IN A LARGE DIAMETER VERTICAL TUBE

A Thesis

by

NICHOLAS ALAN WYNNE

Submitted to the Office of Graduate and Professional Studies of
Texas A&M University
in partial fulfillment of the requirements for the degree of

MASTER OF SCIENCE

Chair of Committee,	Karen Vierow
Committee Members,	Michael Pate
	Yassin Hassan
Head of Department,	Yassin Hassan

December 2015

Major Subject: Nuclear Engineering

ABSTRACT

An experimental investigation to acquire flooding data using steam/water and air/water fluid pairs at elevated pressures was conducted. This research provides the first flooding data above atmospheric pressure in large diameter vertical tubes and can be used to improve the flooding models in one-dimensional system codes. A stainless steel test section consisting of a 3-inch inner diameter tube was modified to permit flooding experiments up to 60 psia for air/water experiments at 25 °C and 30 psia for steam/water experiments at near saturated conditions. Extensive modifications were made to the test facility to allow for high pressure testing, including the addition of a large compressed air supply, two plate type heat exchangers, and extensive instrumentation. The air/water and steam/water flow paths are nearly identical, yielding a test facility capable of providing data that can be directly compared while avoiding influences from complicated geometry effects.

The data at higher pressures suggest that the momentum transfer necessary for the onset of flooding is achievable for lower superficial velocities as the gas density increases. Flooding characteristics are presented in terms of the Kutateladze number, and the effect of fluid properties on flooding, such as density and surface tension, are discussed. If condensation is accounted for, the saturated steam/water data at 30 psia closely trends with the air/water flooding data. This research provides fundamental data that can be used to address the pressure scaling deficiencies in flooding correlations for reactor safety codes and also evaluate the applicability of air/water data for steam/water applications.

ACKNOWLEDGEMENTS

I must thank my advisor Dr. Karen Vierow for her support, encouragement, patience, and openhearted advice during my time here at Texas A&M University. It has sincerely been an honor to work with you since day one, and my success would not be possible without your help. Thank you.

I would like to thank my thesis committee members, Dr. Yassin Hassan and Dr. Michael Pate for their help. In addition, I would like to thank the individuals at Bettis Atomic Power Laboratory for their support.

Next, I would like to thank Will Seward in the chemistry machine shop for letting me use his tools, teaching me how to improve my TIG welding, and fixing all the stuff I consistently messed up.

Many thanks should be given the members of the Nuclear Heat Transfer Systems Laboratory, specifically Nick Luthman, Matt Garza, and Matt Solom.

I need to acknowledge my family for their unwavering support. Finally, I must thank my beautiful wife for always believing in me.

NOMENCLATURE

ABBREVIATIONS

ANSI	American National Standards Institute
ASME	American Society of Mechanical Engineers
ASTM	American Society for Testing and Materials
BSPP	British Standard Parallel Pipe
CFM	Cubic Feet per Minute
DAQ	Data Acquisition System
DC	Direct Current
ECCS	Emergency Core Coolant System
GMAW	Gas Metal Arc Welding
GPM	Gallons per Minute
GTAW	Gas Tungsten Arc Welding
HP	Horsepower
ID	Inner Diameter
LCD	Liquid Crystal Display
MAWP	Maximum Allowable Working Pressure
MIG	Metal Inert Gas
NBR	Nitrile Butadiene Rubber
NPS	Nominal Pipe Size
NPT	National Pipe Thread
OD	Outer Diameter
PTFE	Polytetrafluoroethylene
PVC	Polyvinyl Chloride

PWR	Pressurized Water Reactor
RCIC	Reactor Core Isolation Cooling
RPM	Revolutions per Minute
SBR	Styrene Butadiene Rubber
SRV	Safety Relief Valve
TIG	Tungsten Inert Gas
VAC	Volts Alternating Current
VDC	Volts Direct Current

SYMBOLS

C	Constant in Wallis Correlation
C_k	Constant in the Kutateladze Correlation
C_v	Flow Coefficient
d	Width of Vortex Shedder Bar
D	Characteristic Length
f	Fraction of Steam Condensed
f	Vortex Frequency
g	Acceleration due to Gravity
h	Enthalpy
j_i	Superficial Velocity of Phase i
K	Vortex Correction Factor
Ku_i	Kutateladze number of phase i
Ku_{ge}	Effective Vapor Kutateladze number
m	Constant in Wallis Correlation
m	Constant in Kutateladze Correlation
$\dot{m}$	Mass Flow Rate

Q	Volumetric Flow Rate
T_s	Saturation Temperature
T_{wall}	Inner Tube Wall Temperature
U	Velocity
GREEK SYMBOLS	
μ	Micro, 10^{-6}
ρ_i	Mass Density of Phase i
σ	Surface Tension of Liquid
Ω	Resistance
SUBSCRIPTS	
f	Liquid
in	Inlet
out	Outlet
st	Steam

TABLE OF CONTENTS

Page

ABSTRACT ii

ACKNOWLEDGEMENTS iii

NOMENCLATURE iv

TABLE OF CONTENTS vii

LIST OF FIGURES x

LIST OF TABLES xiii

1. INTRODUCTION 1

    1.1 Project Motivation and Objective 1
    1.2 Importance of the Research 2
    1.3 Technical Approach 3
    1.4 Thesis Organization 3

2. LITERATURE SURVEY 4

    2.1 Early Flooding Studies 4
    2.2 Flooding Studies at Texas A&M University 7
        2.2.1 Air/Water Testing 7
        2.2.2 Steam/Water Testing with Fixed Water Subcooling 8
        2.2.3 Steam/Water Testing with Variable Water Subcooling 10
    2.3 Flooding Studies at Elevated Pressure 11

3. FACILITY DESCRIPTION 14

    3.1 Test Section 14
    3.2 Water Flow Path 19
        3.2.1 Deionized Water System 20
        3.2.2 Water Supply Tank 20
        3.2.3 Water Supply Pump 21
        3.2.4 Holdup Tank 23
        3.2.5 Heat Exchanger 25

3.2.6 Recirculation Pump . . . 28
3.3 Air Flow Path . . . 30
3.3.1 Air Supply . . . 30
3.3.2 Air Filters and Dryer . . . 33
3.3.3 Separator . . . 35
3.3.4 Back Pressure Regulator . . . 36
3.4 Steam Flow Path . . . 38
3.4.1 Steam Generator . . . 38
3.4.2 Steam Condenser . . . 41
3.5 Additional Facility Modifications . . . 43
3.6 Instrumentation . . . 44
3.6.1 Temperatures . . . 45
3.6.2 Pressure Measurements . . . 46
3.6.3 Flow Meters . . . 49
3.6.4 Humidity . . . 52
3.6.5 Data Acquisition System . . . 52
3.6.6 Calibrations . . . 54

4. OPERATING PROCEDURES . . . 57

4.1 Data Acquisition System . . . 57
4.2 Purging Differential Pressure Transmitters . . . 60
4.3 Operating the Air Supply for Air/Water Flooding Tests . . . 62
4.4 Filling the Steam Generator . . . 65
4.5 Draining the Steam Generator . . . 67
4.6 Steam Generator Operation . . . 68
4.7 Water Supply Heatup For Saturated Steam/Water Testing . . . 69
4.7.1 Purging of Water from the Common Pipeline with Air . . . 70
4.7.2 Water Supply Heatup . . . 71
4.7.3 Purging of Steam from the Common Pipeline with Air . . . 73
4.8 Setting System Pressure . . . 74
4.8.1 Setting the Test Section Pressure for Air/Water Flooding . . . 74
4.8.2 Setting the Test Section Pressure for Steam/Water Flooding . . . 75
4.8.3 Setting the Water Supply Tank Pressure . . . 77
4.9 Water Supply Pump Operation . . . 78
4.10 Recirculation Pump Operation . . . 79
4.11 Flooding Procedures for Data Collection . . . 81
4.12 Facility Shutdown . . . 84

5. RESULTS AND DISCUSSION . . . 86

5.1 Test Conditions . . . 86
5.1.1 Air/Water Test Ranges . . . 86

5.1.2 Steam/Water Test Ranges . . . 87
5.2 Air/Water Raw Data and Observations . . . 88
5.3 Steam/Water Raw Data and Observations . . . 96
5.4 Reduced Data . . . 103
5.4.1 Reduced Data in Terms of Superficial Velocities . . . 103
5.4.2 Reduced Data in Terms of Kutateladze Numbers . . . 105
5.4.3 Water Carryover Results . . . 112
5.5 Uncertainty Analysis . . . 116

6. CONCLUSIONS AND FUTURE WORK . . . 118

6.1 Conclusions . . . 118
6.2 Future Work . . . 120

REFERENCES . . . 122

APPENDIX A. EXPERIMENTAL INSTRUMENTATION . . . 125

APPENDIX B. ENGINEERING DRAWINGS . . . 127

APPENDIX C. MATLAB SCRIPTS . . . 139

C.1 Plotting the Data . . . 139
C.2 Finding the Onset of Flooding . . . 143
C.3 Calculating the Average Carryover Flow Rate . . . 145

APPENDIX D. REDUCED DATA SET . . . 147

APPENDIX E. GRAPHICAL DATA . . . 153

APPENDIX F. VITA . . . 301

LIST OF FIGURES

FIGURE Page

2.1 Entrance and exit flange designs for the Wallis test section. 5

2.2 Rothe and Crowley data on the effect of pressure on flooding [11]. . . 12

2.3 Vallée data on the effect of pressure on flooding [17]. 13

3.1 Piping and instrumentation diagram of facility 15

3.2 Exploded diagram of the original test section as designed by Ritchey. 16

3.3 Rendering of the modified steam outlet and long elbow assembly. . . 19

3.4 The Dayton multistage pump and the Liquidflo 620 centrifugal pump. 23

3.5 The holdup tank shown below the test section before insulation was applied. 25

3.6 The AlfaNova 27-30H heat exchanger shown installed with protective blue thermal insulation. 27

3.7 The air supply and supporting equipment. 34

3.8 The Anderson LCCR separator shown without insulation. 37

3.9 The steam generator shown with insulation. 39

3.10 The AlfaNova 27-34H steam condenser shown before installation. . . 42

3.11 The gas outlet absolute pressure transmitter with impulse piping. . . 47

3.12 The Von Karman vortex street. 50

3.13 The data acquisition system 53

3.14 Data acquisition user interface created in LabVIEW. 55

4.1 Piping and instrumentation diagram of facility for operation 58

4.2 Typical impulse tubing and valve arrangement for the differential pressure transmitters. 61

5.1 Test section differential pressure for air/water flooding. 90

5.2 Gas mass flow rate for air/water flooding. 92

5.3 System pressure for air/water flooding. 93

5.4 Water flow rates for air/water flooding. 96

5.5 Test section differential pressure for steam/water flooding. 97

5.6 Gas mass flow rate for steam/water flooding. 98

5.7 System pressure for steam/water flooding. 100

5.8 Water flow rates for steam/water flooding. 101

5.9 Flow temperatures for steam/water flooding. 102

5.10 Superficial flooding velocities for air/water and steam/water tests at various pressures. 104

5.11 Air/water data plotted in terms of the Kutateladze parameters at various pressures. 106

5.12 Steam/water data plotted in terms of the Kutateladze parameters at various pressures. 107

5.13 Air/water and steam/water flooding data at 3 psig plotted in terms of the Kutateladze parameters. 108

5.14 Air/water flooding data by Williams and 97 °C steam/water data by Cullum plotted in terms of the Kutateladze parameters. 110

5.15 Air/water and steam/water flooding data at 15 psig plotted in terms of the Kutateladze parameters. 112

5.16 Average water carryover for air/water and steam/water flooding data at 3 psig. 113

5.17 Average water carryover for air/water at various pressures. 114

5.18 Water down flow rate and average water carryover for air/water flooding at 3 psig. 116

5.19 Flooding data plotted with error bars. 117

LIST OF TABLES

TABLE Page

5.1 Conditions for the air/water tests 87

5.2 Conditions for the steam/water tests 88

5.3 Liquid to gas density ratio for notable pressures, including full scale PWR operating pressure. 110

1. INTRODUCTION

Flooding is defined as the instance in which a gas flowing upward reverses momentum of a liquid flowing downward until both phases are flowing cocurrently. This phenomenon presents challenges in many engineering systems, including nuclear power reactors. As with many topics in two-phase flow, the complexities of the phenomena require empirical correlations to predict and model flooding rather than mechanistic fluid dynamic models. Reactor safety codes use these correlations to predict flooding during hypothetical severe accident analyses, however large uncertainties can be associated with their use due to the lack of models for flooding in high-pressure scenarios. The need in the reactor safety community is to improve these analytical models and correlations by pursuing experimental data for code validation.

1.1 Project Motivation and Objective

This research is the fourth installment of flooding investigations with applications in the pressurizer surge line in a Pressurized Water Reactor (PWR) in the Nuclear Heat Transfer Systems Laboratory. In hypothetical station blackout conditions with loss of auxiliary feedwater, a large quantity of steam can be generated in the reactor core and may vent through the relief valve on top of the pressurizer. This flow path results in counter-current flow in the pressurizer surge line and the probability for flooding at high pressure increases. The pipe wall of the surge line may be exposed to high temperatures and pressures for a long period of time if flooding occurs, and the surge line could fail due to creep rupture. No models currently exist to characterize flooding under high pressure severe accident conditions. A flooding test facility was created in the Nuclear Heat Transfer Systems Laboratory to investigate flooding on

a fundamental level for applications to the pressurizer surge line.

The purpose of this study is to collect fundamental flooding data using steam/water and air/water fluid pairs at multiple pressures in a well characterized vertical tube. This research investigates the onset of flooding, which is considered partial flow reversal of the liquid film by the gas. Complete reversal of the liquid film in which no liquid falls down in the tube is considered full flow reversal. The data between the fluid pairs are directly comparable as the conditions in each test, such as the piping configuration, test section geometry, and system pressures, are nearly identical. The steam/water tests are performed at near saturated conditions to eliminate any mass transfer and are useful data to compare with air/water flooding data. Onset of flooding curves were generated and compared for the fluid pairs at each pressure to investigate variable property effects including viscosity and the liquid-to-gas density ratio.

1.2 Importance of the Research

The significance for this research is that, to the author's knowledge, there has not been any steam/water flooding data at higher pressures in a large diameter vertical tube in the literature. Similar steam/water studies have been performed at above atmospheric pressure in the past, however the facilities used were designed for a very specific geometry, e.g. the pressurized water reactor hot leg [17] or the reactor pressure vessel downcomer [11]. The test section used in this research is a straight vertical tube and provides a unique data set that is independent of reactor-specific geometry. The simplicity of the test section provides the opportunity to investigate the fundamental physics of flooding in the absence of complicated geometry.

1.3 Technical Approach

To conduct the research, the original flooding facility designed by Nicole Ritchey (née Williams) [21] was modified to allow air/water and steam/water flooding data to be generated and collected at pressures up to 60 psia. In the current facility improvements, several components were added for maintaining a pressure boundary and also to operate at higher temperatures than previously considered. A major improvement includes the addition of several flow meters to measure the outlet flow rates of each phase exiting during the flooding test. A brand new air supply was purchased and installed to allow for air/water tests at pressure.

1.4 Thesis Organization

This thesis is divided into six sections. The first section introduces the problem statement and outlines the objectives and relevance of the research. Section 2 contains a literature review of previous work that is relevant to the current research effort. Major correlations are discussed and previous investigations regarding flooding at higher pressure applications are outlined. Section 3 provides a detailed explanation of the design, construction, and installation of the experimental test facility. This section was also intended to be used as a reference for future modifications of the facility. The operating procedures for the experiment are described in Section 4. The results and discussion are presented in Section 5, while the conclusions and suggestions for future work are in Section 6. The appendices contain technical drawings, MATLAB scripts, reduced data, and graphical data.

2. LITERATURE SURVEY

2.1 Early Flooding Studies

The flooding phenomena became a major research topic first in the chemical industry. In the early 20th century, experiments were constructed to investigate the flooding characteristics inside packed columns. The columns were used for a distillation process in which a gas flowing upward through a packing material is separated by interacting with a liquid flowing down called reflux. For any given column geometry, an increase in gas velocity will result in liquid holdup in the packing and eventually will blow all of the reflux out of the top of the vessel. This is referred to as the flooding point, and Sherwood et. al experimentally determined the velocity of the gas at the flooding point in a two inch glass packing tower [12].

The flooding data from the packing towers were then compared to experimental results in vertical tubes by G.B. Wallis. A test facility consisting of an acrylic perspex tube allowed water to flow down in annular flow while air was injected from the bottom to investigate the flooding velocities [20]. The flooding correlations from packed towers were modified by Wallis to obtain two dimensionless parameters referred to as Wallis numbers

$$j_f^* = j_f \sqrt{\frac{\rho_f}{gD(\rho_f - \rho_g)}} \tag{2.1}$$

and

$$j_g^* = j_g \sqrt{\frac{\rho_g}{gD(\rho_f - \rho_g)}} \tag{2.2}$$

where j_i is the superficial velocity of phase i, ρ_i is density of phase i, D is a characteristic length such as tube diameter, and g is the gravitational constant. Four

different tube diameters were tested and a correlation was developed that can be used to approximate the flooding condition in the form

$$\sqrt{j_g^*} + m\sqrt{j_f^*} = C \tag{2.3}$$

where constants m and C are determined by the test section geometry. Equation 2.3 is referred to as the Wallis correlation and often $m = 1.0$. The geometric constant C is determined by the entrance and exit conditions of the media into the test section. Wallis performed flooding tests using flanges with sharp or smooth edges, as shown in Figure 2.1, and determined the values of $C = 0.725$ for sharp edges and $C = 0.9$ for round edges [20]. As will be discussed further in Section 3, the sharp edges were used in the test section for this current research.

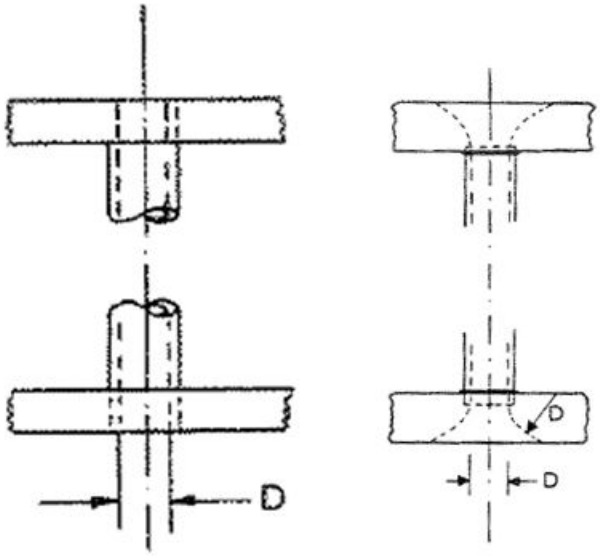

Figure 2.1: Entrance and exit flange designs for the Wallis test section. Flanges with sharp edges (on the left) were designed so that the end of the pipe is flush with the flange face resulting in a 90° edge while smooth flanges (on the right) had a rounded edge with a radius equal to the tube diameter [20].

The Wallis correlation is widely accepted for use in small diameter tubes, however Pushkina and Sorokin did not find agreement when testing the Wallis correlation to a wider range of tubes [10]. The researchers created two vertical test facilities with differing water inlet devices and tube diameters. Pushkina and Sorokin concluded that the Wallis correlation did not support empirical flooding data from these facilities and suggested a new flooding criterion based on earlier work from Sorokin. Sorokin et. al [15] experimentally confirmed that the maximum flooding velocity, i.e. the maximum gas velocity in which no liquid flows down, be described by the dimensionless criterion

$$Ku_g \equiv \frac{j_g \rho_g^{1/2}}{(g\sigma(\rho_f - \rho_g))^{1/4}} = 3.2 \tag{2.4}$$

where Ku_g is the Kutateladze number for the gas phase and σ is the surface tension of the liquid. They claim that the critical flooding velocity (onset of liquid flow reversal) is independent of the liquid flow rate at the inlet due to "drop-shaped formations" at the interface. At flooding, these formations are drawn to the center of the tube and form crests which propagate up the tube in a liquid film as the gas flow rate is increased. The formation dimensions at the interface were found to be independent of liquid flow rate [15]. Sorokin et. al also measured the head loss, or pressure drop, across the test section and used this measurement to confirm the onset of flooding which is a technique also used in the current research.

Equation 2.4 was cast into a more general form analogous to Equation 2.3 by Tien [16] as,

$$Ku_g^{1/2} + mKu_f^{1/2} = C_k \tag{2.5}$$

where

$$Ku_f = \frac{j_f \rho_f^{1/2}}{(g\sigma(\rho_f - \rho_g))^{1/4}}. \tag{2.6}$$

Tien used $m = 1.0$ and $C_k = \sqrt{3.2}$ and later incorporated corrections to include the effects of vapor condensation. An effective vapor flow, Ku_{ge}, was derived by Tien using a simple analytical model that represents the portion of vapor flow that does not condense during the flooding phenomenon. Equation 2.5 is widely regarded as the most applicable correlation for large diameter round tubes [18] and is used in the current research for reporting data. The current research utilizes the correlation by first selecting the desired water flow rate to be injected and gradually increasing the gas flow rate until the corresponding onset of flooding value (j_g predicted by Equation 2.5) is reached. If the gas flow rate were to increase further from the onset of flooding flow rate, Ku_f would decrease according to the correlation [16]. Upon full flow reversal, ie. $j_f = 0$, Equation 2.5 reduces to the maximum gas criterion shown in Equation 2.4.

2.2 Flooding Studies at Texas A&M University

The current research can be considered the fourth installment of flooding investigations performed in the Nuclear Heat Transfer Systems Laboratory at Texas A&M University. These previous studies provide significant information regarding flooding in large diameter tubes and serve as the basis for generating the current flooding data.

2.2.1 Air/Water Testing

In the first series of tests, a transparent test section made of acrylic was designed and constructed for air/water flooding in a large diameter vertical tube at atmospheric pressure [13]. This test section served as the prototype for future test

sections and revealed design characteristics for flooding to be achieved. Specifically, the method for developing annular flow for the falling liquid film was determined and the flow regime was visually confirmed. The air injection device, or the air inlet to the test section, also went through several iterations to find optimum geometry for flooding. Initially a flow diffuser with several holes was installed as the air inlet device; however, the air supply was not large enough to supply enough flow to induce flooding. To reduce the pressure drop, the diffuser was removed and a straight pipe was installed at the bottom of the test section to allow for flooding to be initiated [13].

The scaling analysis by Solmos was also of importance in the air/water tests. The acrylic test section was a scaled version of the 10 inch diameter pipe in the PWR pressurizer surge line. The test section had an inner diameter of 3 inches and was considered within the bounds of the large tube diameter classification by Vijayan [18]. While the Reynolds number of the gas was not matched, the liquid Froude number was used to generate a test matrix that would scale adequately with the pressurizer surge line. The density ratio between air and water for Solmos' test was close to zero and it was acknowledged that further research should be performed to adequately address the density ratio scaling in terms of steam/water flooding [13].

Lastly, a high speed camera was used to capture visualization images of flooding in the test section. The images illustrate the chaotic nature of flooding and document several stages of each flooding event, including the onset of flooding to a stable bidirectional liquid flow.

2.2.2 Steam/Water Testing with Fixed Water Subcooling

The second series of tests used the design information from the air/water acrylic prototype to construct a stainless steel test section intended for steam/water flood-

ing experiments at atmospheric pressure [21]. The test section design followed the prototype as closely as possible to maintain consistency and to have similar operating procedures between the experiments. The existence of annular flow was visually confirmed in the stainless steel test section and a limited set of air/water flooding data was collected to serve as a benchmark. The aformentioned stainless steel test section is used for the current research after undergoing minor modifications.

The benchmark data was later compared to steam/water data to understand the effect of condensation on flooding [21]. The steam/water tests were performed with an inlet water subcooling of 30 °C at atmospheric pressure and the steam was slightly superheated at 110 °C. This resulted in condensation being present during the tests and it was shown by Ritchey that the flooding curves diverge from the air/water curves above a inlet water flow rate of 6 GPM [21]. While the testing range used in the steam/water tests was extended from those done by Solmos, the steam/water and air/water testing was performed at atmospheric pressure and the pressure scaling issues in large diameter tubes were not addressed due to the facility limitations.

The steam/water flooding data was compared to the well-known Wallis and Kutateladze-type correlation; however, neither correlation accurately predicted the flooding data so a new correlation was developed. The correlation was derived to account for the amount of steam that condenses on the film of water by using an energy balance. The amount of energy released by the steam during condensation is equal to the amount of energy absorbed by the water to bring it to saturation conditions. This is expressed as

$$f = \frac{\dot{m}_f c_p (T_s - T_{wall})}{\dot{m}_{st}(h_{st} - h_f)} \tag{2.7}$$

where f is the fraction of steam that condenses inside the test section, T_s is the

saturation temperature at the vapor-liquid interface, T_{wall} is the inner tube wall temperature at the location of flooding, $\dot{m}_{st}$ is the inlet steam mass flow rate, h_{st} is the steam enthalpy, and h_f is the water enthalpy [21].

Using Equation 2.7, the data was fit in terms of the Kutateladze parameters and the final correlation was

$$(Ku_g(1-f))^{0.5} + 0.56Ku_f^{0.5} = 1.45. \tag{2.8}$$

2.2.3 Steam/Water Testing with Variable Water Subcooling

The third series of testing investigated the effects of variable water subcooling on flooding in a large diameter vertical tube at atmospheric pressure [6]. The steam/water facility was modified to allow the water inlet temperatures from 35 °C (65 °C subcooling) to 97 °C (3 °C subcooling). The data confirmed that at high water subcooling the flooding curves diverge from air/water flooding curves due to the large amount of condensation present inside the test section. The low water subcooling data closely followed the air/water flooding data and this result was to be expected in the current testing at higher pressures.

Equation 2.8 provided a good prediction for water subcooling values between 0 °C and 65 °C in large diameter tubes using steam and water [6]. Though the minimum subcooling was 3 °C for Cullum's data, the current research attempts to obtain flooding data even closer to saturated conditions and at varying pressures. The effect of water inlet subcooling on flooding at higher pressures needs to be investigated, though will be outside the scope of the current research.

2.3 Flooding Studies at Elevated Pressure

To the author's knowledge, there is not any data available in the literature for flooding in a large diameter vertical tube at elevated pressure. However, there are some extensive studies for steam/water and air/water flooding at higher pressures in reactor specific geometries. Despite the differences in geometry, the summary below will attempt to focus on the studied effects of pressure on the flooding phenomenon.

Rothe and Crowley investigated the effects of subcooling and pressure during steam/water flooding in a scaled version of a PWR [11]. The study focused on the refill stage from the Emergency Core Coolant System (ECCS) injection during a postulated loss of coolant accident. This study also performed saturated steam/water tests at system pressures ranging from ambient up to 65 psia, similar to the current research. The researchers investigated flooding as it would occur in the annulus or downcomer between the reactor vessel wall and the core barrel. The saturated steam/water data were reported in terms of Wallis parameters and is shown in Figure 2.2. For a fixed inlet water injection flow rate of 60 GPM, Figure 2.2 shows the onset of flooding point, full flow reversal, and points in between for a variety of pressures. The system pressure does not appear to affect the flooding characteristics in this case, and Rothe and Crowley developed a correlation to describe the data. They conclude by claiming that higher pressure data should be acquired to validate the use of small scale data in full scale reactor safety use.

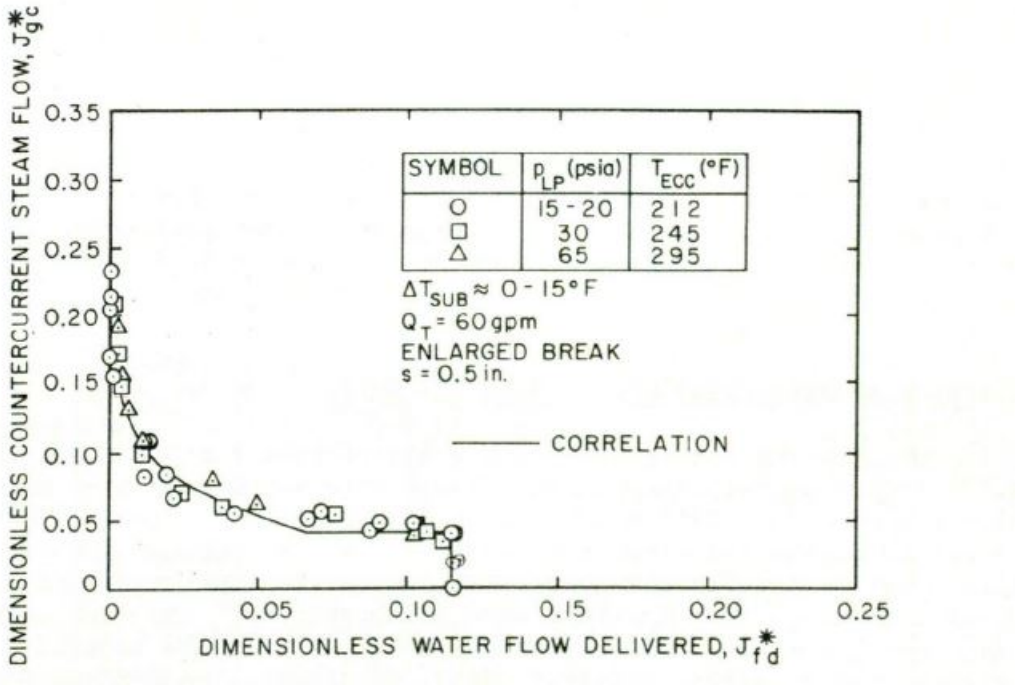

Figure 2.2: Rothe and Crowley data on the effect of pressure on flooding [11].

High pressure air/water and saturated steam water data were obtained by Vallée et. al in a scaled model of the hot leg of a PWR [17]. Air-water tests were conducted at pressures up to 3.0 bar while saturated steam/water tests were performed at 15, 30, and 50 bar with an unavoidable subcooling of about 2 °C. The experiment was designed to simulate a loss of coolant accident and investigate the flooding conditions in a horizontal geometry leading from the hot leg into the steam generator inlet. The saturated steam/water data and air/water data were reported in both the Wallis parameters and the Kutateladze numbers, which is shown in Figure 2.3. As shown in Figure 2.3, the flooding characteristics do seem to be affected by pressure when plotted in terms of the Kutateladze number. The saturated steam/water tests are compared to the air/water results, it is confirmed that the flooding conditions are

very similar for each case when the condensation is accounted for.

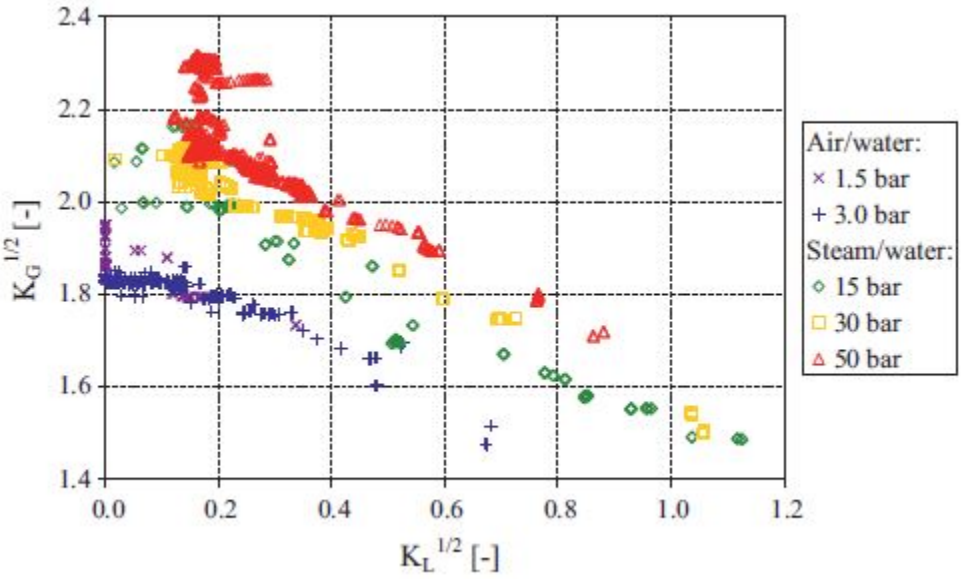

Figure 2.3: Vallée data on the effect of pressure on flooding [17].

3. FACILITY DESCRIPTION

The original flooding facility designed by Nicole Ritchey [21] was modified to allow air/water and steam/water flooding data to be generated and collected at pressures up to 60 psia. In the facility improvements, several components were added for maintaining a pressure boundary and also to operate at higher temperatures than previously considered. A new air supply was procured to allow for high pressure air/water testing and several flow meters were added to measure the outlet flow rates downstream of the test section.

The facility can be divided into three primary flow paths: the water flow path, the air flow path, and the steam flow path. The following summary will explain the major components and subsystems, while a piping and instrumentation diagram of the facility is shown in Figure 3.1.

3.1 Test Section

The majority of the test section was designed and built by Williams [21] and is shown in Figure 3.2. Since the test section was originally designed for steam use, the component labels are referred to in terms of steam; the current research also uses the test section for air testing, therefore the steam inlet is the same as the air inlet.

The test section assembly is a 3 inch inner diameter (ID) tube with wall thickness of 0.25 inches and length of 72 inches. All of the materials used in the test section construction are made of austenitic Type 304 stainless steel. All surfaces on the test section were treated with a citric acid cleaning and passivation solution (Citrisurf 2310) to remove any surface rust and contaminants that were present from previous testing. The test section tube has five 0.125 inch NPT (National Pipe Thread) half couplings welded to the surface to serve as instrumentation ports; three of the ports

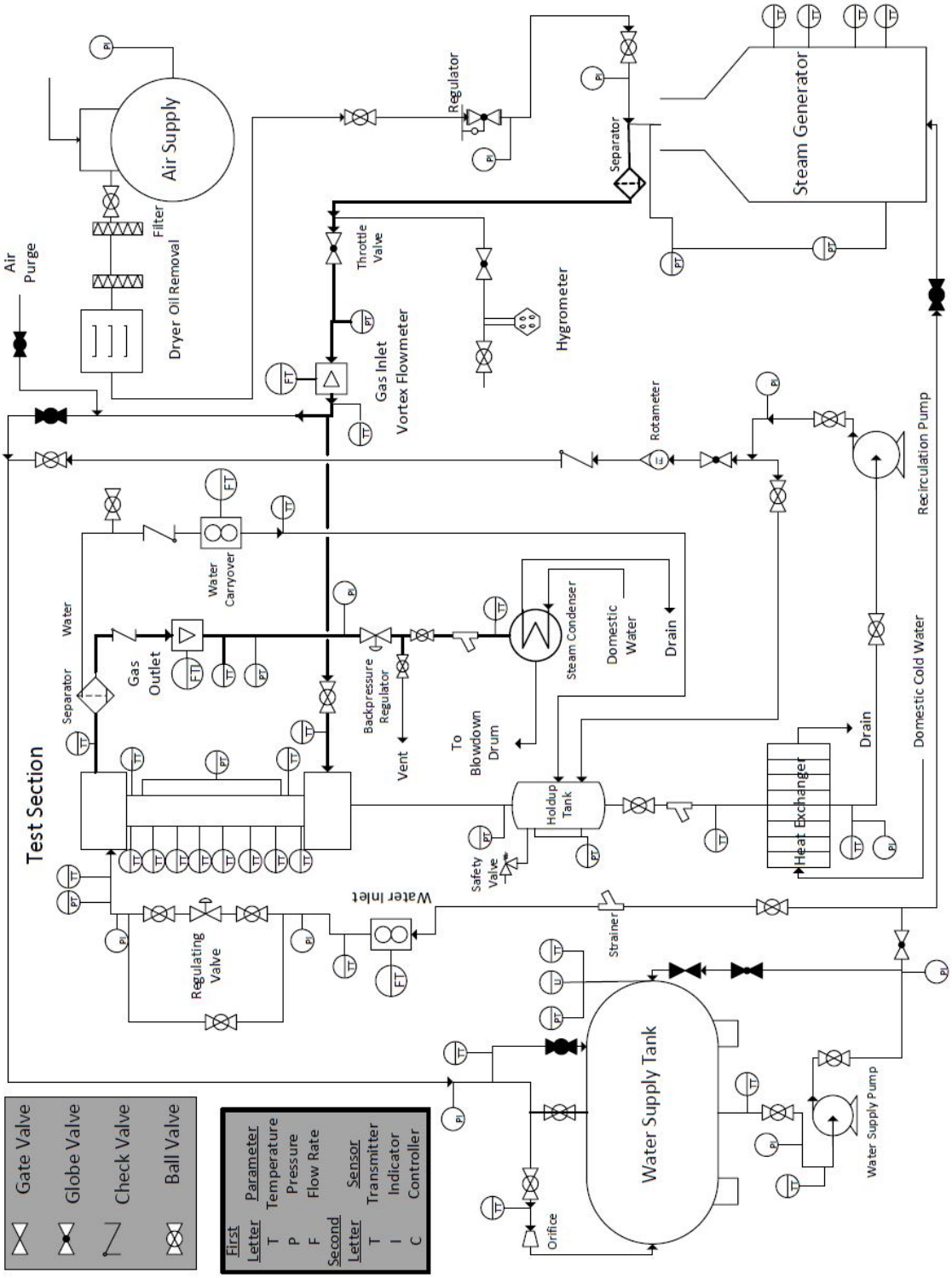

Figure 3.1: Piping and instrumentation diagram of facility

are at the top of the test section and two at the bottom. Both of the bottom ports are used for pressure measurements while only two of the top ports are used, one for pressure and one for centerline temperature measurement of the test section.

The top of the test section tube has a water inlet chamber made of 6 inch nominal pipe size (NPS) welded to two Class 150 socket weld flanges. Four equally spaced ports composed of 0.75 inch NPT half couplings are welded to the 6 inch pipe and direct the inlet water into a plenum to prepare it for annular flow. Only two opposing ports are required for the range of flow rates used in the test matrix.

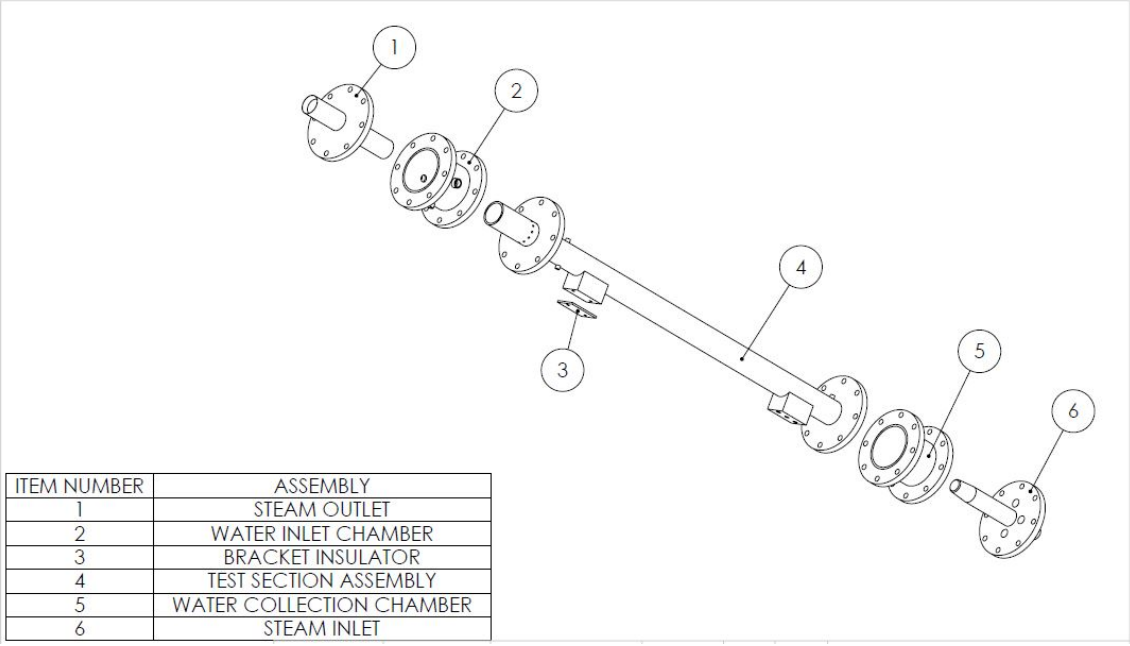

ITEM NUMBER	ASSEMBLY
1	STEAM OUTLET
2	WATER INLET CHAMBER
3	BRACKET INSULATOR
4	TEST SECTION ASSEMBLY
5	WATER COLLECTION CHAMBER
6	STEAM INLET

Figure 3.2: Exploded diagram of the original test section as designed by Ritchey [21]. The major modifications for the proposed research include welding an additional flange to the steam outlet and repairing a broken weld on the steam inlet.

The top of the 3 inch ID test section tube has 12 holes drilled at equal spacing

around the circumference, each with diameter of 0.25 inches. The water flows through these 12 holes from the water inlet chamber and flows down the test section assembly in the annular flow regime. A smaller tube with outer diameter (OD) of 2.75 inches fits concentrically inside the test section assembly and facilitates the formation of the annular film. This same 2.75 inch OD tube has a wall thickness of 0.25 inches and also serves as the steam outlet tube. The distance between the steam outlet tube OD and the test section tube ID is 0.125 inches and is the maximum possible thickness of the annular film at this location. The bottom of the steam outlet tube is beveled to 15° to the vertical axis to prevent vortices in the outlet two-phase mixture.

The bottom of the test section has a water collection chamber that is very similar to the water inlet chamber with the exception that there are not ports on the sides of the 6 inch pipe. Instead, the water exits through a blind flange with four 1 inch NPT threaded holes drilled through to allow the water to exit the test section. These holes were discovered to be poorly tapped during the original assembly, and the threads were chased with a 1 inch NPT pipe tap for the current research. The steam inlet flange has a 1.5 inch NPS pipe that is welded in the center to allow the gas phase to enter into the test section from the bottom. To avoid condensation in the steam inlet, an insulating gap of air is created by welding a 2 inch NPS pipe and concentric reducer over the 1.5 inch steam inlet. During construction of the test facility, a broken weld was discovered between the reducer and the 2 inch pipe. This was likely due to a faulty weld, or thermal expansion of the 1.5 inch steam inlet during previous operation. The broken weld was ground down and repaired using the gas tungsten arc welding (GTAW or TIG) process. A high temperature epoxy was applied over the weld and machined to a sharp edge as opposed to a rounded edge as described by Wallis [20].

In the past, a flexible silicon hose was clamped to the steam outlet to direct

the steam to a blowdown drum where the condensed steam was released to the environment. This arrangement would not permit high pressure operation, so the steam outlet was modified by the addition of a 2.5 inch pipe size blind flange that was machined to fit the steam outlet. The 2.5 inch flange was TIG welded to the steam outlet to create a pressure tight seal. A 2.5 inch flange was chosen so that after machining to size, the remaining gasket thickness would be adequate to meet the Class 150 standards of ANSI 16.5B. A mating flange was machined to reduce the 2.25 inch ID steam outlet to 2 inch NPS, referred to as the reducing flange. The reducing flange was welded to a 2 inch long radius elbow with a centerline curvature of 12 inches. The long radius elbow and reduction in pipe size were chosen to increase the two-phase velocity and gently direct the entrained liquid droplets and slugs out of the test section during flooding. The other end of the long elbow has a 2 inch socket weld flange to easily mate to components downstream. The modified steam outlet and long elbow assembly is shown in Figure 3.3. Engineering drawings of the steam outlet and long elbow assembly are included in Appendix B.

The test section was designed for operation at atmospheric pressure, so certain components required upgrading for use at higher pressures. The previous fasteners for the 6 inch pipe flanges on the test section were hot dipped galvanized hex head bolts with zinc coated hex nuts. The un-galvanized nuts would not thread onto the bolts to compress the flange gasket and required replacement. By calculating the minimum required seating load for the new flange gaskets, the required axial bolt load was found to be 6000 psi for each bolt. The galvanized bolts were replaced with 0.75 inch diameter 18-8 stainless steel hex head bolts and heavy hex nuts that comply with ASTM A193 Grade B8. Upon installation, the bolts were coated with corrosion-resistant antiseize lubricant to transfer more torque to the gasket compression and to avoid galling. The lubricant was nickel based and copper-free to avoid a large

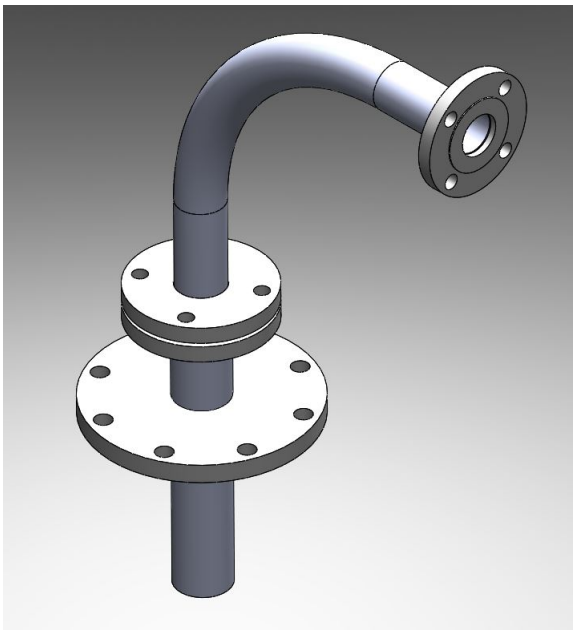

Figure 3.3: Rendering of the modified steam outlet and long elbow assembly.

galvanic potential with the stainless steel and the lubricant is rated for 2200 °F. The existing Aramid/NBR gaskets were replaced with either Aramid/SBR or pure PTFE gaskets for improved resistance to saturated steam at higher temperatures. The test section was isolated with blind flanges and hydrotested to 90 psig for one hour. No leaks were observed and an operating pressure of 45 psig (safety factor of 2) was deemed safe in the test section.

3.2 Water Flow Path

Water used in the experiment is stored in the water supply tank where it is transported to the test section via the water supply pump. If a flooding event occurs, the portion of the water that becomes entrained (referred to as water carryover) will be removed from the gas phase in a separator and drained to the holdup tank. Any water that is not carryover will drain from the bottom of the test section. After exiting the test section, both streams enter the holdup tank, pass through a heat

exchanger, and are returned to the water supply tank through the recirculation pump. This closed loop design reduces the need to continually generate clean deionized water for each flooding test. The major components used in the water flow path will be described in detail below.

3.2.1 Deionized Water System

The water used for both steam/water and air/water testing is supplied by domestic cold water maintained by Texas A&M Utilities. The domestic water is treated by a deionized water system provided by Culligan Water Services. Deionized water is necessary to prevent major corrosion of piping and components in addition to minimizing scale buildup on the steam generator heaters. The deionized system consists of two particulate filters, an activated charcoal filter, two mixed bed resin tanks, and a 50 kΩ conductivity light. The mixed bed tanks consist of a cation and anion resin to produce high purity water with a conductivity of less than 3 μmho/cm. The system is capable of producing roughly 350 gallons before regeneration of the resin is necessary.

3.2.2 Water Supply Tank

The deionized water is stored in a 1400 gallon pressure vessel referred to as the water supply tank. The water supply tank was acquired for another experiment in the lab, though the other experiment is not designed to operate concurrently with the flooding facility. The water supply tank is colloquially referred to as the RCIC tank or the suppression pool tank. The water supply tank is a horizontal tank with diameter of 59 inches and length of 122 inches head-to-head. With exception to the tank legs, the vessel is composed of Type 304 stainless steel and is rated for a maximum allowable working pressure (MAWP) of 88 psig at 400 °F. The water inventory used in the current research was approximately 700 gallons. The outlet of

the tank is a 0.75 inch port on the bottom of the tank to feed the pump suction. The pump suction piping increases to 1 inch NPS and feeds two pumps in parallel. The tank has three penetrations on the top that can be used for injection. The first penetration is an open pipe that vents to the air space of the tank. The second penetration has a tank sparger (commonly referred to as the SRV sparger) that discharges below the water line with a pipe tee. The last penetration also contains a tank sparger (commonly referred to as the RCIC sparger) which consists of an open pipe discharging at the far end of the tank below the water line. Further detailed descriptions of the water supply tank internals are described in Solom et al [14].

3.2.3 Water Supply Pump

In the air/water tests, the supply pump is a Dayton model 5UXF5 five-stage centrifugal booster pump. This pump was used for another experiment and is a high pressure pump that dead-heads close to 93 psid. The pump has a 0.75 horsepower (HP) electric motor wired for 115 VAC and has a cast iron housing with case pressure of 150 psi. The maximum temperature of the pump is published as 194 °F though a viton mechanical seal was installed to allow intermittent use up to 250 °F. The flow rates are controlled via a recirculation line, 1 inch globe valve, and a Jordan Mark 60 pressure regulating valve. The pump discharge piping leading to the test section is primarily 0.75 inch NPS with temperature, pressure, and flow instrumentation throughout. Wye strainers are installed to protect the pump and regulating valves from particles and debris that could become stuck in moving parts. Local pressure gauges were installed on the pump suction and discharge to monitor pump performance, and isolation valves were installed for easy removal of the pump during maintenance. Temperature and pressure measurements are taken close to the test section water inlet chamber to monitor the fluid parameters for each flooding test.

Since the Dayton pump has a relatively low temperature limit on the mechanical seal, a new hot water supply pump was procured for the steam/water flooding tests. The Liquidflo model 620 Century Series is a single stage close coupled centrifugal pump with maximum flow of 45 GPM and maximum head of 65 ft [7]. The use of a single mechanical seal made of silicon carbide along with graphoil seals allow a maximum operating temperature of 500 °F. The impeller and housing are made of Type 316 stainless steel and the impellar diameter is 3.50 inches. The motor is 1 HP and is wired for 115 VAC for a shaft speed of 3500 RPM. This pump is installed in parallel to the Dayton pump though only one pump was operating at any given time during the flooding tests. The discharge piping is identical to that described for the Dayton pump.The required pumping head was calculated to be 65 feet at 12 GPM. During the saturated water tests, the water supply tank was pressurized to approximately 5 psi greater than the test section pressure to maintain the required net positive suction head available to avoid cavitation in the supply pump. The pump discharge transitions from 1 inch NPS to 0.75 inch NPS pipe and the flow rate is recorded using a magnetic flow meter. The two pumps are shown in Figure 3.4.

Figure 3.4: The Dayton multistage pump and the Liquidflo 620 centrifugal pump. The suction and discharge piping is shown prior to the placement of insulation.

3.2.4 Holdup Tank

After the water exits the test section from the water collection chamber, it flows through four stainless steel braided hoses into the holdup tank. The holdup tank serves several functions including accepting water that exits the test section prior to flooding, and storing water as a supply for the recirculation pump after the onset of flooding. The holdup tank is a vertical pressure vessel with a capacity of 80 gallons. The vessel is made of Type 316 stainless steel and is rated for a MAWP of 150 psig at 400 °F. The vessel is also rated for full vacuum, and thus a vacuum breaker was not installed for the steam/water flooding tests. The heads are 0.25 inches thick while the shell is 0.1875 inches in thickness. The tank was manufactured by Kennedy Tank and Manufacturing Co. in 1982 and was procured for the current research. The vessel was hydrotested at 150 psig for one hour and cleaned with citric acid

before being put into service. The holdup tank has two nozzles on top of the vessel, one 6 inch and one 2 inch. Each nozzle has a stainless steel stub-end welded to the nozzle with carbon steel lap joint flanges. Several threaded couplings (2-2inch, 2-1 inch, 3-0.75 inch,and 4-0.5 inch) are welded on the top and sides of the vessel. The vessel is supported by four carbon steel legs made of pipe welded to 7 inch steel angle. Originally the vessel came with a stainless steel overflow pan underneath, however to allow the holdup tank to fit below the test section, the pan was removed and the legs shortened by three inches. Baseplates were fabricated to allow the holdup tank to be securely bolted to the floor and were welded to each leg using the gas metal arc welding (GMAW or MIG) process. A 6 inch pipe size blind flange was machined to seal the holdup tank penetration but also allow the water to drain from the test section. A similar 2 inch pipe size blind flange was machined to seal the smaller nozzle but also allow the water carryover to drain into the holdup tank. Dimensional drawings of both flanges are shown in Appendix B. The modified holdup tank is shown installed in Figure 3.5.

The vessel is protected from overpressure by use of a safety valve manufactured by Kunkle Valve which is factory calibrated to lift at 60 psig for steam service. This bronze safety valve meets ASME Code Section I for Steam and has a capacity of 748 lbs/hr. The capacity was determined by assuming that the steam generator would blowdown all of its inventory into the holdup tank while at full power. Since the water collection chamber on the test section is connected to the holdup tank with no means of isolation, the safety valve also protects the system from overpressure. The safety valve protects the system during air service also, and the valve was verified to lift at 63 psig when using air. A two-wire braided rubber hose with a diameter of 0.75 inches is attached to the safety valve and directs the vented steam to a blowdown drum. The rubber hose is rated for steam service with a working pressure of 250 psi at 450 °F, and

utilizes zinc plated steel boss threaded couplings with two-hole interlocking clamps on each end. The boss couplings are designed for high pressure steam service and are safer than the worm-gear hose clamps found throughout the lab.

Figure 3.5: The holdup tank shown below the test section before insulation was applied. The two inch coupling and piping shown on the left side were later removed and plugged after this photo was taken.

3.2.5 Heat Exchanger

After exiting the holdup tank, the water is returned to the water supply tank via a recirculation pump in a closed loop to conserve the inventory of deionized water. However, to avoid cavitation in the recirculation pump during the saturated water tests, it was necessary to design a cooling system to decrease the vapor pressure of

the water near the eye of the pump impeller. In the past, domestic water running through copper coils was used inside of a 55 gallon drum to cool the hot water exiting the test section. This design was undesirable for the current research since the drum and coils could not be pressurized. Secondly, deionized water will cause pitting and corrosion on copper and will become contaminated by copper ions.

For the current research, a plate-type heat exchanger produced by Alfa Laval was chosen to transfer heat from the saturated water (hot side) to the domestic water supply (cold side). A plate-type heat exchanger was chosen due to the high thermal efficiency and compact size. The unit is 4 inches long, 4 inches wide, and 12 inches tall. Thin corrugated stainless steel plates are bonded together to form sealed flow channels inside the heat exchanger resulting in a large amount of surface area between the two media [1]. The AlfaNova 27-30H heat exchanger operates in counter-current flow and the design limits are 300 psi at 437 °F. The construction is 100% stainless steel and the connections are four externally threaded 0.75 inch NPT ports. The original design assumed a cold side flow rate of 15 GPM, which results in a heat removal rate during saturated water tests of 80 kW. Upon facility shakedowns, it was observed that a maximum cold side flow rate of 22 GPM is possible. The outlet temperature of the cold side should be maintained less than 110 °F to eliminate scaling inside the heat exchanger. A wye strainer was placed upstream of the heat exchanger on the hot side to protect the sealed unit from large particulates and debris that may collect at the bottom of the holdup tank. The installed heat exchanger is shown in Figure 3.6.

The cold side of the heat exchanger is cooled by the domestic cold water supply. The domestic water piping in the laboratory was significantly upgraded to accommodate the heat exchanger and other components in the flooding experiment. Several hoses were used in the past to transport domestic water from the water main to

Figure 3.6: The AlfaNova 27-30H heat exchanger shown installed with protective blue thermal insulation. The hot side inlet is shown on the left while the hot side discharge to the pump suction is on the right. The cold side domestic water is shown in 1 inch PVC piping.

the experiments. These hoses were laying on the ground and presented a tripping hazard in addition to periodically developing leaks. To correct this, the water main was extended by mounting the piping to the wall and vertical structures to extend the domestic water supply closer to the experimental test facilities and eliminate ground level hoses. The water main piping used was 1.5 inch schedule 80 PVC with a combination of threaded and socket-weld joints. A purple primer for PVC pipe was used to comply with most building plumbing codes. A 5 micron particulate filter with a capacity of 45 GPM was installed on the domestic water supply to remove any rust or scale that could contaminate the heat exchanger. The domestic water supplying the heat exchanger is reduced to 1 inch PVC and contains a gate valve and rotameter for precise flow control. Both the heat exchanger inlet and outlet

on the cold side are equipped with local glass thermometers with thermowells for monitoring heat exchanger performance.

3.2.6 Recirculation Pump

For the high pressure steam/water flooding tests, a second Liquidflo Model 620 pump with a 1.5 HP motor and a 3.75 inch diameter impeller was procured as the water supply pump. However, this pump was damaged during shipment and the 1 HP Liquidflo Model 620 was used in its place. This resulted in the use of an AMT Model 489A-98 high head centrifugal pump for the water recirculation pump to propel water from the holdup tank to the water supply tank. The AMT pump has a stainless steel impeller and housing with maximum flow of 118 GPM and maximum head of 149 ft of water [2]. The pump motor is 1.5 HP and is wired to 115 VAC. The mechanical seal is made of viton with a maximum operating temperature of 200 °F. The maximum temperature of the pump limited the steam/water testing matrix for the current research; the maximum system pressure during the steam/water testing was 15 psig to allow for an acceptable saturated water temperature for pumping. Higher pressures will be attainable when the damaged 1.5 HP Liquidflo pump is repaired. The 1 HP Liquidflo Model 620 pump was used as the recirculation pump for the air/water flooding tests.

The recirculated water passes through a 1 inch high temperature Hedland rotameter with flow range from 2-20 GPM. The rotameter is accurate to 2% full scale and can operate up to 3500 psig and 400 °F. The flow rate is controlled with a 0.75 inch globe valve and also with a bypass line that returns water to the holdup tank. The globe valve was chosen to throttle the flow and limit the maximum flow rate while the bypass line enforces a minimum flow rate through the pump. The bypass line ensures that if the pump were ever to run against a closed valve, the minimum

flow rate would be adequate to cool the mechanical seal. As with the supply pump, local pressure gauges and isolation valves are present on the pump suction and discharge for verifying pump performance and easy maintenance. A ball check valve is placed downstream of the rotameter to prevent siphoning of the water supply tank into the holdup tank when the pump is not in operation.

The recirculation water is returned to the water supply tank first through 1 inch NPS piping which then transitions to 1.5 inch NPS over the bay door in the lab. The 1.5 inch NPS line was used in a previous experiment to direct steam into the water supply tank however during the flooding experiments this line is filled with water. This line shall be referred to as the common pipeline. The recirculated water is discharged into the supply tank through one of two spargers constructed for another experiment. The SRV sparger (described in subsection 3.2.2 or in [14]) discharges the recirculation water below the water line through a pipe tee. This sparger promotes mixing of the tank and was primarily used during the air/water flooding tests where tank mixing was not of concern. The RCIC sparger [14] discharges the recirculated water through a straight pipe end and results in more localized heat deposition. The RCIC sparger was used for the steam/water tests since the discharge is on the opposite end of the tank as the water supply pump suction. This allowed the cooler recirculated water to not mix as much with the bulk saturated water needed for the steam/water flooding tests. The RCIC sparger alignment had an orifice plate upstream of the sparger as described in [14] which presented a larger system head for the recirculation pump, but did not affect the overall performance of the flooding facility.

3.3 Air Flow Path

The compressed air used in the flooding tests is generated in a compressor and is then filtered, dried, and regulated before traveling to the steam generator vessel for storage. The compressed air then travels to the test section and upon exiting passes through a phase separator to remove any entrained water during a flooding event. The dry compressed air exiting the separator goes through the back pressure regulator and is vented to outside the lab. The major components used in the air flow path will be described in detail below.

3.3.1 Air Supply

Ritchey recorded a limited set of air/water flooding data in the test section using a regenerative blower that took suction from the lab and discharged to atmosphere [21]. This design was not conducive to high pressure flooding tests since the single stage centrifugal blower was not able to provide enough pressure to induce flooding in a closed loop due to the large pressure losses. A major pressure loss in the closed loop was due to the phase separator.

As a result, a new air supply was designed, procured, and installed for the current research. Larger regenerative blowers were first considered, however none provided enough head to overcome the pressure losses. Centrifugal blowers (like pumps) provide a large capacity at a relatively small differential pressure. Thus, high head compressor systems were considered to supply the required head pressure but at a reduced capacity. The design criteria for the air compressor included cost, noise, oil consumption, and air output quality. A rotary screw compressor was first selected as the best unit however these compressors are very expensive and also do not operate well with intermittent loading. Each flooding test is short in duration, and the air supply is continually loaded and unloaded as the parameters are adjusted for each

test and subsequent tests. The compressor needed to limit the amount of oil that became entrained in the delivered air as oil contamination of the test section and piping was undesirable. Lastly, the compressed air was to be relatively dry and free of moisture to limit corrosion and not affect the flooding phenomenon.

The sizing of the air supply was based from data obtained from previous air/water testing in the current test facility by Ritchey [21]. In those tests, flooding was achieved in the test section for water flow rates ranging from 4 to 12 GPM with air mass flow rates of 47 to 54 g/sec. Based on information from Vallée et al. [17], the steam mass flow rates necessary for flooding are greater at higher pressures than at atmospheric pressure but the air mass flow rates appear unchanged for varying pressures. The air flow rate necessary for flooding is inversely proportional for all water flow rates while subcooled steam/water flooding data do not follow this trend. Therefore it was projected that the air mass flow rates for the proposed tests would be consistent to previous data. However, to have comparable gas supply capabilities and to add conservatism, the air supply was sized to match the maximum steam output of the facility steam generator which is 75 g/sec. The convention in air supply selection is to size the unit in terms of volumetric flow rates at specified conditions, so the mass flow rates of 47 to 75 g/sec is equal to 88 to 140 CFM (ft^3/min) at standard conditions of 14.5 psia, 68 °F, and 36% relative humidity.

The air supply to the test section is from a QT-15 reciprocating air compressor manufactured by Quincy compressor. The compressor is an air cooled, splash lubricated, belt driven unit with two stages of compression. Air is drawn in through the intake valve on the aluminum head into the low pressure cylinder where the first stage of compression takes place. The low pressure air (about 125 psig) exits through the discharge valve and travels to the second stage of compression. The large amount of heat that is produced during the first compression cycle is dissipated to the envi-

ronment through an intercooler made of finned copper tubing. The large cast iron flywheel (also called the compressor sheave) is equipped with fan blades to direct ambient air to the intercooler and cast iron cylinders for the heat exchange. The low pressure air enters the high pressure cylinder and is compressed to 175 psig where it then passes through an air cooled aftercooler. The aftercooler is necessary to cool the compressed air to allow the gross amount of water vapor to condense into a liquid. The condensate is mechanically removed from the air stream through a separator and the compressed air is stored inside a 120 gallon receiver tank. The compression cycle is completed in one revolution of the crankshaft and a dipper on the bottom of the connecting rod splash lubricates the internal components with oil [5]. The V-design of the compressor head results in a balanced unit with four cylinders in total for an output of 51 CFM at 175 psig.

The compressor unit is belt driven by a 15 HP Baldor electric motor that is wired to 460 VAC 3-phase power. The magnetic starter containing the EATON contactor and overload relay is equipped on the front of the unit and a 30 ampere (A) three pole breaker is used to apply electricity to the motor. When energized, a pressure switch will start the compressor when the receiver pressure is below 150 psig and will stop the unit when the pressure is 175 psig. An unloader valve is equipped near the pressure switch to vent air from the pistons when the compressor reaches 175 psig. The unloader valve allows the compressor to easily start during the next compression cycle. Several shutoff valves, check valves, and ASME safety valves are installed on the unit for operation; these valves must not be tampered with. The compressor was installed inside the building since outdoor temperatures during a Texas summer will exceed the maximum ambient operating temperature of 104 °F. The unit was bolted to the floor with 0.5 inch diameter wedge anchors, though the nylon nut was left loose to avoid cracked welds and stresses caused by severe vibrations. Rubber and

cork isolator pads were installed under the compressor feet to reduce the amount of vibration to the piping and building foundation. A metal frame composed of slotted channel strut was constructed around the compressor for future installation of noise dampening boards and a plywood wall to protect the air supply from other large equipment (forklifts, pallet jacks, shelving, etc.) in the laboratory. The metal frame is also used as a support structure for the compressed air piping. A minimum of 12 inches was maintained around the compressor to allow the required air flow for cooling during operation.

During normal operation, the large amount of moisture present in the compressed air will condense inside of the receiver tank. If neglected, this condensate can corrode the receiver tank and compromise the integrity of the vessel. A solenoid operated drain valve was installed on the unit to automatically drain the condensate and oil residue at user-defined time intervals. The outlet of the drain valve was equipped with 0.5 inch NPS black iron piping and fittings to direct the condensate to outside the building. The building penetration used was pre-existing and the asbestos laden building siding was not disturbed. The Texas A&M Environmental Health and Safety office was consulted and confirmed that the oil content of the condensate was below the effluent release limit and could be safely discharged to the environment. A cable protector was installed over the drain line to minimize tripping hazards for personnel accessing the building electrical panels. The air supply and condensate drain piping are shown in Figure 3.7

3.3.2 Air Filters and Dryer

The compressor intake is outfitted with two 10 micron inlet air filters and silencers to remove large particulates. After leaving the receiver tank, the compressed air passes through a 5 micron particulate filter (Quincy Model DCNT00425) and a

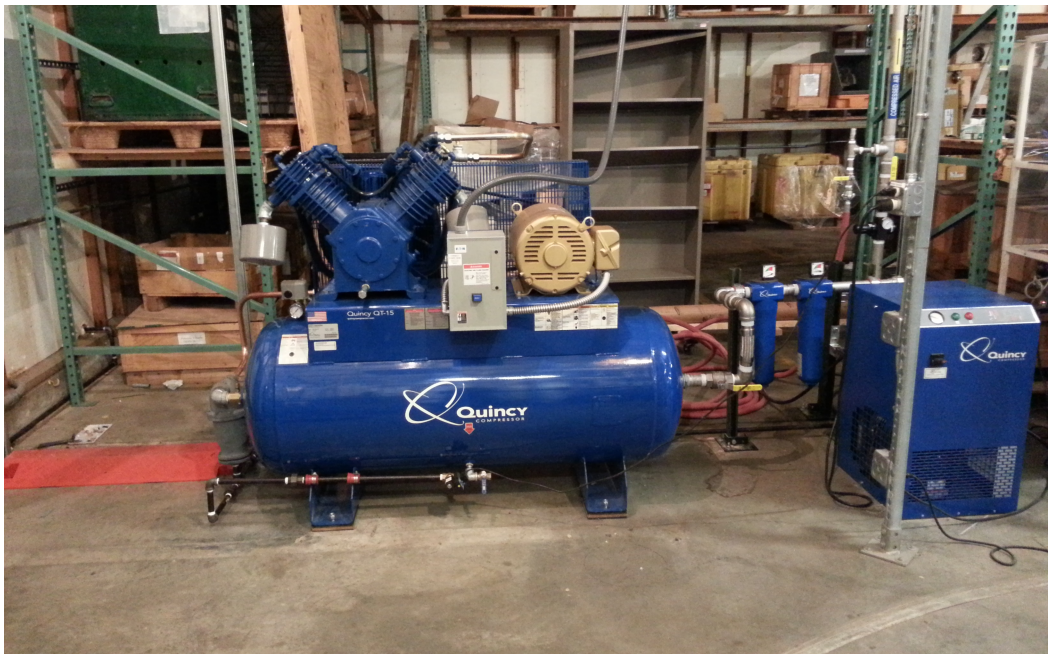

Figure 3.7: The air supply and supporting equipment.

0.01 micron coalescing oil filter (Quincy Model CXNT00425). Both filters have an aluminum housing with 1.5 inch NPT threaded connections. The filters are equipped with automatic condensate drain valves and a differential pressure display to indicate when the filters need to be changed. The combination of these filters provide a clean, relatively oil free air supply to the experimental test facility.

The moisture in the compressed air is reduced further in the refrigerated dryer. The Quincy Model QPNC-100 dryer is a non-cycling refrigerated dryer that lowers the temperature of the incoming compressed air to 39 °F forcing the entrained moisture to condense. The moisture is released through the condensate discharge piping to outside the lab. The dryer operates completely automatically, and maintains a dew point of 39 °F which results in an estimated relative humidity of about 20% during the flooding experiments. The dryer has 1.5 inch NPT connections and is wired to 115V with a 20 A plug.

Interconnecting piping for the air supply is 1.5 inch NPS stainless steel piping (Type 304). The filters and dryer were sized to 1.5 inch connections to decrease the velocity in pipe to reduce the frictional losses and pressure drop for the air supply. The air pressure downstream of the dryer is regulated with a 1.5 inch Speedaire relieving type pressure regulator. Several isolation valves made of nickel plated brass were installed in the compressed air line for easy removal of components during maintenance. Two quick connect air fittings were also installed to provide connections for air hoses to supply other equipment or experiments. The air supply piping was sloped during installation to promote the draining of condensate to traps. The compressed air piping was directed into the steam generator where the regulated pressure is stored for each flooding test. The steam generator was drained of all water during the air/water flooding tests to allow the highest vessel capacity for compressed air storage during the tests. The air travels to the test section in a 1.5 inch NPS line which has a vortex flow meter to measure the volumetric flow rate of the air. The flow rate is varied using a 1.5 inch globe valve referred to as the throttle valve.

3.3.3 Separator

A two-phase mixture of gas and water exit the test section outlet during a flooding event. In order to accurately measure the flow rate of each phase, a separator was procured and installed downsteam of the test section outlet. Initially, a vane-type separator was recommended for the range of flow rates under consideration during the anticipated flooding test matrix. However, the vane type separators were not made in all stainless steel construction and a high efficiency centrifugal type separator was selected. While it was difficult to find a separator that was rated for steam and air use over a range of flow rates, a two-stage separator was chosen to increase the separation efficiency over the operating range. The Anderson LCCR-200-RL-SC is

a high efficiency two-stage separator capable of removing liquid particles down to 1 micron in size [4]. The first separation stage is a stainless steel corrugated mesh at the top of the unit that coalesces liquid droplets by impaction. The second stage utilizes stationary rotor blades that force the liquid droplets to collect on the separator walls using the centrifugal force. The separator has a long body to handle high liquid loading application and is rated for steam service up to 500 °F and 600 psig.

The separator is a 2 inch model and threaded flanges were attached to the unit with close nipples during installation. The flanged connections use Aramid/SBR gaskets and 18-8 stainless steel studs and heavy hex nuts that comply with ASTM A193 Grade B8. The two-phase mixture exiting the test section travels through a section of 2 inch NPS pipe where the centerline temperature is measured. The water carryover that is removed from the two-phase mixture drains from the bottom of the separator through 0.75 inch pipe to the holdup tank. The carryover flow rate is measured with a magnetic flow meter and has a swing check valve inline to prevent backflow into the separator. The dry gas (either air or saturated steam) exits the separator through 2 inch NPS pipe and passes through a wafer disc check valve. The two check valves were installed to prevent backflow into the test section and separator during future steam/water flooding tests with high water subcooling. The disc check valve was chosen due to the compact size, small pressure drop, and high flow coefficient. The installed separator is shown in Figure 3.8.

3.3.4 Back Pressure Regulator

After the air exits the separator, it travels to a back pressure regulator in 1.5 inch NPS piping. A new vortex flow meter was installed downstream of the separator and upstream of the regulator to measure the flow rate of the outlet gas. The back pressure regulator maintains the upstream pressure at a predetermined setpoint;

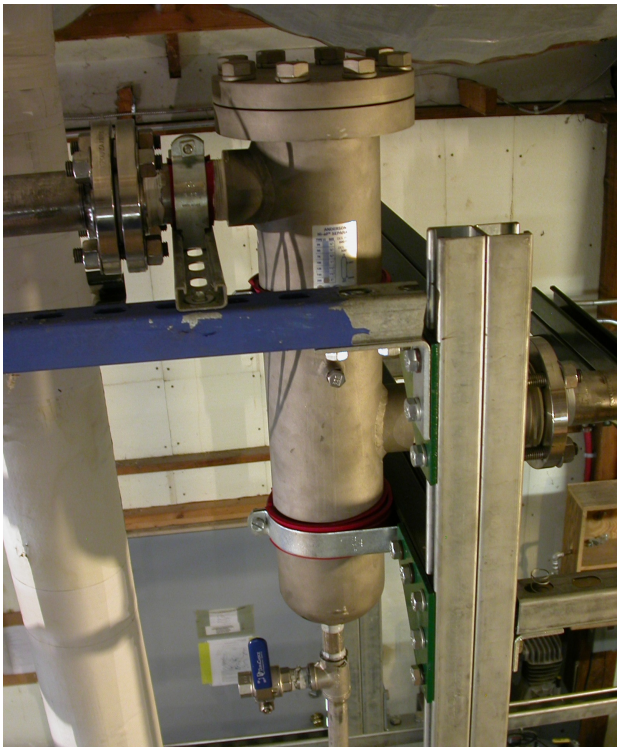

Figure 3.8: The Anderson LCCR separator shown without insulation. The two-phase mixture enters the separator on the left port while dry gas exits through the right port. The liquid drains from the bottom of the separator.

this valve regulates the system pressure for the flooding tests. The valve operates using a sliding disc connected to a stem that is attached to a stainless diaphragm. An adjustable spring is housed above the diaphragm and maintains the disc in the closed position when no flow is present. As the upstream pressure exceeds the force of the spring, the diaphragm lifts the stem and the valve trim opens to decrease the upstream pressure to the set pressure. When the upstream pressure drops below the set pressure, the valve trim closes to maintain the set pressure during flowing conditions.

A Jordan Mark 50 sliding gate back pressure regulator was chosen due to the high flow coefficient and optimal pressure control range. The regulator is a 1.5 inch model

with a ductile iron body and stainless steel trim/seat. The spring range is 15-80 psig and the flow coefficient is $C_v = 15$. The valve has threaded connections and is rated for 650 °F steam service at 300 psig. Since the air compressor discharge is below the standards for breathable air, the vented air from the regulator is discharged to outside the lab through a 2 inch ID SBR nylon braided hose.

3.4 Steam Flow Path

Deionized water from the water supply tank is directed to the steam generator where a series of high power immersion heaters generate a large quantity of saturated steam. The steam is sent to the test section and then passes through the separator to remove any carryover. The dry saturated steam travels through the gas outlet piping to the back pressure regulator and is vented to the steam condenser. The condensate is sent to a blowdown drum which releases to the drain. It is very important to note that the air flow path and steam flow path are identical from the steam generator to the back pressure regulator. This was intentionally designed to allow consistency between the flooding experiments so that accurate comparisons can be made when comparing the flooding behavior of each gas. The major components used in the steam flow path, that were not described in the air flow path, will be described in detail below.

3.4.1 Steam Generator

The steam used for the flooding tests is generated inside a 135 gallon vertical pressure vessel manufactured by Kennedy Tank and Manufacturing Co. for previous experiments in the Nuclear Heat Transfer Systems Laboratory. The vessel is made of Type 304 stainless steel and is 24 inches in diameter with a head-to-head distance of roughly 72 inches. The shell is Schedule 10 pipe and the MAWP of the vessel is 135 psig at 350 °F. Several penetrations were added for a vent line, a vacuum breaker,

two safety valves, and six heaters. The vessel is filled from a 0.75 inch NPS pipe from the water supply tank. The steam generator and associated equipment are shown in Figure 3.9.

Figure 3.9: The steam generator shown with insulation. The control panel is on the right and the blowdown drum is shown in yellow.

The deionized water is boiled to steam using six electric immersion heaters produced by Watlow Process Systems. Three of the heaters are 8-inch flanged models and output 50 kW each. The remaining three heaters are threaded with power levels of 2 kW, 2kW, and 3 kW. This results in a maximum operating power of 157 kW. Some of the heaters can be operated at lower power levels using subdivided circuits. Two of the 50 kW heaters have two 25 kW circuits and one heater has eight 6.25 kW

circuits. Therefore the operator can select the operating power level in fine increments using the control panel to select the appropriate heater circuits. The control panel is supplied by a 200 A three pole breaker at 480 VAC-3 phase. Safety interlocks protect the heaters from either low water level or thermal overload. A reed switch attached to the magnetic liquid level indicator will open the heater circuits if the liquid level drops below 35 cm on the sight glass. The heater temperature is regulated by Watlow Series 146 Temperature Regulators and will also open the circuits if the inconel sheath temperature exceeds 600 °F [21].

The steam generator is protected from overpressure by two 0.5 inch safety valves manufactured by Kunkle valve and are set to lift at 115 psig. The safety valves direct vented steam to a blowdown drum partially filled with water for condensation. A vacuum breaker valve is installed on the vessel to prevent a vacuum from developing inside the vessel after facility shutdown while the vessel cools. The vacuum breaker has an inline air filter to prevent debris from entering the vessel. A ball valve upstream prevents leakage of steam from the vacuum breaker during full power operation.

The saturated steam exiting the vessel has entrained water droplets present in the flow. A separator is installed at the steam generator outlet to remove those droplets and produce nearly dry saturated steam. The separator is an Anderson Type TL high efficiency centrifugal type separator and is compliant with ASME Pressure Vessel Code Section 8. The unit is a flanged 1 inch model and is constructed of stainless steel. The condensate that is removed is directed back into the steam generator and the dry saturated steam is expanded into 1.5 inch NPS piping. The same 1.5 inch globe valve used during air service regulates the flow rate of the steam to the test section. The flow path of the steam after this point is the same as that described for the air.

3.4.2 Steam Condenser

Since the high temperature steam cannot be discharged to the laboratory due to safety concerns, a steam condenser was designed to safely condense all of the steam that is vented from the back pressure regulator. The original intention of the condenser was to recycle the condensate to conserve the deionized water inventory, however during shakedown testing it was discovered that the condenser outlet was affecting the boundary conditions during the flooding tests. Water hammer was also present during shakedowns, and the condenser outlet was later directed to a blowdown drum to correct these two issues. The condensate is later drained to outside from the blowdown drum.

The steam condenser is a plate type heat exchanger produced by Alfa Laval (model AlfaNova 27-34H), and is nearly identical to the heat exchanger on the recirculation flow loop. The primary difference between the two units is that the steam condenser is larger in capacity and has unique connections. The heat exchanger operates in counter-current flow and condenses steam on the hot side by exchanging heat to domestic water on the cold side. The unit was sized based on data from previous saturated steam/water flooding tests by Cullum [6]. By using the effective superficial velocity of the steam during the saturated water flooding tests, the heat load for condensation to occur was estimated to be 64 kW. By assuming a domestic water flow rate of 22 GPM, the unit is designed to remove 107 kW of heat and can continually condense 400 lb/hr (or 50 g/sec) of steam. The condenser is made entirely of Type 316 stainless steel and is 5 inches long, 4 inches wide, and 12 inches tall. The steam condenser is shown before installation in Figure 3.10.

The first design of the steam condenser was a 1 inch NPT model, however this would result in a steam velocity of over 130 ft/sec inside the condenser. This was

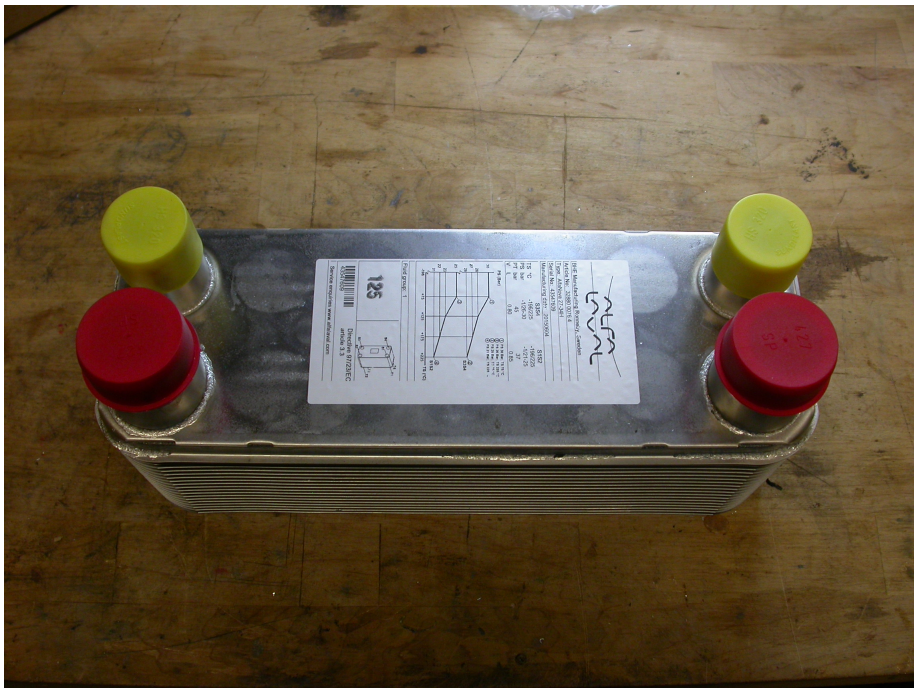

Figure 3.10: The AlfaNova 27-34H steam condenser shown before installation. The hot side ports are shown with red caps and the cold side with yellow caps for protection during shipment.

undesirable due to concerns of erosion of the thin stainless steel plates, high pressure drop, and high flow noise inside the condenser. The AlfaNova 27-34H steam condenser has 1.25 inch connections on the hot side and 0.75 inch connections on the cold side. This results in an acceptable steam velocity of 77 ft/sec. The unit is manufactured to be used as an oil cooler in European facilities, and the standard connections use British Standard Parallel Pipe (BSPP) threads. The parallel threads require a bonded seal ring to prevent leakage and four BSPP to weld-on adapters were installed. Standard NPT nipples were welded to the adapters using the TIG process. The condensate is drained to a blowdown drum through a 1.5 inch diameter two-wire steel braided hose rated for 450 °F and 250 psig. The hose is equipped with zinc plated steel boss threaded couplings with four-hole interlocking clamps on

each end. The cold side is supplied from the domestic water supply and has similar instrumentation and components as described in subsection 3.2.5.

3.5 Additional Facility Modifications

The additional piping that was installed throughout the facility was predominantly Type 304 stainless steel schedule 40 piping with a welded seam. The piping was purchased in 20 ft lengths and cut to size during the facility construction. The majority of the piping was threaded to national pipe threads using a Ridgid threading system. In some cases, butt weld fittings were used, especially near instruments that require a constant bore diameter such as the flow meters. The NPT connections were sealed with either thread seal tape, thread seal paste, or an anaerobic resin compound. The thread seal tape was a heavy duty grade laced with nickel to prevent galling of the stainless steel and has a density of 1.5 g/cm^3 and thickness of 0.005 inches. The anaerobic resin (Loctite 567) is a solvent free compound that fills the voids between threads and cures slowly to form a strong seal that resists the effects of temperature, pressure, and vibration. The cure time can be decreased with use of a primer (Loctite 7471) and joint disassembly is possible by using a heat gun.

The addition of several new components to the test section required the facility structure to be upgraded. The structure used in the past was composed of slotted channel strut, however this structure was not adequate to carry the additional load of the new heavy components, specifically the modified steam outlet, long elbow, separator, and associated piping. Secondly, the outlet vortex flow meter required several feet of straight length piping for proper operation and the test section needed to be relocated to allow all of the components to fit in the laboratory space. The test section was lowered from the structure and several modifications were made to reinforce the structure. Slotted hole channel strut (1.625 inch x 1.625 inch) was

used to create additional cross members, gussets, and braces while double back-to-back channel strut (3.25 inch x 1.625 inch) was used for additional posts. The double strut was also used for structural beams that would support heavy loading over long distances. All of the channel strut was attached using 0.5 inch diameter zinc plated bolts and spring nuts, while the base plates were anchored to the floor with 0.5 inch wedge anchors for added stability. The test section was installed in a new location and was leveled using a laser level and plumb bob. All of the facility piping was mounted to the structure using strut-mount clamps. An isolation material (Bline Vibra-cushion) was used to insulate the piping, inhibit galvanic corrosion, and dampen vibration to the facility.

The piping and components were insulated with at least 1.5 inch thick fiberglass insulation with an all surface jacketing to reduce heat loss and protect personnel from burns. PVC covers were used to insulate common pipe fittings such as elbows, tees, and flanges. Pipe markers indicating the fluid and flow direction were added to the outside of the jacketing for easy identification of piping. A computer monitor was mounted near the throttle valve so that the experimenter can monitor system parameters more conveniently in real time.

3.6 Instrumentation

The test facility has an array of instruments to measure several properties during each flooding test including temperature, pressure, flow, level, and relative humidity. A total of 27 temperatures, 4 absolute pressures, 3 gauge pressures, 4 differential pressures, 1 humidity, and 4 flow rates are recorded during each flooding test. The data are recorded with a data acquisition system manufactured by National Instruments. A LabVIEW user interface was created to display, interpret, and save the data for each test. The instrumentation is summarized in Appendix A and the lo-

cation of each instrument is shown in Figure 3.1. The instrumentation is described below.

3.6.1 Temperatures

All of the temperatures recorded during the flooding tests are measured using thermocouples. Two wires composed of dissimilar metals are joined at a junction inside the thermocouple and generate a voltage when heated due to the Seebeck effect. All the thermocouples used in the experiment are Type T, meaning the dissimilar metals are copper and constantan, and have a temperature range of -250 °C to 350 °C with an uncertainty of 0.5 °C. The thermocouples are the quick connect type and most have a 0.0625 inch diameter stainless steel sheath around the wires. All of the thermocouples are considered ungrounded at the junction and must be grounded inside the data acquisition terminal block. With exception to the thermocouples on the test section surface, all the thermocouples are mounted using CONAX PG series packing glands with viton sealants and 0.125 NPT connections. A shielded two wire (20 American Wire Gauge) insulated extension cable is attached to most of the thermocouples to provide noise immunity for the millivolt signals generated by the sensors.

There are 7 thin film thermocouples attached to the outside of the test section surface using a high temperature, thermally conductive epoxy. One thermocouple is inserted into the centerline of the test section using one of the top 0.125 inch NPT ports to measure the centerline temperature during flooding. This thermocouple has a reduced diameter of 0.020 inches for faster response time to capture transient data during flooding. All other thermocouples are inserted into the facility piping to measure temperatures of the process fluid. Four thermocouples are used to measure the steam generator axial temperatures, while 10 thermocouples are used inside the

water supply tank to monitor the thermal stratification during heatup. These 10 thermocouples are only monitored and not recorded in the data file. Locations of these thermocouples are described in [14]. Temperature measurements in the gas flow loop are taken at: the gas inlet vortex flow meter, the gas inlet right before injection into the test section, the two-phase outlet before the separator, the gas outlet vortex flow meter, the steam condenser inlet, and inside the blowdown drum. Temperature measurements in the water flow loop are taken at: the suppression pool outlet, the water supply pump suction, the water inlet magnetic flow meter, the water inlet before injection to the water inlet chamber, the water carryover magnetic flowmeter, and the heat exchanger inlet and outlet.

3.6.2 Pressure Measurements

Pressure is monitored throughout the facility by either pressure transmitters or local Bourdon gauges. The local gauges are typically not used for data collection, but are used for facility operation and maintenance. The pressure transmitters consist of a sensing element, typically a diaphragm, that flexes in response to changes in pressure from either the high or low port of the transmitter. The flexing is translated into a change in resistance due to piezoresistive technology unique to each transmitter and the output responds accordingly.

The absolute pressure is measured at the gas inlet vortex flowmeter, the gas outlet vortex flow meter, and inside the steam generator using the Honeywell ST3000 STA940 pressure transmitter. The transmitter is able to measure absolute pressures up to 500 psia, though the range is set from 0-130 psia for the gas inlet, 0-100 psia for the gas outlet, and 0-150 psia for the steam generator transmitter. These transmitters output a 4-20 mA signal and are able to be configured using the Honeywell Smart Field Communicator. Since the meter body temperature is limited to only 158 °F,

impulse lines made of 0.25 inch stainless steel tubing and Yor-Lok compression fittings were installed. The impulse lines were filled with deionized water and were not insulated to protect the meter body from high temperature steam. The wet impulse lines must be free of all trapped air to have accurate pressure measurements and must be purged with water occasionally. The meter body was intentionally installed on its side to allow any trapped air around the diaphragm to be easily purged. The gas outlet absolute pressure measurement is shown in Figure 3.11.

Figure 3.11: The gas outlet absolute pressure transmitter with impulse piping. The transmitter is shown in the foreground while the outlet vortex flow meter is shown in the background.

The absolute pressure of the test section is also measured using a new Keller Valueline High Accuracy pressure transmitter procured for this research. The Keller transmitter has a factory set pressure range from 0-150 psia with an accuracy of ± 0.1% full scale. The output of the transmitter is 4 to 20 mA and the transmitter is installed at the lower end of the test section through a 0.125 inch NPT port with impulse tubing. An absolute pressure transmitter was chosen for the test section to detect vacuum conditions that may be present during future steam/water flooding tests with high water subcooling.

Three of the differential pressure measurements use the Honeywell ST3000 STD924 pressure transmitter. These transmitters can measure a differential pressure from 0 to 400 inH2O and have a MAWP of 4500 psig. The range of the transmitters can be adjusted using the Honeywell Smart Field Communicator and the output is 4 to 20 mA. Two of the transmitters are used to determine the liquid level in the steam generator and the water supply tank. These transmitters use a compensating wet leg configuration with the high side of the transmitter measuring the top port.

The remaining Honeywell transmitter is used to measure the differential pressure across the test section. The impulse piping connects the low side of the transmitter to the bottom 0.125 inch NPT port on the test section, while the high side measures the pressure at the top port on the test section. This transmitter is the direct indicator to identify the presence of flooding inside the test section and is used to determine the time at which the onset of flooding occurs. The distance between the top and bottom port of the test section is 55.75 inches and this is the expected differential pressure reading when no gas or water is flowing through the test section. The transmitter was also rotated on its side during installation to facilitate air purging from the sensing element.

A Rosemount 3051 differential pressure transmitter was installed on the holdup

tank to measure liquid level. The transmitter has a pressure range from -25 to 25 inH2O, however the range was calibrated from 0-25 inH2O for this research. This transmitter is not adjustable with the smart field communicator and the range was set during calibration offsite. The impulse lines are connected in a compensated wet leg configuration described earlier and the high side of the transmitter measures the top port on the vessel.

Three gauge pressure transmitters produced by Dwyer (Model 673-7) are used to measure the pressure inside of the holdup tank, water supply tank, and at the water inlet to the test section. These transmitters are set to a fixed range of 0 to 100 psig and have an uncertainty of ± 0.25 % full scale from the factory.

3.6.3 Flow Meters

The inlet and outlet flow rate of each of the phases used during the flooding tests are recorded. The gas phase flow rates are recorded using two vortex flow meters while the water inlet and carryover are measured using two magnetic flow meters.

The vortex flow meters function by placing a blunt object (called the shedder bar) in the flow path to generate a stable array of vortices that are formed downstream of the shedder bar. These vortices are referred to as the Von Karman vortex street [8]. The number of vortices, or the shedding frequency, is proportional to the velocity of the fluid, and a piezoelectric sensor measures the frequency of the Von Karman vortex street. An illustration of the principle of operation is shown in Figure 3.12. Vortex meters are very accurate and do not require a need to compensate for fluid density when used for volumetric flow measurements. Thus, the air and steam flow rates are easily measured using the same flow meter with minimal adjustments.

The volumetric flow rate measured by the meter is

$$Q = \frac{f}{K} \tag{3.1}$$

where f is the vortex shedding frequency and K is the factor that describes the linearity between the fluid velocity, width of the shedding body, and cross sectional area of the meter bore. The factor K is determined at the factory for each meter manufactured. Under proper installation, the only instance that the factor K should be changed is when accounting for the thermal expansion of the meter body during high temperature operation, as this changes the cross sectional area of the meter. The mass flow measurements used during the research are then determined as

$$\dot{m} = \rho Q = \rho \frac{f}{K} \tag{3.2}$$

where ρ is the gas density determined by property tables from the pressure and temperature measurements close to the flow meter.

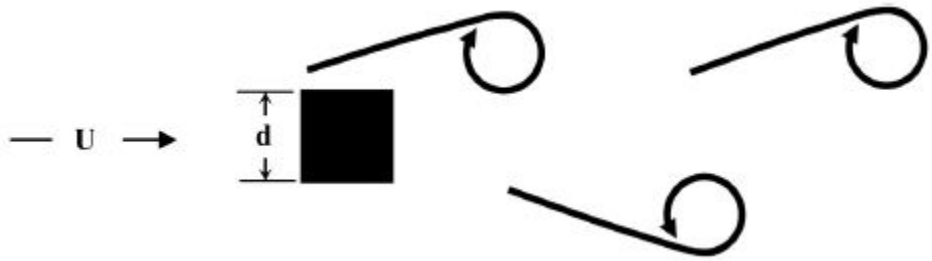

Figure 3.12: The Von Karman vortex street [8]. A fluid at velocity U impacting on a shedder bar of width d will generate vortices at a frequency f. The vortex frequency is linear for certain ranges of Reynold's numbers.

The gas inlet uses a Foxboro Model 83W-A with a bore size of 1.5 inch. The flow meter is a wafer design and has a stainless steel body. The output of the flow

meter is 4 to 20 mA and, as this is an older meter, all of the electronics are analog and require external corrections for the factor K when accounting for temperature. The gas outlet uses a new Foxboro Model 84F intelligent vortex flow meter with a bore size of 1.5 inch that was procured for this research. The meter body is flanged and is of stainless steel construction. The meter has an LCD display and local indicator to configure the flow meter for the fluid parameters to be used. The digital microprocessor incorporates the user defined input parameters to compute the corrections for the factor K internally. The output is a 4 to 20 mA signal based on volumetric flow rates.

Magnetic flow meters generate a magnetic field around a conductive liquid flowing inside the pipe. Following Faraday's Law, a voltage is generated in the conductive liquid as it passes through the magnetic field and the voltage is measured by two electrodes on the walls of the flow tube. The voltage generated is proportional to the velocity of the liquid, and the electronics inside the converter output a volumetric flow rate. Magnetic flow meters were chosen for this research due to the high accuracy for low flows and the small induced pressure drop. This is especially important for the water carryover measurement, as this is typically a small flow rate driven by the force of gravity. The minimum conductivity needed for measurement is 3 μmhos/cm, however since the facility does not have a resin bed to continually recycle the deionized water, there were not any measurement difficulties during the research.

The magnetic flow meters used on the water inlet and carryover are two identical units procured for this research. They are both Azbil (formerly Yamatake) MagneW 3000 Plus flow meters consisting of a 0.5 inch wafer style detector (Model MGG18) and remote converter (Model MGG14C). The remote converter was necessary since this feature allows a maximum operating temperature of the flow meter to be 160 °C. The maximum measurable flow rate is 28 GPM and the output is a 4 to 20 mA signal

[3].

3.6.4 Humidity

To fully define the density of the compressed air during the research, a hygrometer was procured and installed to measure the relative humidity of the incoming air. A Dwyer HHT humidity/temperature transmitter was used to measure the relative humidity of the inlet air to an accuracy of ± 2%. The sensor has a maximum temperature of 140 °F so the hygrometer was installed on a secondary air line using uninsulated 1 inch NPS piping to avoid high temperatures of the gas inlet piping during steam operation.

3.6.5 Data Acquisition System

The data acquisition system consists of hardware produced by National Instruments to read the data outputted from the sensors; the software, specifically LabVIEW, is used to interpret and save the data. With the exception to the LabVIEW virtual interface, the hardware portion of the experimental set up is largely based on the work by Solom [14]. The major components used in data acquisition will be described below.

The National Instruments SCXI system is used to collect the data and output to a Dell Precision personal computer through a NI PCIe-6341 card. The SCXI system consists of a SCXI-1000 chassis that houses four modules that filter and amplify the incoming signals. Only three modules are used for the current research and each module has a specific bandwidth for data collection. Therefore, data that were anticipated to be steady, e.g. the heat exchanger temperatures, were placed on the lowest bandwidth modules (SCXI-1102, 2 Hz bandwidth). Transient data, e.g. test section surface temperatures, are placed on the faster modules such as the SCXI-1102B and SCXI-1102C with bandwidths of 200 Hz and 10 kHz respectively. The

physical cables for each instrument are connected into SCXI-1303 terminal blocks which can accept up to 32 channels each and direct the signals to the SCXI-1102 modules.

The SCXI system is only able to measure voltages, not current signals. A converter box was created by Solom that accepts the signals from the instruments with 4-20 mA analog outputs and places a 249 Ω precision resistor in the current loop [14]. The voltage across the resistor is measured and a 1-5 V signal is sampled by the SCXI system. The 4 to 20 mA instruments require a DC voltage to drive the current circuit, and a power supply is set to a constant output of 24.0 VDC. The hardware of the DAQ is shown in Figure 3.13.

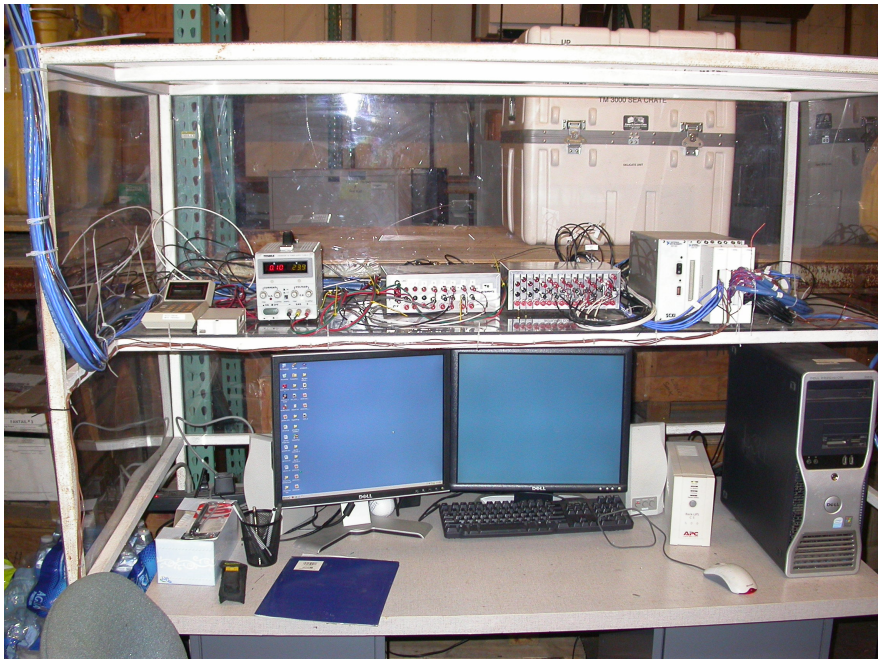

Figure 3.13: The data acquisition system. The data acquisition system consists of the LabVIEW software, the Dell personal computer, the SCXI chassis, the converter box, and the DC power supply [14].

A LabVIEW virtual interface was created to save and interpret the raw voltages read by the SCXI system. The foundation of the interface was based on work from previous researchers in the Nuclear Heat Transfer Systems Laboratory, specifically in terms of data logging. The raw voltages are averaged and the mean and standard deviation of each signal are recorded. The thermocouple voltages are directly converted to temperatures using DAQmx in LabVIEW. All other instrument voltages are first normalized from 0 to 1.0. Then, the upper/lower range values are applied to output the data into known quantities (such as psia, GPM, inH2O, etc.). When computing densities or displaying liquid levels, unit conversions and formulae are computed. The final values for each instrument are saved to a .dat file. The data are sampled at 200 Hz and every 20 samples collected are averaged to a single data point that is recorded. Therefore, the data are recorded to the file at a rate of 10 Hz. The LabVIEW virtual interface is shown in Figure 3.14.

3.6.6 Calibrations

All of the instruments used for data collection were verified to be operating as expected by either a channel check or a channel calibration. A channel check is a qualitative verification of acceptable performance of a channel (including sensor, line, and DAQ output) with comparison to other independent channels measuring the same variable. A channel calibration is an adjustment of the channel such that the output is within acceptable accuracy to a known value.

The thermocouples were verified using a channel check as they are not able to be calibrated; thermocouples that did not have acceptable outputs were replaced with equivalent sensors. The new equipment that was procured was assumed to be properly calibrated at the factory and calibration profiles were obtained from the vendor when possible. The Honeywell and Rosemount pressure transmitters

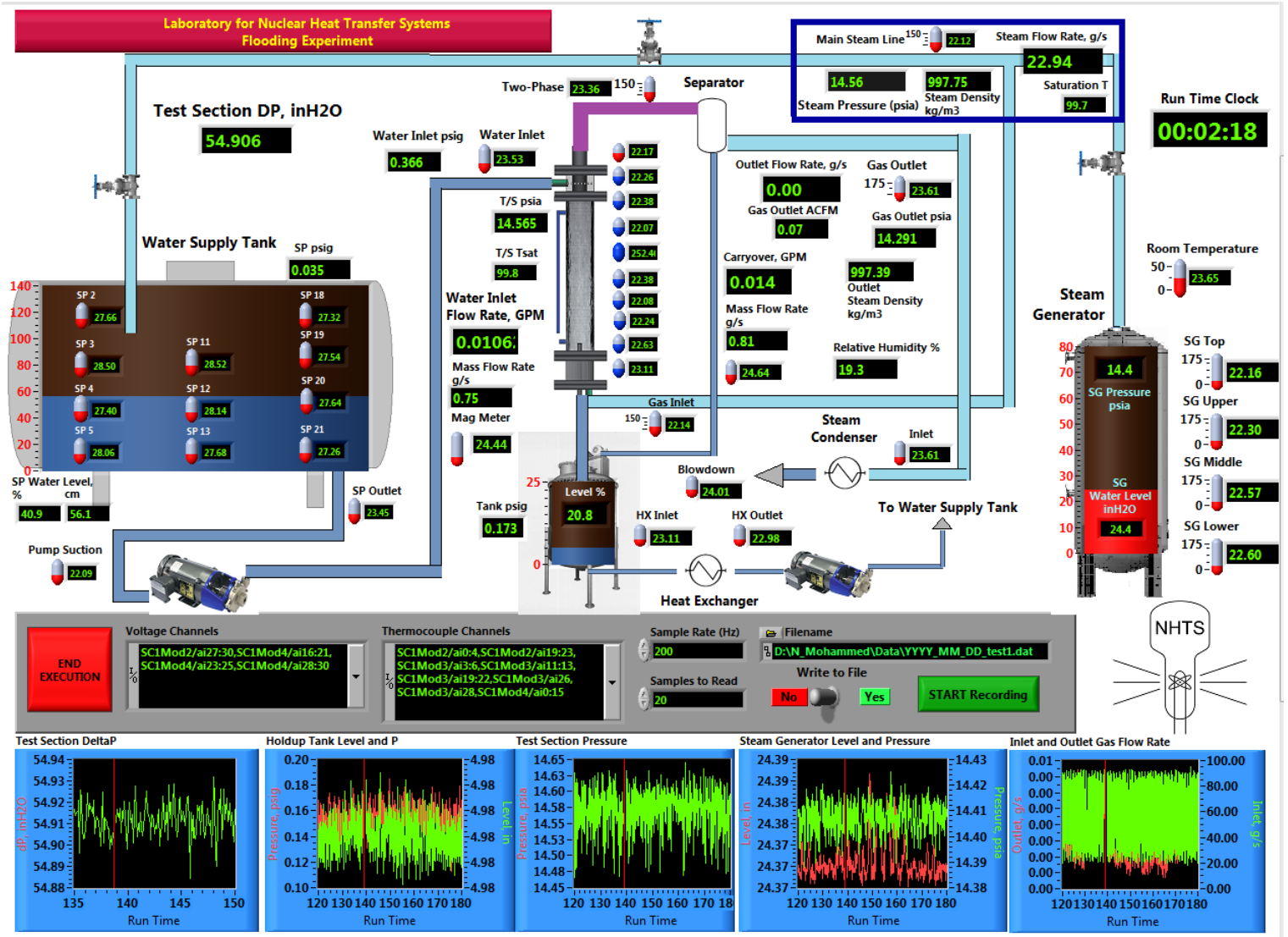

Figure 3.14: Data acquisition user interface created in LabVIEW.

were either verified to have a recent calibration or were sent to an offsite facility in Houston to be properly calibrated. The inlet vortex flow meter was recently calibrated using the procedures outlined in the user manual and was also channel checked with the outlet vortex flow meter. The Dwyer pressure transmitters are not able to be adjusted for calibration, but were channel checked and deemed acceptable since they are primarily used as monitors during facility operation.

The 4-20 mA instruments use a two-point calibration to ensure that the signal from the sensor corresponds to 0% and 100% in the DAQ. First, the sensor output is set to 0% with either a local configurator or the smart field communicator. A LabVIEW virtual interface reads the output and records the average of this signal for a minimum of 100 seconds. This process is repeated for 100% output and a calibration profile is created assuming that the output is linear. The profile is saved and is incorporated with the instrument range to determine the upper and lower range values.

4. OPERATING PROCEDURES

After incorporating the major modifications, the flooding facility is now more complex than it has ever been. The use of pressurized vessels and high fluid temperatures require safety to be the primary focus on the facility design and operation. Operating procedures were developed to ensure the safety of the experimenter, to protect equipment from damage, and to maintain consistency during data collection. The procedures for operating the systems and subsystems for the flooding facility for data collection are listed below. The sections are chronologically ordered in terms of a daily startup. All valves that are referenced in the operating procedures are highlighted in Figure 4.1 and are physically labeled with valve tags on the facility. Minor deviations from the routine operating procedures may be approved however routine deviations must require procedure amendment and lab supervisor approval.

4.1 Data Acquisition System

The data acquistion system is used to monitor system performance and should be operating during facility startup. It is not mandatory to record the data to file during startup, however it is imperative that the record function be utilized properly during data collection.

1. Startup and/or login to the data acquisition computer. The username is "vierowlab" and password "Riverside3pc".

2. Power ON the remote computer monitor near the throttle valve.

3. Open $D:\backslash N\_Mohammed\backslash SteamFlooding\_Version3.vi$ for steam/water flooding operation.

   Open $D:\backslash N\_Mohammed\backslash AirFlooding\_Version2.vi$ for air/water flooding

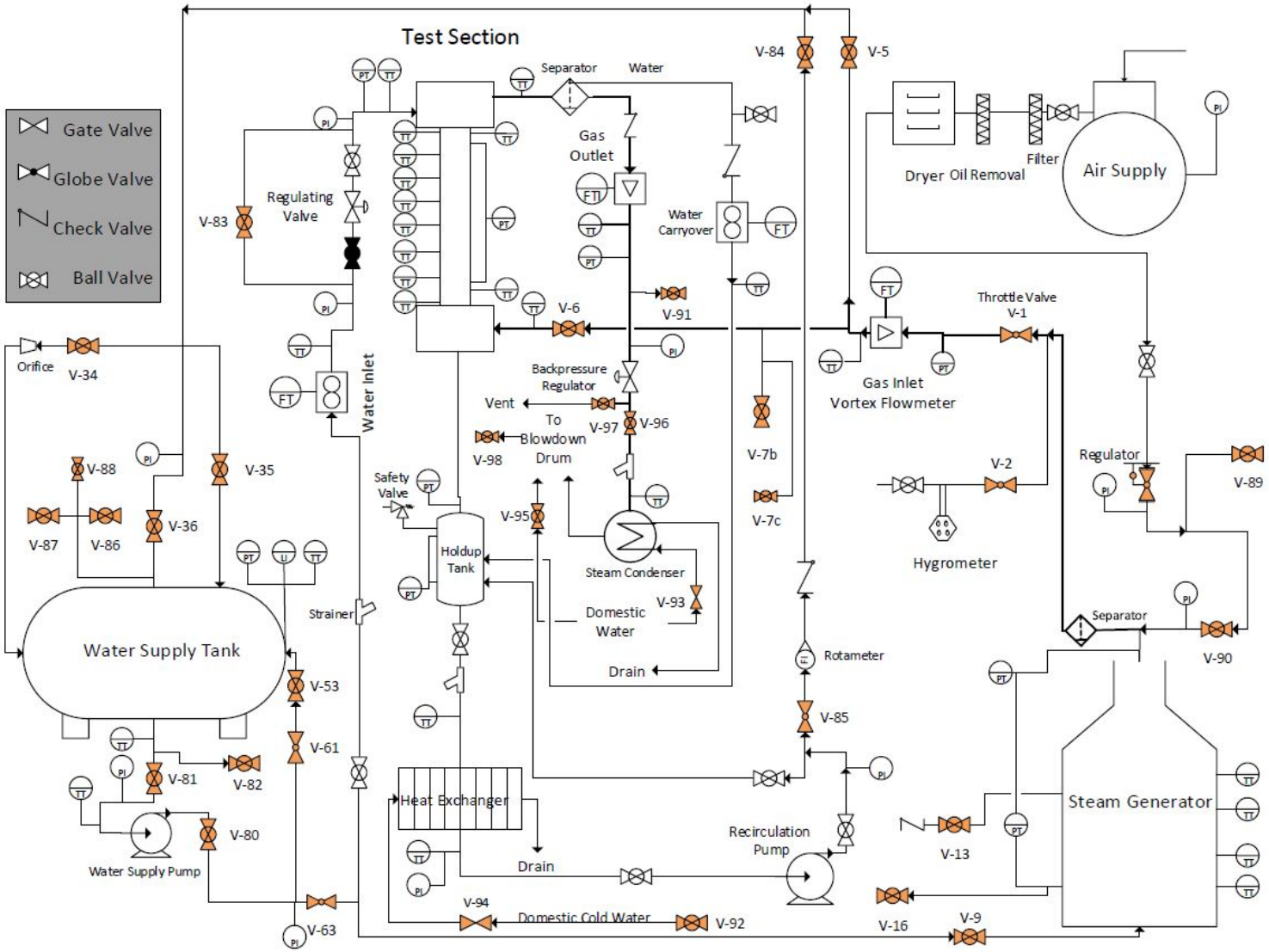

Figure 4.1: Piping and instrumentation diagram of facility for operation. The valves to be routinely used during data collection are highlighted in orange.

operation.

4. Turn ON the DC power supply. The output should be set to 24.0 V.

5. Turn ON the National Instruments SCXI chassis.

6. Acquire data by selecting the "Run" button in LabVIEW.

7. Verify all instruments are reporting expected values. Corrective action should be taken for instruments that are not operable.

    - The test section differential pressure readings may drift due to evaporation of water from the impulse tubing from exposure to steam. The transmitter should output 55.75 inH2O ±5% during no flow of gas or water. If the output is outside this range, refer to Section 4.2 to purge the impulse tubing.

    - Verify the outlet gas vortex flow meter is set for the appropriate gas to be measured. The gas density, temperature, and viscosity must be changed locally in the meter fluid parameters when using air versus steam. These parameters are used for the internal correction for the factor K. Enter the appropriate fluid parameters or pick an average value in the testing range. Refer to the user manual for details in setting the fluid parameters.

8. Input the desired filename for the data to be recorded. An example filename is "YYYY_MM_DD_TestXX.dat".

9. Turn the Write Data toggle switch on the LabVIEW front panel to YES.

10. Select the "START" button on the LabVIEW front panel to begin writing data to file.

11. Select the large "End Execution" button on the front panel to end data recording. The program will automatically stop acquiring all data.

12. Repeat steps 4-10 for each subsequent test.

13. Power OFF the remote computer monitor near the throttle valve after facility shutdown. No extension cords should be energized when not in use.

4.2 Purging Differential Pressure Transmitters

The following procedure can be used to purge the impulse tubing on the differential pressure transmitters. Caution should be used in this procedure to maintain the calibration or prevent damage to the transmitter diaphragm. Refer to Figure 4.2 for valve descriptions.

1. Fill the pump-up sprayer with deionized water.

    - Pump up to a reasonable pressure. Overpressurizing will lift the relief valve. Pump up as necessary during this procedure to repressurize.
    - The fill valve in Figure 4.2 is on the sprayer hose. Close the fill valve. Then detach the wand at the compression fitting after the fill valve.
    - Attach the compression fitting to the impulse tubing near the isolation valve.

2. Close the high side valve.

3. Verify the equalization valve is closed.

4. Verify the low side valve is open.

5. Open the isolation valve.

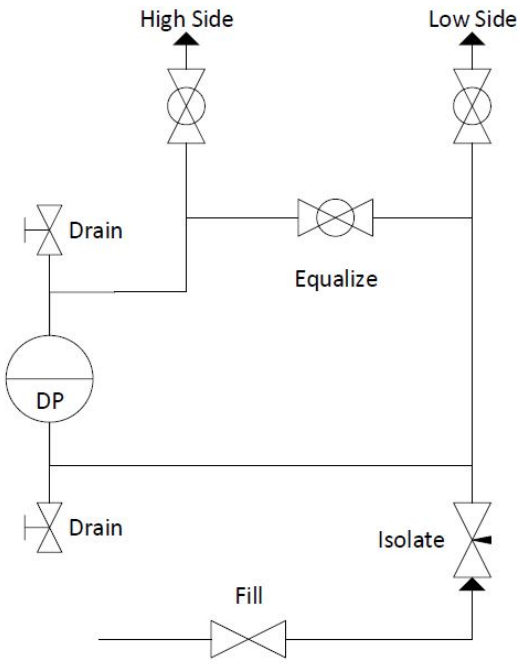

Figure 4.2: Typical impulse tubing and valve arrangement for the differential pressure transmitters.

6. Open the fill valve to allow water to purge any air out of the low side tubing. You should hear water traveling through the low side measuring port.

7. Open the low side drain. Do not let the transmitter electronics get wet.

8. Close the low side drain when a continuous stream of water (no air bubbles) is exiting the drain.

9. Close the fill valve.

10. Close the low side valve.

11. Open the high side valve.

12. Open the equalizing valve.

13. Open the fill valve to allow water to purge any air out of the high side tubing. You should hear water traveling through the high side port.

14. Open the high side drain. Do not let the transmitter electronics get wet.

15. Close the high side drain when a continuous stream of water (no air bubbles) is exiting the drain.

16. Close the fill valve.

17. Close the equalizing valve.

18. Open the low side valve.

19. Close the isolation valve.

20. Verify the transmitter output is reading correctly. If not, repeat steps 1-19.

21. Disconnect the compression fitting from the transmitter impulse tubing.

4.3 Operating the Air Supply for Air/Water Flooding Tests

The air compressor is used to supply a large amount of compressed air to the test section. The steam generator should be adequately drained of most water to act as a receiver tank for the compressed air. Refer to Section 4.5 for procedures to drain the steam generator of water. The air compressor tank and steam generator should slowly pressurize together during the pump up time.

1. Turn the refrigerated dryer power switch to ON at least 5 minutes before air compressor startup. This ensures the compressed air piping is free of condensate.

    - The dryer must be switched ON while the air compressor is operating.

- The condensate filter of the auto drain must be inspected and/or cleaned once a month. For periods of heavy use, double the maintenance frequency.
- The condenser fins must be inspected and/or cleaned once every two months. For periods of heavy use, double the maintenance frequency.
- Refer to the dryer user manual for maintenance procedures.

2. Inspect the air compressor. Verify the compressor is in good working order and that all rotating components are free from obstructions. All guards and shields should be in place. Check that the fasteners are tight with exception to the mounting anchors on the feet. Visually inspect the wiring to be in good condition. Ensure the regular scheduled maintenance, as described in the user manual [5], has been completed.

3. Check the lubricant level in the crankcase. The lubricant level must register between the high and low marks on the dipstick.

    - If lubricant is low or contaminated, drain and replace. Refer to the user manual for replacement oil viscosity and capacity.
    - The lubricant must be replaced after the first 100 hours of operation. Subsequent lubricants should then be changed after 500 hours of operation [5].

4. Visually inspect the drive belt. The belt should be free of cracks, frays, or tears.

    - The belt tension must be checked after every 160 hours of operation. A belt tension gauge was procured for this purpose.

5. Plug in the electronic drain valve to drain condensate from the air compressor tank.

6. Verify the isolation valves leading to the pressure regulator are OPEN.

7. Close the air hose valve (V-89).

8. Open the steam generator air isolation valve (V-90).

9. Verify throttle valve (V-1) is closed.

10. Verify the steam generator vent (V-16) is closed.

11. Turn the 30A breaker in the 480 VAC electrical panel to ON to start compressor.

12. Ensure the air supply regulator is set to 110 psig or less. The steam generator must not be pressurized above 135 psig.

13. Monitor the steam generator pressure and the air compressor tank pressure during the pump up.

    - The air compressor will turn OFF automatically when the compressor tank reaches 175 psig.
    - It is normal to hear air leaking or hissing out of the air compressor pressure switch shortly after automatic shutdown. This is due to air exiting the unloader valve and the venting will stop after 3-5 minutes.
    - The electronic drain valve will automatically vent the condensate to outside the lab every 45 minutes.

14. The air supply system is now ready for use.

4.4 Filling the Steam Generator

Before using the steam generator for steam production, the water level inside the vessel must be adequate to ensure all of the immersion heaters are covered with water. The reed switch will automatically open the heater circuits if the water level decreases below 35-40 cm on the magnetic liquid level indicator. It is not desirable to run out of steam during the flooding tests, so this procedure should be performed whenever the water level is less than 48 cm on the level indicator. The steam generator can be filled directly from the water supply tank, and does not necessarily have to be depressurized or powered off during the fill. That is, it is possible to continuously fill the steam generator with the heaters powered on, provided that the liquid level is above the automatic trip setpoint. The procedures below can be used to fill the steam generator for all ranges of pressure.

1. Verify the steam generator pressure is below 90 psia. This ensures the vessel pressure is low enough to prevent the RCIC pump from dead-heading.

    - To lower the steam generator pressure, either decrease the heater power or open the steam generator vent valve (V-16) to vent to outside the lab . Ensure no personnel are near the steam vent exhaust point before venting the steam to outside.

2. Close the supply pump discharge valve (V-80).

3. Open the RCIC pump suction valve (V-82).

4. Open V-53.

5. Open the bypass valve (V-61).

6. Crack the flow control valve slightly open (V-63). This ensures that a large amount of potentially cold water does not suddenly inject into the hot steam generator, and also reduces water hammer in the piping.

7. Turn ON the RCIC pump fan to highest setting.

8. Turn the RCIC pump switch to ON.

9. Open the steam generator fill valve (V-9).

10. Observe the water injection fill rate on the Yamatake magnetic flowmeter used for the RCIC experiment. The flowmeter upper range value is set to 5.75 GPM. Flow capacities above this range will cause the meter to show offscale high. A fill flow rate of 1.2 GPM will maintain a constant water level in the steam generator when operating at full power.

11. Ensure the water inlet temperature to the RCIC pump is below the thermal limits. Avoid cavitation or excessive pump whining.

12. Verify the steam generator water level is increasing in LabVIEW and on the magnetic liquid level indicator. The orange level marker inside the sight glass of the liquid level indicator may need to be adjusted so that it is always in contact with the magnetic float.

13. Fill the steam generator to 58-60 cm on the liquid level indicator.

14. Close the steam generator fill valve (V-9).

15. Turn the RCIC pump switch to OFF.

16. Turn OFF the RCIC pump fan.

4.5 Draining the Steam Generator

The steam generator must be drained of water to allow more compressed air to be stored during the air/water flooding tests. The goal is to pressurize the steam generator with compressed air to drive the liquid out of the vessel and back to the water supply tank. The water will travel in reverse flow through the fill piping to the water supply tank. This procedure will not drain 100% of the water from the steam generator due to the axial location of the fill penetration, however most of the water will be evacuated. The procedures are described below.

1. Close the water supply pump discharge valve (V-80).
2. Close the RCIC pump suction valve (V-82).
3. Open the water flow control valve (V-63) to 100%.
4. Open the bypass valve (V-61).
5. Open V-53.
6. Complete the procedures in Section 4.3.
7. Slowly open the steam generator fill valve (V-9). Water will begin to reverse flow back to the water supply tank.
8. Verify the steam generator water level is decreasing.
9. Close V-9 when air is audibly heard to be exiting the steam generator.
10. Shutdown the air supply and depressurize the steam generator if necessary.

4.6 Steam Generator Operation

The steam generator is used to create steam for two purposes during the flooding tests. First, steam is used to heatup the water supply to saturated temperatures before the flooding tests begin. Secondly, the steam generator supplies steam to the test section during the approach to the onset of flooding. The procedures for steam generator operation from cold shutdown to heatup are described below.

1. Verify that a second person is present in the laboratory for steam generator operation. Operation of the steam generator is not allowed unless this criterion is met.

2. Verify the steam generator water level is above 48 cm, otherwise fill the steam generator. Refer to Section 4.4.

3. Close the steam generator air isolation valve (V-89).

4. Close valve V-2 TIGHTLY.

5. Close the throttle valve (V-1).

6. Close the vacuum breaker valve (V-13).

7. Close the 200 A breaker in the 480 VAC panel for the steam generator heater circuits.

8. Unlock the padlock from the heater power switch. Turn the heater power switch to ON.

9. Power on the appropriate amount of heaters to the desired power level.

10. Vent the noncondensable gases from the steam generator when the vessel pressure is 30 psia.

- Open the steam generator vent valve (V-16) for 20 seconds. Close when steam is verified to be exiting to outside.

11. Verify the steam generator axial thermocouples are all reading the saturated water temperature for the corresponding vessel pressure. Otherwise, repeat step 10.

12. Monitor steam generator heatup. Do not let vessel pressure exceed 130 psia.

13. When the desired vessel pressure is reached, power OFF all heaters.

14. The steam generator is now ready for use.

4.7 Water Supply Heatup For Saturated Steam/Water Testing

Before the saturated steam/water flooding tests can be performed, the large volume of water inside the water supply tank must be heated to near saturated conditions. Steam from the steam generator is injected directly below the water line in the supply tank to heat up the water to the desired saturation temperature for the flooding tests. The water supply tank pressure must be maintained high enough to prevent boiling inside the vessel and also to avoid cavitation in the water supply pump. The tank pressure is typically maintained to 5 psi greater than the desired test section pressure at flooding. The steam generator delivers steam to the water supply tank in a common pipeline that is also used for the recirculation water flow loop during the flooding tests. The common piping must be purged with air to vent all of the water out before any steam is injected in this line. This is to prevent issues associated with water hammer. The water supply heatup procedure is detailed below.

4.7.1 Purging of Water from the Common Pipeline with Air

1. Close the throttle valve (V-1).
2. Verify V-5 is closed.
3. Close the RCIC sparger valve (V-34).
4. Verify the SRV sparger valve (V-36) is closed.
5. Open the air space sparger valve (V-35).
6. Drain any condensate from steam trap #1.
    - Close the test section gas inlet valve (V-6).
    - Open V7b to drain condensate into a partially filled bucket of water.
    - Close V7b when finished.
7. Connect the 0.25 inch air hose from the quick connect air taps to the air purge coupling.
8. Slowly open the air purge valve (V-7c). Crack to 50% with 50 psig of compressed air.
9. Slowly open V-5 to purge water from common pipeline.
10. Close the air purge valve (V-7c) when the water supply tank pressure increases by 0.5 psi or more.
11. Close the recirculation valve (V-84).

4.7.2 Water Supply Heatup

1. Verify the common pipeline has been purged with air and is free of water. Refer to subsection 4.7.1.

2. Startup the steam generator. Refer to Section 4.6.

3. Verify V-5 is open and V-6 is closed.

4. Verify the air space sparger valve (V-35) is open.

5. Open the SRV sparger valve (V-36).

6. If this is the first heatup cycle for the day, and the water supply tank pressure is close to ambient pressure, then open the suppression pool vent (V-86). Otherwise, close (V-86).

7. Crack the throttle valve to allow 7-10 g/sec of steam to flow from the steam generator to the water supply tank.

8. If the facility piping is cold, drain the collected condensate during heatup from steam trap #1 by opening and closing valve V-7b.

9. Close the air space sparger valve (V-35) when the suppression pool pressure begins to increase. The air space temperatures will also be increasing which indicates that steam is entering the water supply tank air space.

10. Increase the steam flow using the throttle valve (V-1).

    - The steam generator power is typically set to 157 kW during water supply heatup.
    - Maintain the steam generator pressure to around 80 psia.

- Fill the steam generator when the water level is below 48 cm on the sight glass. See Section 4.4.

11. If the water supply tank requires to be pressurized and is not already at this point, close the suppression pool vent (V-86) when the bulk water temperature is 94 °C. This will allow the water supply tank to naturally pressurize as energy is continually added to the water by the steam.

12. Heat the water to the desired saturation temperature.

13. Close the throttle valve (V-1) when the desired saturation temperature has been reached.

14. Turn the steam generator heater power switch to OFF.

15. Adjust the water supply tank pressure if necessary.

    - Vent steam through the CASHCO back pressure regulator that is attached to the water supply tank air space to lower the water supply tank pressure.
    - Fill the water supply tank with compressed air to increase the pressure. Refer to Section 4.8 for details on pressurizing the water supply tank with air.

4.7.3 Purging of Steam from the Common Pipeline with Air

1. Verify the throttle valve (V-1) is closed.
2. Close V-5.
3. Verify the RCIC sparger valve (V-34) is closed.
4. Close the SRV sparger valve (V-36).
5. Open the air space sparger valve (V-35).
6. Verify the test section gas inlet valve (V-6) is closed.
7. Drain any condensate from steam trap#1.
    - Open V7b to drain any condensate into a partially filled bucket of water.
    - Close V7b when finished.
8. Connect the 0.25 inch air hose from the quick connect air taps to the air purge coupling.
9. Slowly open the air purge valve (V-7c). Crack to 50% with 50 psig of compressed air.
10. Slowly crack V-5 to purge steam from common pipeline.
11. Close V-5 when the water supply tank pressure increases by 0.5 psi or more.
12. Close the air purge valve (V-7c).
13. Open V-7b to vent the compressed air from the steam line. Close V-7b when finished.

4.8 Setting System Pressure

Before the water supply pump and the recirculation pump can be turned on, the system pressure must be set. This means that the water supply tank must be pressurized to the desired system pressure and the back pressure regulator must be adjusted to allow the set pressure to equal the desired system pressure. This ensures large pressure differentials between closed vessels are avoided and results in steady system parameters during the flooding tests.

4.8.1 Setting the Test Section Pressure for Air/Water Flooding

1. Review the desired system pressure for the flooding test.
2. Set the air inlet and outlet flow paths.
    - Close V-5.
    - Open the test section gas inlet valve V-6.
    - Close steam trap#1 (V-7b).
    - Close the air purge valve (V-7c).
    - Close steam trap #2 (V-91).
    - Close the steam condenser isolation valve (V-96).
    - Open the air vent (V-97).
    - Route the 2 inch ID SBR nylon braided hose to outside to release the vented air to atmosphere.
3. Inject air into the test section at a flow rate close to a predicted flooding velocity by using the throttle valve (V-1).

4. Adjust the back pressure regulator set pressure by turning the adjusting screw with a 0.5 inch combination wrench. Turning the screw clockwise (when viewed from above) increases the set pressure, while turning counter-clockwise decreases the set pressure. Continue to adjust the regulator until the test section pressure is equal to the desired system pressure.

    - If the desired system pressure is atmospheric pressure, turn the adjusting screw counter-clockwise until the screw is no longer in contact with the spring. The change in torque required to turn the screw will indicate the loss of contact. Verify the test section pressure is approximately 3 psig.

5. Close the throttle valve (V-1).

4.8.2 Setting the Test Section Pressure for Steam/Water Flooding

1. Review the desired system pressure for the flooding test.

2. Set the steam inlet and outlet flow paths.

    - Close V-5.
    - Open the test section gas inlet valve V-6.
    - Open steam trap#1 (V-7b).
    - Close the air purge valve (V-7c).
    - Open steam trap #2 (V-91).
    - Open the steam condenser isolation valve (V-96).
    - Close the air vent (V-97).

3. Heatup system piping.

- Slowly crack the throttle to allow 10-15 g/sec of steam flow to the test section.
- Close steam trap #1 (V-7b) when steam exits the trap.
- Open the steam condenser isolation valve (V-96) when steam exits steam trap #2.
- Using a heat-resistant glove, close steam trap #2 (V-91).

4. Inject steam into the test section at a flow rate close to a predicted flooding velocity by using the throttle valve (V-1).

5. Adjust the back pressure regulator set pressure by turning the adjusting screw with a 0.5 inch combination wrench. Turning the screw clockwise (when viewed from above) increases the set pressure, while turning counter-clockwise decreases the set pressure. Continue to adjust the regulator until the test section pressure is equal to the desired system pressure.

    - If the desired system pressure is atmospheric pressure, turn the adjusting screw counter-clockwise until the screw is no longer in contact with the spring. The change in torque required to turn the screw will indicate the loss of contact. Verify the test section pressure is approximately 3 psig.

6. Close the throttle valve (V-1).

4.8.3 Setting the Water Supply Tank Pressure

1. Pressurize the water supply tank to the desired system pressure with air. Omit this step for testing at atmospheric pressure.

2. Close the water inlet valve (V-83).

3. Connect the 0.75 inch ID air hose from the quick connect air tap near the air supply regulator to the water supply tank.

4. Close the 0.75 inch air hose vent valve (V-88).

5. Close the suppression pool vent (V-86).

6. Open the suppression pool air space fill valve (V-87).

7. Slowly crack open the 0.75 inch air hose fill valve (V-89).

8. Close the 0.75 inch air hose fill valve (V-89) when the water supply tank is at the desired system pressure.

9. Close the suppression pool air space fill valve (V-87).

10. Vent the compressed air that is trapped in the air hose by opening the 0.75 inch air hose vent valve (V-88). This is very important, since the crow's foot connectors on the air hose do not have an internal valve. Therefore, any time that this air hose has to be disconnected, the experimenter MUST vent the compressed air from inside the hose or else injury may occur. Close V-88 when the venting is completed.

11. Disconnect the hose from the water supply tank.

4.9 Water Supply Pump Operation

The water supply pump sends water to the test section to form the annular film. Procedures for operating this pump during steam/water and air/water flooding tests are the same and are described below.

1. For saturated steam/water tests, ensure that the water supply tank is pressurized to 5 psi greater than the desired test section pressure during flooding. This ensures that the water supply pump will not cavitate during operation.
2. Open the water supply pump suction valve (V-81).
3. Close the RCIC pump suction valve (V-82).
4. Open the water supply pump discharge valve (V-80).
5. Open V-53.
6. Slowly open the water inlet valve (V-83).
7. Turn the switch for the water supply pump ON.
8. Regulate the flow to the desired flow rate using the flow control valve (V-63) and the bypass valve (V-61).

4.10 Recirculation Pump Operation

The recirculation pump returns water from the holdup tank to the water supply tank and ensures that the holdup tank never overfills into the test section. Depending on the inlet water flow rate, the recirculation pump does not necessarily need to be operating during the flooding test itself, as long as the holdup tank water level is acceptable. During the saturated steam/water flooding tests, it is necessary to run the heat exchanger to avoid cavitation in the recirculation pump. The recirculation pump discharges the water through a common pipeline that is also used for steam use during the pool heatup procedures for the steam/water testing. The common piping must be purged with air to avoid water hammer when alternating between pool heatup operation and recirculation use.

1. Verify that the common piping has been purged with air and is free of steam. Refer to subsection 4.7.3 for procedures to purge the common piping.
2. Open the recirculation water valve (V-84).
3. Verify V-5 is closed.
4. Close the air space sparger valve (V-35).
5. Close the SRV sparger valve (V-36).
6. Open the RCIC sparger valve (V-34).
7. Turn the recirculation pump switch to ON.
8. Monitor the return water flow rate on the rotameter. Use the recirculation throttle (V-85) to regulate flow.

9. Ensure that the heat exchanger outlet temperature is within the thermal limits of the pump. If not, or if cavitation is present, proceed to turn on the heat exchanger to cool the water to sufficient levels.

10. Turn on the heat exchanger if necessary.

    - Verify the water fill line from the blowdown drum is connected to the auxiliary domestic water supply.
    - Open the auxiliary domestic water valve (V-95). This is to relieve the water hammer effects on the PVC piping.
    - Slowly open the domestic water supply valve (V-92).
    - Slowly close the auxiliary domestic water valve (V-95) when water is observed to be discharging into the blowdown drum.
    - Open the heat exchanger domestic water supply valve (V-94). Use the rotameter to monitor the amount of domestic water supplied to the heat exchanger to regulate the cooling capacity. Full capacity for the domestic water is about 20 GPM. Do not let the heat exchanger domestic water drain piping get too hot, as the schedule 80 PVC is rated for 140 °F.
    - Secure the heat exchanger when cooling is no longer needed.

11. Ensure that the holdup tank level does not fall below 5%. If neglected, air can become trapped in the pump suction piping and lead to air lock.

4.11 Flooding Procedures for Data Collection

The procedures for collecting data for steam/water and air/water flooding are described below. Minor deviations particular for each gas are explicitly stated.

1. Turn ON data acquisition system. See Section 4.1.

2. Collect baseline data with no steam or water flow at the beginning of each day. This data file could be helpful in troubleshooting instrumentation if testing abnormalities are observed during data analysis.

3. Determine the type of flooding test for the day.

   - Select either steam/water operation or air/water operation.
   - Select the desired system pressure.
   - Select the desired water inlet flow rate to begin testing.

4. Configure the steam generator for flooding tests.

   - For air/water testing, refer to Section 4.3.
   - For steam/water testing, refer to Section 4.6.

5. Verify the steam generator is at the correct pressure.

   - For steam/water testing, ensure the steam inside the steam generator has the desired enthalpy content. Use the heaters to adjust accordingly, see Section 4.6 for procedures to operate the steam generator.

6. In the air/water flooding tests, purge the hygrometer by opening valve V-2 to measure the humidity content of the air. This valve may be left cracked open during the air/water tests for a delayed real time measurement. However,

experience has shown that the humidity content of the air is relatively constant for each day and occasional measurements every few tests should be adequate.

- Valve V-2 should be TIGHTLY closed at all times during steam/water flooding tests.
- Verify the hygrometer temperature (on the local display) is below 140 °F during steam generator operation.

7. For steam/water flooding tests, turn ON the steam condenser.
   - Verify the domestic water supply is ON to the steam condenser. If not, refer to the heat exchanger ON procedures in Section 4.10.
   - Open the steam condenser domestic water supply valve (V-93). Use the rotameter to monitor the amount of domestic water supplied to the steam condenser to regulate the cooling capacity. Full capacity for the domestic water to the condenser is about 22 GPM. Do not let the steam condenser domestic water drain piping get too hot, as the schedule 80 PVC is rated for 140 °F.
   - Secure the steam condenser when cooling is no longer needed.
8. Set the system pressure. Refer to Section 4.8.
9. Turn ON the water supply pump. Refer to Section 4.9.
10. Turn ON the recirculation pump if necessary. Refer to Section 4.10.
11. Use the flow control valve (V-63) and the bypass valve (V-61) to obtain a water flow rate of at least 8 GPM into the test section. This flow rate ensures the annular film is properly formed inside the test section.

12. Use the flow control valve (V-63) and the bypass valve (V-61) to set the desired water flow rate to the test section.

13. Verify the desired inlet water flow rate and temperature to the test section.

14. Begin data collection. See Section 4.1.

15. Slowly open the throttle valve (V-1) to increase the gas flow rate in small increments until the onset of flooding occurs.

    - The onset of flooding is marked by a rapid decrease in the test section differential pressure.
    - Do not open the throttle valve any further after the onset of flooding is achieved.
    - Monitor system parameters to ensure the system is flooding. The water carryover flow rate will increase roughly 5 seconds after the onset of flooding. The gas outlet flow rate will oscillate during flooding.

16. Record data for 20-30 seconds during the onset of flooding. Afterwards, close the throttle valve (V-1) to stop flooding.

17. Stop data collection when the test section differential pressure and gas outlet flow rate stabilize.

18. Prepare the system for the next test, or shut down the facility.

4.12 Facility Shutdown

After testing is complete, it is not permissible to leave the laboratory if any vessels are pressurized or if any major heat source is present. Therefore, all vessels must be depressurized and the water supply must be subcooled liquid at atmospheric pressure. All pumps, heaters, and compressors are turned off and the steam generator is allowed to vent and cool down.

1. Turn the 30 A breaker in the 480 VAC electrical panel to OFF to stop the air compressor.

2. Turn the refrigerated dryer power switch to OFF at least 5 minutes after air compressor is turned off. This ensures the compressed air piping is free of condensate.

3. Unplug the electronic drain valve.

4. Shutdown the steam generator.

    - Turn OFF power to all heaters.
    - Turn the heater power switch to OFF. Lockout the switch using the padlock.
    - Open the 200 A breaker in the 480 VAC electrical panel for the heater circuits.
    - Open the steam generator vent valve (V-16) to blowdown the steam generator. Vent the vessel until the steam generator thermocouples all read below 100 °C.
    - Blowdown the air compressor tank to outside through the steam generator.
    - Blowdown the test section to outside through the steam generator.

- Close V-16 when blowdown is complete.
- Open the vacuum breaker valve (V-13).

5. Close the RCIC sparger valve (V-34).
6. Open the air space valve (V-35).
7. Operate the water supply pump and recirculation pump until the bulk water supply temperatures are below 100 °C.
    - Discharge the recirculated water through the air space of the water supply tank to bring the vessel pressure down and promote mixing inside the vessel during cooldown.
8. Secure the pumps when finished.
9. Depressurize the test section by opening the condensate traps (V-7b or V-91) to the lab.
10. Secure the heat exchanger and the steam condenser.
    - Close V-93 and V-94.
    - Close the domestic water supply valve (V-92).
11. Power OFF the data acquisition system. See Section 4.1.

5. RESULTS AND DISCUSSION

In this section, a flooding test is specified as one facility operation in which a predetermined water flow rate is injected into the test section and the gas flow rate is incrementally increased until the onset of flooding occurs. The system parameters at the onset of flooding are recorded and represent one data point on a flooding curve. A collection of data points at similar conditions, yet different water inlet flow rates, that can be used to generate a flooding curve is considered a flooding set.

5.1 Test Conditions

All tests for each gas phase were performed using the same procedures to maintain consistency to the most reasonable extent. The test matrices were based on work from previous researchers in the Nuclear Heat Transfer Systems Laboratory [13, 21, 6].

5.1.1 Air/Water Test Ranges

The test ranges for the air/water flooding tests are shown in Table 5.1. The test section pressure range was determined by considering the MAWP of the steam generator and also the required pressure ratio to maintain choked flow through the throttle valve. Since the steam generator safety valves are set to lift at 115 psig and the minimum pressure ratio for choked flow is approximately 1.8 (using air or steam), the nominal test section pressure range of 3-45 psig was chosen. The lowest test section pressure achievable during flooding was 3 psig with the regulator adjusted to the minimum set pressure. Air/water flooding data sets were obtained for three nominal pressures of 3, 15, and 45 psig. The mean pressure of the test section for each set had a standard deviation of less than 1.8%. The steam generator was pressurized with air in the range of 100-110 psig to allow for the maximum amount of compressed

air to be stored during the air/water flooding tests. The inlet water flow rate was maintained consistent to that used in [21] to allow the liquid Froude number of the test section to match the liquid Froude number of the pressurizer surge line. The minimum water flow rate for which flooding was detectable was 4.5 GPM.

Table 5.1: Conditions for the air/water tests

Parameter	**Range**
Test Section Pressure	3-45 psig
Air Inlet Flow Rate	36-86 g/sec
Air Outlet Flow Rate	36-86 g/sec
Air Temperature	15 °C
Steam Generator Pressure	114-124 psia
Water Inlet Flow Rate	4.5-12 GPM
Water Carryover	0.5-7.4 GPM
Water Temperature	25 °C

5.1.2 Steam/Water Test Ranges

The test ranges for the steam/water flooding tests are shown in Table 5.2. As mentioned before, the test section pressure range for steam/water flooding tests was limited to 15 psig due to the unavailability of the correct water supply pump. However, the test facility was designed, and is projected to function correctly, for steam/water flooding tests up to 45 psig. Flooding data sets were collected for nominal pressures of 3 psig and 15 psig. The steam outlet flow range is less than the inlet range due to small amounts of condensation present during testing. The steam inlet temperature was near saturation (slightly superheated) during each flooding test.

The steam generator pressure was verified to meet the minimum pressure required for choked flow. This ensured that a steady steam flow rate was supplied to the test section during the approach to the onset of flooding. The water temperature was maintained as close as reasonable to the saturation temperature for the given system pressure. The water inlet subcooling was less than or equal to 3.2 °C for all tests.

Table 5.2: Conditions for the steam/water tests

Parameter	**Range**
Test Section Pressure	3-15 psig
Steam Inlet Flow Rate	22-43 g/sec
Steam Outlet Flow Rate	22-34 g/sec
Steam Inlet Temperature	105-123 °C
Steam Generator Pressure	32-85 psia
Water Inlet Flow Rate	4.5-12 GPM
Water Carryover	1.2-8.3 GPM
Water Temperature	101-122 °C

5.2 Air/Water Raw Data and Observations

Since the test section is opaque, it is not possible to detect the onset of flooding by visual means similar to Solmos [13]. Instead, the onset of flooding is inferred from measurements by the test section differential pressure transmitter. An example of a typical differential pressure trend is shown in Figure 5.1. During zero flow inside the test section, the differential pressure between the high and low ports of the transmitter is equal to the liquid head in the impulse tubing between the measurement ports on the test section. Therefore, the output of the transmitter

during no flow of air or water is equal 55.75 inH2O. When water is injected into the test section and the annular flow regime is established, the differential pressure output increases slightly and fluctuates around a steady state value. The data file starts recording after the water inlet flow rate is established and differential pressure has stabilized. The throttle valve is then cracked, and air is injected into the bottom of the test section at a flow rate below that which will induce flooding and is slowly increased. On some, but not all instances, the differential pressure will suddenly decrease by 1-2 inH2O when the throttle valve is cracked. This corresponds to a small transient pressure pulse of air traveling through the test section that marks the beginning of air flow. The pulse typically does not perturb the annular flow of water and soon disappears as steady flow resumes. The test section is now in a stable counter-current flow regime and the differential pressure remains at steady state.

The air flow is steadily increased until the differential pressure across the test section suddenly decreases by more than 1 inH2O. This designates the onset of flooding and corresponds to a large portion of the liquid film becoming entrained with the air flowing upward. Right before flooding, the interface of the annular film is likely developing oscillatory waves of increasing amplitude. At the onset of flooding, the wave growth and droplet detachment is such that the cross sectional area for gas flow upward has been reduced, resulting in a local pressure wave which propagates up the tube. This pressure wave is detected by the lower differential pressure measurement port on the test section. Since the lower port is measured by the low side of the differential pressure transmitter, the output signal suddenly decreases upon rapid detection of the positive pressure. The formation of the pressure wave was confirmed by Solmos in the acrylic prototype facility [13] and the location of flooding inside the stainless steel test section is projected to be in the lower third based on steam/water temperature data from [6]. The differential pressure continues to oscillate during the

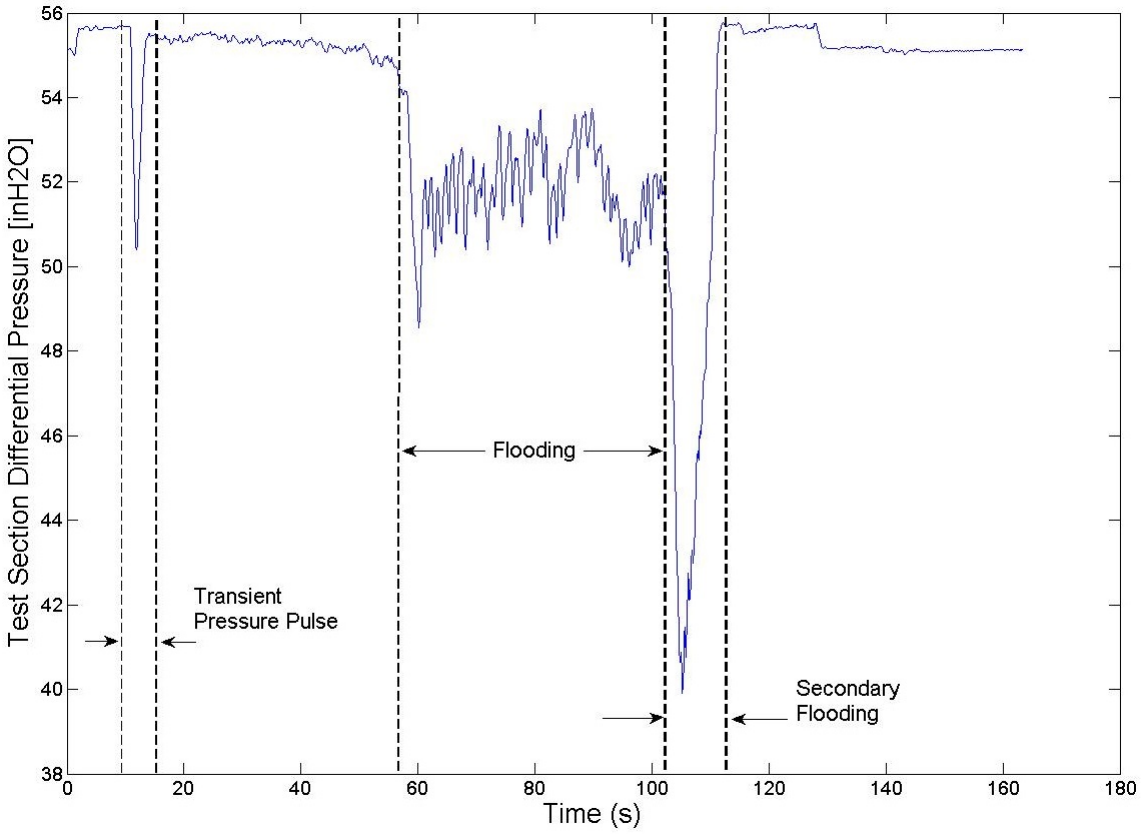

Figure 5.1: Test section differential pressure for air/water flooding. This test corresponds to Run #5, Test #9 in Appendix D.

flooding event until the throttle valve is shut.

After the inlet gas flow rate ceases, the back pressure regulator continues to vent the outlet gas until the valve seat reaches a tight shutoff. This results in a very large drop in differential pressure across the test section as the top measurement port is sensing a decreasing pressure during the venting. This is shown between 105 to 112 seconds in Figure 5.1. The bottom measurement port senses positive pressure as the buildup of pressure inside the holdup tank is trying to vent upward to reach equilibrium. The influx of air rushing out of the holdup tank may come in contact with water that may be flowing down in the test section, and a secondary flooding

event occurs inside the test section. No air is being injected from the air supply during the secondary flooding event. The pressure pulse, flooding, and secondary flooding are shown in Figure 5.1. Eventually after the regulator closes, the pressures will equalize and the differential pressure will return to the steady state value before any air was injected at the beginning of the test. The water then returns to a stable annular flow.

A typical plot of the air flow rate during a flooding test is shown in Figure 5.2. The flow rate of the air entering the test section is controlled by the throttle valve. The valve is opened in large increments below the flow rate required to initiate the onset of flooding, referred to as the onset flow rate. The large flow increments are shown from 18 to 25 seconds in Figure 5.2. Once a steady flow rate is established, the throttle valve is opened slowly until the onset flow rate is determined, as shown between 40 to 55 seconds in Figure 5.2. In some cases, an initial flooding test was performed with smaller increments throughout to determine the approximate onset flow rate. By determining the approximate onset flow rate beforehand, the probability to surpass or "overshoot" the onset of flooding is diminished. Secondly, less compressed air is used in the approach to flooding when the onset flow rate is predetermined. The large flow rate increments leading up to flooding allow the test section pressure to converge close to the desired set pressure as the flow rate through the back pressure regulator is stabilizing. The throttle valve is then opened slowly and until the onset of flooding is determined from the differential pressure measurement. The throttle valve is not opened any further during the flooding event. The inlet mass flow rate during the flooding event is observed to trend down in some cases due to the decreasing pressure inside the steam generator. Since the air is not able to change phase with the water, the outlet mass flow rate of air is equal to the inlet mass flow rate within the accuracy of the vortex flow meters. The

outlet gas flow rate displays a delay in response from changes in the throttle valve position compared to the inlet gas flow rate. This is due to the relative location of the flow meters; the outlet vortex flow meter is far downstream from the inlet vortex flow meter.

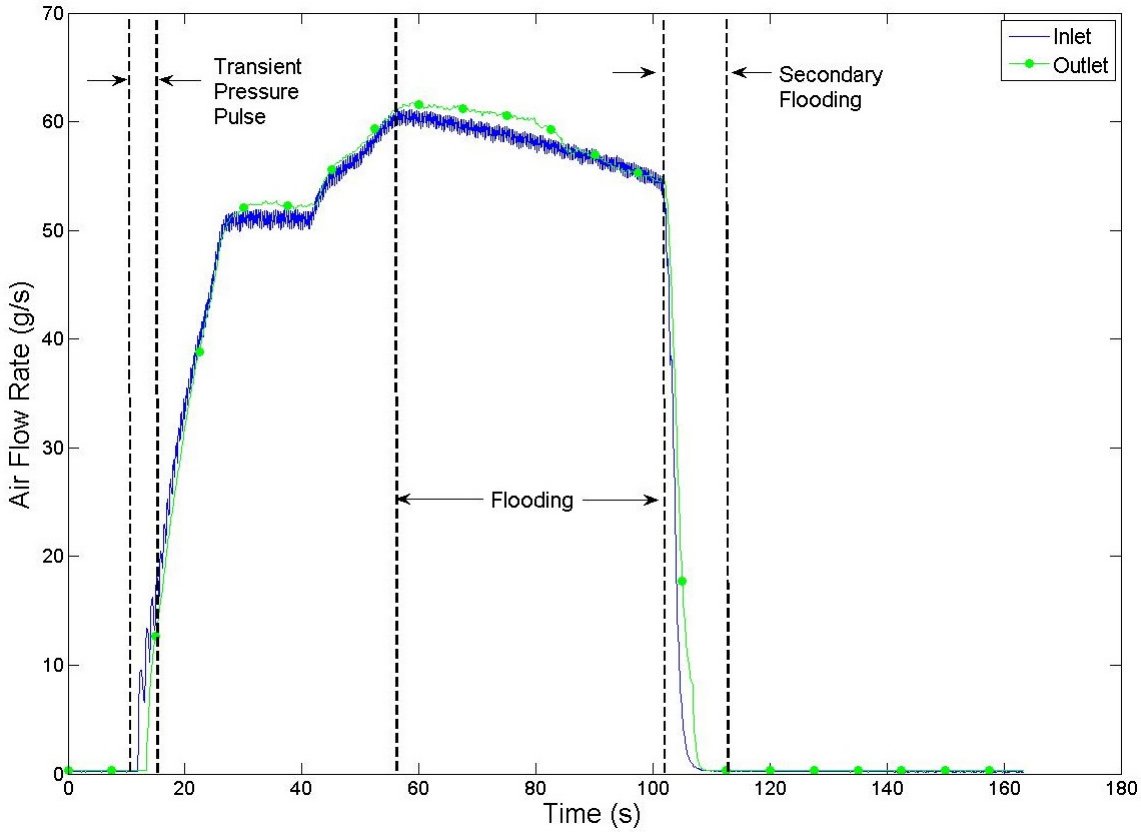

Figure 5.2: Gas mass flow rate for air/water flooding. This test corresponds to Run #5, Test #9 in Appendix D.

A plot of the system pressure during a 45 psig flooding test is shown in Figure 5.3. The system pressure is controlled by the back pressure regulator which works to maintain the regulated pressure to the set pressure. During the air/water tests, if the system pressure is above the set pressure, the regulator vents the necessary

amount of air to atmosphere to maintain the set pressure upstream of the valve. If the system pressure is below the set pressure, the valve trim closes to raise the system pressure to the set pressure. As the throttle valve is opened and air is injected into the test section, the system pressure increases until converging near the desired set pressure for the flooding test. This is shown between 0-22 seconds in Figure 5.3.

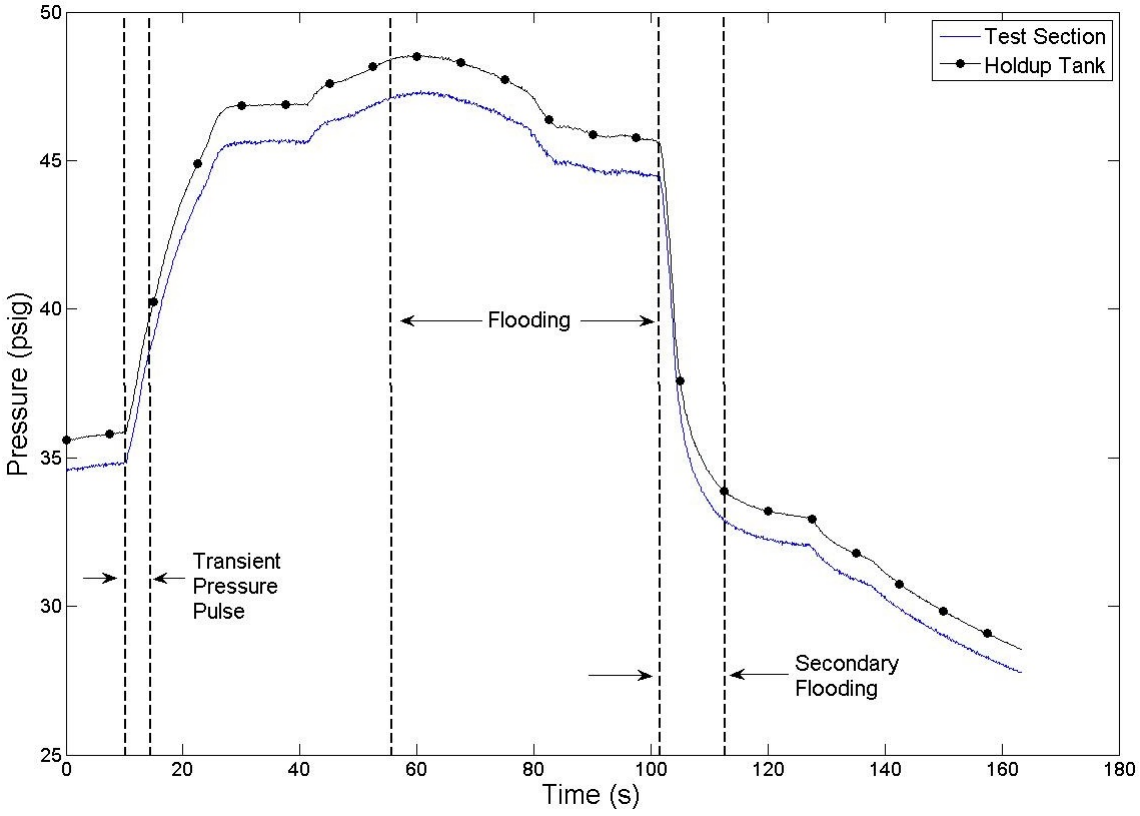

Figure 5.3: System pressure for air/water flooding. This test corresponds to Run #5, Test #9 in Appendix D.

The increase in pressure is accomplished inside the valve by maintaining a force balance between the inlet pressure impinging on the bottom of the diaphragm and the compressive spring force on top of the diaphragm. In an ideal case, the regulator will

maintain the set pressure for all ranges of flow rates through the valve. In practice, this is not the case for direct-operated regulators due to two primary factors. First, as the flow rate increases through the valve, the inlet pressure increases and the diaphragm lifts the valve trim to allow more flow to pass through. The spring is compressed slightly and a new equilibrium will be reached in the force balance between the flow and the spring. However, the spring is now exerting more force on the diaphragm due to Hooke's Law. The inlet pressure must now increase to reach equilibrium with the greater spring force. Therefore, the increase of flow is easily allowed to pass through the valve, just at a slightly higher pressure than before. Secondly, the apparent area of the diaphragm in the force balance is dependent on the inlet pressure and is commonly referred to as the diaphragm effect [9]. The combination of the valve spring behavior and diaphragm effect results in the buildup of pressure as the flow rate through the valve increases. This affects the accuracy of the valve and is referred to as buildup (or droop in pressure regulators). The buildup during the flooding tests is small in effect over the range of flow rates used. This is illustrated in Figure 5.3 between 22 and 50 seconds when the air flow rate is slowly increased to the onset flow rate.

After sufficient data has been collected during the flooding event, the throttle valve is closed and the inlet pressure to the regulator decreases. The diaphragm inside the regulator pushes the valve trim down and the spring is extended. The spring force is now smaller than with full flow, and a new equilibrium is reached between the diaphragm and the inlet pressure until a tight shutoff of the seat occurs. Typically in the flooding tests, the system pressure vents down to 10 psi less than the desired set pressure when flow is going through the valve. The venting of pressure once gas flow ceases is shown after 100 seconds in Figure 5.3.

In all of the tests, the holdup tank gauge pressure is typically greater than the

test section pressure since it is farther from the back pressure regulator. In some tests, the holdup tank gauge pressure is shown to oscillate during flooding similar to water exit tank results presented by Ritchey [21]. The evidence of secondary flooding is shown in Figure 5.3 in which the holdup tank pressure drops rapidly and tries to reach equilibrium with the test section pressure while the regulator vents down.

The water flow rates during the same aforementioned test are shown in Figure 5.4. The inlet water flow rate decreases slightly during the approach to flooding due to the increase of pressure in the test section. After the onset of flooding, the water carryover rapidly increases and fluctuates greatly. This is likely due to the chaotic conditions inside the test section as an unpredictable amount of water is becoming entrained at a given point in time. This results in an average value of carryover for a flooding test. The water carryover flow rate does not respond immediately at the onset of flooding; there is a time delay (or travel time) associated with the entrained liquid slugs to be carried out of the test section, separated, and then measured by the flow meter. The average travel time is 5 seconds. In some instances, the secondary flooding event will indeed contribute to the water carryover flow rate at the end of the flooding test. This contribution is not included in the average water carryover determined for each flooding event. A MATLAB script was created to determine the average carryover from the beginning of water carryover to the end of gas injection. Any carryover that is recorded after the gas injection has ceased (and including the travel time) must be from the secondary flooding event and is discarded from the averaging. The inlet water flow rate increases during the secondary flooding due to the decrease in test section pressure. The inlet water flow rate is isolated after each test.

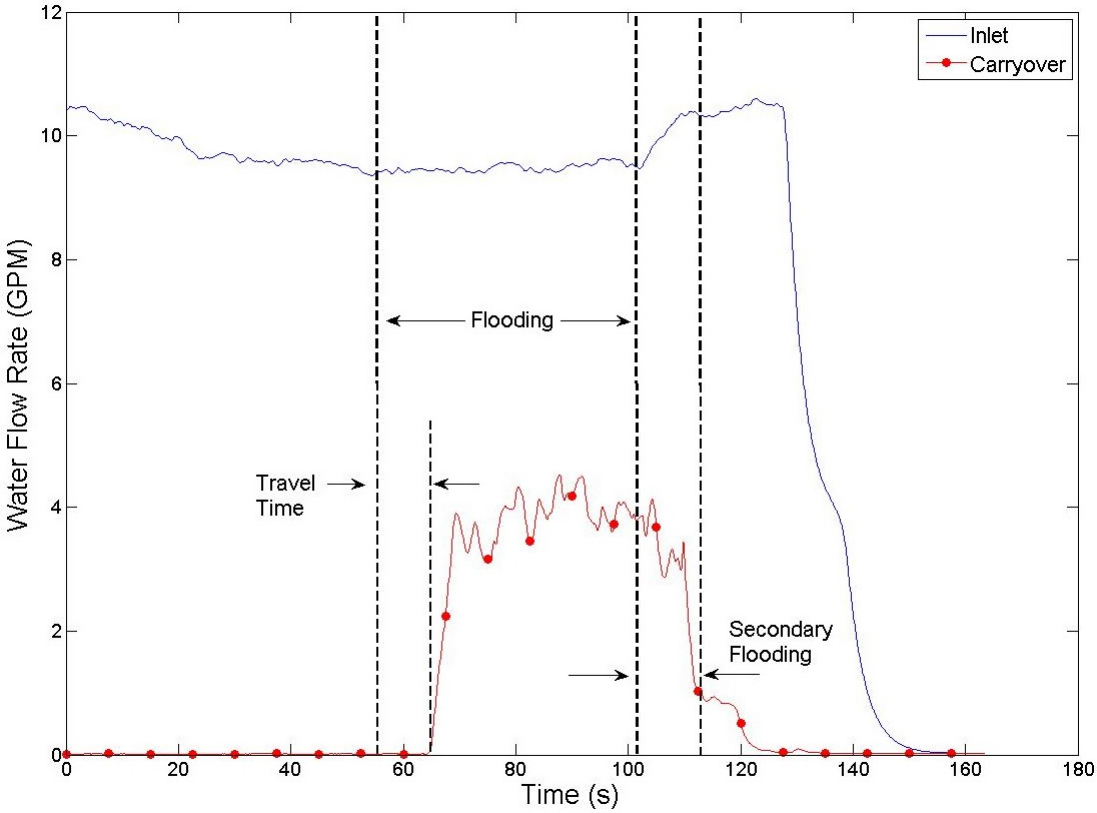

Figure 5.4: Water flow rates for air/water flooding. This test corresponds to Run #5, Test #9 in Appendix D.

5.3 Steam/Water Raw Data and Observations

The general trends described in section 5.2 were observed in the steam/water flooding data. The notable differences, particularly due to phase changes, are discussed herein.

The approach to flooding and data logging procedures during the steam tests are near identical to the air/water flooding tests. The trends in the test section differential pressure seem to be unaffected by the differences in using steam or air. A typical plot of a steam/water flooding test is shown in Figure 5.5. This test was performed at a water flow rate of 6.83 GPM and will be used to illustrate other trends

in the steam/water observations.

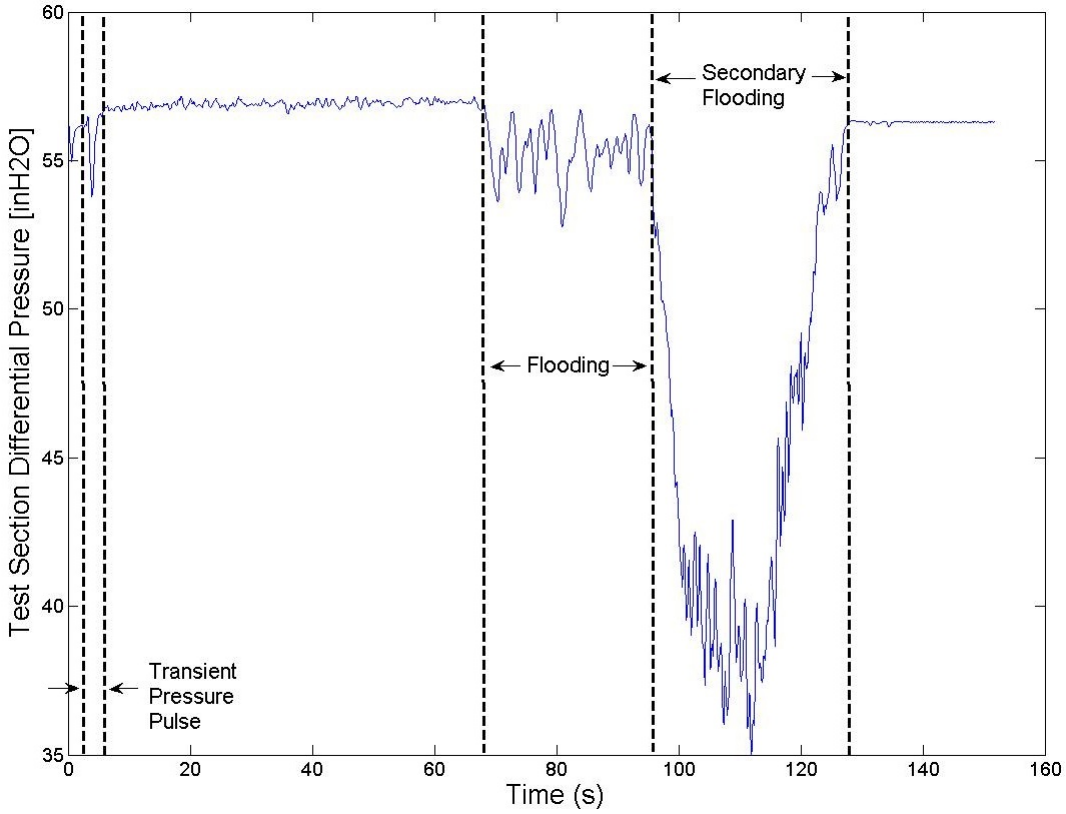

Figure 5.5: Test section differential pressure for steam/water flooding. This test corresponds to Run #15, Test #3 in Appendix D.

The gas inlet flow rate is controlled using the throttle valve, just as in the air/water flooding tests. The approach to flooding is nearly the same, using large increments to pressurize the system before flooding while then using small increments to determine the onset flow rate. However, the throttle valve is more difficult to turn during the steam/water flooding tests due to the thermal expansion of internal valve components. This results in a slightly different trend for the inlet gas flow rate when compared to the air tests. The steam outlet flow rate exhibits the same time delay

as in the air outlet flow rate, however the magnitude is affected by the thermodynamic conditions of each test. The water temperature is near saturation during each steam/water flooding test, however some small amount of water inlet subcooling was unavoidable. This results in a small amount of condensation of the inlet steam inside the test section. This is illustrated in Figure 5.6, in which the inlet steam flow rate is greater than the outlet steam flow rate during the test.

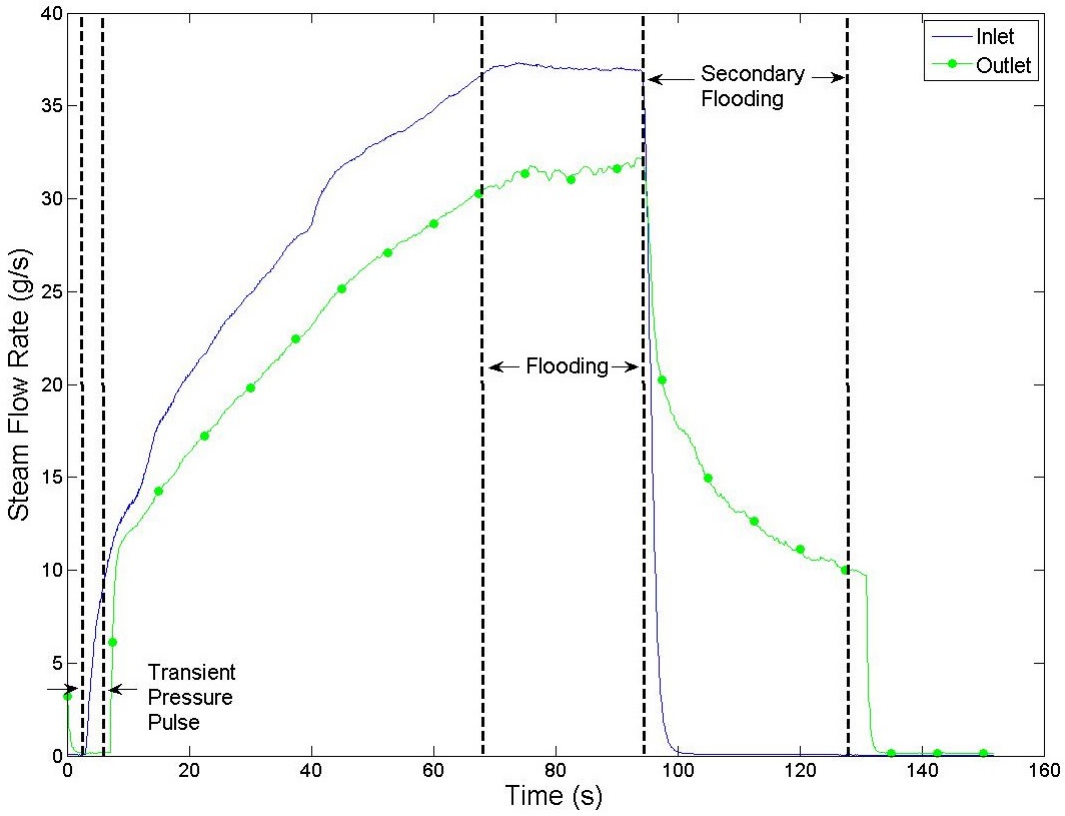

Figure 5.6: Gas mass flow rate for steam/water flooding. This test corresponds to Run #15, Test #3 in Appendix D.

System characterization tests were performed with steam only and no water flow to better understand the amount of condensation taking place. In these tests, steam

was injected into the cold test section while the inlet and outlet flow rates were measured as the facility heated up. It was observed that even with no water present, the inlet steam would condense inside the test section during facility heatup and drain into the holdup tank thereby increasing the liquid level. After a long period of time, a steady state heat flux was established through the test section and condensation was minimal. The outlet steam flow rate was then observed to be within instrument accuracy of the inlet steam flow rate, confirming that the vortex flow meters were functioning properly. The time to reach thermal equilibrium was at least 20 minutes. It is probable that during the flooding tests with an annular flow of water, some portion of the steam condensation is due to heat loss through the test section components that may have cooled slightly in between tests. However, the majority of the condensation is largely affected by the inlet water temperature.

The large venting of steam through the regulator is shown in the secondary flooding portion of Figure 5.6. The vented steam is mostly from the higher pressure vapor space of the holdup tank. However, a second contributer to this mass flow rate is actually from water that is in the holdup tank that may be flashing to steam. As the back pressure regulator drops the system pressure by 10 psi after the throttle valve is closed, the once saturated water during testing is now driven to evaporate due to the lower system pressure. This contribution to the vented steam is assumed to be small but non-zero.

The system pressures during the steam/water flooding tests follow the same trends as the air/water tests. This is expected since the back pressure regulator is also designed for steam use; the only difference is the vented steam is not released to the lab and is condensed inside the steam condenser. A plot of the system pressures during a typical steam/water test is shown in Figure 5.7.

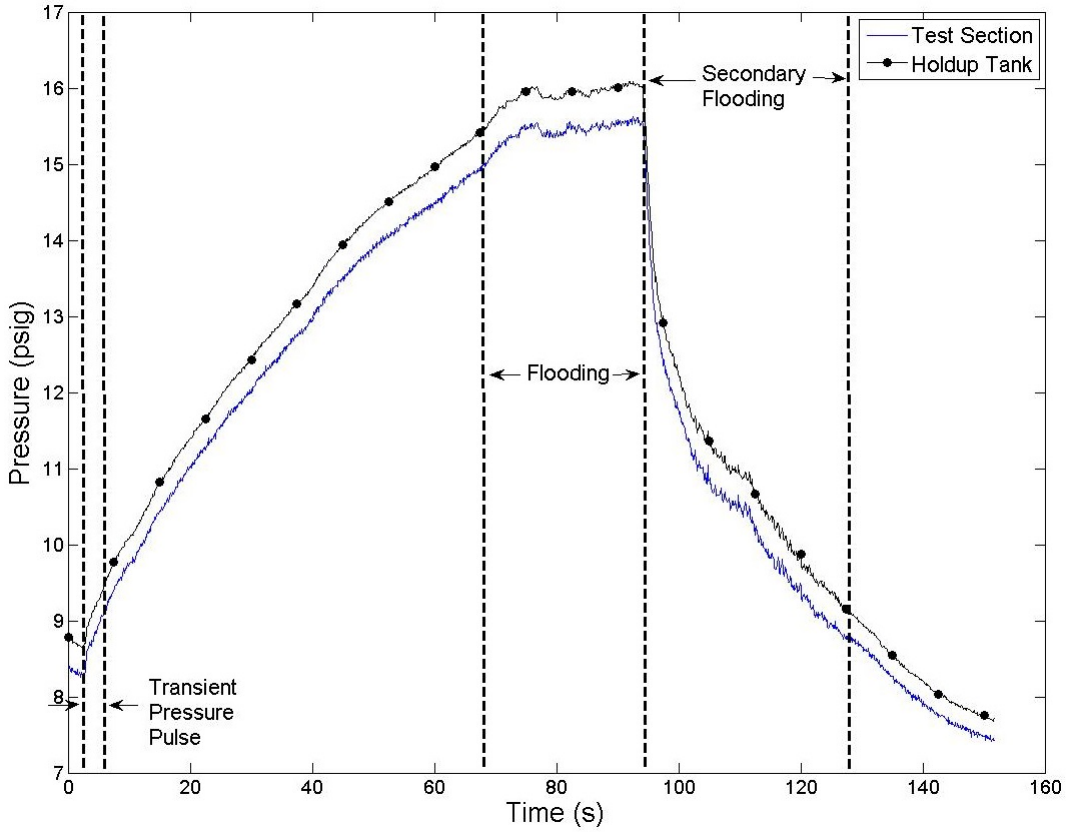

Figure 5.7: System pressure for steam/water flooding. This test corresponds to Run #15, Test #3 in Appendix D.

The water flow rate for a typical steam/water flooding test is shown in Figure 5.8. For the majority of the tests, no observable differences are noted in the water flow rate trends between steam/water and air/water testing. During the steam/water testing, it is now possible to have a water carryover flow rate that is greater than the inlet water flow rate. This is due to the condensation of inlet steam inside the test section. This behavior was observed in a handful of testing.

Unique to the steam/water tests, the temperature of the inlet/outlet gas and liquid flow rates add a new dimension of parameters to control during the flooding tests. The steam inlet temperature is determined by the enthalpy content of

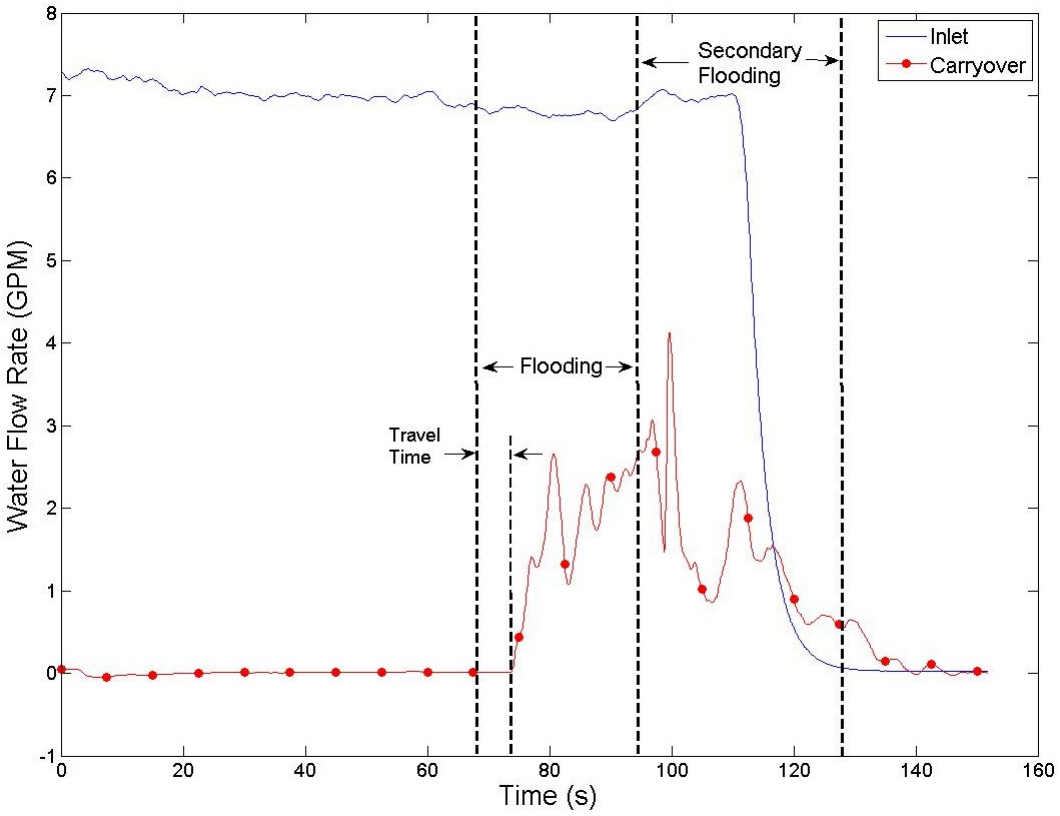

Figure 5.8: Water flow rates for steam/water flooding. This test corresponds to Run #15, Test #3 in Appendix D.

the steam in the steam generator. The steam inside the steam generator vessel is wet saturated steam at the given vessel pressure. The vessel pressure and rate of steam generation are controlled by the heat input, or heater power, applied to the water in the steam generator. As the wet steam is dried in the separator, it then passes through the throttle valve where the high pressure steam is reduced to a lower pressure. Assuming that the throttling process across the valve is isenthalpic, the temperature decreases to a state that results in superheated steam at the reduced pressure. Thus the superheated steam temperature depends on the steam generator heater power and also the flow rate through the throttle valve. This trend is shown

in Figure 5.9 as the steam inlet temperature increases during the approach to the onset flow rate. The saturation temperature is also increasing during the approach to flooding, however this is an artifact of the increasing test section pressure due to the back pressure regulator. The water inlet temperature is maintained close to the saturation temperature inside the test section during flooding. The steam outlet temperature is typically very close to the saturation temperature during flooding, indicating that some steam is indeed condensing inside the test section.

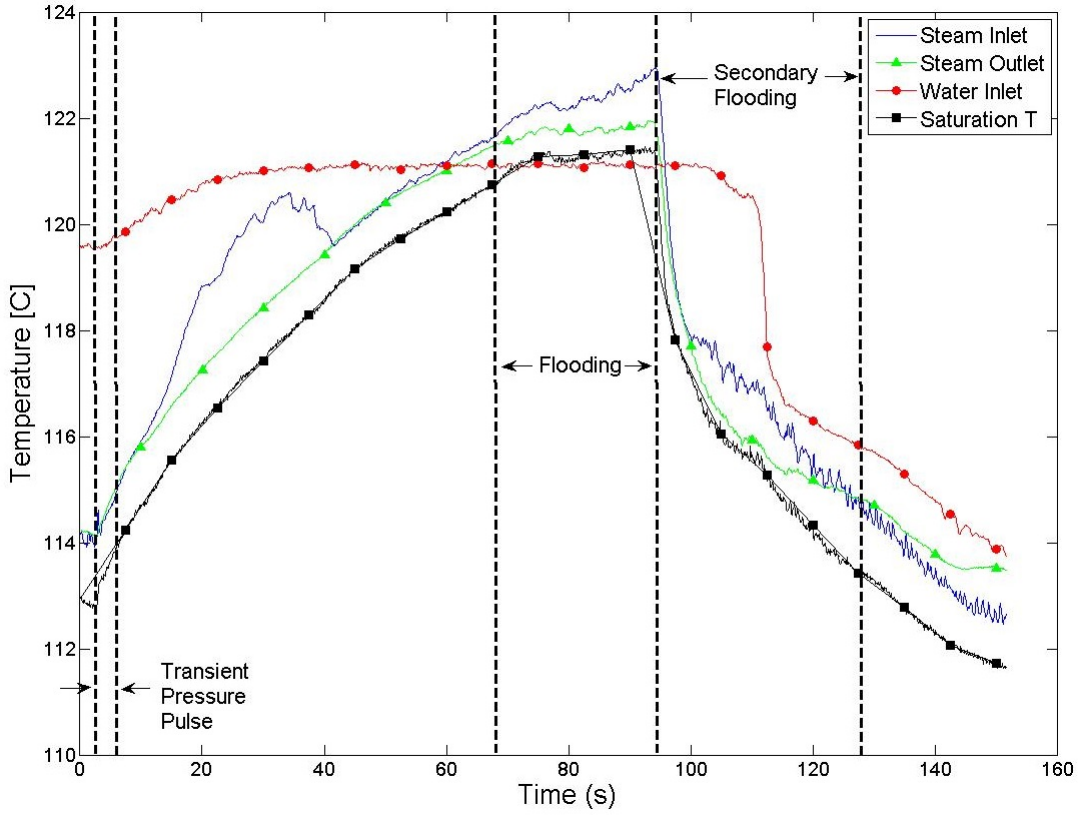

Figure 5.9: Flow temperatures for steam/water flooding. This test corresponds to Run #15, Test #3 in Appendix D.

5.4 Reduced Data

The raw data for each flooding test was analyzed using a MATLAB script that determines the onset of flooding. The script searches the data file and selects the instant in time in which the test section differential pressure is observed to decrease by 1.0 inH2O from a steady state value. This instant is regarded as the onset of flooding. The system parameters right before the onset of flooding are at steady state and are considered the flooding conditions to constitute the data point for the flooding test. The script outputs all measured variables right before the onset of flooding. The MATLAB script is included in Appendix C and the reduced data is in Appendix D. The raw data is shown graphically for each test in Appendix E. The measured variables were then analyzed and are presented herein.

5.4.1 Reduced Data in Terms of Superficial Velocities

The flooding data are plotted in terms of the superficial velocities in Figure 5.10. The superficial velocities in Figure 5.10 correspond to the gas and water flow rate at the test section inlet. The superficial velocity was determined by dividing the volumetric flow rate reported by the flow meters by the area of the test section. The air velocity required for the onset of flooding is shown to be inversely related to the inlet water velocity for all pressures. This is consistent with other atmospheric air/water data in the literature [21, 13]. For a fixed water flow rate, the air velocity required for flooding decreases as the system pressure increases. This is likely due to the increase of gas density for a greater system pressure. The momentum transfer between the gas and liquid that is necessary for flooding can be achieved at a lower velocity as the gas becomes more dense.

The steam velocity required for the onset of flooding decreases as the water inlet velocity increases. This trend is different than that observed by Ritchey, in which

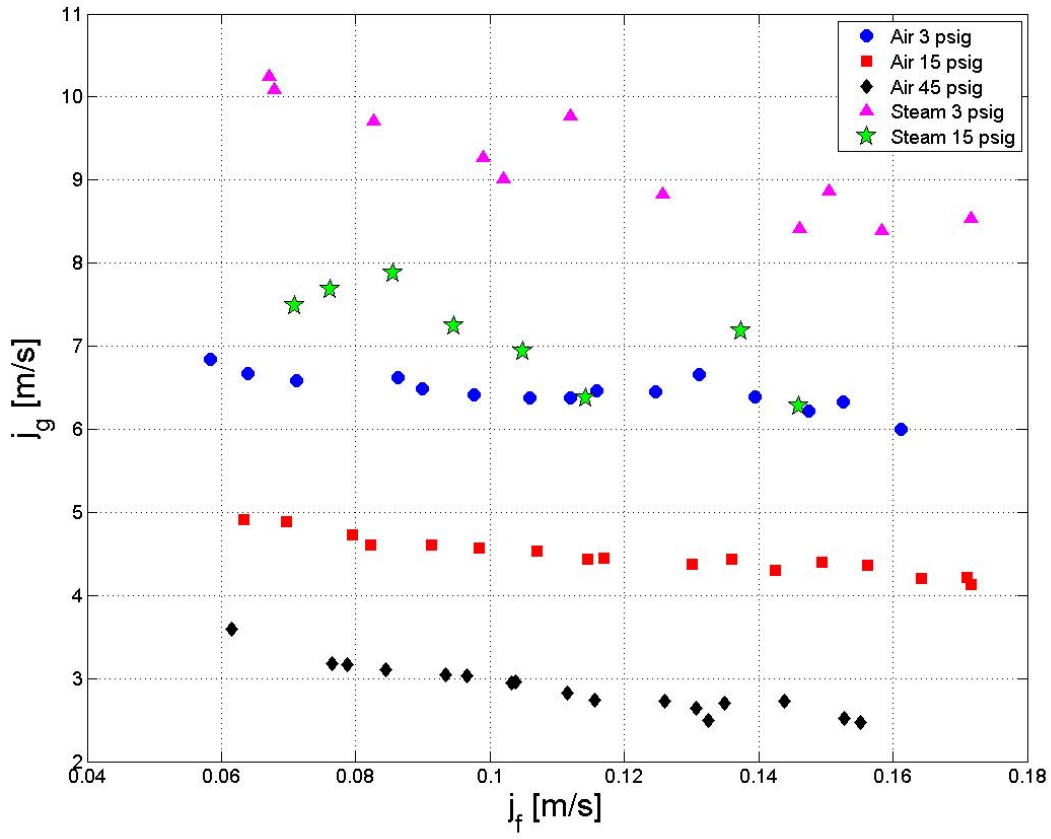

Figure 5.10: Superficial flooding velocities for air/water and steam/water tests at various pressures.

the steam velocity decreased for water flow rates below 6 GPM and then increased for water flow rates above 6 GPM [21]. This difference can be attributed to the water temperature used in the tests, as the water inlet temperature for Ritchey's test was 70 °C. The highly subcooled water condensed more steam at high water flow rates above 6 GPM. Since the water inlet temperature in the current research was near saturation, the condensation effects during the onset of flooding are of lesser importance than during subcooled flooding tests. The onset flow velocity is less dependent on thermodynamic properties when the fluids are near saturation.

Therefore, the steam velocity trend is similar to the adiabatic air/water velocity trend and agrees well with other saturated water data presented by Rothe and Crowley [11]. The water inlet temperature during the steam/flooding testing was more difficult to regulate due to the thermal stratification inside the water supply tank, and therefore the water subcooling during the tests ranged from 0-3.2 °C. This unavoidable amount of subcooling may have contributed to the deviation from linearity in the steam/water data when compared to the air/water data. The steam velocity required for flooding at 15 psig is less than at 3 psig for a fixed water flow rate. This is consistent with the air/water tests, and is likely due to the same differences in momentum transfer due to higher densities.

5.4.2 Reduced Data in Terms of Kutateladze Numbers

The air/water flooding data are plotted in terms of the Kutateladze parameters in Figure 5.11. The abscissa is the Kutateladze number for the constant flow rate of water injected into the test section before flooding occurs and will be denoted as $Ku_{f,in}$. For $Ku_{f,in}^{1/2} > 0.65$, the flooding curves do not have the same slope and diverge for higher water flow rates. As the flooding test pressure increases, the corresponding $Ku_g^{1/2}$ decreases for higher water flow rates. Since water is incompressible over this pressure range and the temperature was unchanged for all air/water tests, the water density and surface tension were mostly constant between the three flooding data sets. Therefore, the parameters that are affected the most by the pressure change is the air density, ρ_g, and the superficial flooding velocity, j_g. The varying slope between the three pressures may suggest that the gas momentum necessary to achieve flooding at higher pressures is less than at lower pressures when the water parameters are held constant.

In contrast, the saturated steam/water data are plotted in terms of the Kutate-

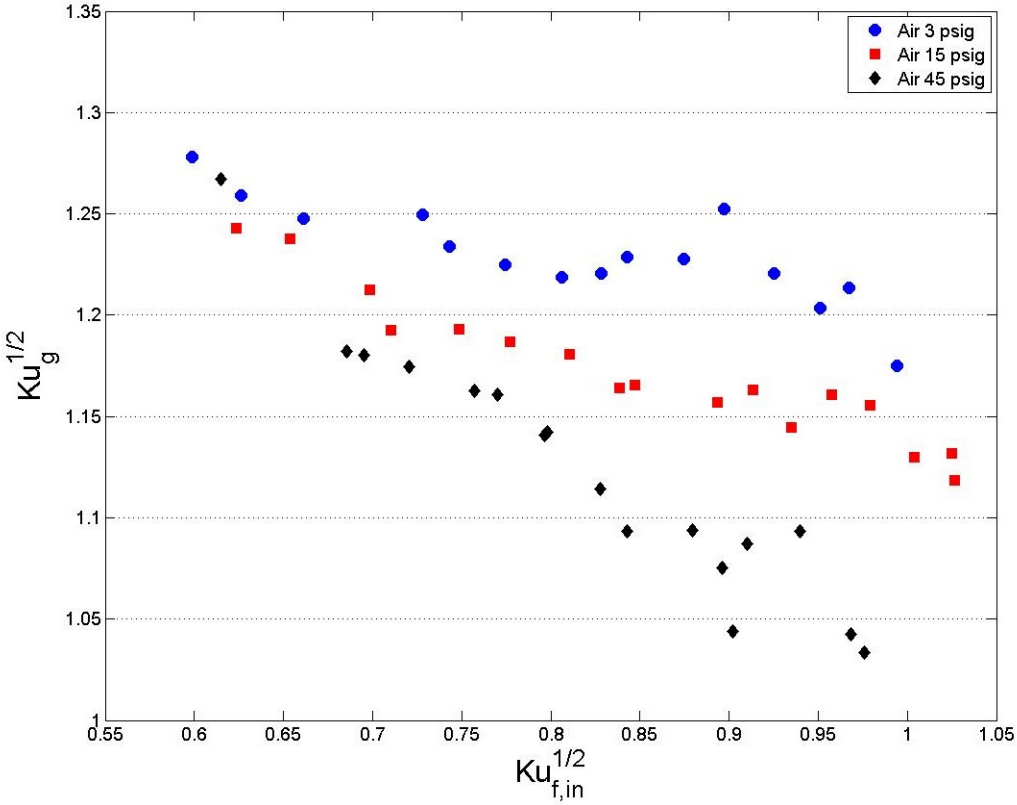

Figure 5.11: Air/water data plotted in terms of the Kutateladze parameters at various pressures.

ladze parameters in Figure 5.12. The data were fitted with a linear polynomial and are shown for comparison. The slopes are nearly parallel with each other, and may suggest that the change in fluid properties across different pressures are balanced by the change in momentum required for the onset of flooding. This hypothesis assumes that the saturated/steam water and air/water flooding data agree with each, as suggested in [6]. During the saturated steam water tests, the water density and surface tension do indeed change for different flooding pressures. Further investigation should be conducted by comparing a saturated steam/water flooding data set to the air/water flooding data set at 45 psig.

Since saturated steam/water data should ideally have no phase change, the flood-

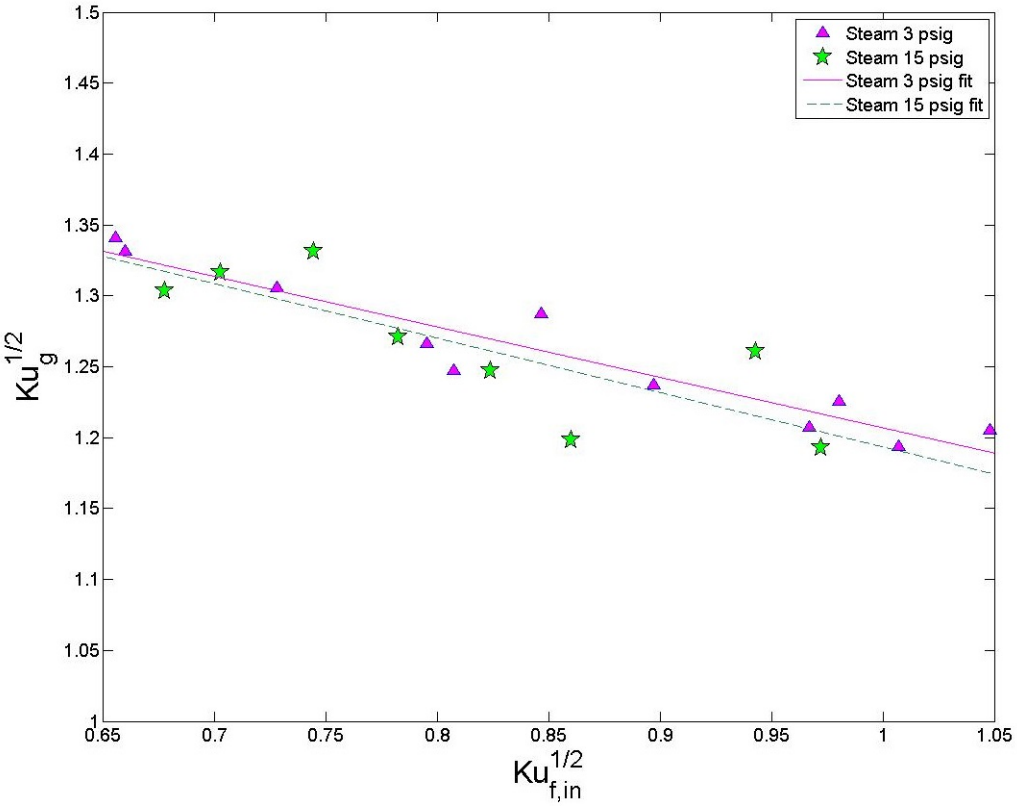

Figure 5.12: Steam/water data plotted in terms of the Kutateladze parameters at various pressures.

ing curves should be comparable to the air/water flooding data at the same pressure. In fact, the correlations developed by Ritchey and Wallis suggest that when steam condensation is accounted for, the flooding curves for steam/water and air/water should be near the same [21, 19]. The saturated steam/water and air/water flooding data at 3 psig are shown in Figure 5.13. The steam/water data at 3 psig does trend closely to the air data, however it is offset vertically. This can be explained as slight subcooling of the water inlet was unavoidable and more steam was needed to initiate the onset of flooding than if it were purely saturated water.

Equation 2.8 has been used in the past to correct for the steam condensation and develop an effective steam flow rate that represents the amount of steam that

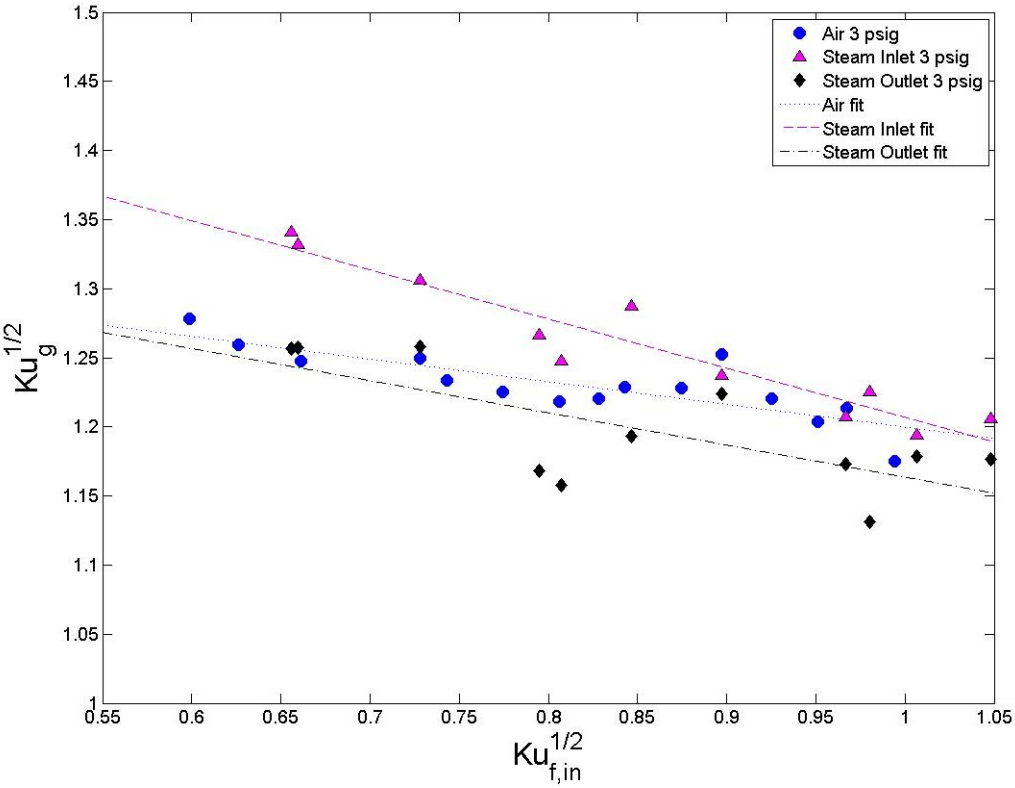

Figure 5.13: Air/water and steam/water flooding data at 3 psig plotted in terms of the Kutateladze parameters.

has not condensed at the location of flooding. The development of this correlation was necessary since a direct measurement of the steam mass flow rate inside the test section was not available. However, the current research does measure the amount of steam that leaves the test section outlet after the onset of flooding has occurred. The outlet steam flow measurement is equal to the amount of steam that has not condensed once leaving the test section. Plotting the outlet steam flow in Figure 5.13 shows better agreement with the air data at 3 psi. The trend in this case is slightly lower than the air data which could suggest that the outlet steam flow rate underestimates the effective steam flow rate in the test section due to condensation at varying axial locations. Specifically, the effective steam flow rate should be equal

to the inlet flow rate minus the amount of condensation up to the axial flooding location; the outlet steam flow rate accounts for all condensation that occurs inside the test section. Therefore, knowledge of the axial flooding location would allow for stricter estimations of the effective steam flow rate during near saturated steam/water flooding. Attempts to analyze the test section outer surface temperatures were not conclusive in determining the exact location of flooding in the tube, since the thermal gradient between the steam/water or air/water fluid pairs is too small.

The slope and intercept between the air/water and steam/water data at 3 psig agree with Cullum's results [6] as shown in Figure 5.14. In both Figures 5.14 and 5.13, the air/water data has a smaller slope than the near saturated steam data and the corrected steam data. Cullum attributes this difference to the test facility modifications between the air/water data collection and the 97 °C data collection. The test section outlet collection tank used by Williams was later modified by Cullum. In the current research, the discrepancy cannot be due to the test facility modifications since the facility is unchanged between the air/water and steam/water tests. Therefore, the test section outlet geometry does not appear to have a major effect on the onset of flooding. Currently, the difference in slope between the air/water and steam/water data is unclear but may be attributed to the water properties at differing temperatures or also the variation in liquid-gas density ratio. The liquid to gas density ratios are shown in Table 5.3.

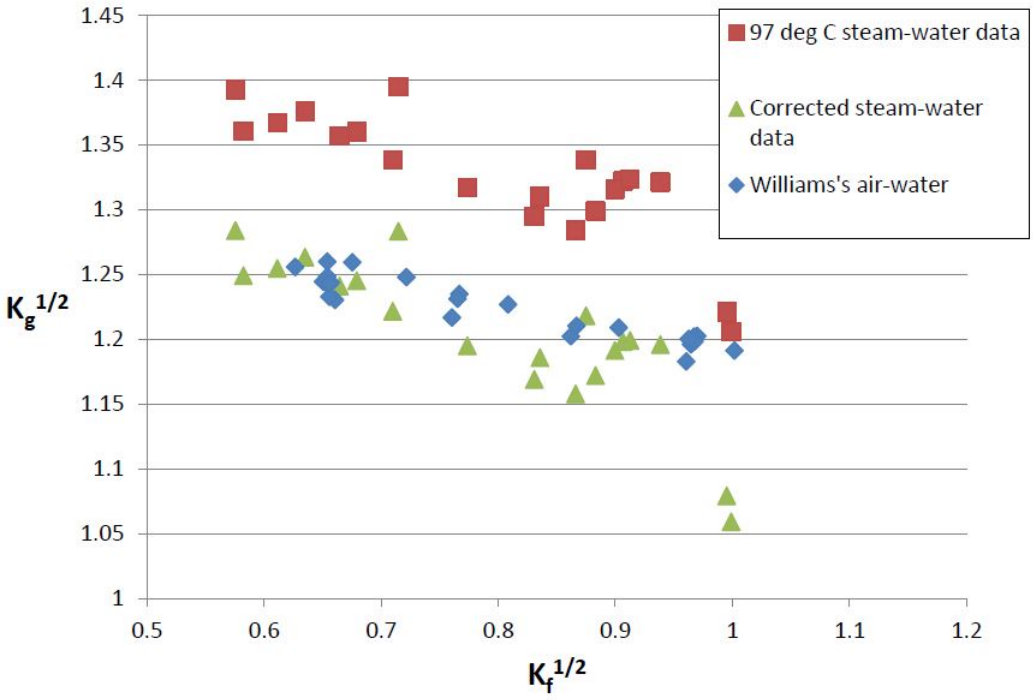

Figure 5.14: Air/Water flooding data by Williams and 97 °C steam/water data by Cullum plotted in terms of the Kutateladze parameters [6]. The abscissa refers to the inlet water flow rate during the onset of flooding.

Table 5.3: Liquid to gas density ratio for notable pressures, including full scale PWR operating pressure.

ρ_f/ρ_g	3 psig	15 psig	45 psig	2175 psig
Air	686	400	195	7.5
Steam	1376	830	414	6.1

The steam/water and air/water flooding data at 15 psig is shown in Figure 5.15. The trends are similar to that in Figure 5.13, however the steam outlet data agrees

quite well to the air/water flooding data. This is in contrast to the 3 psi data in which the steam outlet may have underestimated the effective steam flow rate. One possibility for this difference may be that the location of flooding changes at higher pressures. If the onset of flooding occurred at a higher axial location, then the outlet steam flow rate would be closer the effective steam flow rate than during the 3 psi tests. A second possibility could be that the heat loss through the test section and insulation is greater at higher pressures and temperatures due to Newton's Law of Cooling. This would result in more steam condensation inside the test section and would require more steam to initiate the onset of flooding. Additional data at higher pressures is needed to test these hypotheses.

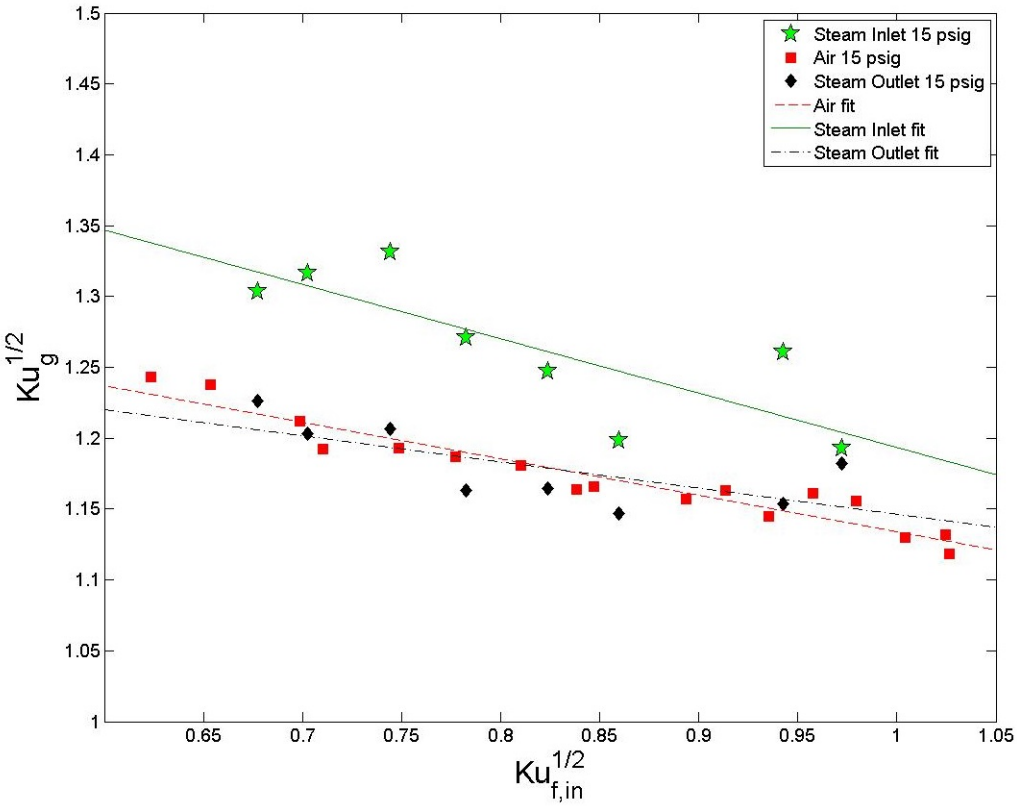

Figure 5.15: Air/water and steam/water flooding data at 15 psig plotted in terms of the Kutateladze parameters.

5.4.3 Water Carryover Results

A MATLAB script was created to determine the average flow rate of the water carryover during the onset of flooding. The average flow rate during flooding is considered the portion of the carryover between the ramp rate of the flow signal leading up to secondary flooding. The carryover flow rate may increase during the secondary flooding portion of the tests, and this contribution was not included in the averaging calculation. For example, referring to Figure 5.8, the average water carryover flow rate is computed between the end of the flow ramp up portion (at 80 seconds) until the beginning of secondary flooding (at 97 seconds) to yield an average

carryover flow rate of 2.1 GPM. The script searches for the increase in carryover flow rate after the onset of flooding and terminates the averaging scheme at the end of the inlet gas flow injection. This intricate calculation eliminates the influences on the average due to the low flow rates during ramp up and high flow rates from secondary flooding. The MATLAB script is included in Appendix C.

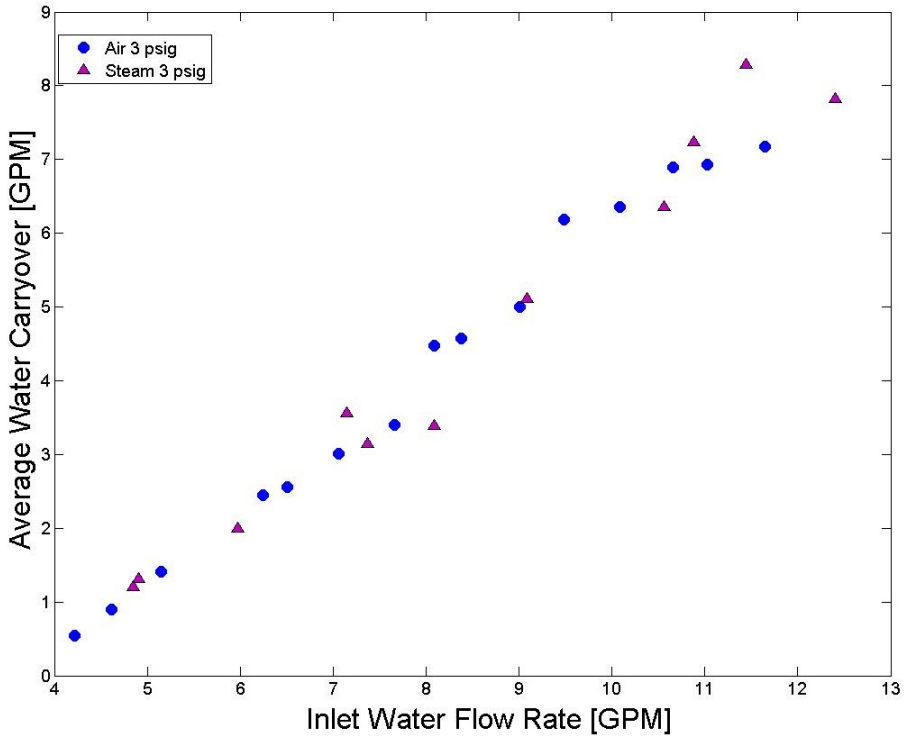

Figure 5.16: Average water carryover for air/water and steam/water flooding data at 3 psig.

The average water carryover flow rate for air/water and steam/water tests at 3 psig is shown in Figure 5.16. As the inlet water flow rate increases, the amount of entrained water that is carried out of the test section with the gas increases. However, for the majority of the inlet water flow range, the average carryover to inlet water

ratio is roughly 0.48. If the gas inlet flow rate were to be increased further after the onset of flooding, the carryover to inlet water ratio would be expected to increase. The amount of carryover seems to be independent of the gas used; the air/water data closely predicts the amount of entrained carryover in the saturated steam/water data. This trend is also consistent in the 15 psig air/water to steam/water flooding data.

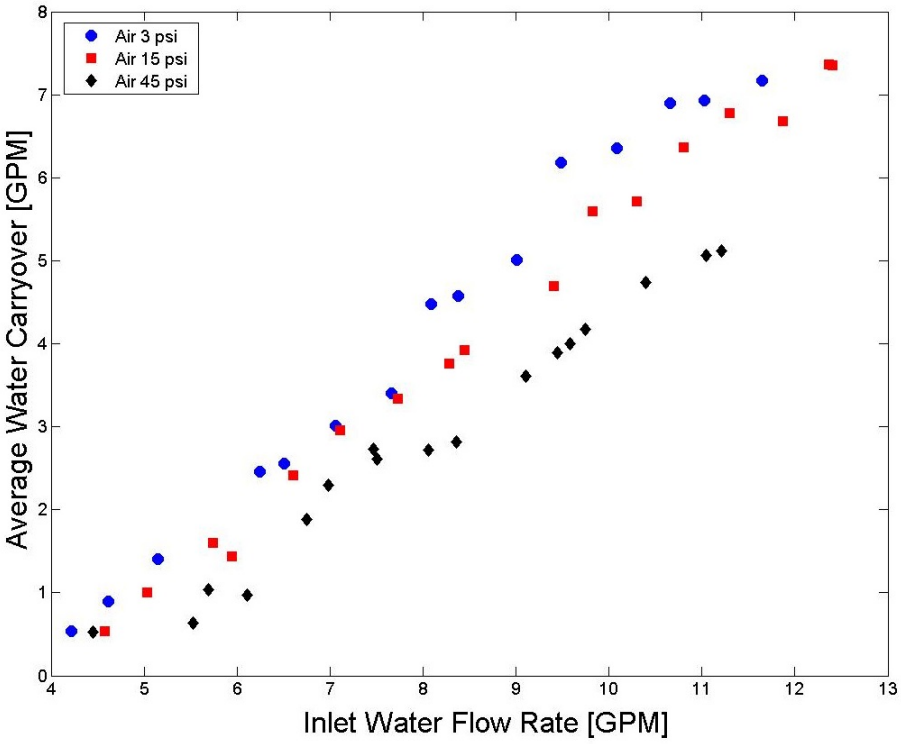

Figure 5.17: Average water carryover for air/water at various pressures.

The water carryover for air/water flooding at different pressures is shown in Figure 5.17. The similar trend and slope is common between the air pressures, however there is an offset present as pressure increases. That is, as pressure increases, the amount of entrained water in the gas decreases at the onset of flooding. The

average carryover to inlet water ratio is 0.44 and 0.32 for the 15 psig and 45 psig data respectively.

Lastly, the average water carryover was subtracted from the inlet water flow rate to determine the amount of water that falls down in the test section and into the holdup tank. This shall be referred to as the water down flow rate. The water down flow rate and average water carryover for air/water testing at 3 psig is shown in Figure 5.18. As shown, the amount of water that falls down in the test section is relatively constant at the onset of flooding across the testing range. This illustrates that the carryover to inlet water ratio is not constant across the inlet water flow range. The water down trend for all the other tests are similar to Figure 5.18. Further investigation into characteristics past the onset of flooding will provide more insight into the effects of pressure on the water down flow rate leading up to full flow reversal.

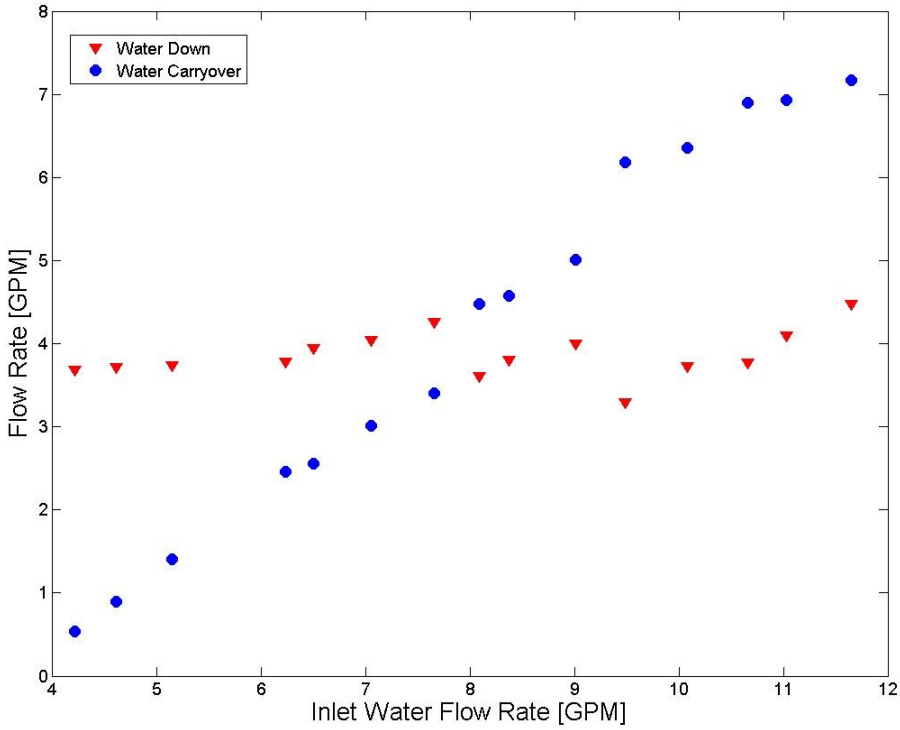

Figure 5.18: Water down flow rate and average water carryover for air/water flooding at 3 psig.

5.5 Uncertainty Analysis

The error associated with the flooding velocity was calculated using standard error propagation techniques. The primary sources of uncertainty include the random error associated with determining the flooding velocity, the measurement of the system parameters, and the error in converting the analog data to digital values. The random error was determined by repeating an air/water flooding test 22 times at the same water inlet flow rate to determine the mean flooding velocity. The average water inlet flow rate for the tests was 9.5 $\pm$0.2 GPM and the system pressure was 3 psig. The average gas inlet flooding velocity was 6.16 $\pm$ 0.10 m/s. The instrument error of the vortex flow meters is 1.0%. The error associated with data conversion

is considered very small and can be neglected. The flooding velocity is plotted with error bars in Figure 5.19.

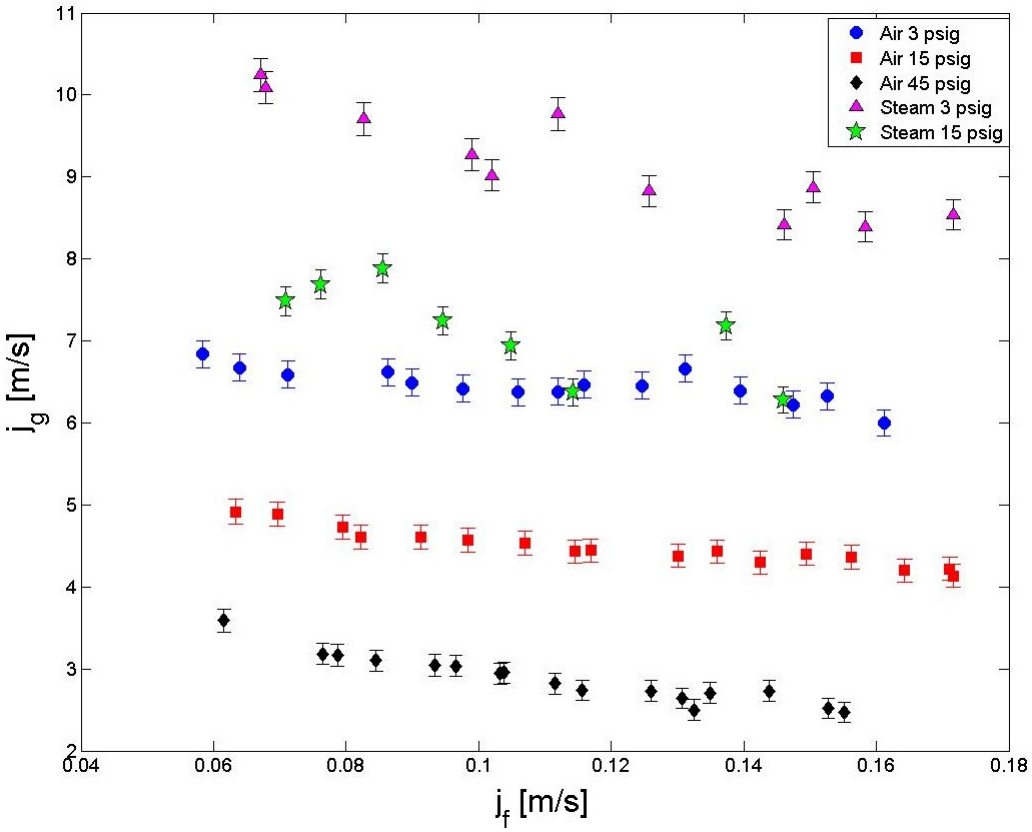

Figure 5.19: Flooding data plotted with error bars.

6. CONCLUSIONS AND FUTURE WORK

6.1 Conclusions

The flooding test facility in the Nuclear Heat Transfer Systems Laboratory was extensively modified to allow testing for air/water and steam/water flooding data at higher pressures. An experimental investigation to acquire fundamental flooding data at elevated pressures has been conducted. The major modifications made to the test facility are listed below:

1. A large capacity air supply was designed and installed in the laboratory to allow for high pressure air/water flooding tests.

2. The test facility piping was altered to allow the steam/water and air/water flow paths to be nearly identical. This produces flooding data that is directly comparable, unaffected by reactor-specific geometry.

3. Flow instrumentation was sized and installed to measure the outlet gas and liquid flow rates exiting the test section.

4. The facility connections and vessels were upgraded to withstand high pressure testing. A back pressure regulator was installed to control the system pressure during the flooding tests.

5. The water flow paths were extensively upgraded with the addition of two new hot water pumps and two compact plate type heat exchangers.

6. A phase separator was added to the test section outlet to adequately separate the two-phase mixture for measurement.

7. The facility structure was reinforced and additional instrumentation was added for future flooding experiments.

8. The laboratory domestic water plumbing and electrical were upgraded for increased safety for lab personnel. A machine shop was established in the lab for the current research and for future projects within the Nuclear Engineering Department.

The steam/water tests were performed at up to 30 psia and the air/water tests were performed at up to 60 psia, yielding some of the first fundamental flooding data at higher pressures in a large diameter vertical tube. The data at higher pressures suggest that the momentum transfer necessary for the onset of flooding is achievable for lower superficial velocities as the gas density increases.

Onset of flooding curves for elevated pressure data were generated using the non-dimensional Kutateladze numbers, which are more suitable for large diameter vertical tubes. The curves can be used to further investigate the fluid property effects, such as density and viscosity, in the flooding correlations used in practice. If condensation is accounted for, the saturated steam/water data at higher pressure closely trends with the air/water flooding data. This information can be used for improving empirical flooding models with the eventual goal to develop a mechanistic model that can be incorporated into nuclear reactor safety codes. The data can be used for code validation in preventing flooding in the pressurizer surge line of a PWR.

6.2 Future Work

The suggestions for future work involving this flooding facility include:

1. Saturated steam/water flooding data should be obtained at full system pressure of 45 psig. This will provide a good comparison to the acquired air/water data to investigate the effects of the liquid-gas density ratio.

2. Improvements should be made to the facility to precisely maintain the water inlet temperature at the saturation temperature. By eliminating the water subcooling, better comparisons can be made to the air/water data without regard to the effect of phase change on the momentum transfer at the interface. Reducing the heat loss from the test section would also help make for a more accurate comparison.

3. Efforts should be made to find the location of flooding inside the test section. This information would be very useful since one could then determine and/or measure the effective steam flow rate at the onset flooding location. An impedance sensor or probe could be installed near this axial location to measure the annular film thickness prior to flooding. The thickness could then be used to improve the flooding correlation developed by Ritchey to adequately account for condensation inside the test section.

4. Air/water flooding tests should be performed with near saturated water to understand and quantify the effect of the liquid density and surface tension on the flooding correlations. The facility can reasonably achieve a water inlet temperature of 95 °C for atmospheric air/water tests as an initial scoping analysis.

5. Curves defining the conditions of full flow reversal using steam/water and air/water fluid pairs have not been created for large diameter vertical tubes at higher pressure. These tests would fully define the flooding spectrum of the test section and can be used to validate the full flow reversal prediction that can be inferred from the Ritchey correlation, that is $Ku_{ge}^{1/2} = 1.45$.

6. The test facility has design features that allow subcooled steam/water tests to be conducted at higher pressures. This data would be unique for large diameter tubes. The hysteresis effect mentioned by Tien [16] can be investigated for subcooled steam/water testing.

REFERENCES

[1] AlfaLaval. *AlfaNova 27 Datasheet*. 5400 International Trade Drive, Richmond, VA 23231 USA. Document No: PCT0034EN 0801.

[2] AMT. *489A-98 High Heat Straight Centrifugal Pump Datasheet*. 400 Spring Street, Royersford, PA 19468 USA. Document No: STE-10.

[3] Azbil. *MagneW 3000 PLUS Smart Electromagnetic Flowmeter Detector Datasheet*. 1-12-2 Kawana, Fujisawa, Kanagawa 251-8522 Japan, 12 edition, 2012.

[4] Anderson Separator Company. *Line Type Models Type LC Separator Datasheet*. 16633 Foltz Industrial Parkway, Strongsville, OH 44149 USA, Jun. 2002. Bulletin: A100.50c.

[5] Quincy Compressor. *QT and QTS Series Compressors Instruction Manual*. 701 North Dobson Avenue, Bay Minette, AL 36507, Jan. 2013. Manual No. 50161-108.

[6] Wes Cullum. Subcooling effects for flooding experiments with steam and water in a large diameter vertical tube. Master's thesis, Texas A&M University, 2012.

[7] Liquidflo. *Installation, Operation, and Maintenance Manual*. 443 North Avenue, Garwood, NJ 07027 USA, Dec. 2006. Document No: 3.20.023.

[8] W Mattar and J Vignos. Vortex shedding tutorial. Technical report, Invensys, Foxboro, January 2010. Retrieved from `http://iom.invensys.com/EN/pdfLibrary/WhitePaper_Foxboro_VortexSheddingTutorial_01-10.pdf`, Accessed March 5, 2015.

[9] Emerson Process. Principles of direct-operated regulators. Technical report, Emerson Process Management. Retrieved from `http://www.documentation.emersonprocess.com/groups/public/documents/reference/d351798x012_05.pdf`, Accessed October 9, 2015.

[10] OL Pushkina and Yu L Sorokin. Breakdown of liquid film motion in vertical tubes. *Heat Transfer Sov. Res*, 1(5):56–64, 1969.

[11] Paul H Rothe and Christopher J Crowley. Scaling of pressure and subcooling for countercurrent flow, quarterly progress report, 1 april-30–june 1978. Technical report, Creare, Inc., Hanover, NH (USA), 1978.

[12] TK Sherwood, GH Shipley, and FAL Holloway. Flooding velocities in packed columns. *Industrial & Engineering Chemistry*, 30(7):765–769, 1938.

[13] Matthew Aaron Solmos. An experimental investigation of the countercurrent flow limitation. Master's thesis, Texas A&M University, 2008.

[14] M Solom, K Vierow, and A Nosek. Experimental investigation of thermal hydraulic limits of bwr rcic system operation under long-term operation. Hyatt Regency, Chicago, IL, 2015. Proc. of 16th International Topical Meeting on Nuclear Reactor Thermal Hydraulics (NURETH-16).

[15] Yu L Sorokin, AA Kirdyashkin, and BG Pokusaev. Investigation of the stability of the film flow of liquid in a vertical pipe with an upward flow of gas. *Chemical and Petroleum Engineering*, 1(5):401–405, 1965.

[16] CL Tien. A simple analytical model for counter-current flow limiting phenomena with vapor condensation. *Letters in Heat and Mass Transfer*, 4(3):231–237, 1977.

[17] Christophe Vallée, Tobias Seidel, Dirk Lucas, Matthias Beyer, Horst-Michael Prasser, Heiko Pietruske, Peter Schütz, and Helmar Carl. Counter-current flow

limitation in a model of the hot leg of a pwrcomparison between air/water and steam/water experiments. *Nuclear Engineering and Design*, 245:113–124, 2012.

[18] M Vijayan, S Jayanti, and AR Balakrishnan. Effect of tube diameter on flooding. *International journal of multiphase flow*, 27(5):797–816, 2001.

[19] GB Wallis. Dc desieyes, rj rosselli, and j. lacombe. *Countercurrent Annular Flow Regimes for Steam and Subcooled Water in a Vertical Tube, NP-1336, Research Project 443*, 2, 1980.

[20] Graham B Wallis. Flooding velocities for air and water in vertical tubes. Technical report, United Kingdom Atomic Energy Authority, Reactor Group, Winfrith (United Kingdom), 1961.

[21] Susan Nicole Williams. Flooding experiments with steam and water in a large diameter vertical tube. Master's thesis, Texas A&M University, 2009.

APPENDIX A

EXPERIMENTAL INSTRUMENTATION

The details of each instrument including the location, manufacturer, model, calibrated range, and accuracy are shown in Table A.1.

Table A.1: Instrumentation used for flooding tests.

Instrument	**Location**	**Model**	**Range**	**Accuracy**
Thermocouples	Throughout Facility	Omega Type T	-250-350 °C	0.5 °C
Absolute Pressure Transmitter	Gas Inlet	Honeywell ST3000 STA940	0-130 psia	0.1% Span
Absolute Pressure Transmitter	Gas Outlet	Honeywell ST3000 STA940	0-100 psia	0.1% Span
Absolute Pressure Transmitter	Steam Generator	Honeywell ST3000 STA940	0-150 psia	0.1% Span
Absolute Pressure Transmitter	Test Section	Keller Valueline	0-150 psia	0.1% Span
Differential Pressure Transmitter	Steam Generator Level	Honeywell ST3000 STD924	0-110 inH2O	0.075% Span
Differential Pressure Transmitter	Water Supply Tank Level	Honeywell ST3000 STD924	0-80 inH2O	0.075% Span
Differential Pressure Transmitter	Test Section	Honeywell ST3000 STD924	0-100 inH2O	0.075% Span
Differential Pressure Transmitter	Holdup Tank Level	Rosemount 3051S	0-25 inH2O	0.035% Span
Gauge Pressure Transmitter	Holdup Tank	Dwyer 673-7	0-100 psig	0.25% Span
Gauge Pressure Transmitter	Water Supply Tank	Dwyer 673-7	0-100 psig	0.25% Span
Gauge Pressure Transmitter	Water Inlet	Dwyer 673-7	0-100 psig	0.25% Span
Vortex Flow Meter	Gas Inlet	Foxboro Model 83W-A	0-2400 Hz	1% Value
Vortex Flow Meter	Gas Outlet	Foxboro Model 84F	0-140 CFM	1% Value
Magnetic Flow Meter	Water Inlet	Azbil MagneW 3000 Plus	0-20 GPM	0.5% Value
Magnetic Flow Meter	Water Carryover	Azbil MagneW 3000 Plus	0-10 GPM	0.5% Value
Hygrometer	Gas Inlet	Dwyer HHT	0-100% RH	2% Value

APPENDIX B

ENGINEERING DRAWINGS

Dimensional drawings of the modified steam outlet and long elbow assembly are provided below. Drawings of the holdup tank nozzle flanges are also included. The initials "NM" refer to the author's former name.

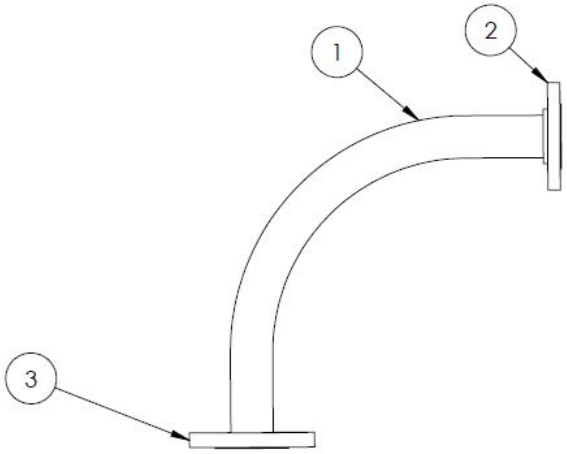

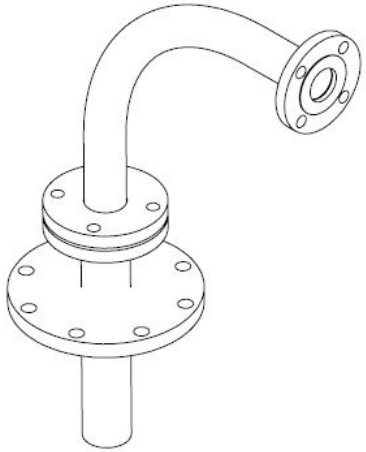

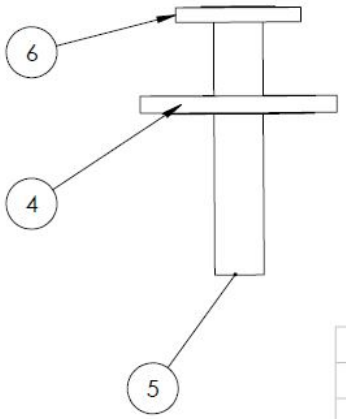

ITEM NO.	SW-Part Number	DESCRIPTION	QTY.
1	LONG ELBOW	2 INCH SCH40 LONG ELBOW	1
2	SMALL ELBOW FLANGE	STOCK 2 INCH SOCKET WELD FLANGE	1
3	REDUCING FLANGE	2.5 INCH FLANGE	1
4	LARGE STEAM OUTLET FLANGE	6 INCH FLANGE	1
5	STEAM OUTLET TUBE	TUBING 2.75OD 2.25ID INCH	1
6	SMALL STEAM OUTLET FLANGE	2.5 INCH FLANGE	1

		UNLESS OTHERWISE SPECIFIED:		NAME	DATE
		DIMENSIONS ARE IN INCHES TOLERANCES: FRACTIONAL ± 1/64 ANGULAR: MACH ± 0.1 BEND ±	DRAWN		19JAN2015
		TWO PLACE DECIMAL ± 0.01 THREE PLACE DECIMAL ± 0.005	CHECKED		
			ENG APPR.		
		INTERPRET GEOMETRIC TOLERANCING PER:	MFG APPR.		
		MATERIAL	Q.A.		
		FINISH	COMMENTS: REMOVE ALL BURRS, SHARP EDGES, LOOSE SCALE, AND WELD SPATTER		
NEXT ASSY	USED ON				
APPLICATION		DO NOT SCALE DRAWING			

TEXAS A&M UNIVERSITY

TITLE:

STEAM OUTLET AND ELBOW ASSEMBLY

SIZE	DWG. NO.	REV
A	1-1	
SCALE: 1:12	WEIGHT:	SHEET 1 OF 9

5 4 3 2 1

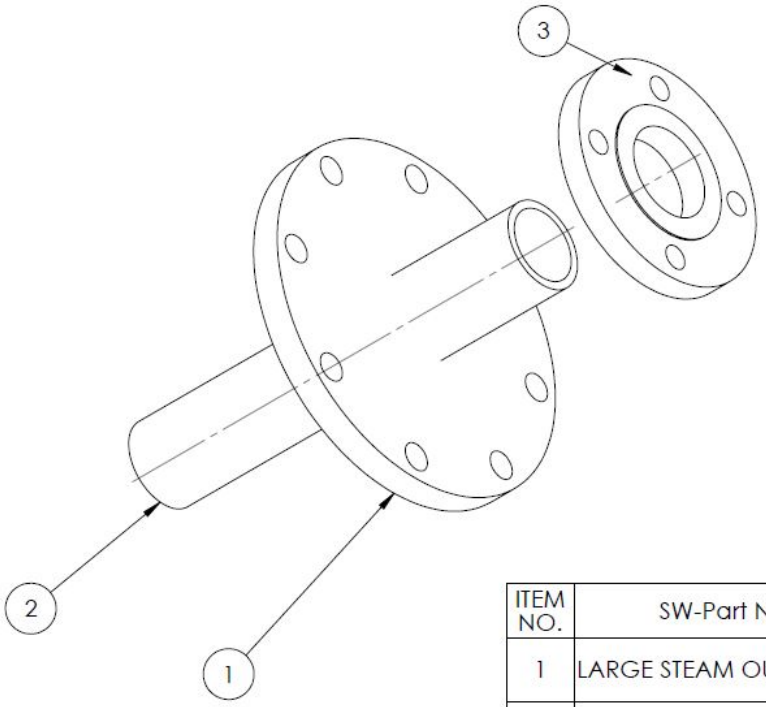

TOP VIEW

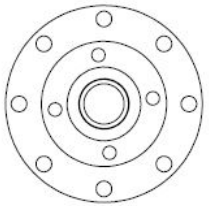

ITEM NO.	SW-Part Number	DESCRIPTION	QTY.
1	LARGE STEAM OUTLET FLANGE	6 INCH FLANGE	1
2	STEAM OUTLET TUBE	TUBING 2.75OD 2.25ID INCH	1
3	SMALL STEAM OUTLET FLANGE	2.5 INCH FLANGE	1

UNLESS OTHERWISE SPECIFIED:

DIMENSIONS ARE IN INCHES
TOLERANCES:
FRACTIONAL ± 1/64
ANGULAR: MACH ± 0.1 BEND ± 1
TWO PLACE DECIMAL ± 0.01
THREE PLACE DECIMAL ± 0.005

INTERPRET GEOMETRIC TOLERANCING PER:

MATERIAL
SS304

FINISH

NEXT ASSY | USED ON

APPLICATION | DO NOT SCALE DRAWING

	NAME	DATE
DRAWN	N.M.	19JAN2015
CHECKED		
ENG APPR.		
MFG APPR.		
Q.A.		

COMMENTS:

REMOVE ALL BURRS, SHARP EDGES, LOOSE SCALE, AND WELD SPATTER

TEXAS A&M UNIVERSITY

TITLE:
STEAM OUTLET EXPLODED VIEW

SIZE A | DWG. NO. 2-1 | REV

SCALE: 1:8 | WEIGHT: | SHEET 2 OF 9

5 4 3 2 1

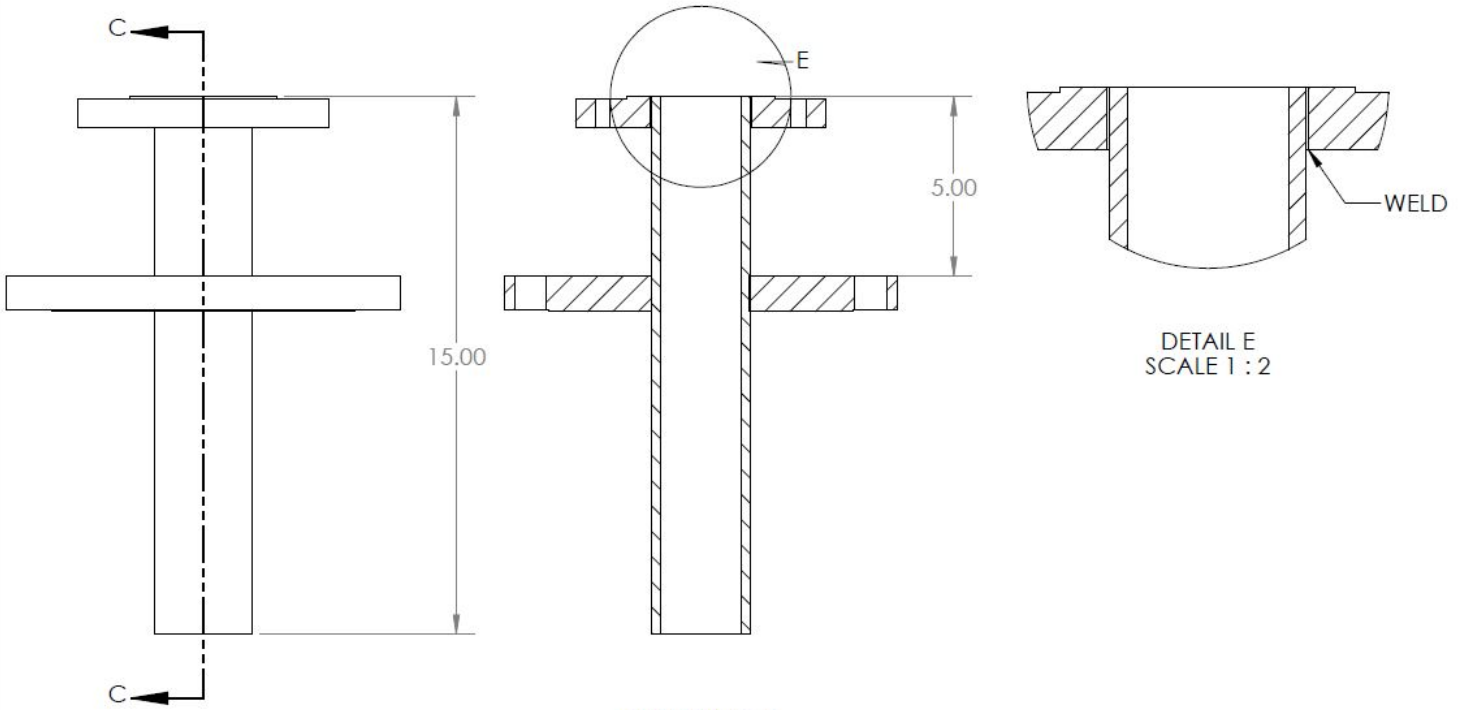

UNLESS OTHERWISE SPECIFIED:		NAME	DATE	TEXAS A&M UNIVERSITY	
DIMENSIONS ARE IN INCHES TOLERANCES: FRACTIONAL ± 1/64 ANGULAR: MACH ± 0.1 BEND ± TWO PLACE DECIMAL ± 0.01 THREE PLACE DECIMAL ± 0.005	DRAWN	N.M.	19JAN2015	TITLE: STEAM OUTLET	
	CHECKED				
	ENG APPR.				
	MFG APPR.				
INTERPRET GEOMETRIC TOLERANCING PER:	Q.A.				
MATERIAL SS304	COMMENTS: REMOVE ALL BURRS, SHARP EDGES, LOOS SCALE, AND WELD SPATTER			SIZE A	DWG. NO. 2-2 REV
FINISH				SCALE: 1:8	WEIGHT: SHEET 3 OF 9
DO NOT SCALE DRAWING					

USED ON
APPLICATION
NEXT ASSY

5 4 3 2 1

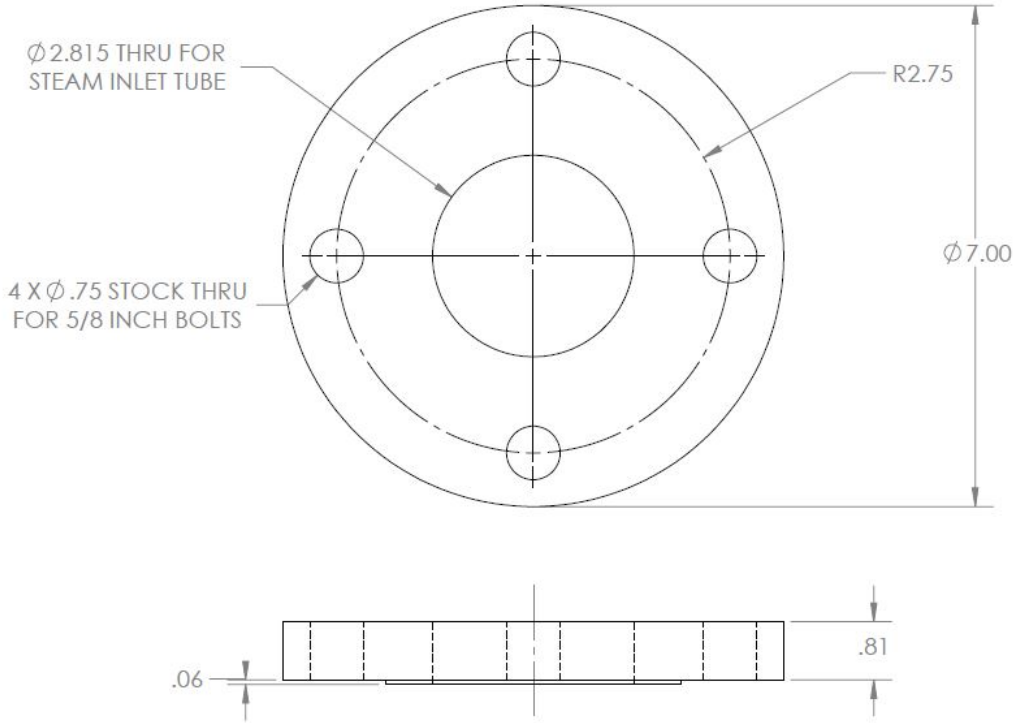

UNLESS OTHERWISE SPECIFIED:		NAME	DATE	TEXAS A&M UNIVERSITY	
DIMENSIONS ARE IN INCHES TOLERANCES: FRACTIONAL ± 1/64 ANGULAR: MACH ± 0.1 BEND ± TWO PLACE DECIMAL ± 0.01 THREE PLACE DECIMAL ± 0.005	DRAWN	N.M.	19JAN2015	TITLE: SMALL STEAM OUTLET FLANGE	
	CHECKED				
	ENG APPR.				
	MFG APPR.				
INTERPRET GEOMETRIC TOLERANCING PER:	Q.A.				
MATERIAL SS 304	COMMENTS: STOCK 2.5 INCH BLIND FLANGE, DO NOT DAMAGE FACE			SIZE A	DWG. NO. 2-3 REV
FINISH				SCALE: 1:2	WEIGHT: SHEET 4 OF 9
APPLICATION / USED ON					
DO NOT SCALE DRAWING					

5 4 3 2 1

ITEM NO.	SW-Part Number	DESCRIPTION	QTY.
1	LONG ELBOW	2 INCH SCH40 LONG ELBOW	1
2	SMALL ELBOW FLANGE	STOCK 2 INCH SOCKET WELD FLANGE	1
3	REDUCING FLANGE	2.5 INCH FLANGE	1

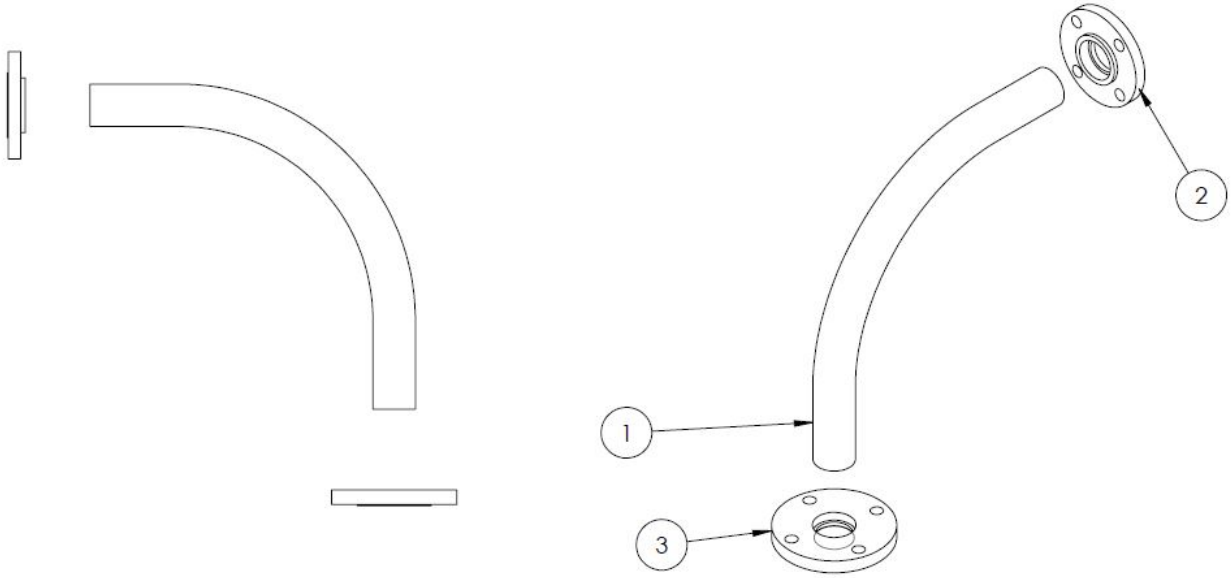

UNLESS OTHERWISE SPECIFIED:

DIMENSIONS ARE IN INCHES
TOLERANCES:
FRACTIONAL ± 1/64
ANGULAR: MACH ± 0.1 BEND ± 1
TWO PLACE DECIMAL ± 0.01
THREE PLACE DECIMAL ± 0.005

INTERPRET GEOMETRIC TOLERANCING PER:

MATERIAL: SS 304

FINISH

	NAME	DATE
DRAWN	N.M.	19JAN2015
CHECKED		
ENG APPR.		
MFG APPR.		
Q.A.		

COMMENTS:
REMOVE ALL BURRS, SHARP EDGES, LOOSE SCALE, AND WELD SPATTER

NEXT ASSY | USED ON

APPLICATION | DO NOT SCALE DRAWING

TEXAS A&M UNIVERSITY

TITLE: ELBOW EXPLODED VIEW

SIZE A | DWG. NO. 3-1 | REV

SCALE: 1:12 | WEIGHT: | SHEET 5 OF 9

5 4 3 2 1

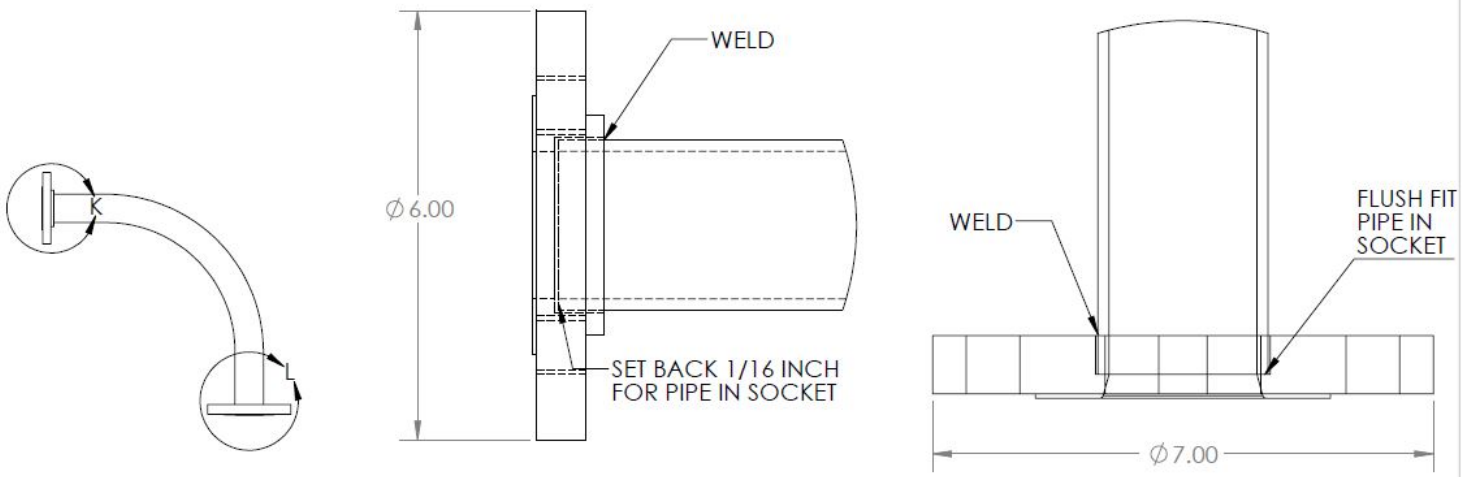

DETAIL K
SCALE 1 : 2

DETAIL L
SCALE 1 : 2

UNLESS OTHERWISE SPECIFIED:		NAME	DATE	TEXAS A&M UNIVERSITY	
DIMENSIONS ARE IN INCHES TOLERANCES: FRACTIONAL ± 1/64 ANGULAR: MACH ± 0.1 BEND ±	DRAWN	N.M.	19JAN2015	TITLE:	ELBOW
	CHECKED				
TWO PLACE DECIMAL ± 0.01 THREE PLACE DECIMAL ± 0.005	ENG APPR.				
	MFG APPR.				
INTERPRET GEOMETRIC TOLERANCING PER:	Q.A.				
MATERIAL SS 304	COMMENTS: REMOVE ALL BURRS, SHARP EDGES, LOOS SCALE, AND WELD SPATTER			SIZE A	DWG. NO. 3-2
FINISH				SCALE: 1:12	WEIGHT:
DO NOT SCALE DRAWING					SHEET 6 OF 9

5 4 3 2 1

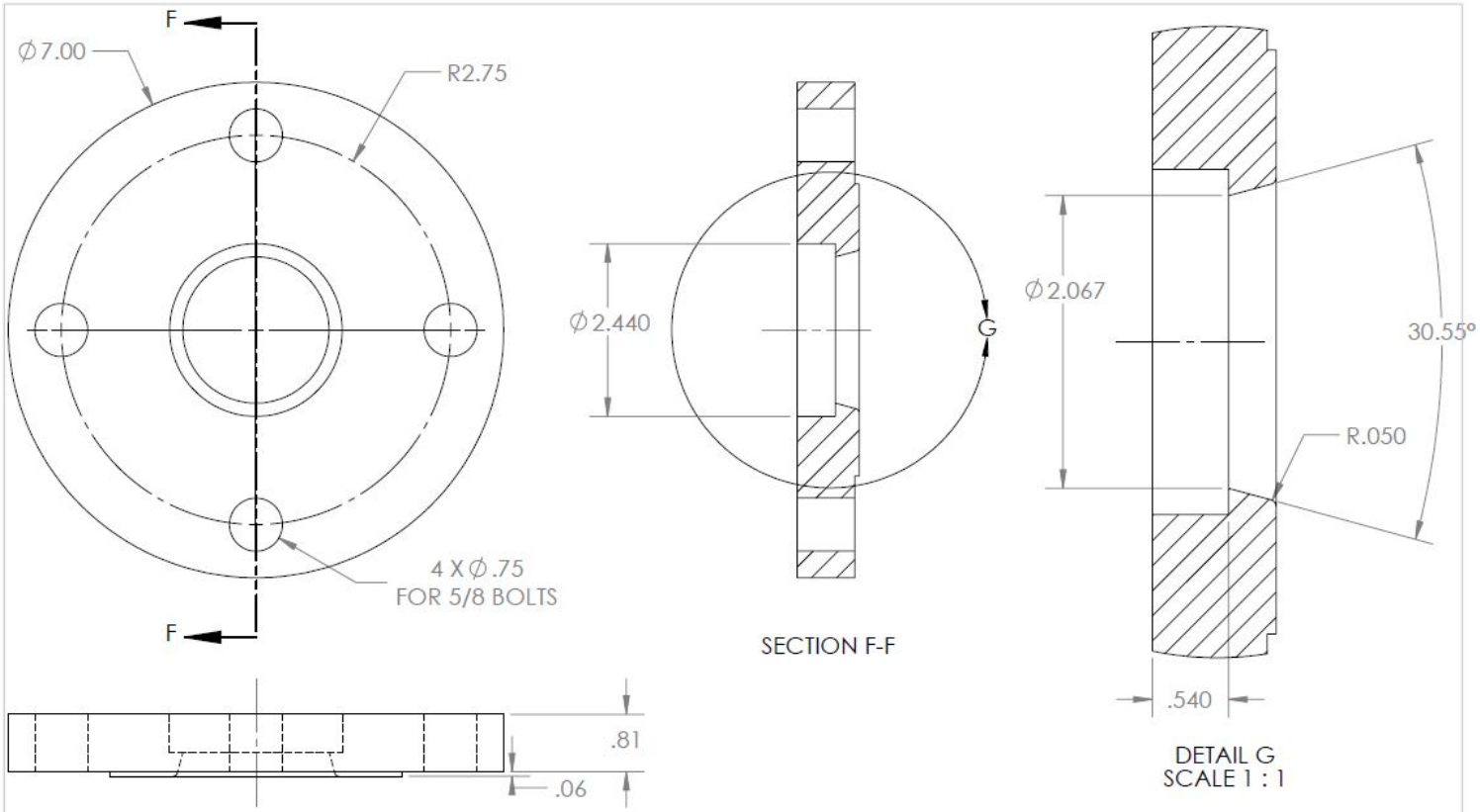

		UNLESS OTHERWISE SPECIFIED:		NAME	DATE
		DIMENSIONS ARE IN INCHES TOLERANCES: FRACTIONAL± 1/64 ANGULAR: MACH± 0.1 BEND ± TWO PLACE DECIMAL ± 0.01 THREE PLACE DECIMAL ± 0.005	DRAWN	N.M.	19JAN2015
			CHECKED		
			ENG APPR.		
			MFG APPR.		
		INTERPRET GEOMETRIC TOLERANCING PER:	Q.A.		
		MATERIAL SS 304	COMMENTS: STOCK 2.5 INCH BLIND FLANGE DO NOT DAMAGE FACE		
		FINISH			
NEXT ASSY	USED ON				
APPLICATION		DO NOT SCALE DRAWING			

TEXAS A&M UNIVERSITY

TITLE: REDUCING FLANGE

SIZE	DWG. NO.	REV
A	3-3	

SCALE: 1:2 | WEIGHT: | SHEET 7 OF 9

5 4 3 2 1

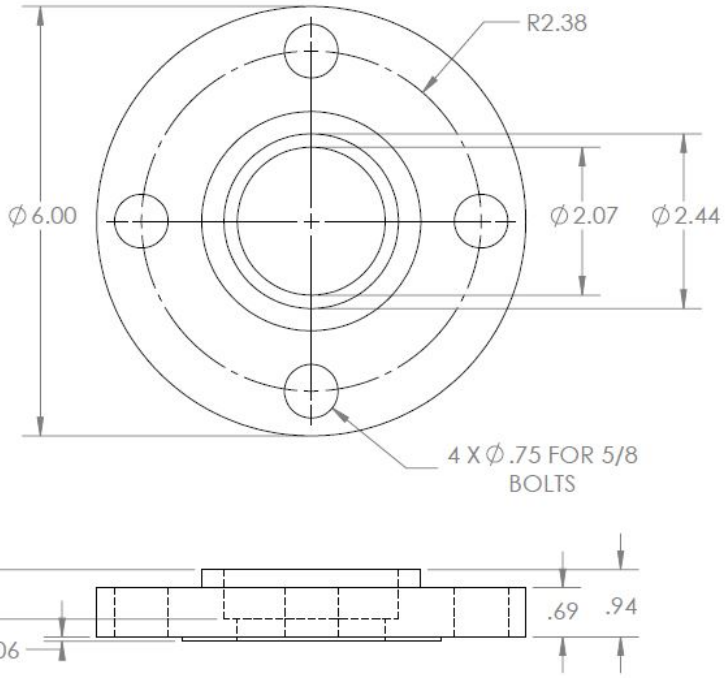

		UNLESS OTHERWISE SPECIFIED:		NAME	DATE
		DIMENSIONS ARE IN INCHES TOLERANCES: FRACTIONAL ± 1/64 ANGULAR: MACH ± 0.1 BEND ± 1 TWO PLACE DECIMAL ± 0.01 THREE PLACE DECIMAL ± 0.005	DRAWN	N.M.	20JAN2015
			CHECKED		
			ENG APPR.		
			MFG APPR.		
		INTERPRET GEOMETRIC TOLERANCING PER:	Q.A.		
		MATERIAL	COMMENTS:		
	USED ON	FINISH SS 304	STOCK 2 INCH SOCKET WELD FLANGE, CLASS 150		
	APPLICATION	DO NOT SCALE DRAWING			

TEXAS A&M UNIVERSITY

TITLE: SMALL ELBOW FLANGE

SIZE	DWG. NO.	REV
A	3-4	
SCALE: 1:2	WEIGHT:	SHEET 8 OF 9

5 4 3 2 1

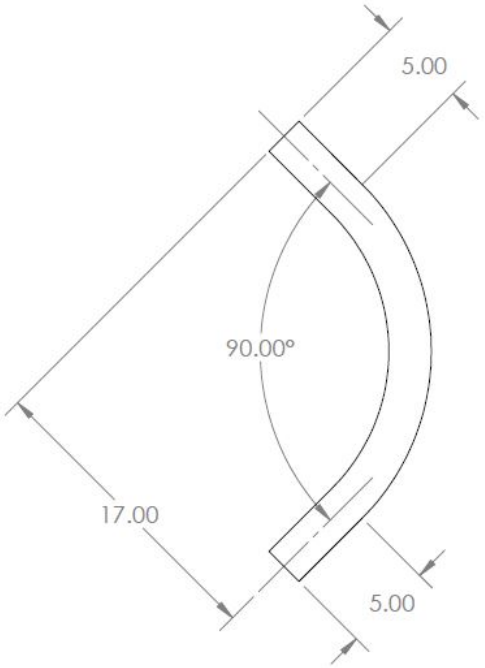

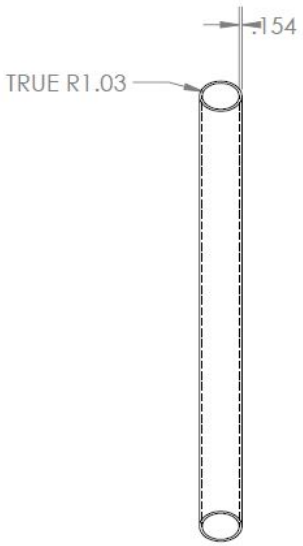

UNLESS OTHERWISE SPECIFIED:		NAME	DATE	TEXAS A&M UNIVERSITY	
DIMENSIONS ARE IN INCHES TOLERANCES: FRACTIONAL ± 1/64 ANGULAR: MACH ± 0.1 BEND ±	DRAWN	N.M.	19JAN2015	TITLE: LONG ELBOW	
TWO PLACE DECIMAL ± 0.01 THREE PLACE DECIMAL ± 0.005	CHECKED				
	ENG APPR.				
	MFG APPR.				
INTERPRET GEOMETRIC TOLERANCING PER:	Q.A.				
MATERIAL	COMMENTS: STOCK 2 INCH SCH 40 PIPE			SIZE A	DWG. NO. 3-5 REV
FINISH				SCALE: 1:8	WEIGHT: SHEET 9 OF 9
DO NOT SCALE DRAWING					

NEXT ASSY	USED ON
APPLICATION	

5 4 3 2 1

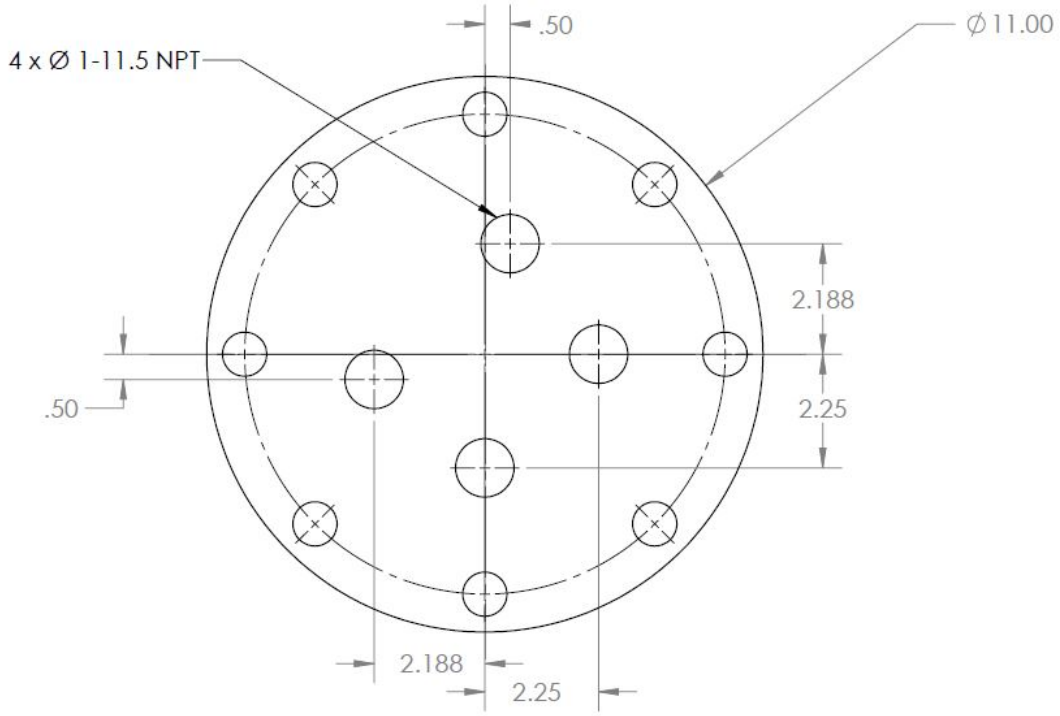

		UNLESS OTHERWISE SPECIFIED:		NAME	DATE
		DIMENSIONS ARE IN INCHES TOLERANCES: FRACTIONAL ± ANGULAR: MACH ± BEND ± TWO PLACE DECIMAL ±.01 THREE PLACE DECIMAL ± .01	DRAWN		
			CHECKED		
			ENG APPR.		
			MFG APPR.		
		INTERPRET GEOMETRIC TOLERANCING PER:	Q.A.		
		MATERIAL SS 304	COMMENTS:		
NEXT ASSY	USED ON	FINISH	STOCK BLIND FLANGE		
APPLICATION		DO NOT SCALE DRAWING			

TEXAS A&M UNIVERSITY

TITLE:

Nozzle 1

SIZE	DWG. NO.	REV
A	4-1	
SCALE: 1:3	WEIGHT:	SHEET 1 OF 1

5 4 3 2 1

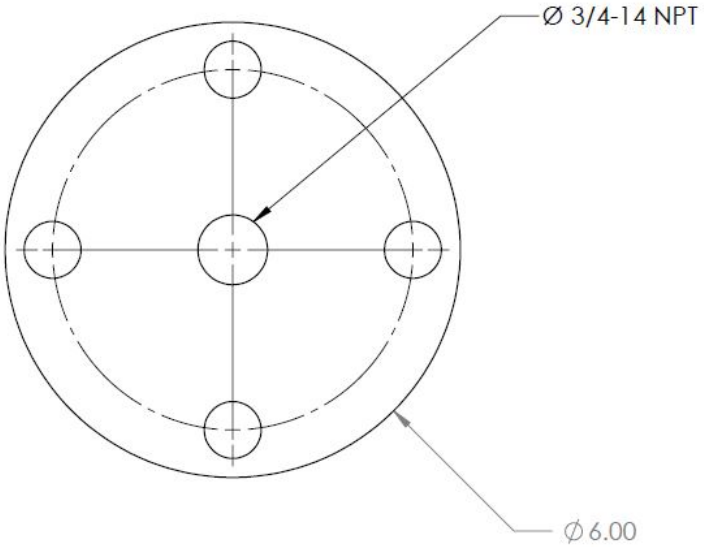

		UNLESS OTHERWISE SPECIFIED:		NAME	DATE
		DIMENSIONS ARE IN INCHES TOLERANCES: FRACTIONAL ± ANGULAR: MACH ± BEND ± TWO PLACE DECIMAL ± .01 THREE PLACE DECIMAL ± .01	DRAWN		
			CHECKED		
			ENG APPR.		
			MFG APPR.		
		INTERPRET GEOMETRIC TOLERANCING PER:	Q.A.		
		MATERIAL: SS304	COMMENTS: STOCK 2 INCH BLIND FLANGE		
NEXT ASSY	USED ON	FINISH			
APPLICATION		DO NOT SCALE DRAWING			

TEXAS A&M UNIVERSITY

TITLE: Nozzle 2

SIZE	DWG. NO.	REV
A	4-2	

SCALE: 1:2 | WEIGHT: | SHEET 1 OF 1

5 4 3 2 1

APPENDIX C

MATLAB SCRIPTS

This appendix includes the MATLAB scripts used to graph the time dependent data, to reduce the raw data, and to compute the average carryover flow rate during flooding.

C.1 Plotting the Data

Below is the MATLAB script used to graph the time dependent data. The scripts used to graph steam and air are nearly identical, the only differences are in some of the column numbers in the data matrix.

```
cvin=load('filename.dat'); %Steam data has different column numbers
gasflowin=cvin(:,83);
gasflowout=cvin(:,92);
gasflowoutq=cvin(:,90);
gasflowinq=cvin(:,84);
gasoutdensity=cvin(:,91);
gasoutp=cvin(:,95);
tsdp=cvin(:,110);
tsabsp=cvin(:,101);
holdupgaugep=cvin(:,107);
holduptanklevel=cvin(:,104);
waterflowin=cvin(:,72);
carryover=cvin(:,77);
relativehumid=cvin(:,98);
mainsteamt=cvin(:,26);
```

```
mainsteamp=cvin(:,87);

timeend=0.1*(length(gasflowin)-1);
time=0:0.1:timeend;
time=time'; %Transpose

%Uncomment to Trim Plots
%start=find(time==0); %Begins the start of the trimmed data
%len=1500; %last index of untrimmed data
%time=time(1:len+1-start);
%gasflowin=gasflowin(start:len);
%gasflowout=gasflowout(start:len);
%gasflowoutq=gasflowoutq(start:len);
%gasflowinq=gasflowinq(start:len);
%gasoutdensity=gasoutdensity(start:len);
%tsdp=tsdp(start:len);
%tsabsp=tsabsp(start:len);
%holdupgaugep=holdupgaugep(start:len);
%holduptanklevel=holduptanklevel(start:len);
%waterflowin=waterflowin(start:len);
%carryover=carryover(start:len);
%relativehumid=relativehumid(start:len);
%mainsteamt=mainsteamt(start:len);
%mainsteamp=mainsteamp(start:len);

plot(time,tsdp);
xlabel('Time (s)','fontsize',16);
ylabel('Test Section Differential Pressure [inH2O]','fontsize',16);
print('-djpeg','TestSectionDP')

    plot(time,gasflowin,'LineWidth',1);
```

```
    hold on
    plot(time(1),gasflowout(1),'-go','LineWidth',1,...
'MarkerFaceColor','g');
    plot(time,gasflowout,'g','LineWidth',1);
    plot(time(1:75:end),gasflowout(1:75:end),'go','LineWidth',1,...
'MarkerFaceColor','g');
    legend('Inlet','Outlet')
    hold off;
    xlabel('Time (s)','fontsize',16);
    ylabel('Air Flow Rate (g/s)','fontsize',16);
    print('-djpeg','MassGasFlow');




    plot(time,gasflowinq,'LineWidth',1);
    hold on
    plot(time(1),gasflowoutq(1),'-go','LineWidth',1,...
'MarkerFaceColor','g');
    plot(time,gasflowoutq,'g','LineWidth',1);
    plot(time(1:50:end),gasflowoutq(1:50:end),'go','LineWidth',1,...
'MarkerFaceColor','g');
    legend('Inlet','Outlet');
    hold off;
    xlabel('Time (s)','fontsize',16);
    ylabel('Air Flow Rate (ft^3/min)','fontsize',16);
    print('-djpeg','VolumeGasFlow.jpg');
```

```
    plot(time,waterflowin,'LineWidth',1);
    hold on
    plot(time(1),carryover(1),'-ro','LineWidth',1,...
'MarkerFaceColor','r');
    plot(time,carryover,'r','LineWidth',1);
    plot(time(1:75:end),carryover(1:75:end),'ro','LineWidth',1,...
'MarkerFaceColor','r');
    legend('Inlet','Carryover');
    hold off;
    xlabel('Time (s)','fontsize',16);
    ylabel('Water Flow Rate (GPM)','fontsize',16);
    print('-djpeg','WaterFlow.jpg');

    plot(time,tsabsp-14.540,'LineWidth',1);
    hold on
    plot(time(1),holdupgaugep(1),'-ko','LineWidth',1,...
'MarkerFaceColor','k');
    plot(time,holdupgaugep,'k','LineWidth',1);
    plot(time(1:75:end),holdupgaugep(1:75:end),'ko','LineWidth',1,...
'MarkerFaceColor','k');
    legend('Test Section','Holdup Tank')
    hold off;
    xlabel('Time (s)','fontsize',16);
    ylabel('Pressure (psig)','fontsize',16);
    print('-djpeg','SystemP.jpg');


plot(time,holduptanklevel,'LineWidth',1);
xlabel('Time (s)','fontsize',16);
ylabel('Holdup Tank Level (inches)','fontsize',16);
print('-djpeg', 'HoldupTankLevel.jpg');
```

C.2 Finding the Onset of Flooding

Below is the MATLAB script used to reduce the data and determine the conditions at the onset of flooding.

```
clear all

datafile='filename.dat';
rootname='directory';

for i = 1:1
    filename=[rootname datafile];
    M = load(filename);
    dp = M(:,110);
    len = length(dp);
    dx = 1.0;
    vel_cmpr = dp(1);
    for j = 1:len-1
       if (((dp(j+1)-vel_cmpr))>2*dx)
            vel_cmpr = dp(j+1);
       end
       if (dp(j+1)<(vel_cmpr - 1*dx))
           fprintf('The onset of flooding at row = %d \n', j-1)
     %row of onset of flooding
           fprintf('Time of Flooding in file = %8.4f seconds \n',...
     M(j-1,1)) % time at onset of flooding in raw file
           fprintf('Time of Flooding in plots = %8.3f seconds \n',...
     M(j-1,1)-M(1,1)) %time at onset of flooding in plots
           fprintf('The minimum dP during flooding = %8.4f inH2O\n',...
    min(M(j-1:j+200,110)))  % min dp
```

```
            fprintf('The mean dP during flooding = %8.4f inH2O\n',...
        mean(M(j-1:j+200,110))) % mean dp
            fprintf('The test section pressure at onset = %8.2f psia\n',...
        M(j-1,101)) %Test section abs P at onset of flooding
            M(j-1,:)              % parameters at flooding
            break
        end
    end
end
```

C.3 Calculating the Average Carryover Flow Rate

Below is the MATLAB script for determining the average carryover flow rate after the onset of flooding.

```
cvin=load('filename.dat');
gasflowin=cvin(:,84); %Steam has different columns
tsdp=cvin(:,111); %Steam has different columns
carryover=cvin(:,77);

%%%%%%%%%%%%%%%%%%%%%%%%%%%%%%%%%%%%%%%%%%%%%%%%%%%%%%%%
%                CARRYOVER CALCULATION
%%%%%%%%%%%%%%%%%%%%%%%%%%%%%%%%%%%%%%%%%%%%%%%%%%%%%%%%

for i = 1:1
    len = length(tsdp); %Sets the length of index
    dx = 1.0;     % Adjusts the space for searching in deltaP
    vel_cmpr = tsdp(1); % Is the comparison counter in deltaP search
    for j = 200:len-1
    %This loop searches for onset of flooding
       if (((tsdp(j+1)-vel_cmpr))>2*dx)
            vel_cmpr = tsdp(j+1);
       end
       if (tsdp(j+1)<(vel_cmpr - 1*dx))
           rowstart=j+1;
            fprintf('The onset of flooding = %8.3f seconds \n',...
 rowstart/10) %row of gas flow
           for k= j+1:len
    %This loop searches for the end of gas inlet flow
               if(1000*gasflowin(k)<10)
```

```
                    rowend=k;
                    fprintf('The end of gas flow = %8.3f seconds \n',...
 rowend/10) %row of gas flow
                    for l=rowstart:len
          %This loop searches for the beginning of carryover
                        if carryover(l)>0.1
                            carrystart=l;
                            delay=carrystart-rowstart;
                            fprintf('The carryover starts' =...
               '%8.3f seconds \n', carrystart/10)
                        timedelay=delay/10;
                            fprintf('The time delay is ='...
              ' %8.3f seconds \n', timedelay)
                            averagecarryover=...
             mean(carryover(carrystart+80:rowend)) %Add 8 seconds to start
                            break
                        end
                    end
                    break
                end
            end
            break
        end
    end
end
```

APPENDIX D

REDUCED DATA SET

The major flow rates and temperatures for each test at the onset of flooding are shown below. Data that were within acceptable ranges and were also collected without any testing abnormalities are considered qualified data.

Table D.1: Air/Water Reduced Data Set at 3 psig.

Gas	Run#	Test	P_{Test} psia	$Q_{carryover}$ GPM	$Q_{f,in}$ GPM	$\dot{m}_{g,in}$ g/s	$\dot{m}_{g,out}$ g/s	$T_{f,in}$ °C	$T_{g,in}$ °C	$T_{g,out}$ °C	Qualify
Air	1	1									No
Air	1	2									No
Air	1	3	17.13	7.17	11.65	36.39	38.76	24.99	13.28	21.80	Yes
Air	1	4	17.29	6.93	11.03	39.06	41.33	25.17	12.81	20.74	Yes
Air	1	5	17.33	6.89	10.66	38.36	41.24	25.19	15.12	21.18	Yes
Air	1	6	17.44	6.35	10.08	39.64	42.19	25.34	19.82	20.64	Yes
Air	1	7	17.77	6.19	9.48	41.82	44.38	25.46	20.08	21.06	Yes
Air	1	8	17.47	5.01	9.01	40.07	42.65	25.57	15.22	21.15	Yes
Air	1	9	17.51	4.57	8.37	40.05	42.58	25.77	14.92	22.04	Yes
Air	1	10	17.46	4.48	8.09	39.54	42.63	25.86	14.46	21.44	Yes
Air	1	11	17.44	3.40	7.66	39.51	42.54	25.98	14.55	21.50	Yes
Air	1	12	17.51	3.01	7.06	39.97	43.29	26.06	16.21	20.92	Yes
Air	1	13	17.61	2.56	6.50	40.49	43.60	26.08	15.21	21.52	Yes
Air	1	14	17.77	2.45	6.24	41.76	45.46	26.19	15.72	20.99	Yes
Air	1	15	17.78		5.66	41.16	44.81	26.2	15.58	21.55	No
Air	1	16	17.83	1.41	5.15	41.41	45.32	26.23	12.17	22.72	Yes
Air	1	17	18.00	0.90	4.62	42.27	46.60	26.29	13.73	22.23	Yes
Air	1	18	18.20	0.54	4.22	43.78	47.97	26.39	13.49	21.80	Yes

Table D.2: Air/Water Reduced Data Set at 15 psig.

Gas	Run#	Test	P_{Test} psia	$Q_{carryover}$ GPM	$Q_{f,in}$ GPM	$\dot{m}_{g,in}$ g/s	$\dot{m}_{g,out}$ g/s	$T_{f,in}$ °C	$T_{g,in}$ °C	$T_{g,out}$ °C	Qualify
Air	7	1									No
Air	7	2	29.30	7.35	12.41	45.67	45.50	26.29	15.35	22.86	Yes
Air	7	3	29.44	7.36	12.37	46.90	46.08	26.32	15.04	23.59	Yes
Air	7	4	29.55	6.68	11.87	46.80	46.83	26.33	14.62	23.88	Yes
Air	7	5	29.96	6.78	11.30	49.30	49.09	26.35	14.22	23.89	Yes
Air	7	6	29.90	6.37	10.81	49.75	47.57	26.37	14.24	24.07	Yes
Air	7	7	29.77	5.72	10.30	48.21	47.98	26.41	14.07	23.76	Yes
Air	7	8	29.85	5.60	9.83	49.86	48.31	26.42	15.11	22.04	Yes
Air	7	9	29.84	4.70	9.40	49.32	48.30	26.44	15.17	23.29	Yes
Air	7	10	29.88	3.93	8.45	50.12	49.69	26.44	14.05	23.63	Yes
Air	7	11	29.85	3.76	8.28	49.98	49.55	26.44	13.62	23.58	Yes
Air	7	12	30.08	3.34	7.73	51.68	50.94	26.50	13.74	23.39	Yes
Air	7	13	30.34	2.96	7.11	52.39	52.26	26.54	13.45	23.36	Yes
Air	7	14									No
Air	7	15	30.36	2.41	6.60	52.96	52.26	26.60	14.51	23.57	Yes
Air	7	16	30.39	1.44	5.94	52.98	53.18	26.59	13.47	23.39	Yes
Air	7	17	30.76	1.60	5.75	55.14	54.87	26.59	13.51	23.21	Yes
Air	7	18	31.16	1.01	5.03	57.87	57.02	26.64	13.12	23.27	Yes
Air	7	19	31.32	0.54	4.58	58.54	57.99	26.59	12.94	22.97	Yes

Table D.3: Air/Water Reduced Data Set at 45 psig.

Gas	Run#	Test	P_{Test} psia	$Q_{carryover}$ GPM	$Q_{f,in}$ GPM	$\dot{m}_{g,in}$ g/s	$\dot{m}_{g,out}$ g/s	$T_{f,in}$ °C	$T_{g,in}$ °C	$T_{g,out}$ °C	Qualify
Air	5	1									No
Air	5	2									No
Air	5	3	60.25	5.07	11.04	56.57	57.41	26.06	19.00	23.87	Yes
Air	5	4	60.54	5.12	11.22	55.71	53.36	26.09	18.97	24.20	Yes
Air	5	5									No
Air	5	6	61.66	4.73	10.39	63.01	60.65	26.09	18.54	24.26	Yes
Air	5	7	61.43	4.17	9.75	62.19	59.11	26.11	18.22	24.37	Yes
Air	5	8	61.29	4.00	9.58	57.30	59.04	26.17	18.20	24.15	Yes
Air	5	9	61.76	3.89	9.45	61.05	61.29	26.16	18.00	24.48	Yes
Air	5	10	61.62	3.61	9.11	63.12	60.69	26.23	17.67	23.20	Yes
Air	5	11	61.10	2.81	8.36	62.88	61.91	26.28	17.17	23.85	Yes
Air	5	12	62.03	2.72	8.06	65.79	63.58	26.31	17.34	23.87	Yes
Air	5	13a	62.53	2.61	7.50	69.38	66.77	26.40	16.94	24.08	Yes
Air	5	13b	62.73	2.73	7.46	69.32	66.92	26.35	16.75	24.30	Yes
Air	5	14	63.07	2.30	6.98	71.99	70.33	26.41	16.85	24.13	Yes
Air	5	15	63.16	1.88	6.75	72.26	70.77	26.49	16.72	24.27	Yes
Air	5	16	63.42	0.97	6.11	73.92	72.04	26.59	16.90	24.21	Yes
Air	5	17	62.06	1.03	5.69	73.84	72.89	26.55	16.65	24.23	Yes
Air	5	18	61.91	0.64	5.52	73.91	72.09	26.71	18.15	23.59	Yes
Air	5	19	64.12	0.52	4.45	86.49	86.34	26.77	16.47	23.59	Yes

Table D.4: Steam/Water Reduced Data Set at 3 psig.

Gas	Run#	Test	P_{Test} psia	$Q_{carryover}$ GPM	$Q_{f,in}$ GPM	$\dot{m}_{g,in}$ g/s	$\dot{m}_{g,out}$ g/s	$T_{f,in}$ °C	T_{sat} °C	$T_{g,in}$ °C	$T_{g,out}$ °C	Qualify
Steam	11	5	18.18	1.20	4.85	28.18	28.28	104.60	106.05	107.00	106.13	Yes
Steam	11	6	18.18	1.32	4.91	28.74	28.28	105.00	106.05	106.89	106.13	Yes
Steam	11	4	18.24	2.00	5.97	27.22	28.27	106.10	106.15	107.55	106.18	Yes
Steam	11	3	17.23	3.56	7.15	29.64	23.65	101.55	104.49	105.19	104.70	Yes
Steam	11	2	17.19	3.15	7.37	31.72	23.24	101.21	104.43	105.15	104.62	Yes
Steam	15	7	17.55	3.38	8.09	25.67	25.34	104.51	105.03	106.12	105.27	Yes
Steam	11	1	17.27	3.98	8.14	26.19	23.6	103.57	105.27	104.58	104.56	No
Steam	15	6	17.56	4.28	8.60	31.67	25.12	104.86	105.04	105.83	105.138	No
Steam	12	1	17.95	5.11	9.08	33.50	26.69	105.13	105.68	115.51	105.65	Yes
Steam	12	6	17.32	6.36	10.56	26.28	24.02	104.39	104.65	105.32	104.78	Yes
Steam	12	2	16.96	7.23	10.88	33.01	22.44	101.30	104.04	105.23	104.32	Yes
Steam	12	4	17.48	8.28	11.44	26.81	24.85	105.09	104.92	115.48	105.01	Yes
Steam	12	5	17.46	7.82	12.40	29.88	24.66	104.71	104.88	108.58	104.90	Yes

Table D.5: Steam/Water Reduced Data Set at 15 psig.

Gas	Run#	Test	P_{Test} psia	$Q_{carryover}$ GPM	$Q_{f,in}$ GPM	$\dot{m}_{g,in}$ g/s	$\dot{m}_{g,out}$ g/s	$T_{f,in}$ °C	T_{sat} °C	$T_{g,in}$ °C	$T_{g,out}$ °C	Qualify
Steam	14	6	30.48	1.31	5.12	39.45	34.27	121.58	121.78	122.59	122.35	Yes
Steam	14	5	30.19	1.33	5.51	39.98	32.98	121.84	121.48	122.25	122.08	Yes
Steam	15	3	29.61	2.13	6.84	36.93	30.65	121.08	120.86	121.81	121.55	Yes
Steam	15	2	29.78	2.32	7.58	35.71	30.61	121.29	121.04	121.79	121.63	Yes
Steam	15	4	30.39	3.04	6.18	40.76	33.40	122.06	121.69	123.47	122.23	Yes
Steam	14	3	30.21	2.85	6.30	43.45	33.21	120.11	121.50	122.27	122.14	No
Steam	14	2	29.99	1.97	6.97	33.47	31.64	121.59	121.27	122.14	121.8	No
Steam	14	1	29.85	3.76	7.93	30.49	30.55	120.69	121.12	122.91	122.14	No
Steam	15	1	29.65	3.99	8.26	33.26	29.70	119.59	120.90	121.69	121.55	Yes
Steam	13	8	29.29	5.45	9.92	36.12	30.01	120.17	120.52	121.38	121.13	Yes
Steam	13	7	29.62	6.90	10.55	33.04	31.12	121.41	120.87	121.60	121.39	Yes

APPENDIX E

GRAPHICAL DATA

This appendix contains the time dependent data in graphical form for all of the qualified tests. The figure caption identifies the test which corresponds to the numbers in Appendix C.

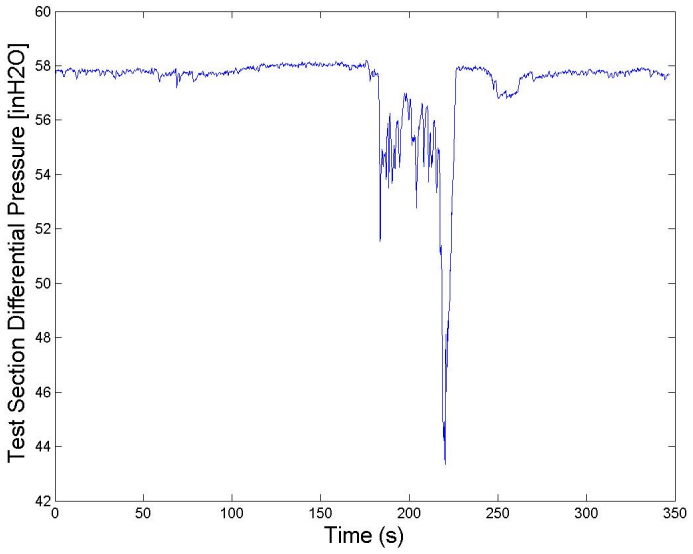

Figure E.1: Test Section Differential Pressure for Run #1, Test 3.

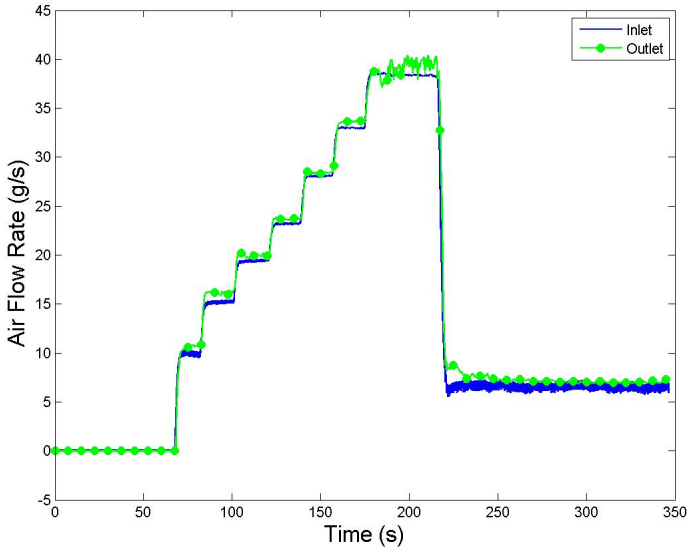

Figure E.2: Gas Mass Flow Rate for Run #1, Test 3.

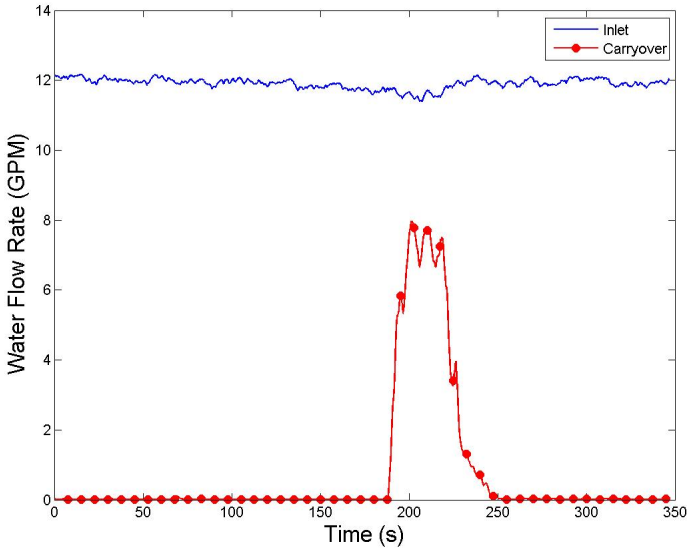

Figure E.3: Water Flow Rate for Run #1, Test 3.

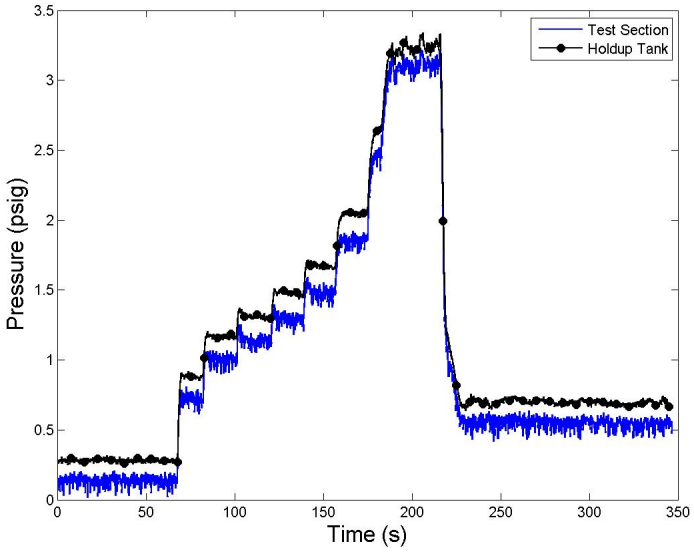

Figure E.4: System Pressure for Run #1, Test 3.

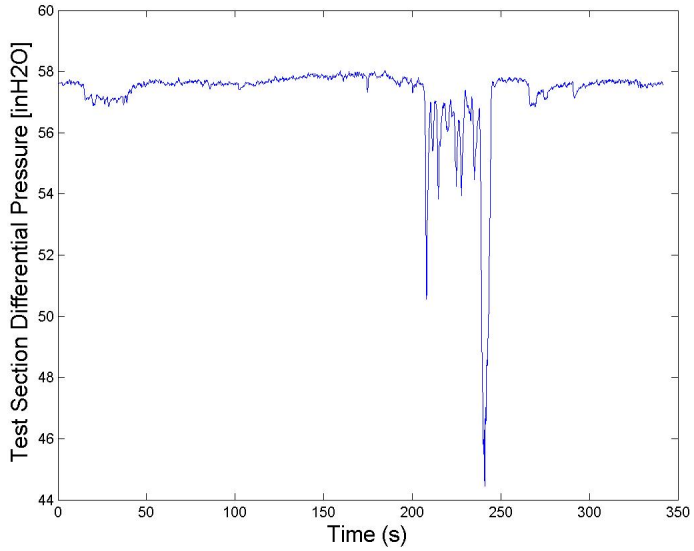

Figure E.5: Test Section Differential Pressure for Run #1, Test 4.

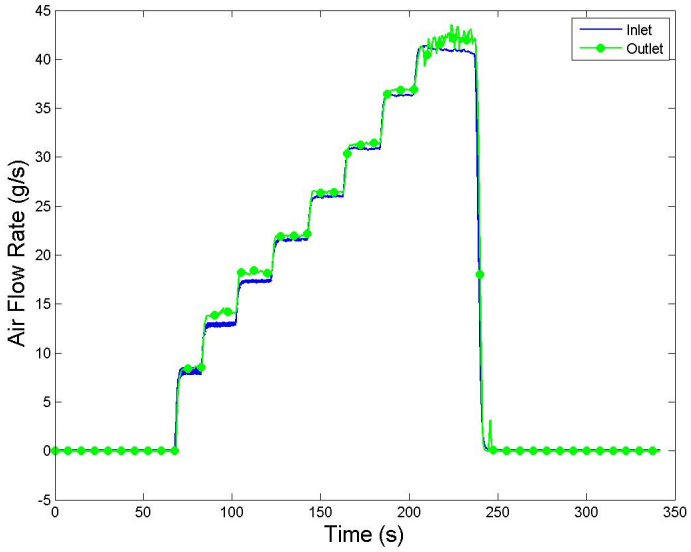

Figure E.6: Gas Mass Flow Rate for Run #1, Test 4.

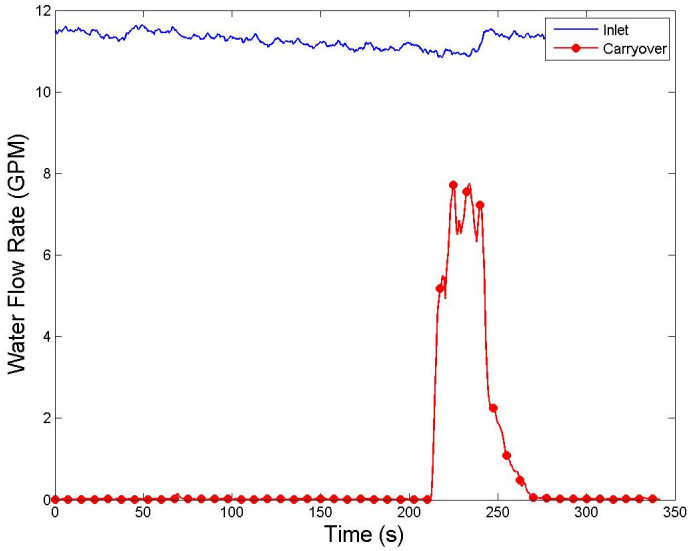

Figure E.7: Water Flow Rate for Run #1, Test 4.

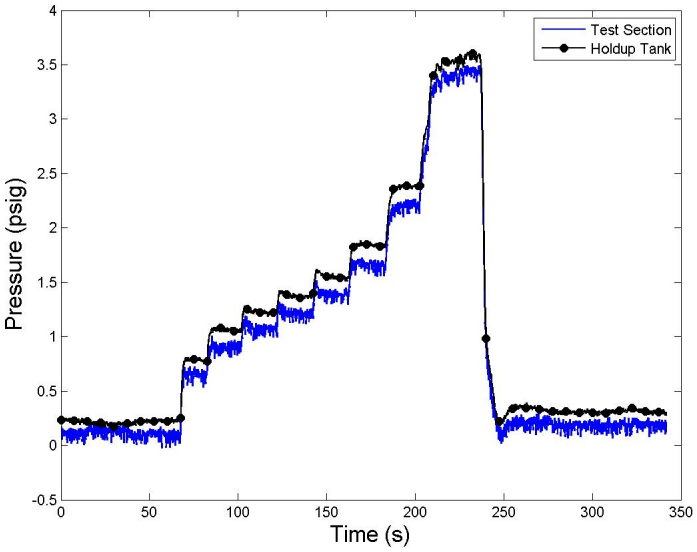

Figure E.8: System Pressure for Run #1, Test 4.

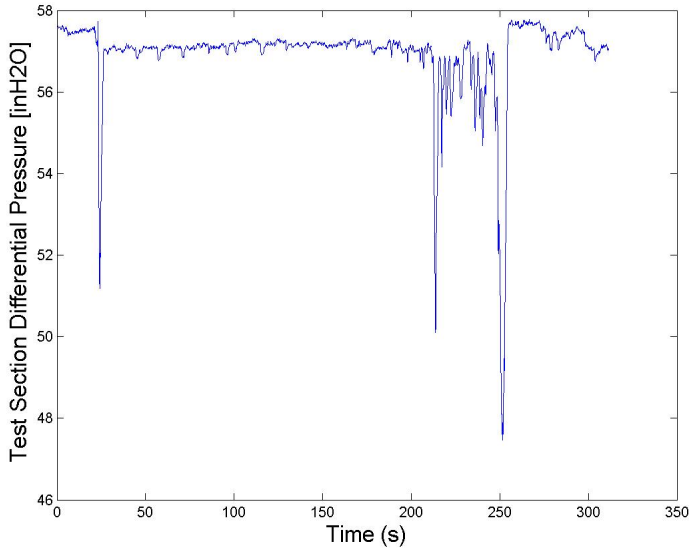

Figure E.9: Test Section Differential Pressure for Run #1, Test 5.

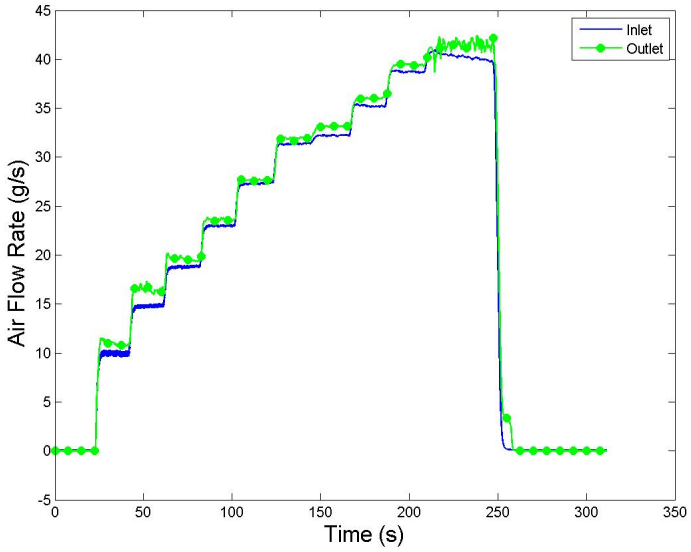

Figure E.10: Gas Mass Flow Rate for Run #1, Test 5.

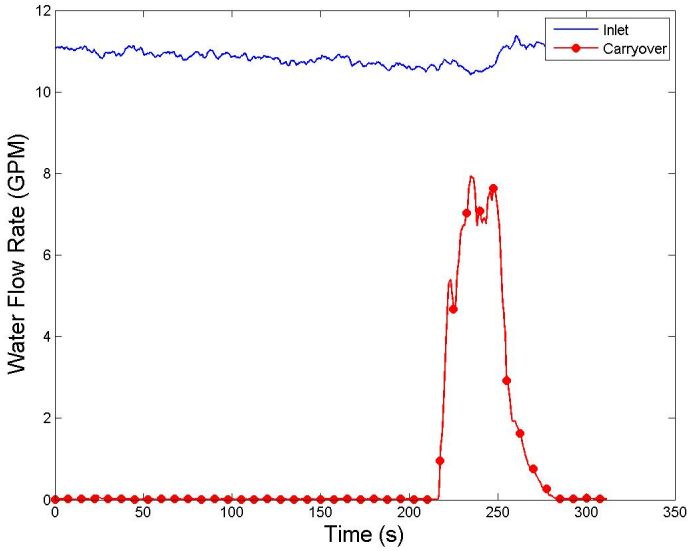

Figure E.11: Water Flow Rate for Run #1, Test 5.

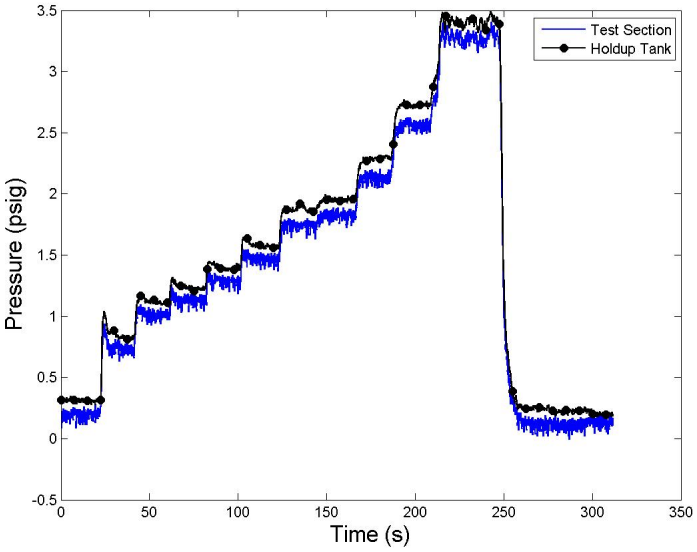

Figure E.12: System Pressure for Run #1, Test 5.

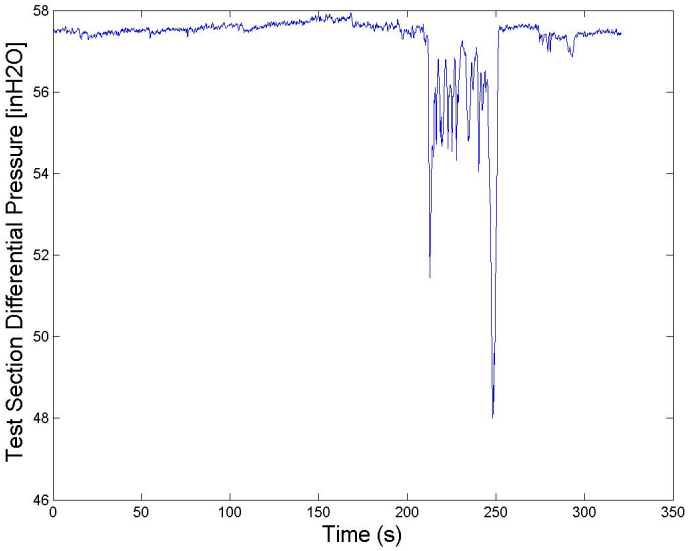

Figure E.13: Test Section Differential Pressure for Run #1, Test 6.

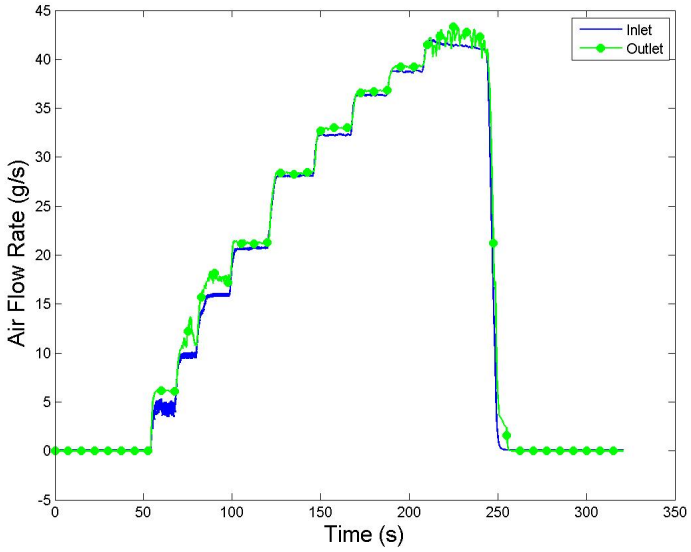

Figure E.14: Gas Mass Flow Rate for Run #1, Test 6.

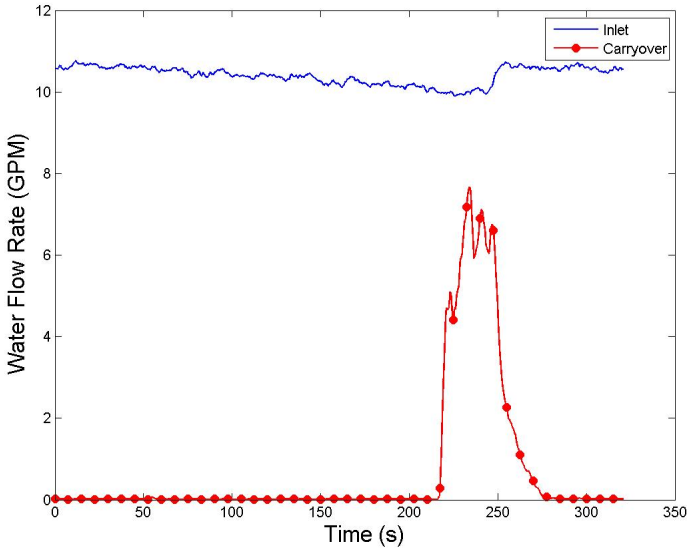

Figure E.15: Water Flow Rate for Run #1, Test 6.

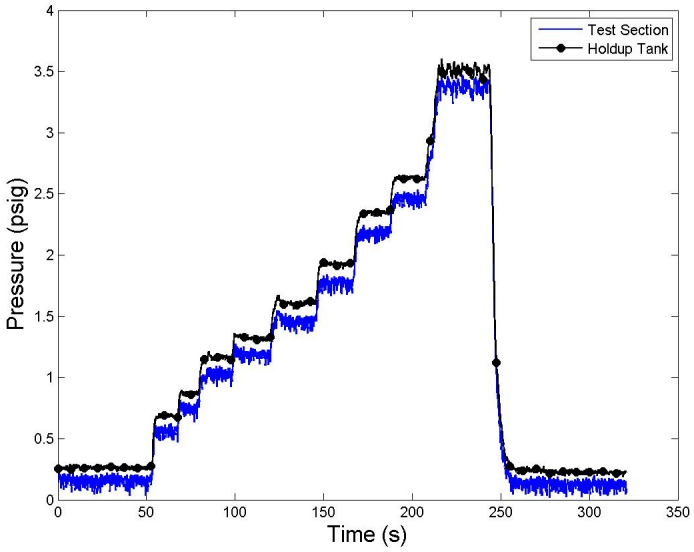

Figure E.16: System Pressure for Run #1, Test 6.

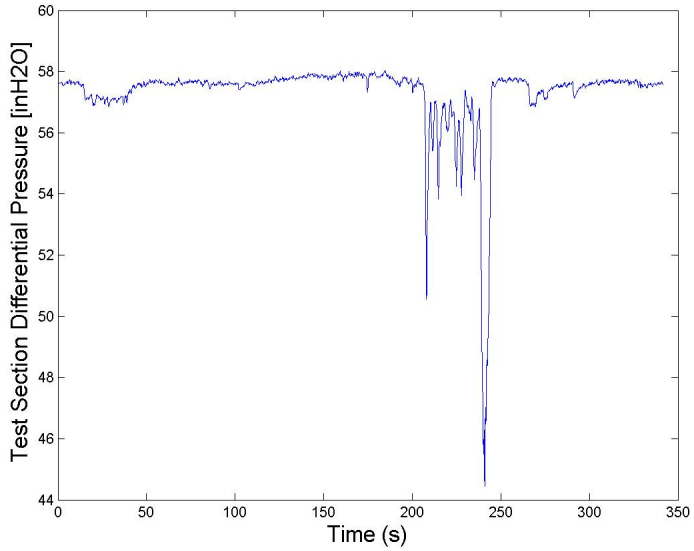

Figure E.17: Test Section Differential Pressure for Run #1, Test 4.

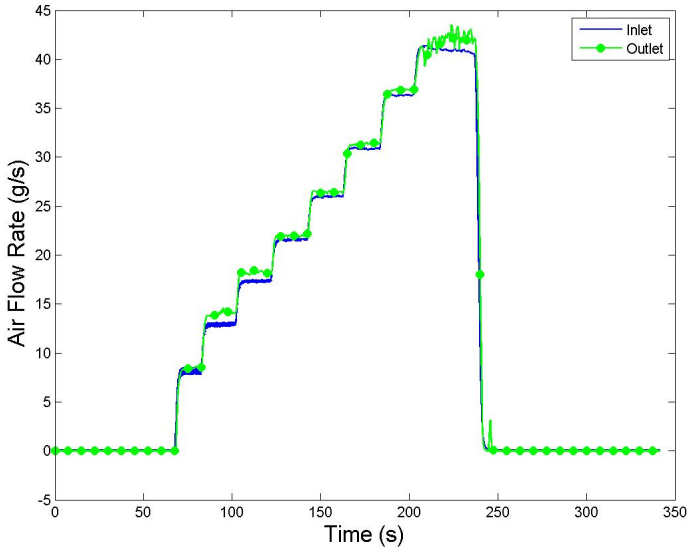

Figure E.18: Gas Mass Flow Rate for Run #1, Test 4.

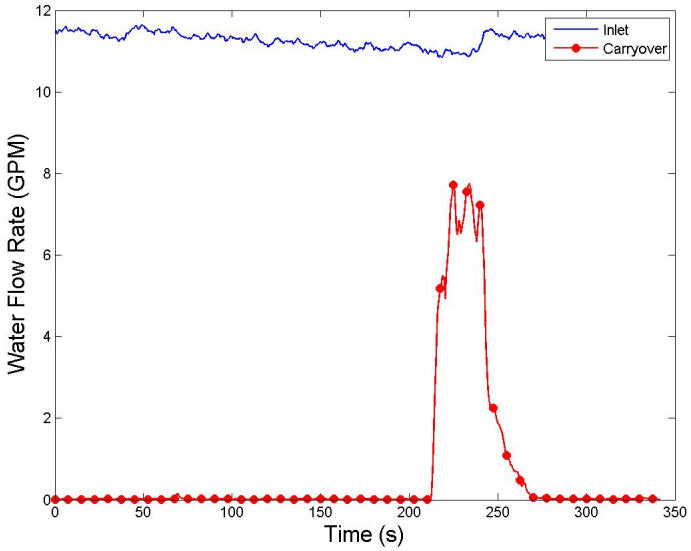

Figure E.19: Water Flow Rate for Run #1, Test 4.

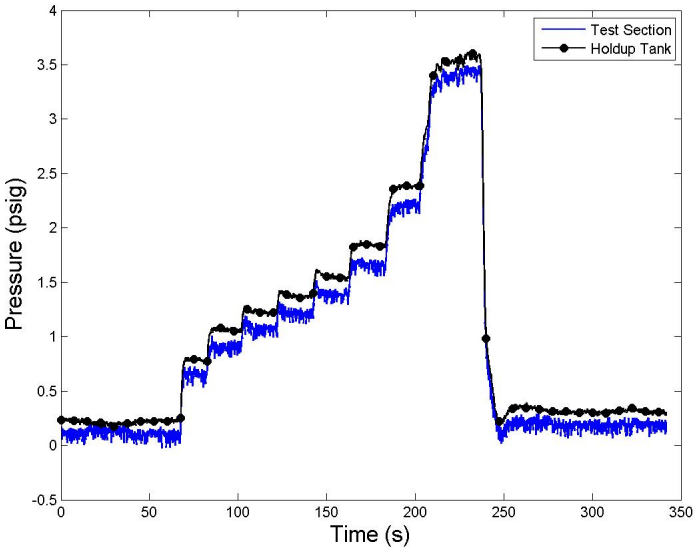

Figure E.20: System Pressure for Run #1, Test 4.

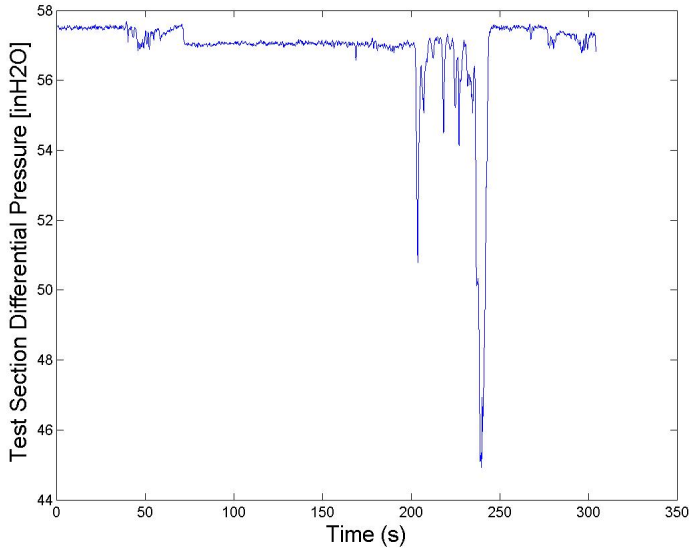

Figure E.21: Test Section Differential Pressure for Run #1, Test 7.

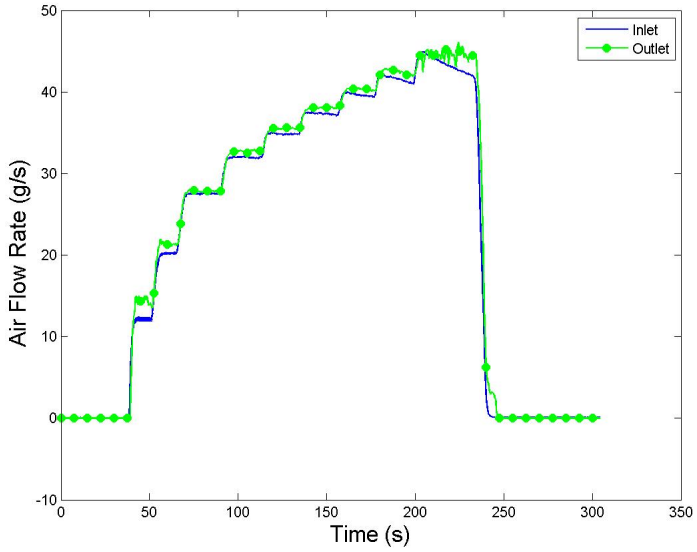

Figure E.22: Gas Mass Flow Rate for Run #1, Test 7.

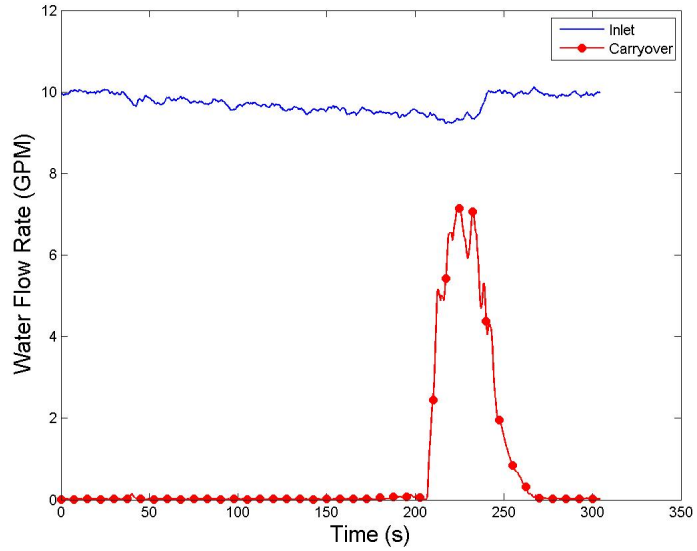

Figure E.23: Water Flow Rate for Run #1, Test 7.

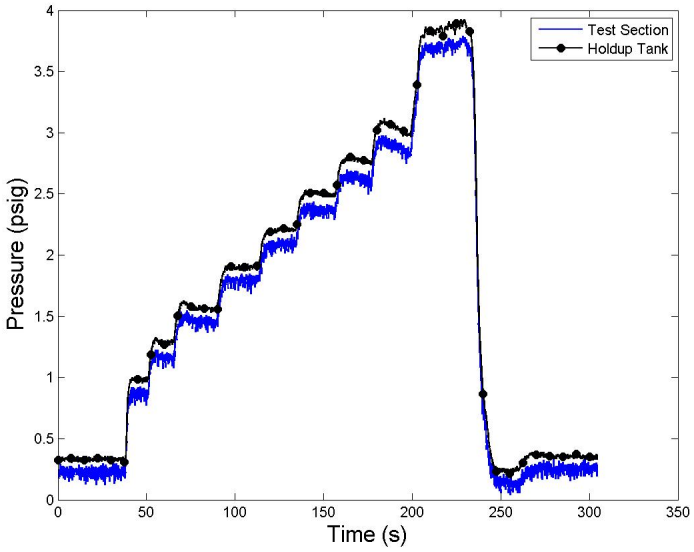

Figure E.24: System Pressure for Run #1, Test 7.

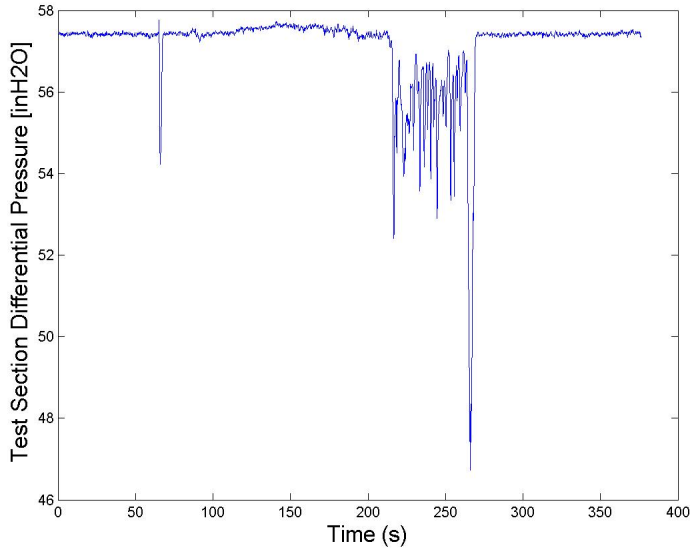

Figure E.25: Test Section Differential Pressure for Run #1, Test 8.

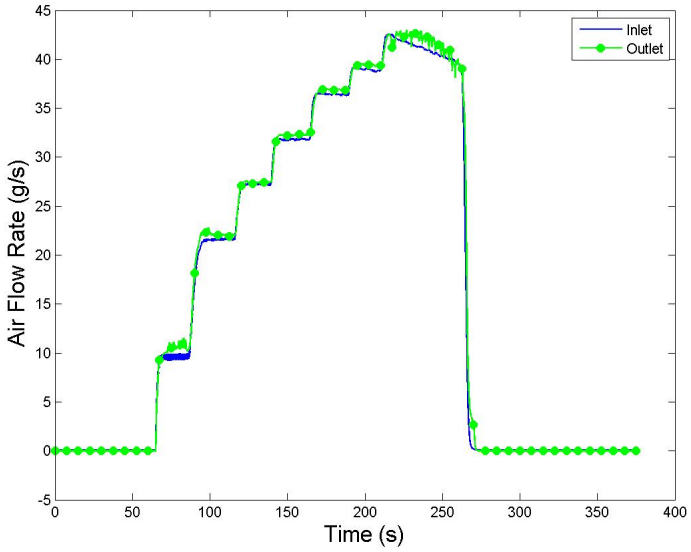

Figure E.26: Gas Mass Flow Rate for Run #1, Test 8.

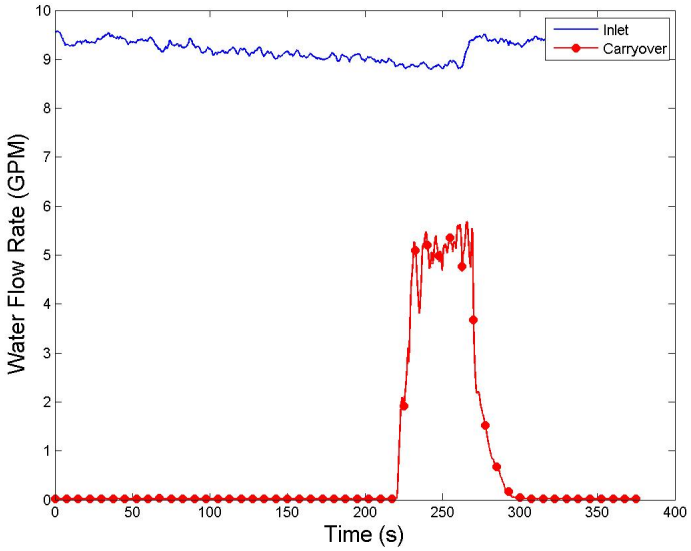

Figure E.27: Water Flow Rate for Run #1, Test 8.

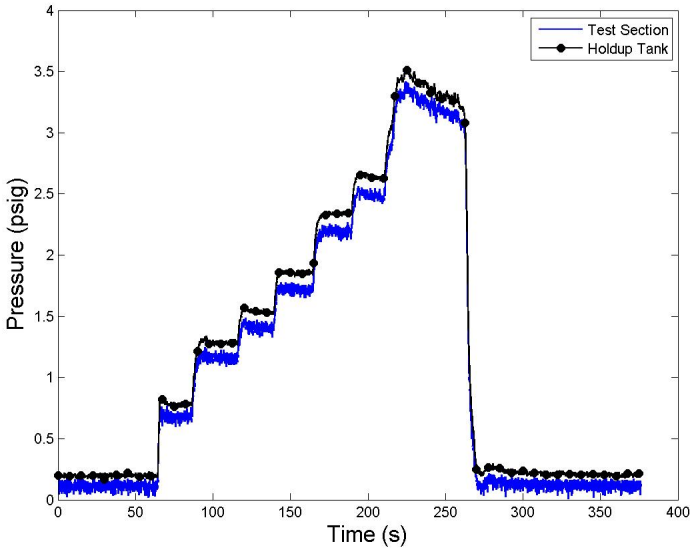

Figure E.28: System Pressure for Run #1, Test 8.

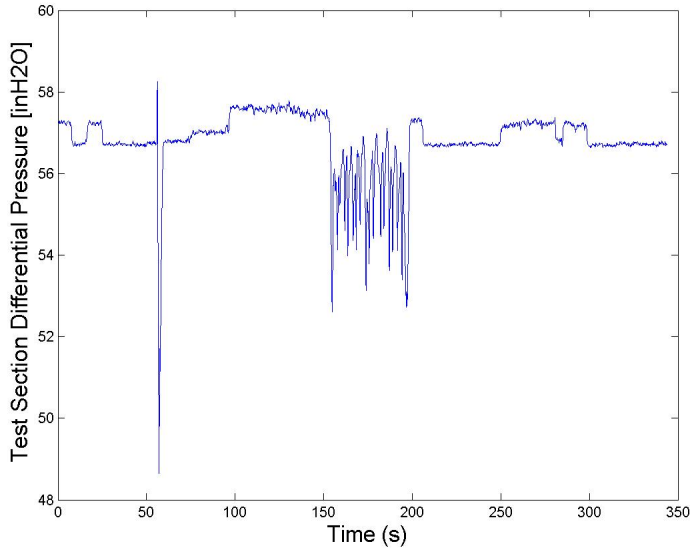

Figure E.29: Test Section Differential Pressure for Run #1, Test 9.

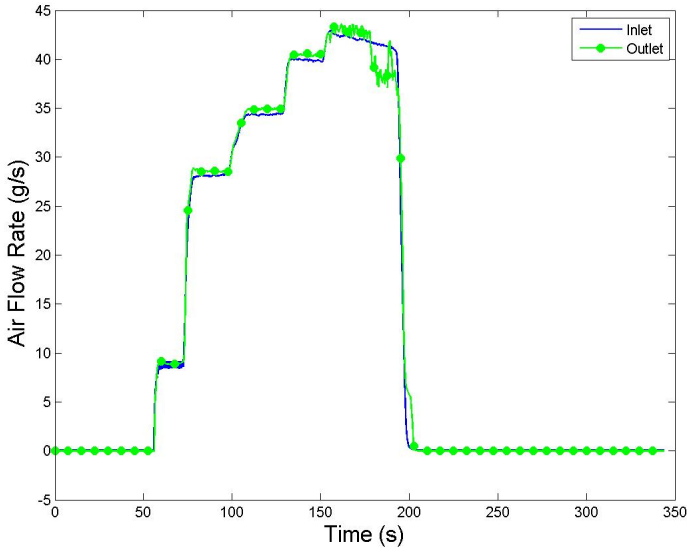

Figure E.30: Gas Mass Flow Rate for Run #1, Test 9.

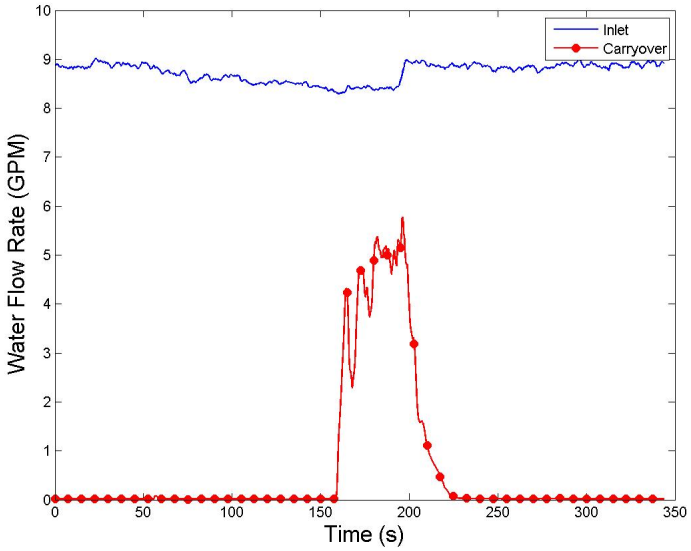

Figure E.31: Water Flow Rate for Run #1, Test 9.

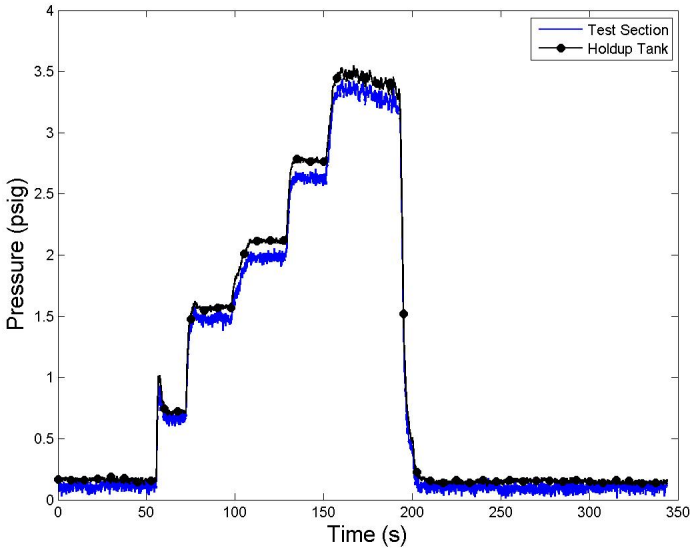

Figure E.32: System Pressure for Run #1, Test 9.

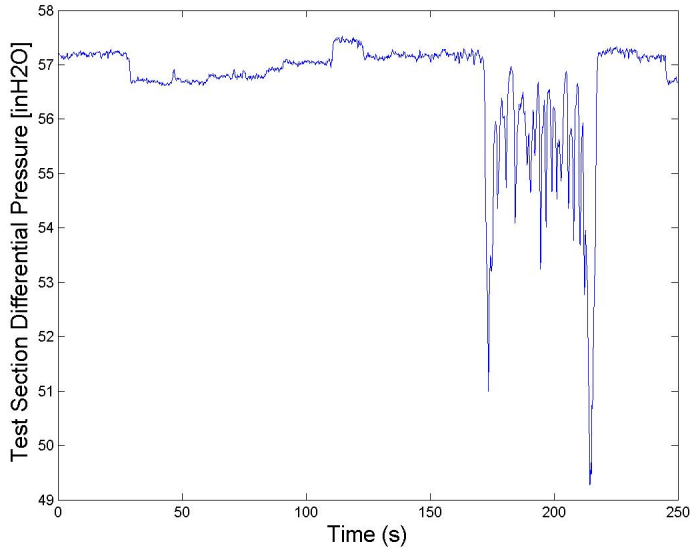

Figure E.33: Test Section Differential Pressure for Run #1, Test 10.

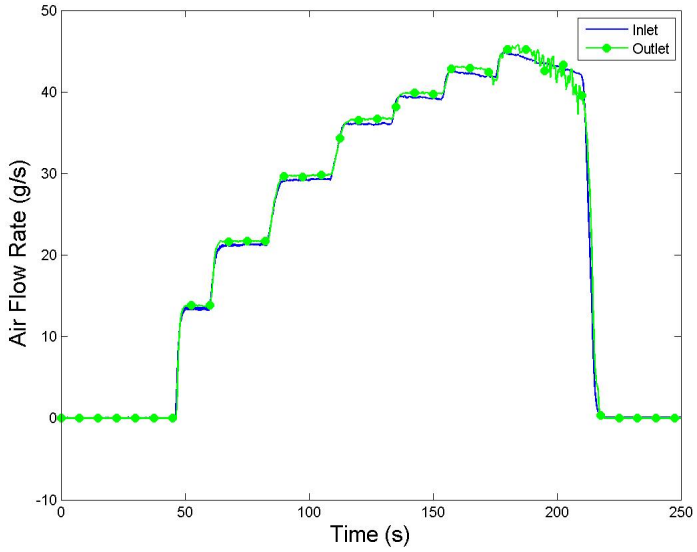

Figure E.34: Gas Mass Flow Rate for Run #1, Test 10.

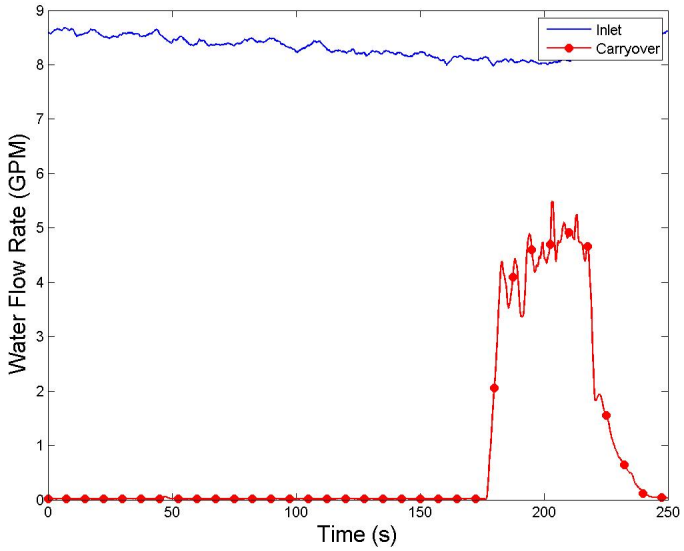

Figure E.35: Water Flow Rate for Run #1, Test 10.

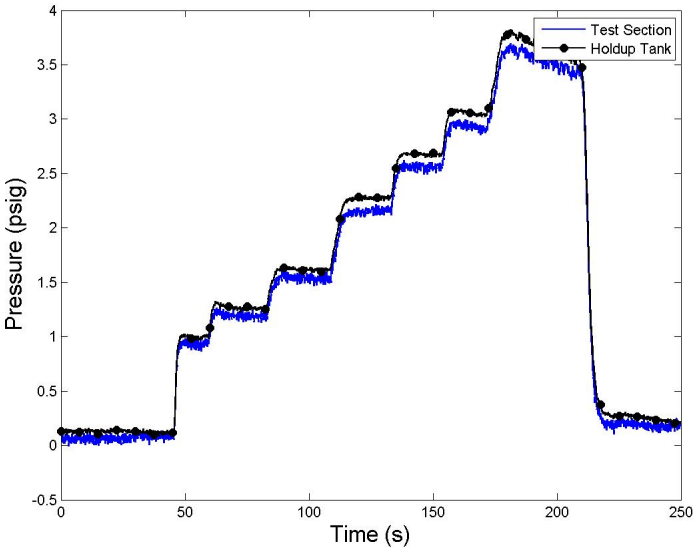

Figure E.36: System Pressure for Run #1, Test 10.

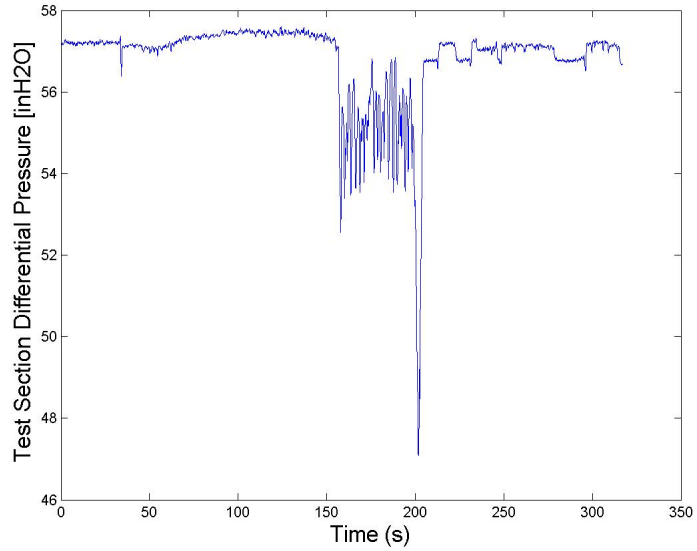

Figure E.37: Test Section Differential Pressure for Run #1, Test 11.

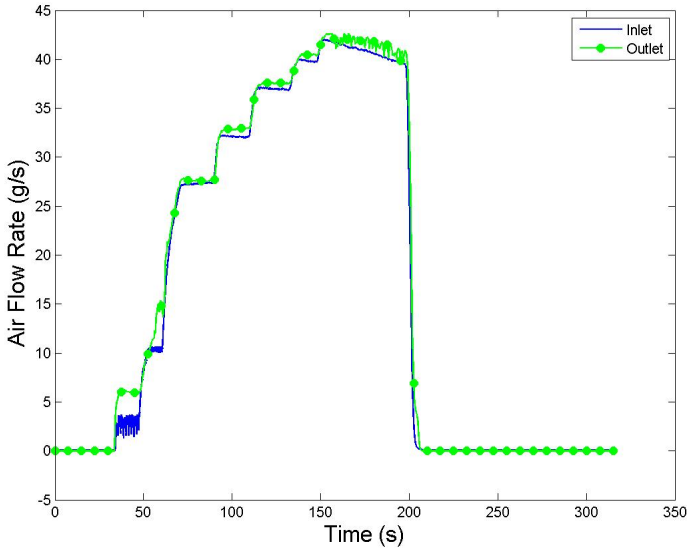

Figure E.38: Gas Mass Flow Rate for Run #1, Test 11.

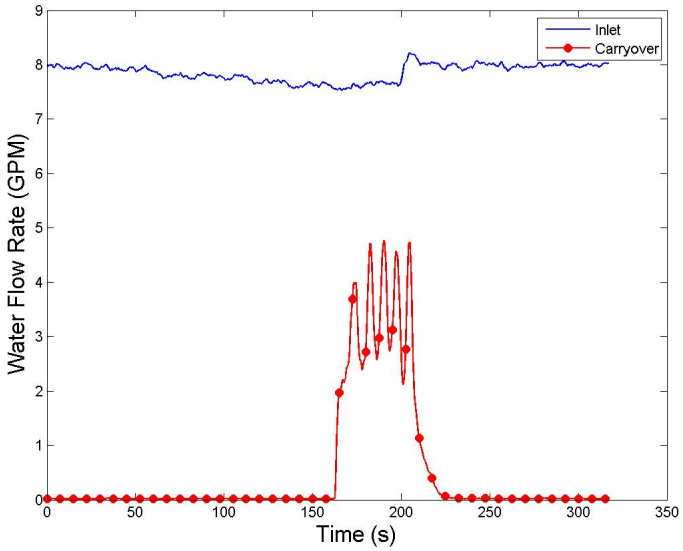

Figure E.39: Water Flow Rate for Run #1, Test 11.

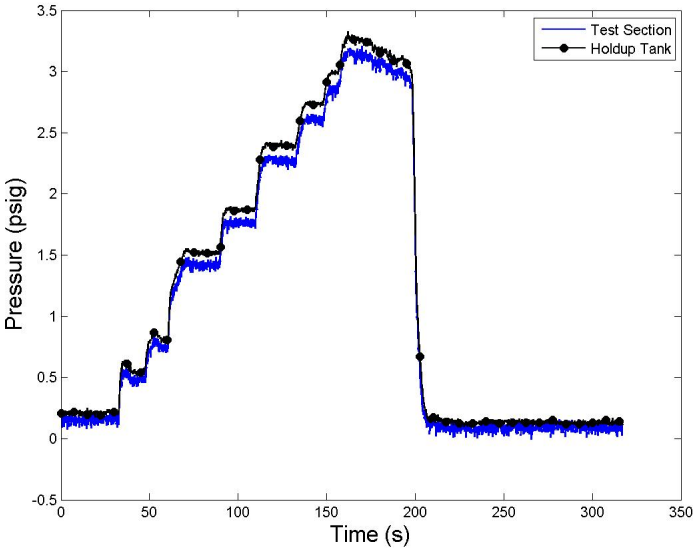

Figure E.40: System Pressure for Run #1, Test 11.

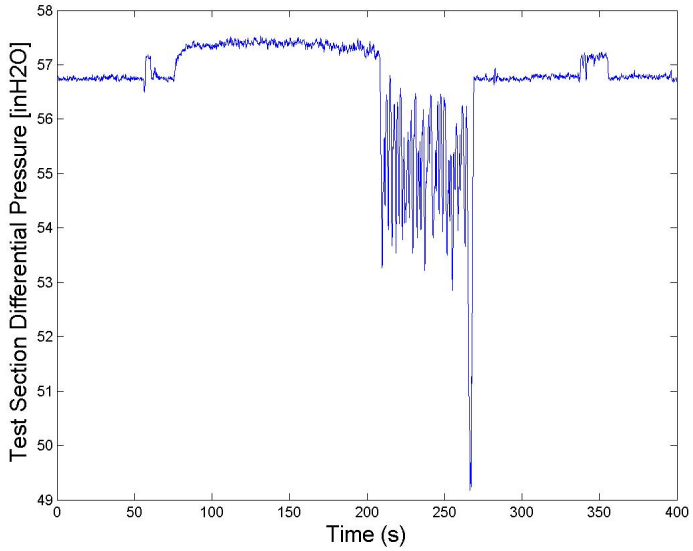

Figure E.41: Test Section Differential Pressure for Run #1, Test 12.

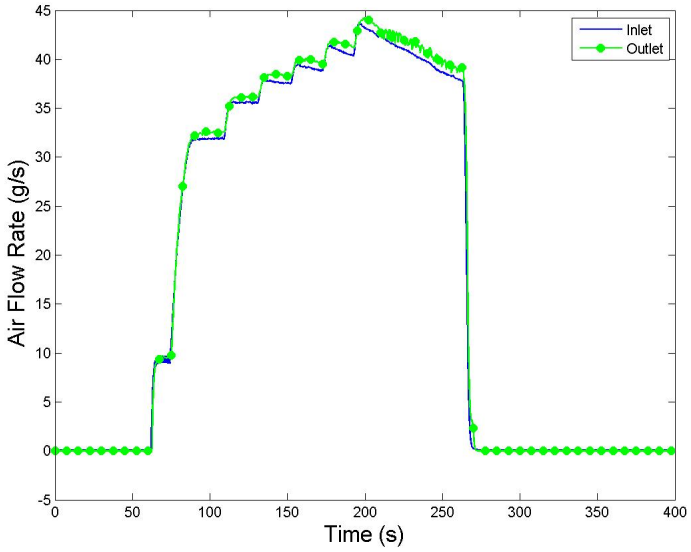

Figure E.42: Gas Mass Flow Rate for Run #1, Test 12.

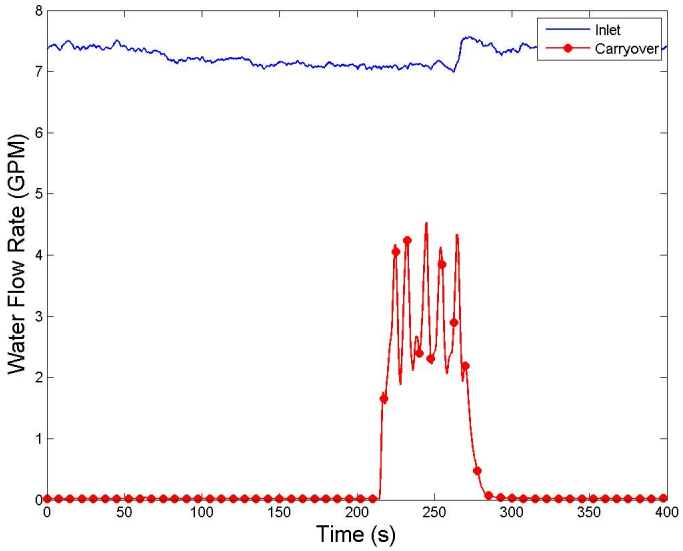

Figure E.43: Water Flow Rate for Run #1, Test 12.

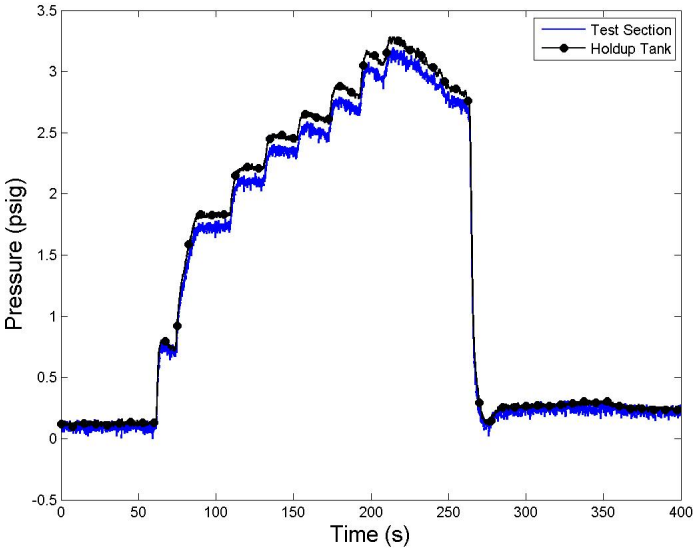

Figure E.44: System Pressure for Run #1, Test 12.

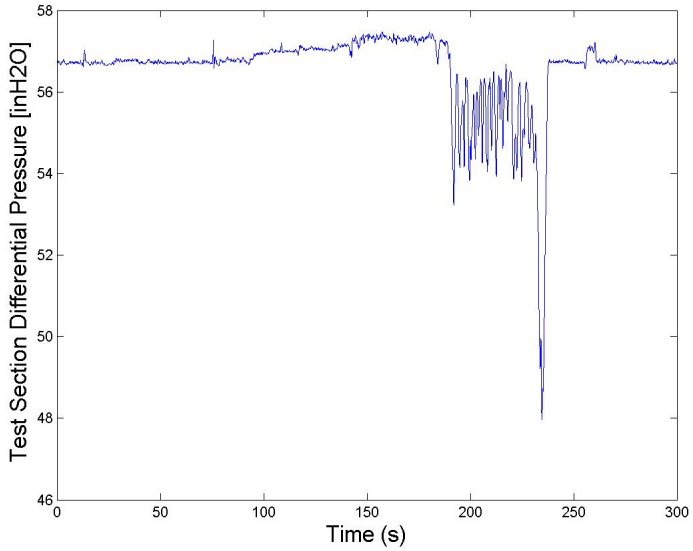

Figure E.45: Test Section Differential Pressure for Run #1, Test 13.

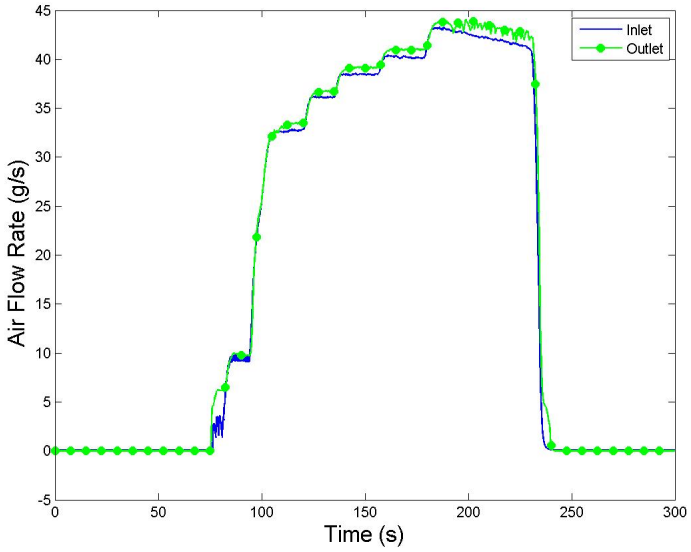

Figure E.46: Gas Mass Flow Rate for Run #1, Test 13.

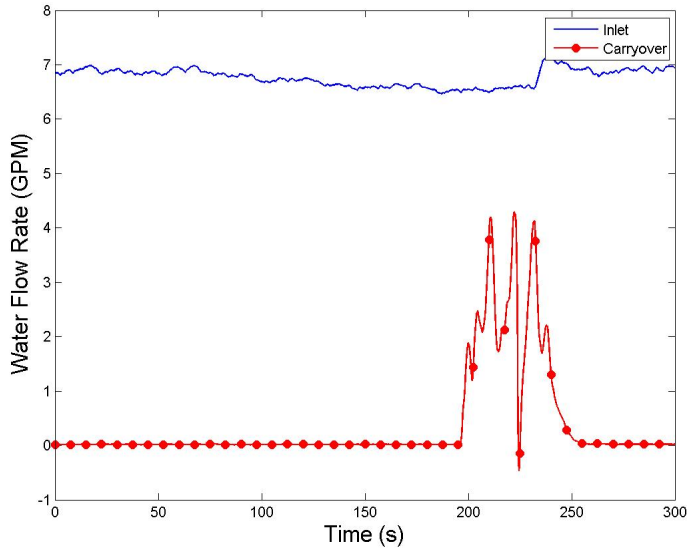

Figure E.47: Water Flow Rate for Run #1, Test 13.

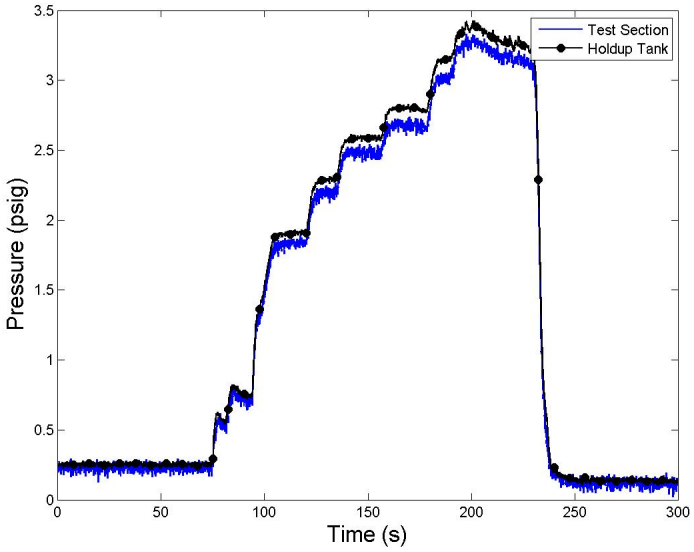

Figure E.48: System Pressure for Run #1, Test 13.

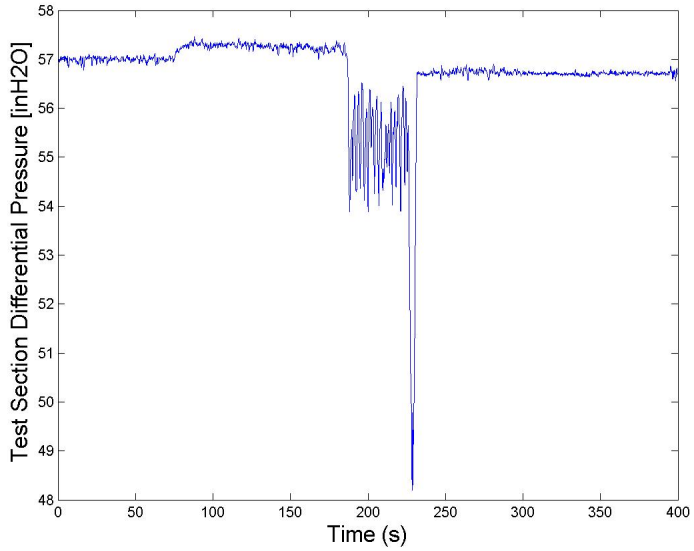

Figure E.49: Test Section Differential Pressure for Run #1, Test 14.

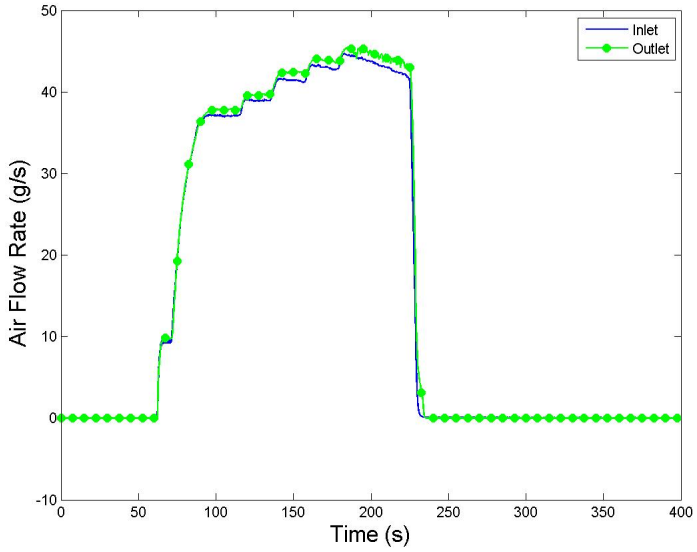

Figure E.50: Gas Mass Flow Rate for Run #1, Test 14.

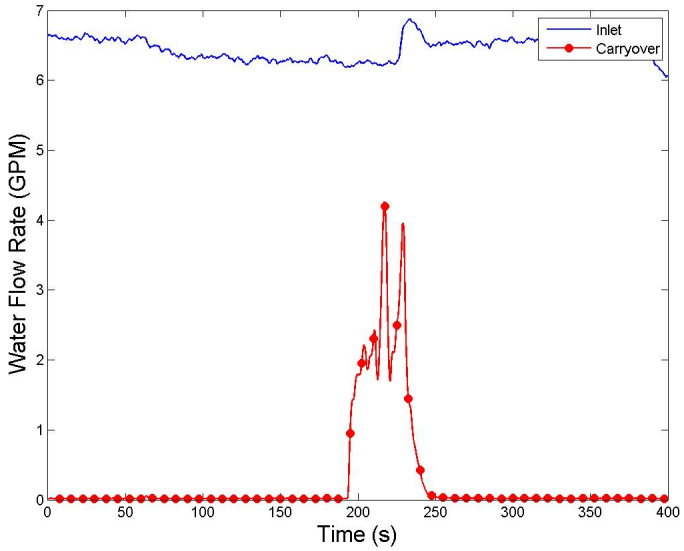

Figure E.51: Water Flow Rate for Run #1, Test 14.

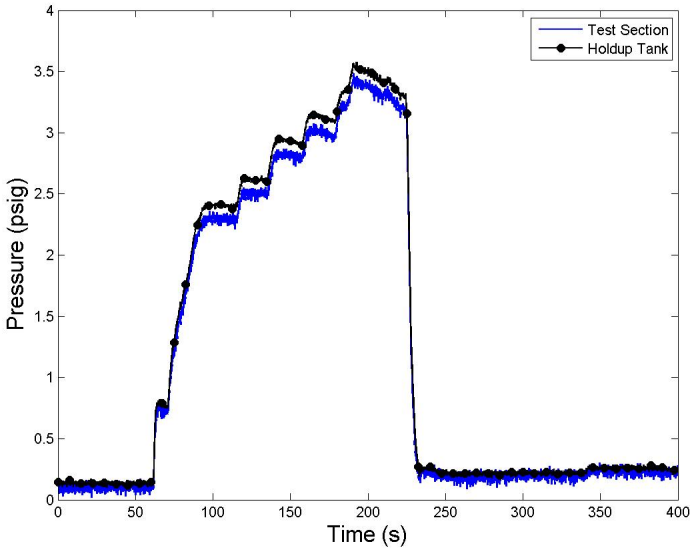

Figure E.52: System Pressure for Run #1, Test 14.

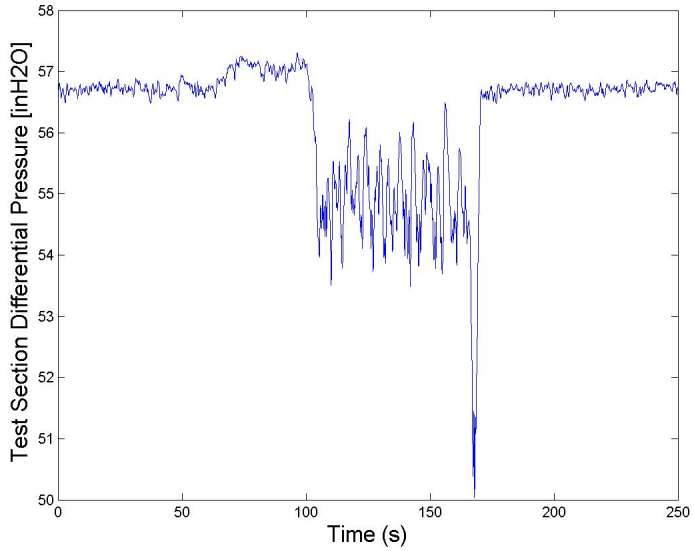

Figure E.53: Test Section Differential Pressure for Run #1, Test 16.

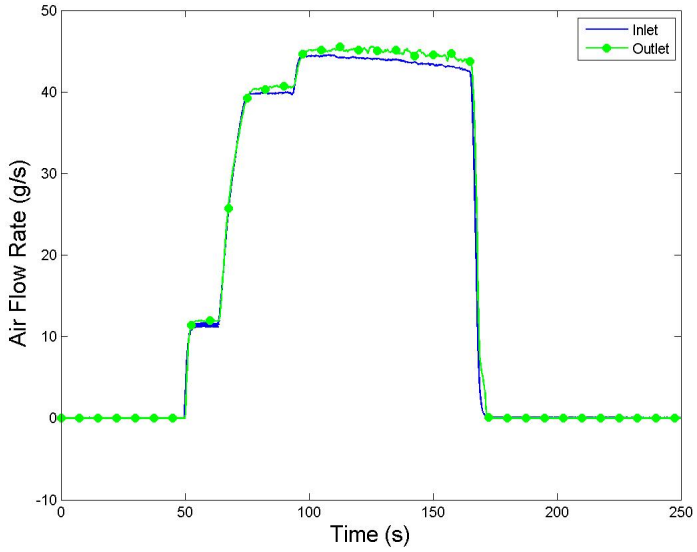

Figure E.54: Gas Mass Flow Rate for Run #1, Test 16.

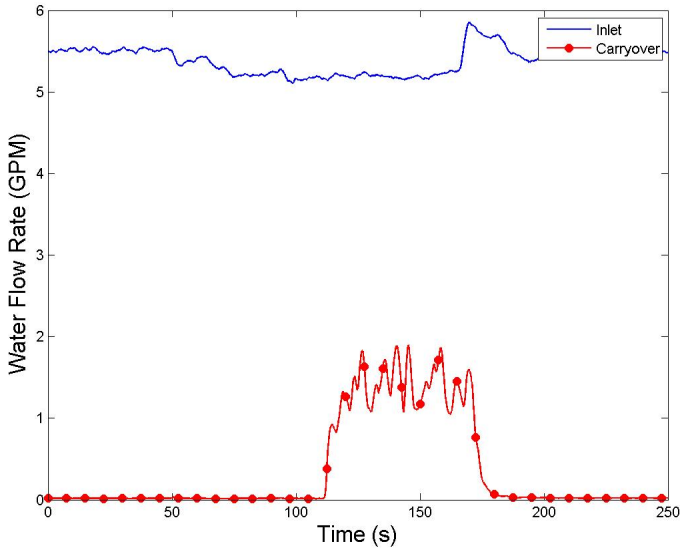

Figure E.55: Water Flow Rate for Run #1, Test 16.

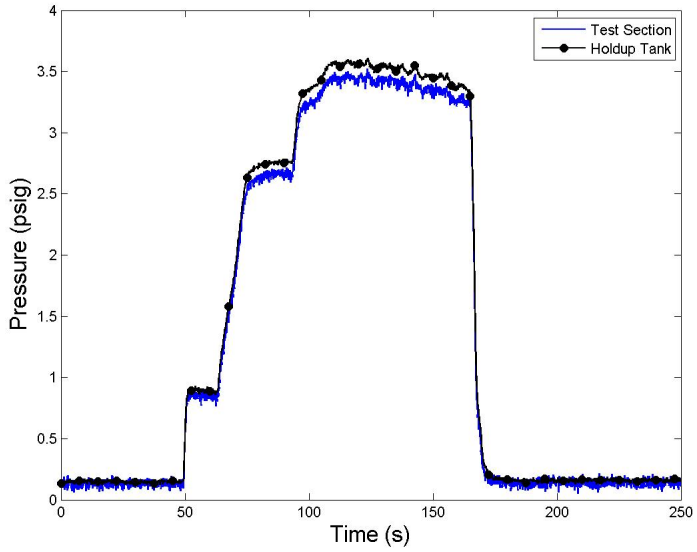

Figure E.56: System Pressure for Run #1, Test 16.

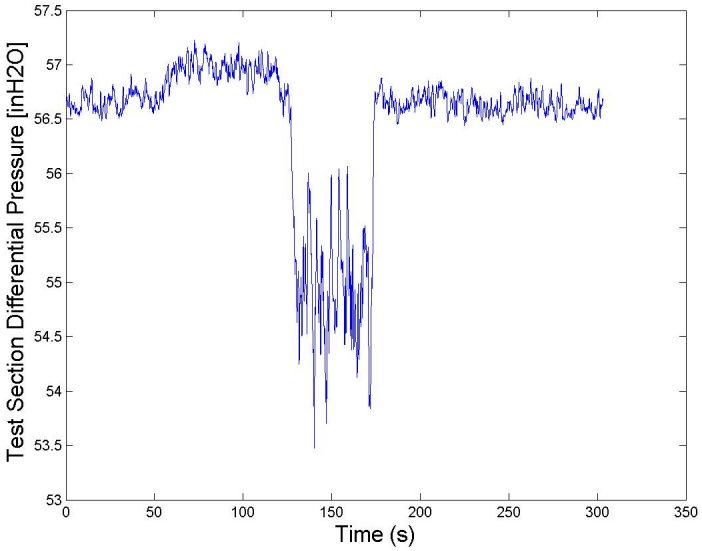

Figure E.57: Test Section Differential Pressure for Run #1, Test 17.

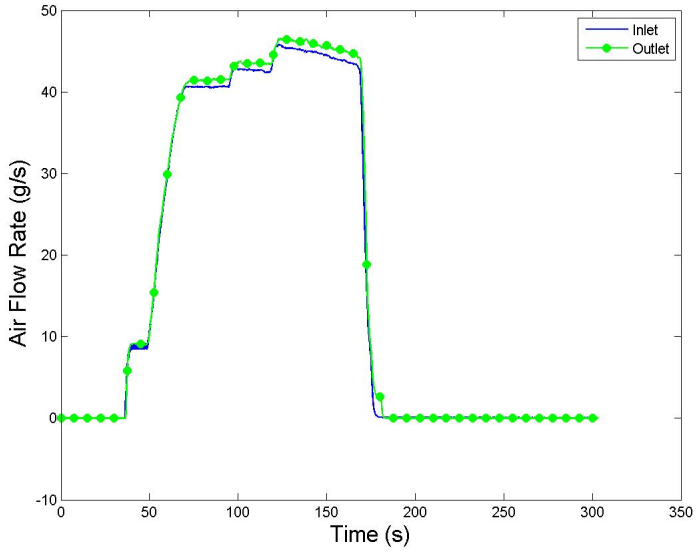

Figure E.58: Gas Mass Flow Rate for Run #1, Test 17.

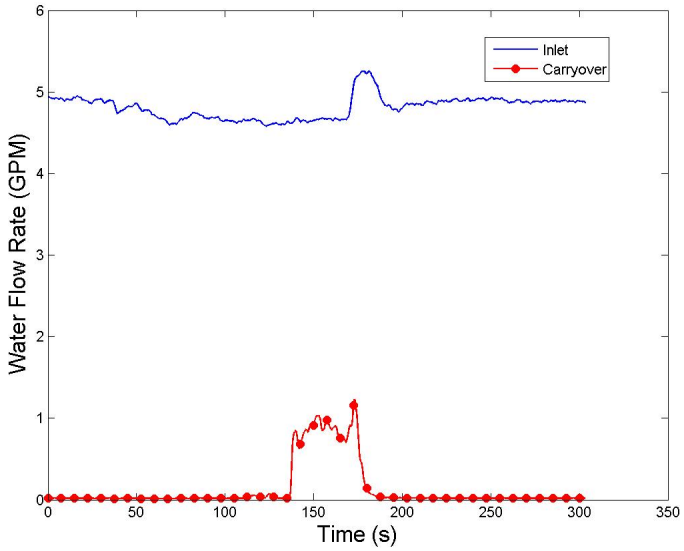

Figure E.59: Water Flow Rate for Run #1, Test 17.

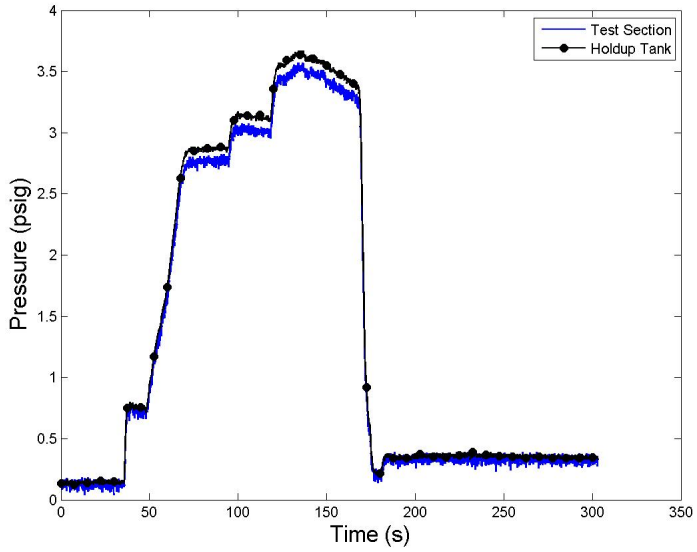

Figure E.60: System Pressure for Run #1, Test 17.

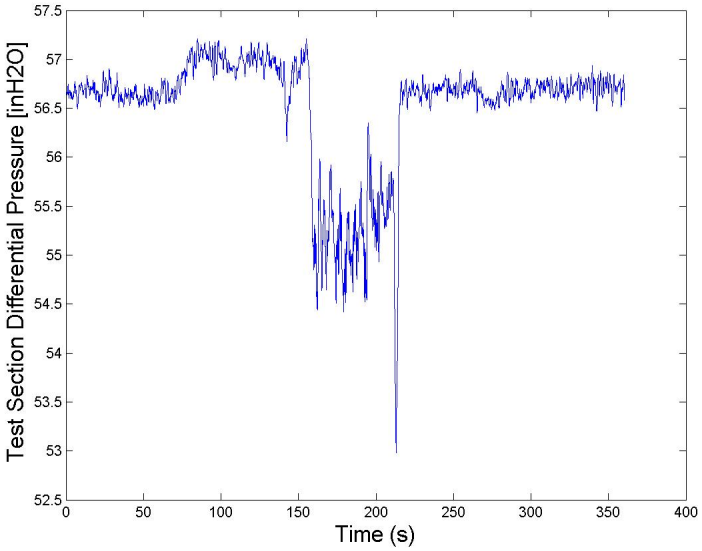

Figure E.61: Test Section Differential Pressure for Run #1, Test 18.

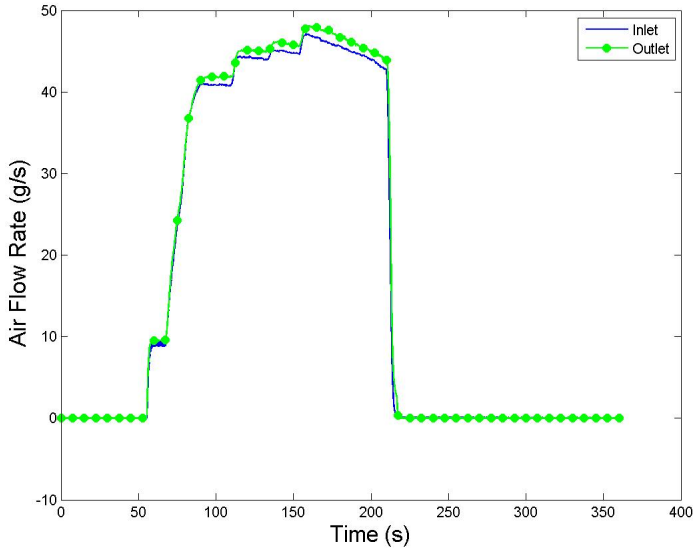

Figure E.62: Gas Mass Flow Rate for Run #1, Test 18.

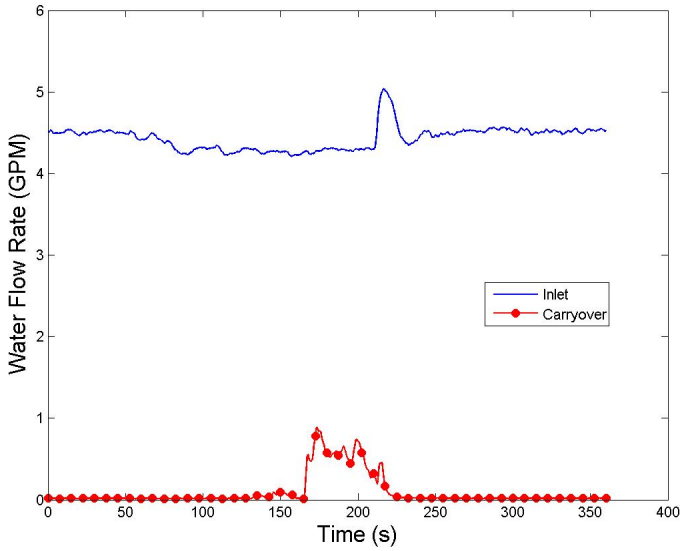

Figure E.63: Water Flow Rate for Run #1, Test 18.

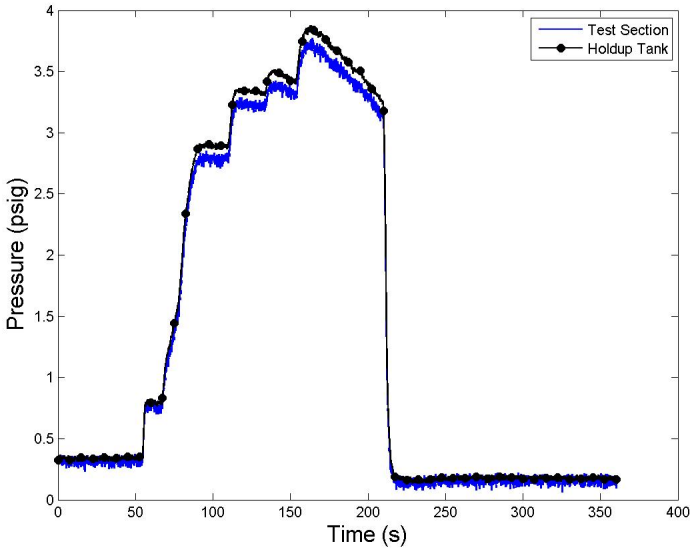

Figure E.64: System Pressure for Run #1, Test 18.

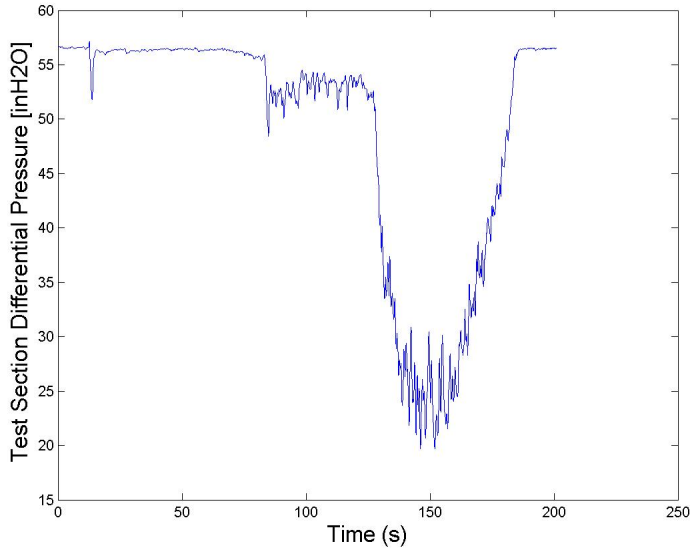

Figure E.65: Test Section Differential Pressure for Run #7, Test 2.

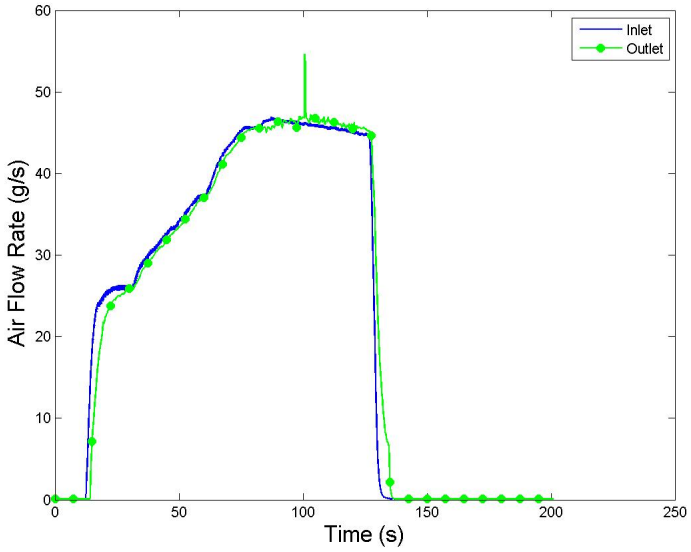

Figure E.66: Gas Mass Flow Rate for Run #7, Test 2.

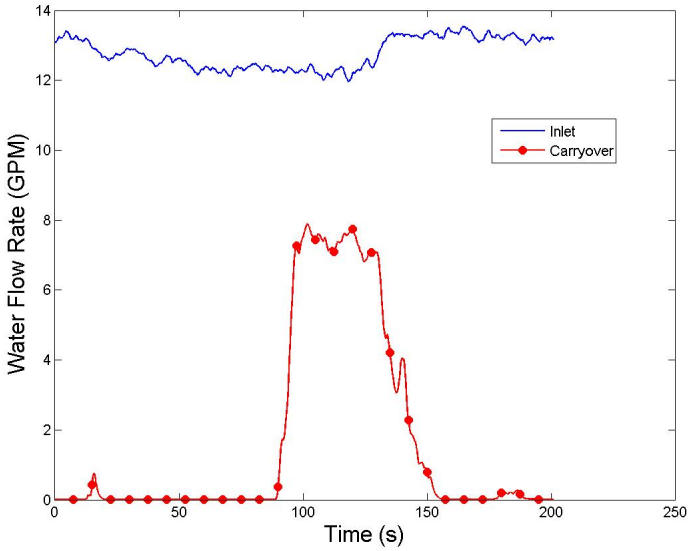

Figure E.67: Water Flow Rate for Run #7, Test 2.

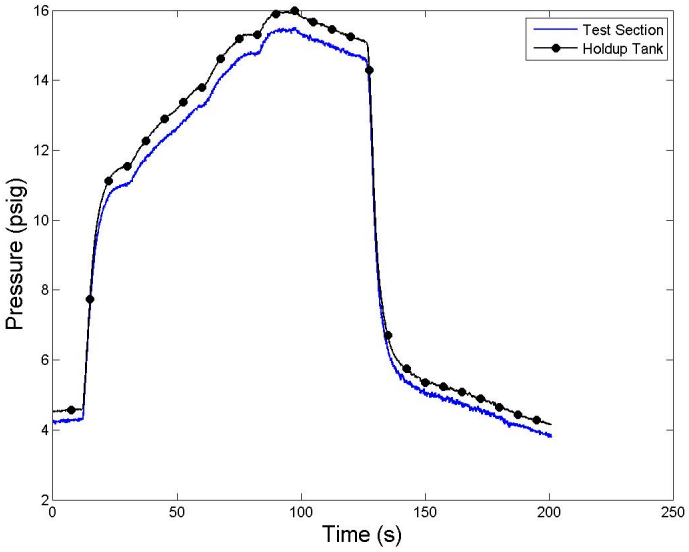

Figure E.68: System Pressure for Run #7, Test 2.

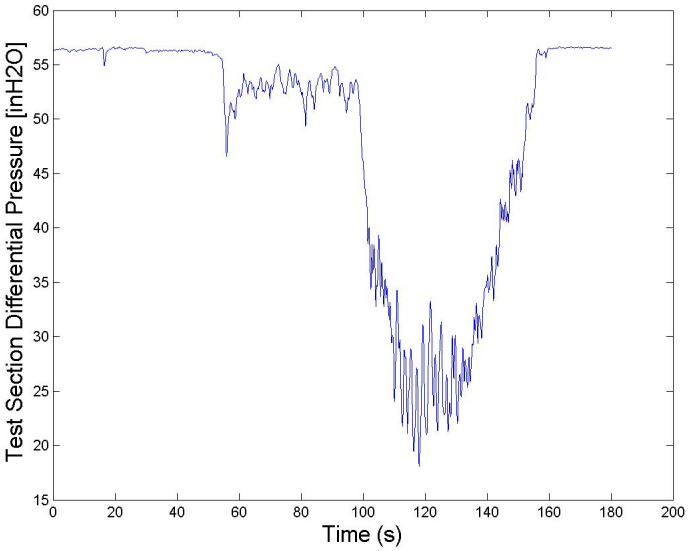

Figure E.69: Test Section Differential Pressure for Run #7, Test 3.

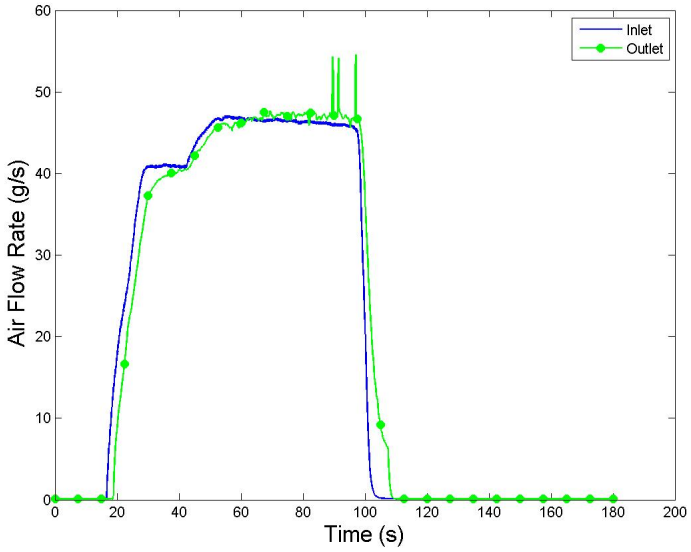

Figure E.70: Gas Mass Flow Rate for Run #7, Test 3.

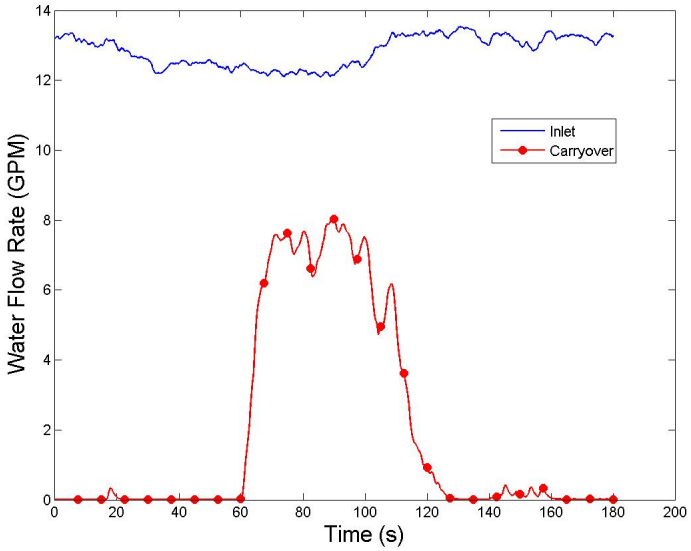

Figure E.71: Water Flow Rate for Run #7, Test 3.

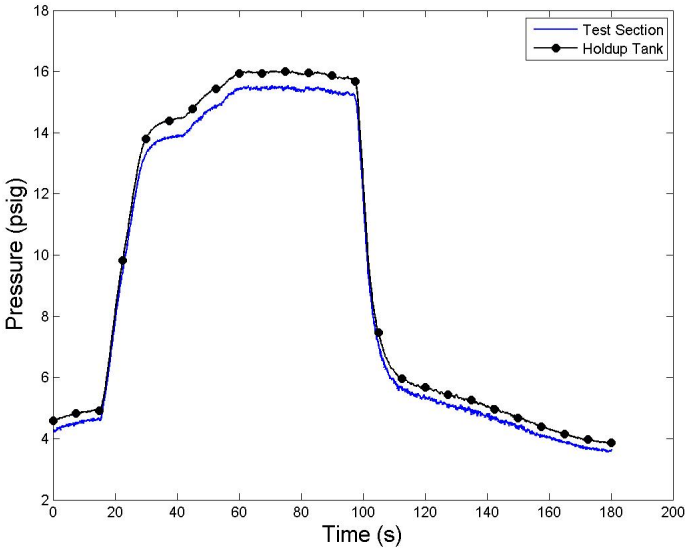

Figure E.72: System Pressure for Run #7, Test 3.

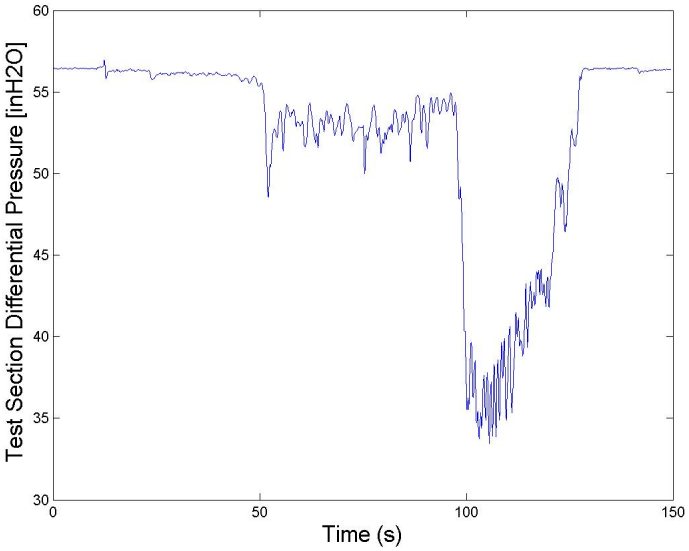

Figure E.73: Test Section Differential Pressure for Run #7, Test 4.

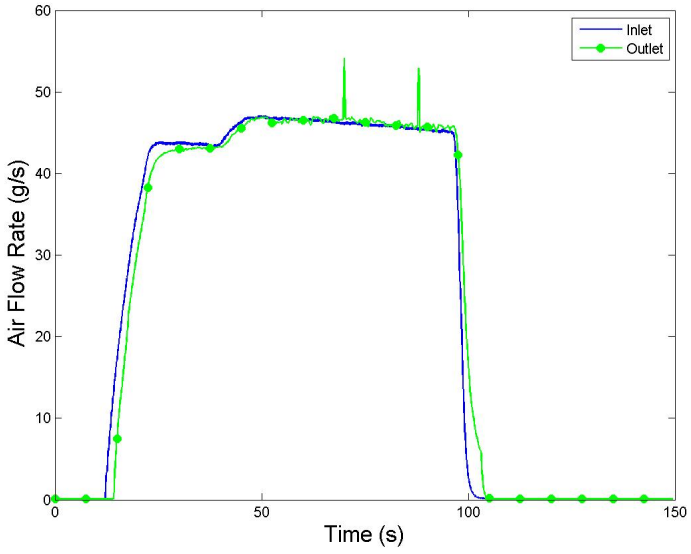

Figure E.74: Gas Mass Flow Rate for Run #7, Test 4.

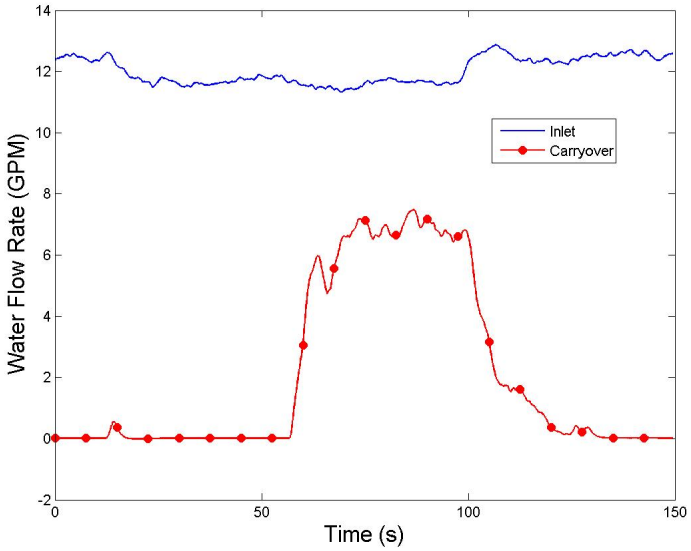

Figure E.75: Water Flow Rate for Run #7, Test 4.

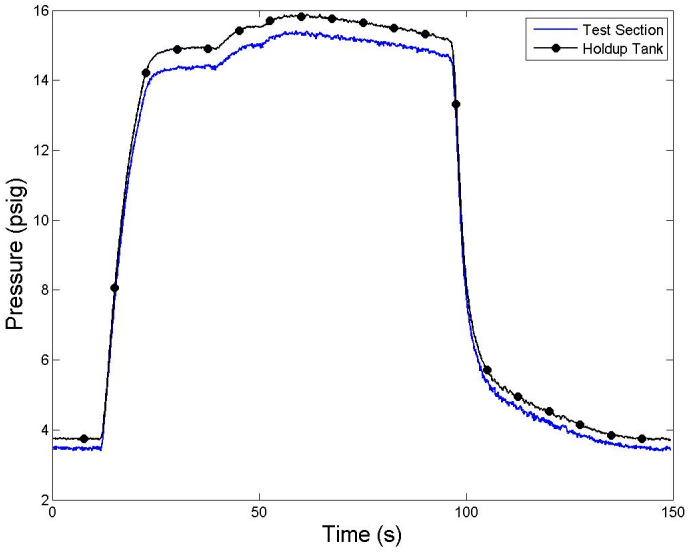

Figure E.76: System Pressure for Run #7, Test 4.

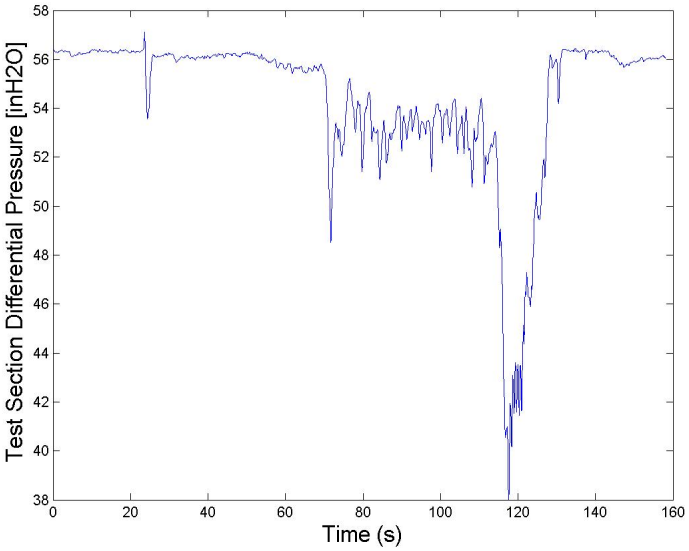

Figure E.77: Test Section Differential Pressure for Run #7, Test 5.

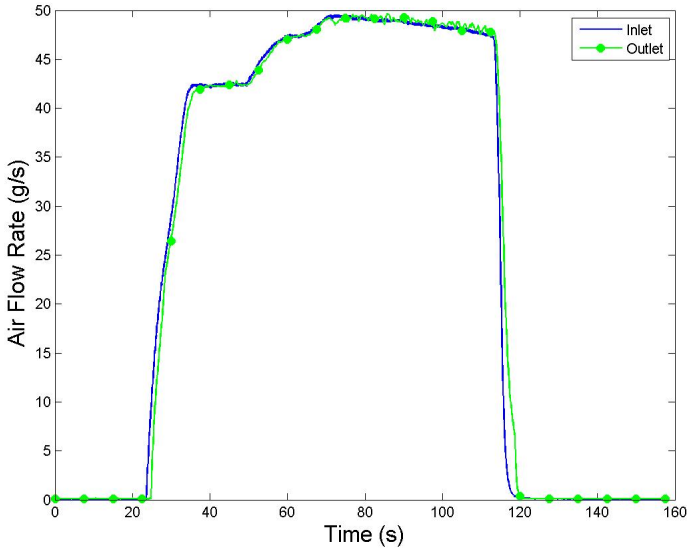

Figure E.78: Gas Mass Flow Rate for Run #7, Test 5.

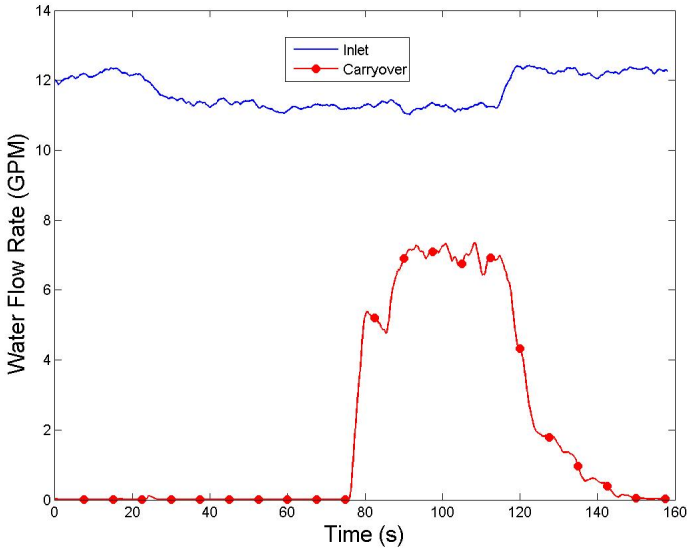

Figure E.79: Water Flow Rate for Run #7, Test 5.

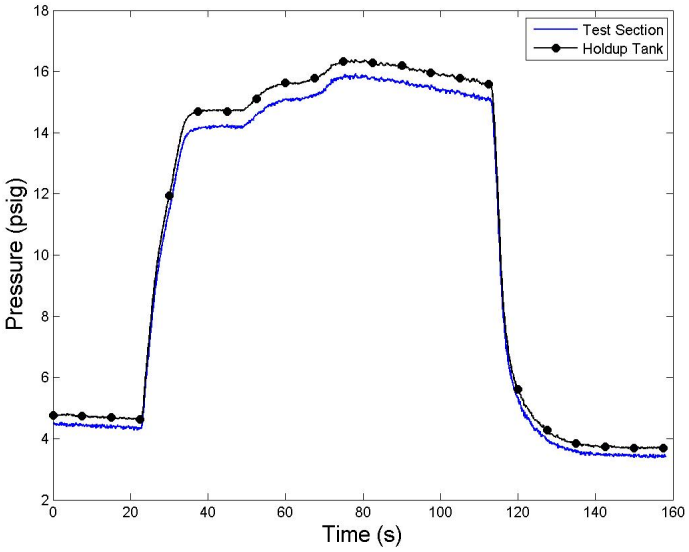

Figure E.80: System Pressure for Run #7, Test 5.

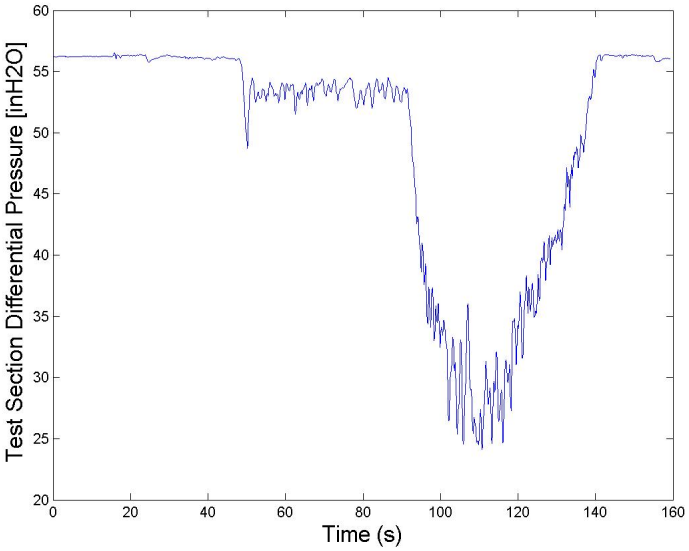

Figure E.81: Test Section Differential Pressure for Run #7, Test 6.

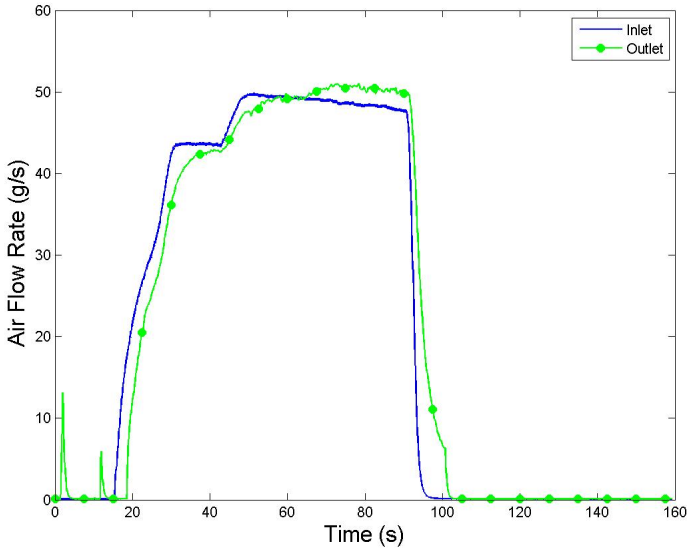

Figure E.82: Gas Mass Flow Rate for Run #7, Test 6.

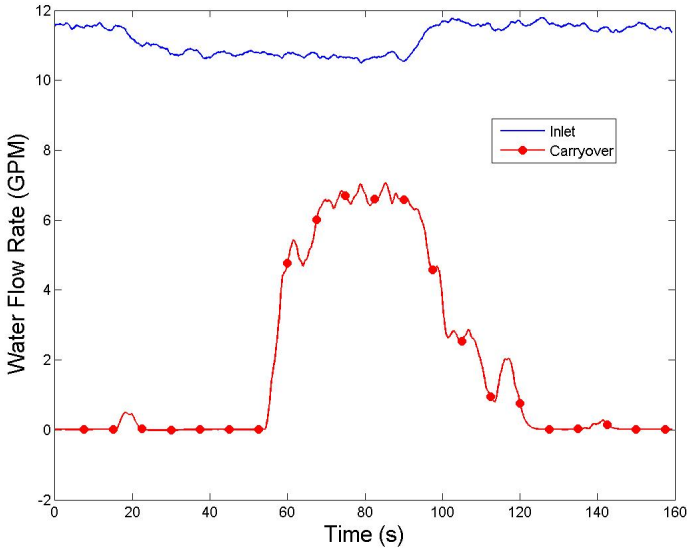

Figure E.83: Water Flow Rate for Run #7, Test 6.

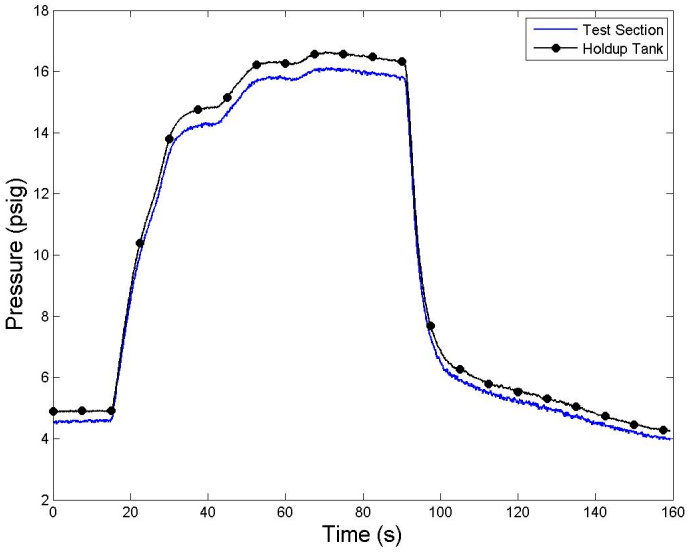

Figure E.84: System Pressure for Run #7, Test 6.

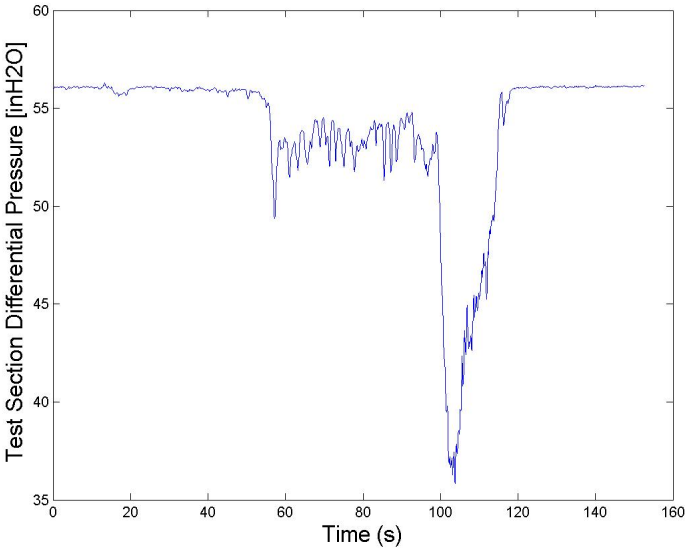

Figure E.85: Test Section Differential Pressure for Run #7, Test 7.

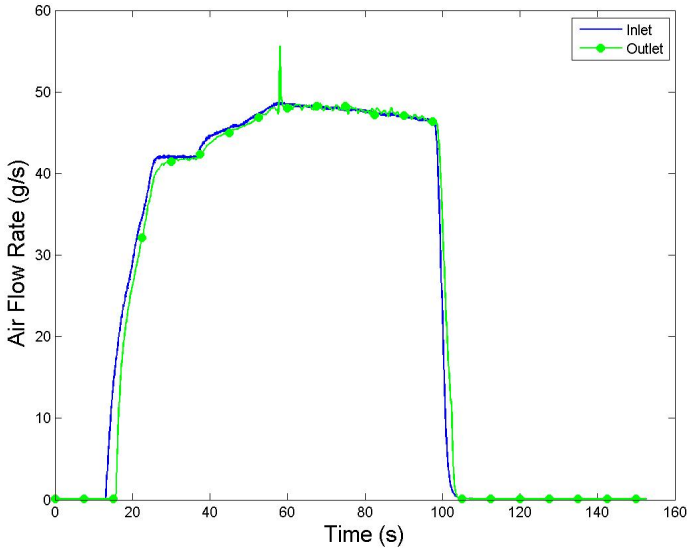

Figure E.86: Gas Mass Flow Rate for Run #7, Test 7.

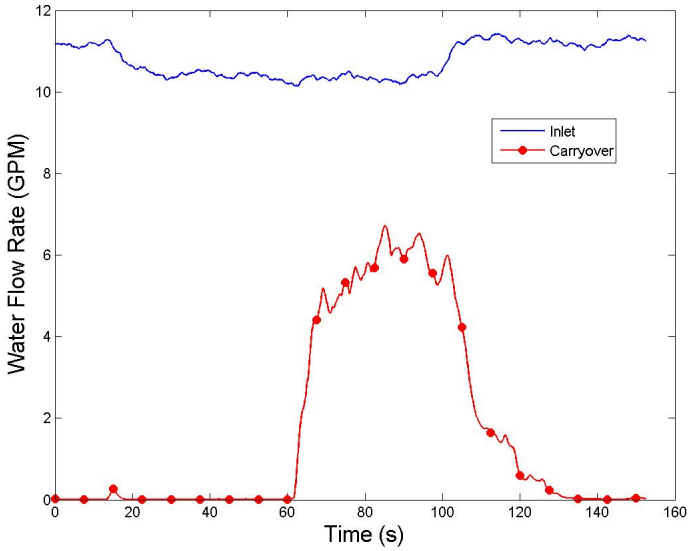

Figure E.87: Water Flow Rate for Run #7, Test 7.

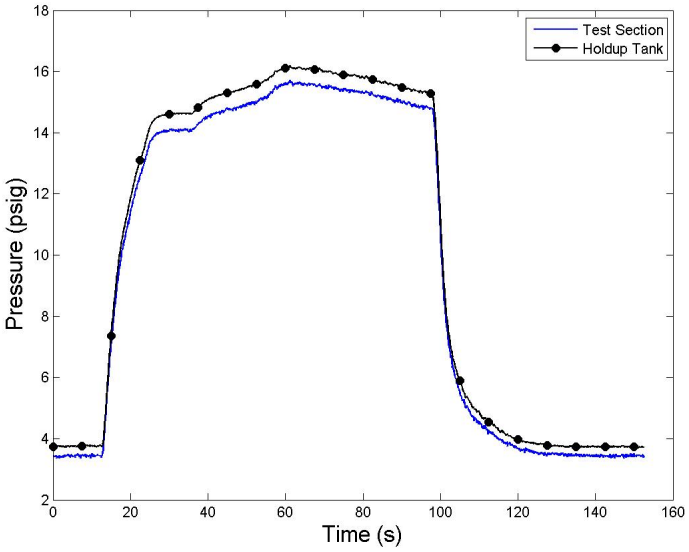

Figure E.88: System Pressure for Run #7, Test 7.

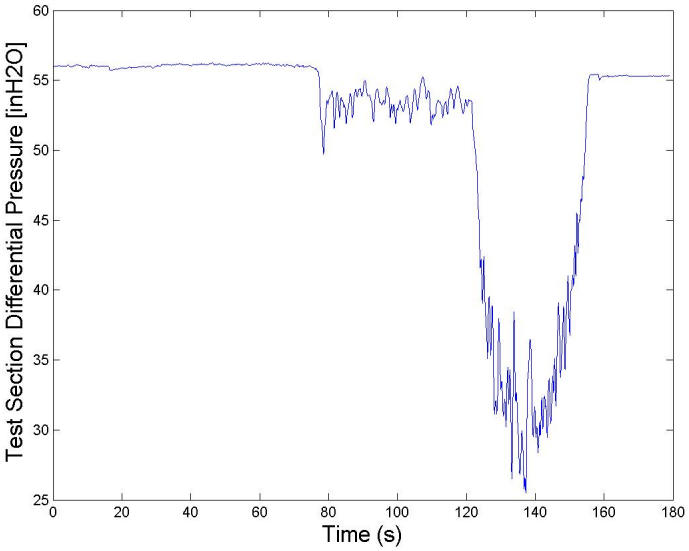

Figure E.89: Test Section Differential Pressure for Run #7, Test 8.

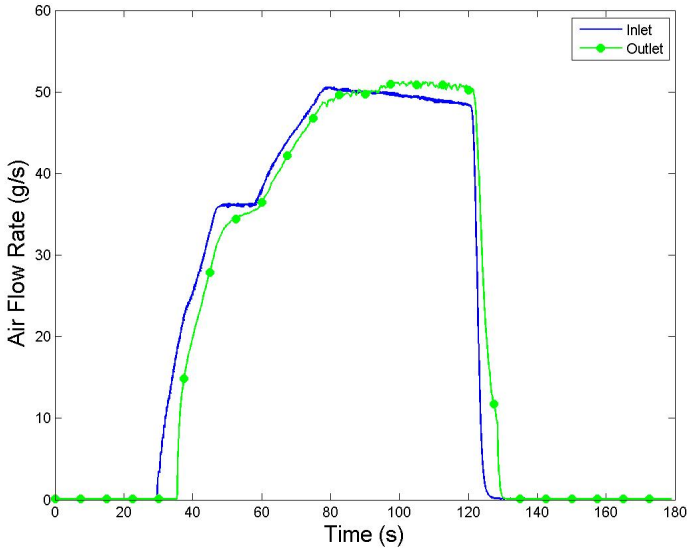

Figure E.90: Gas Mass Flow Rate for Run #7, Test 8.

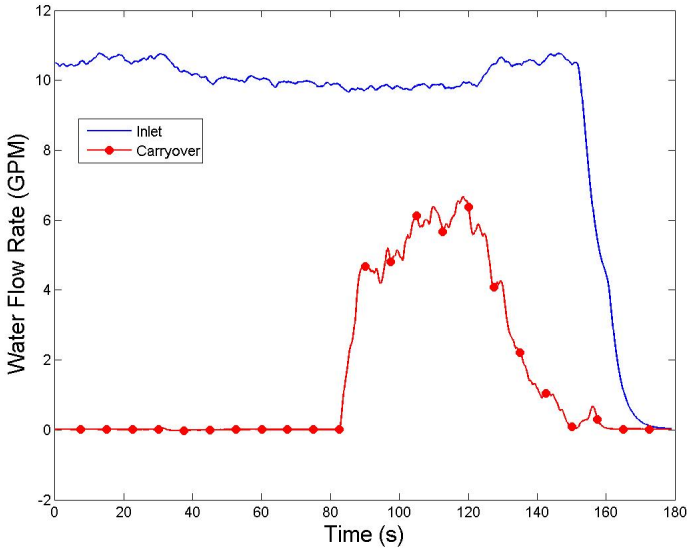

Figure E.91: Water Flow Rate for Run #7, Test 8.

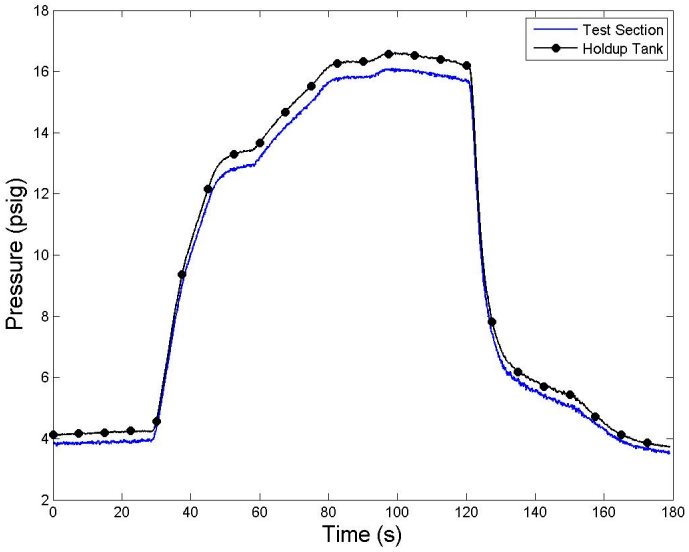

Figure E.92: System Pressure for Run #7, Test 8.

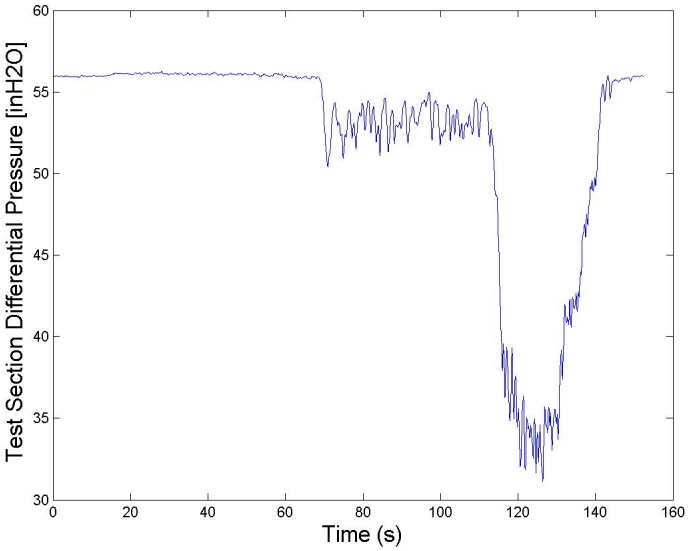

Figure E.93: Test Section Differential Pressure for Run #7, Test 9.

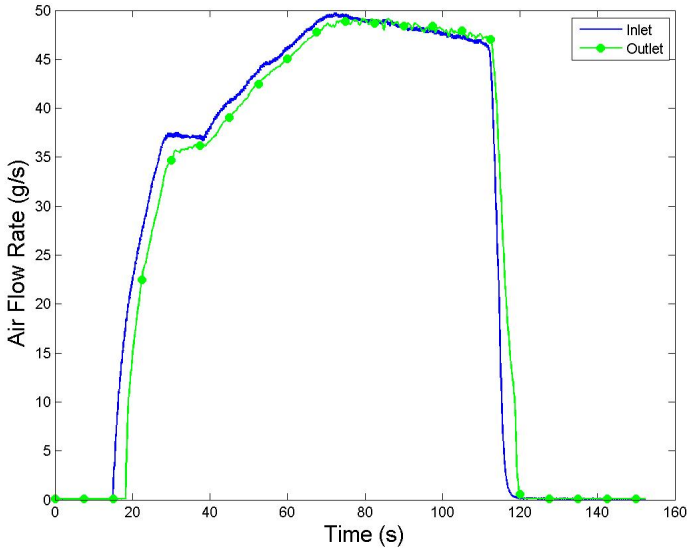

Figure E.94: Gas Mass Flow Rate for Run #7, Test 9.

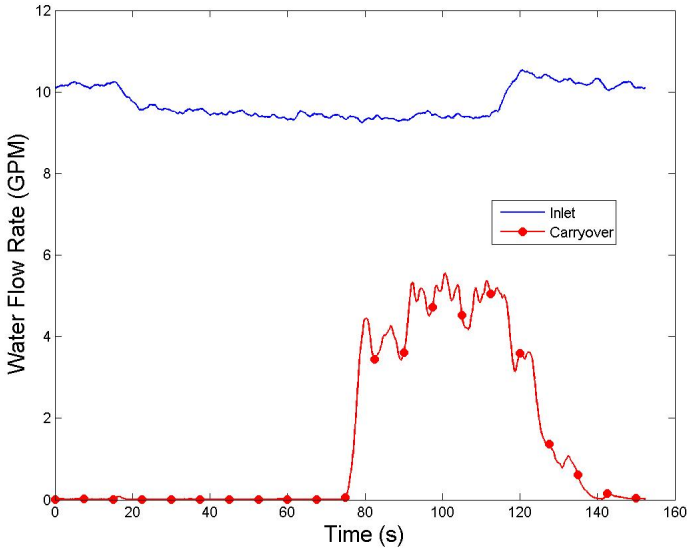

Figure E.95: Water Flow Rate for Run #7, Test 9.

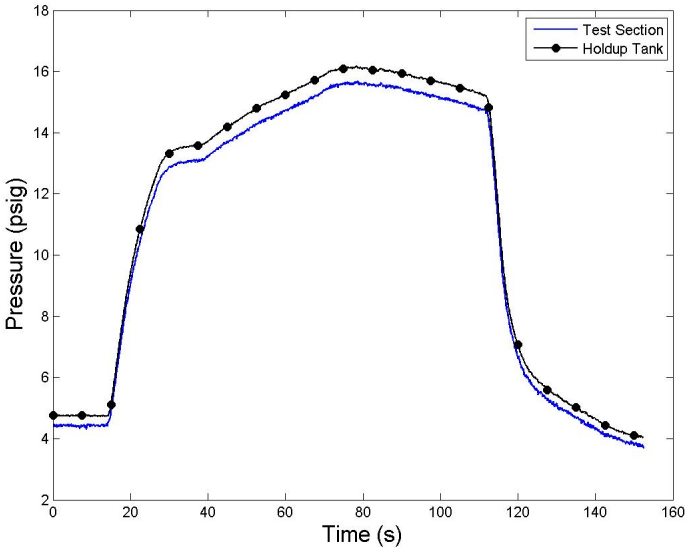

Figure E.96: System Pressure for Run #7, Test 9.

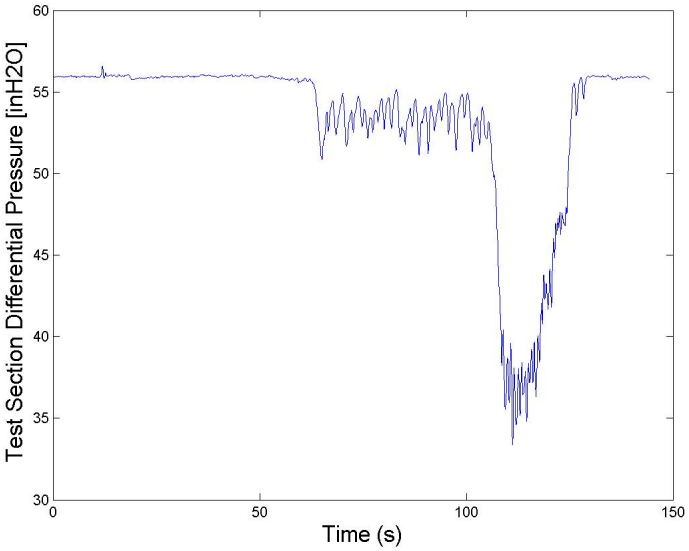

Figure E.97: Test Section Differential Pressure for Run #7, Test 10.

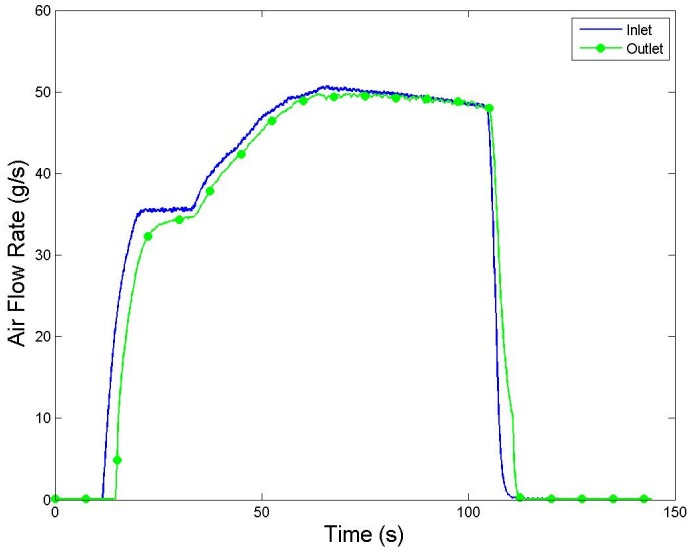

Figure E.98: Gas Mass Flow Rate for Run #7, Test 10.

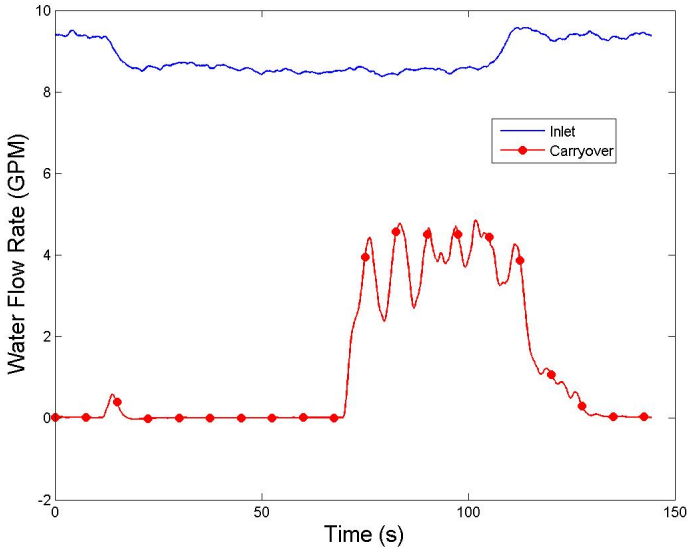

Figure E.99: Water Flow Rate for Run #7, Test 10.

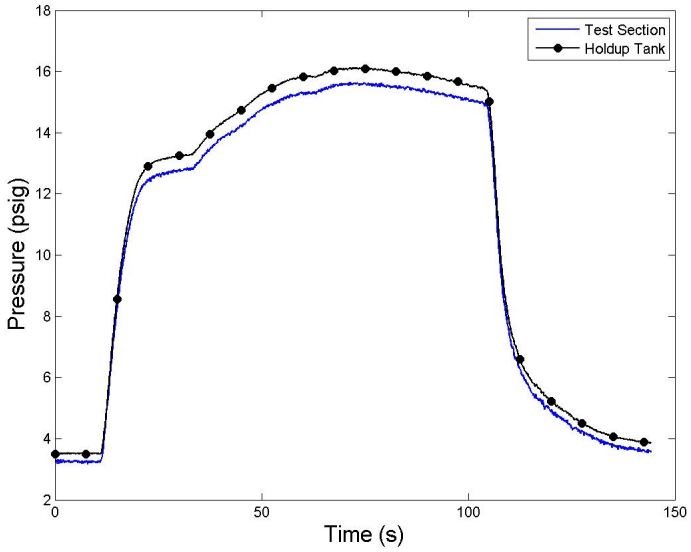

Figure E.100: System Pressure for Run #7, Test 10.

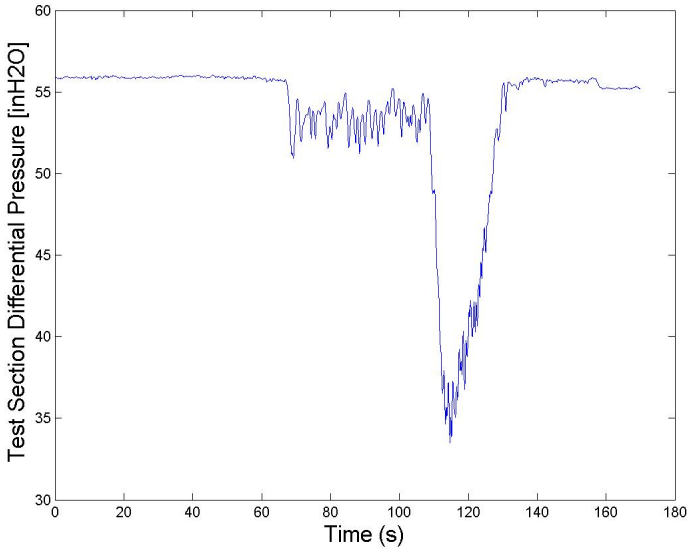

Figure E.101: Test Section Differential Pressure for Run #7, Test 11.

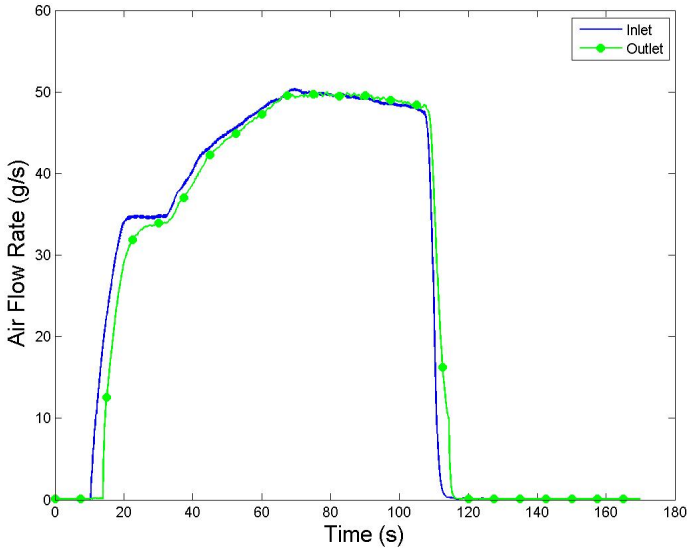

Figure E.102: Gas Mass Flow Rate for Run #7, Test 11.

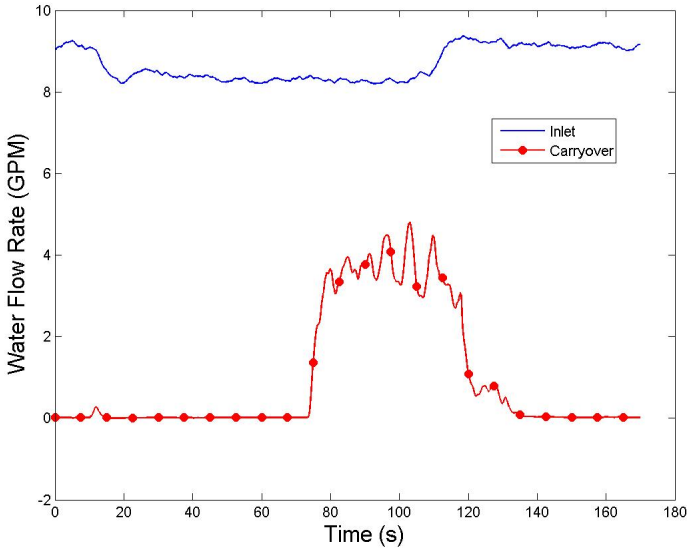

Figure E.103: Water Flow Rate for Run #7, Test 11.

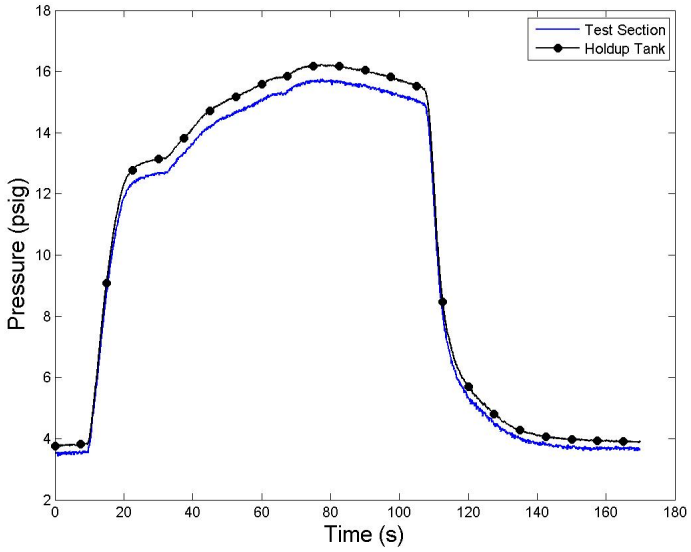

Figure E.104: System Pressure for Run #7, Test 11.

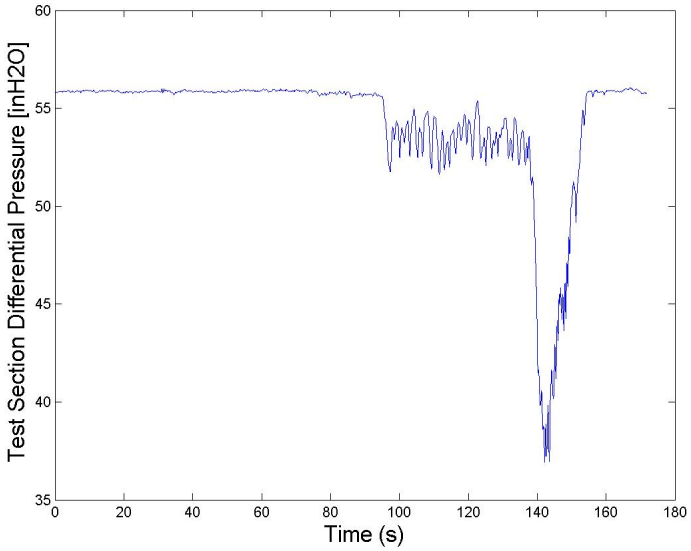

Figure E.105: Test Section Differential Pressure for Run #7, Test 12.

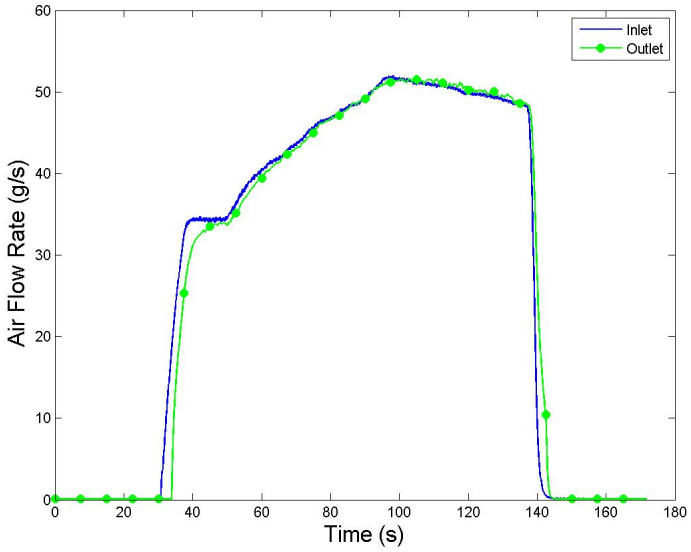

Figure E.106: Gas Mass Flow Rate for Run #7, Test 12.

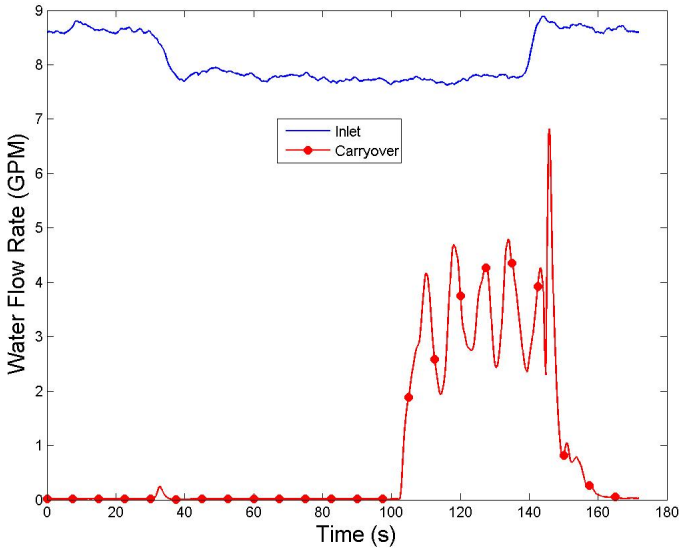

Figure E.107: Water Flow Rate for Run #7, Test 12.

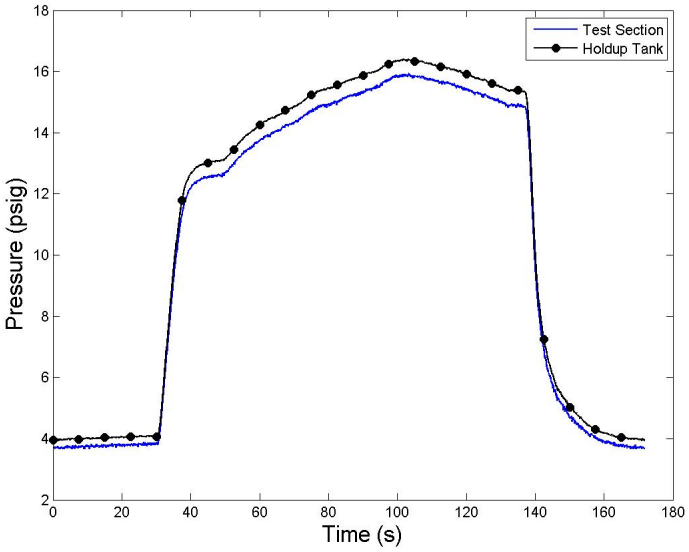

Figure E.108: System Pressure for Run #7, Test 12.

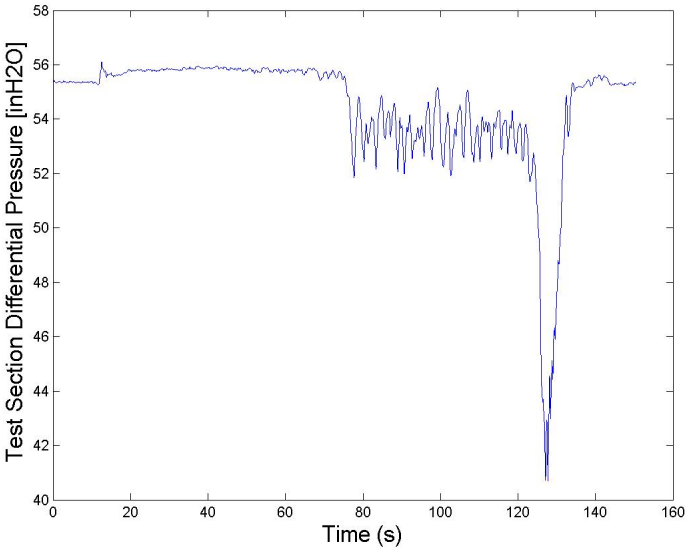

Figure E.109: Test Section Differential Pressure for Run #7, Test 13.

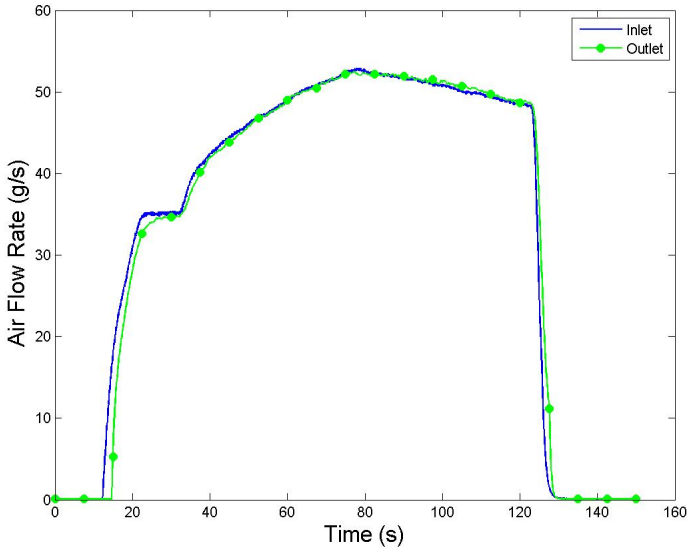

Figure E.110: Gas Mass Flow Rate for Run #7, Test 13.

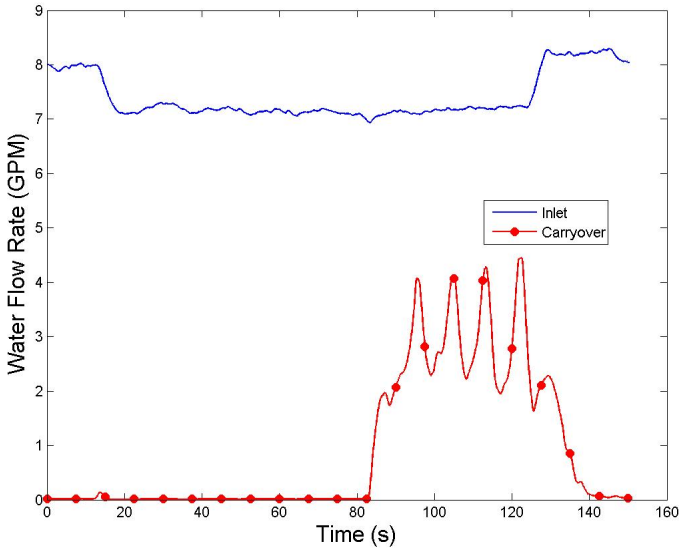

Figure E.111: Water Flow Rate for Run #7, Test 13.

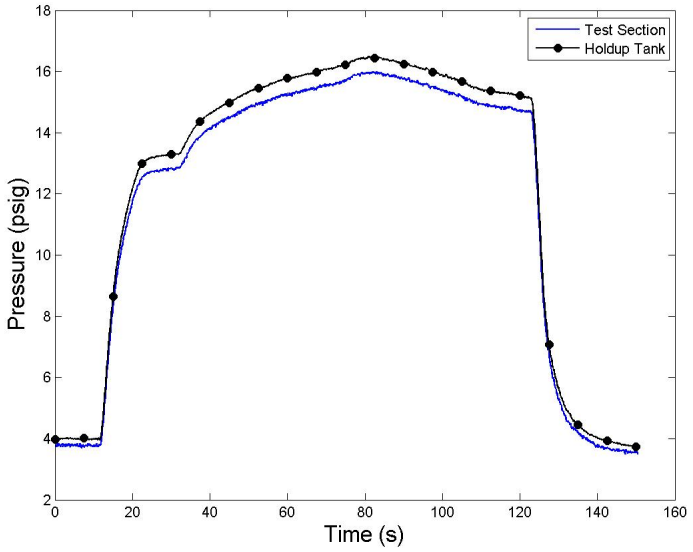

Figure E.112: System Pressure for Run #7, Test 13.

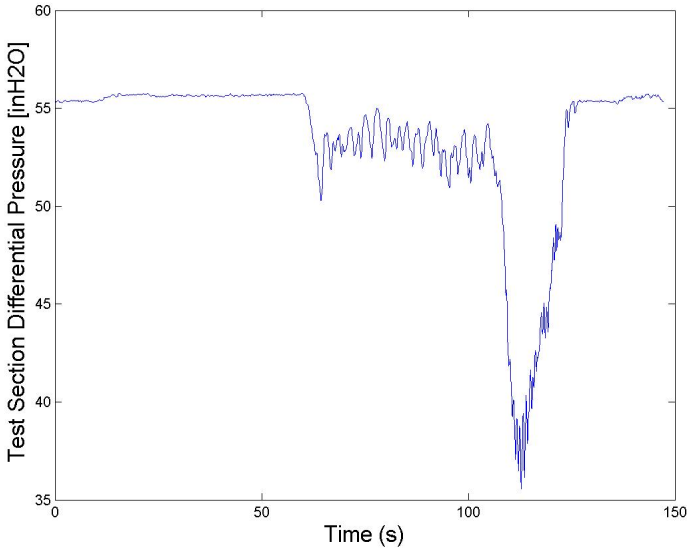

Figure E.113: Test Section Differential Pressure for Run #7, Test 15.

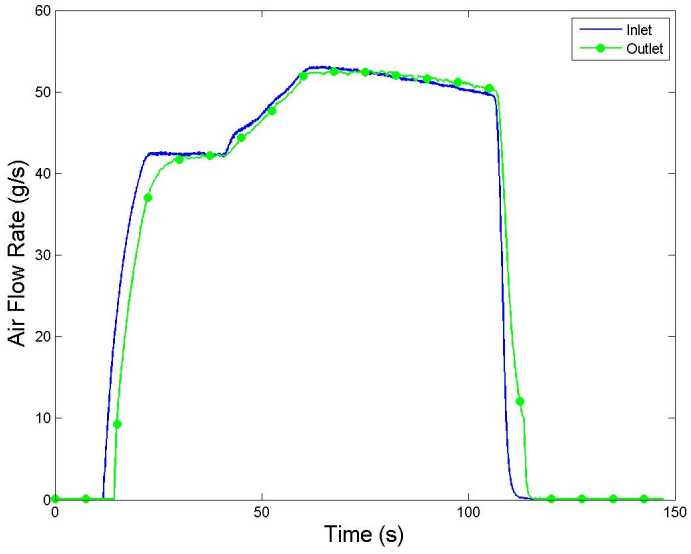

Figure E.114: Gas Mass Flow Rate for Run #7, Test 15.

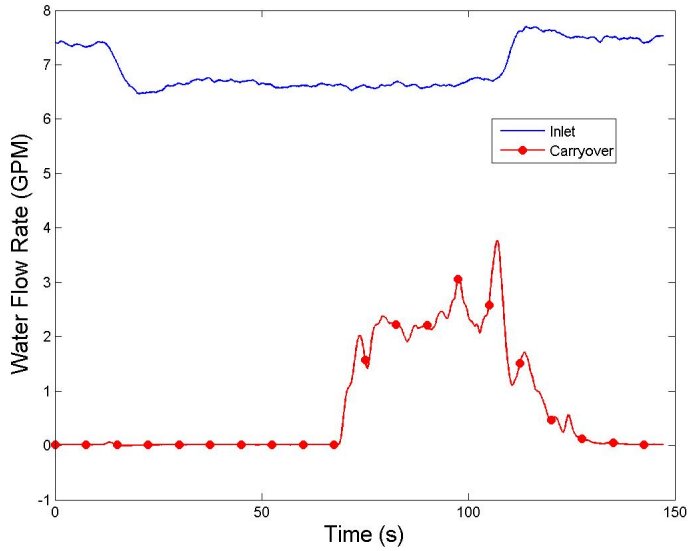

Figure E.115: Water Flow Rate for Run #7, Test 15.

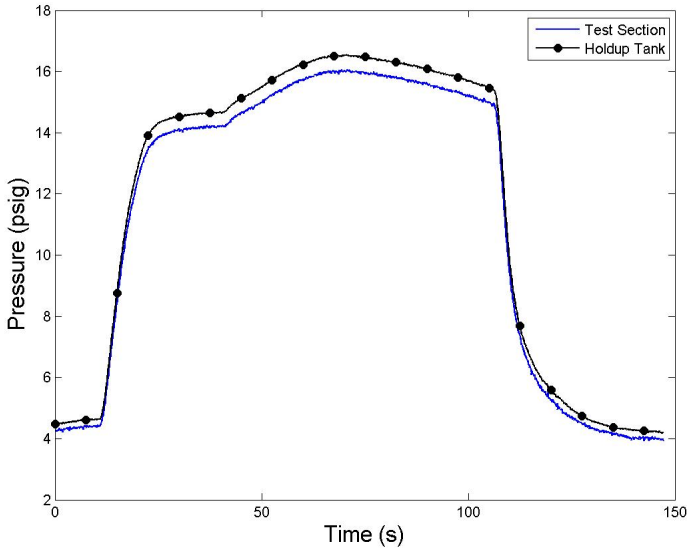

Figure E.116: System Pressure for Run #7, Test 15.

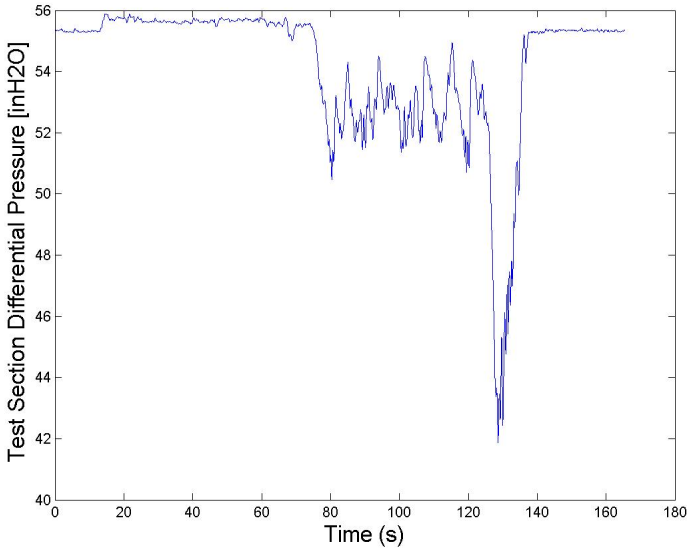

Figure E.117: Test Section Differential Pressure for Run #7, Test 16.

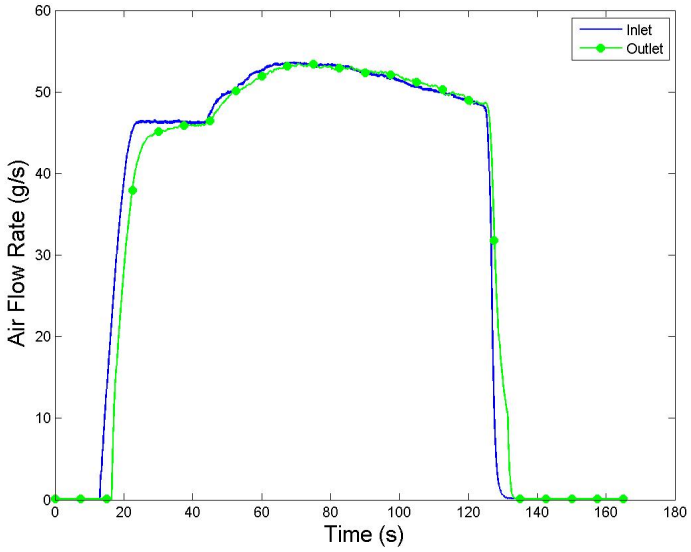

Figure E.118: Gas Mass Flow Rate for Run #7, Test 16.

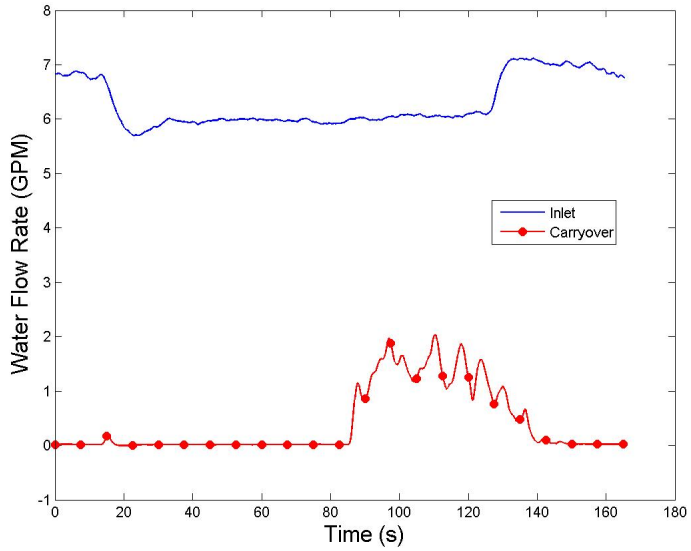

Figure E.119: Water Flow Rate for Run #7, Test 16.

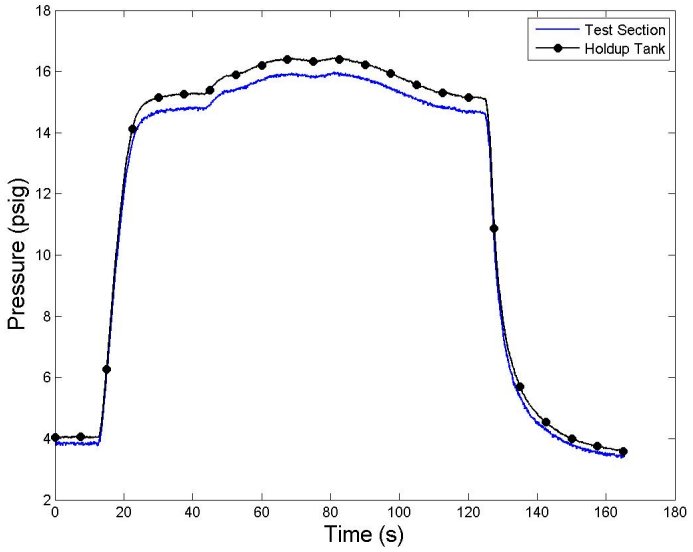

Figure E.120: System Pressure for Run #7, Test 16.

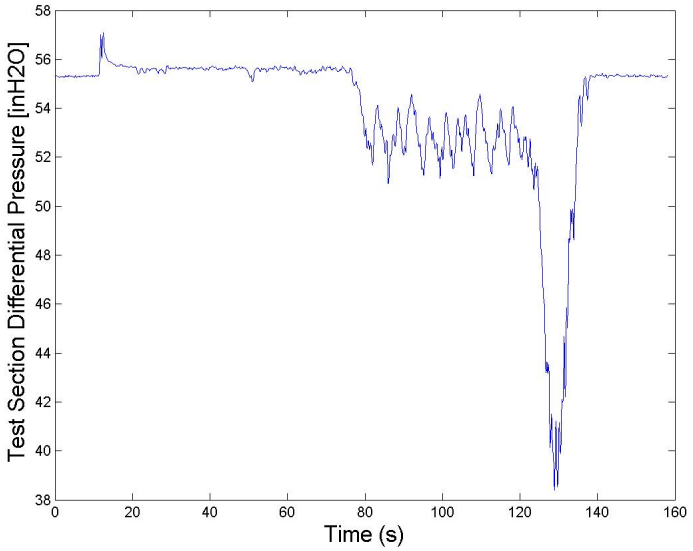

Figure E.121: Test Section Differential Pressure for Run #7, Test 17.

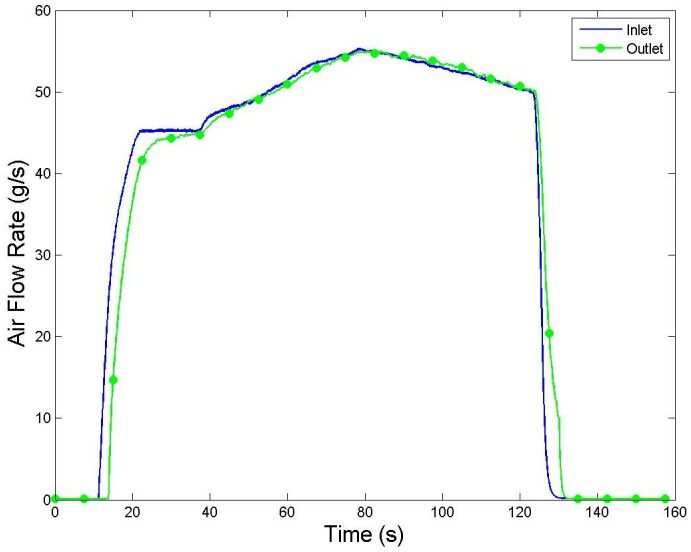

Figure E.122: Gas Mass Flow Rate for Run #7, Test 17.

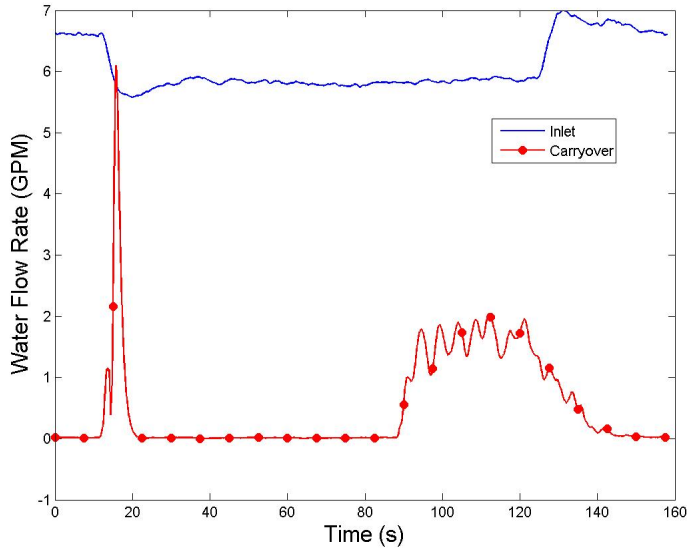

Figure E.123: Water Flow Rate for Run #7, Test 17.

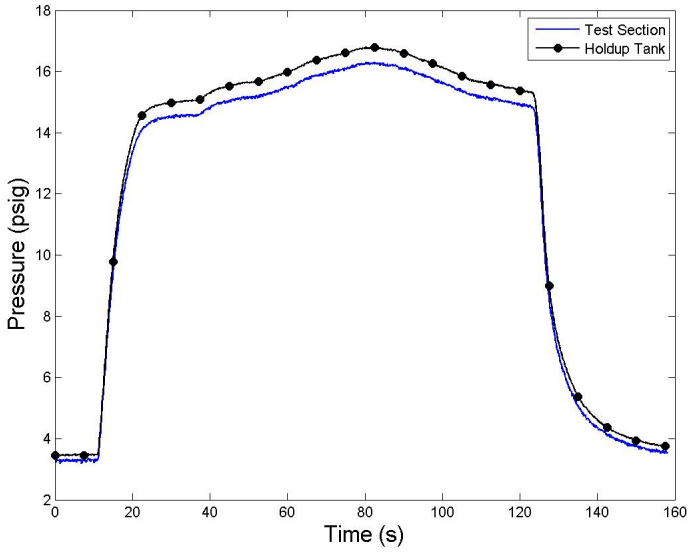

Figure E.124: System Pressure for Run #7, Test 17.

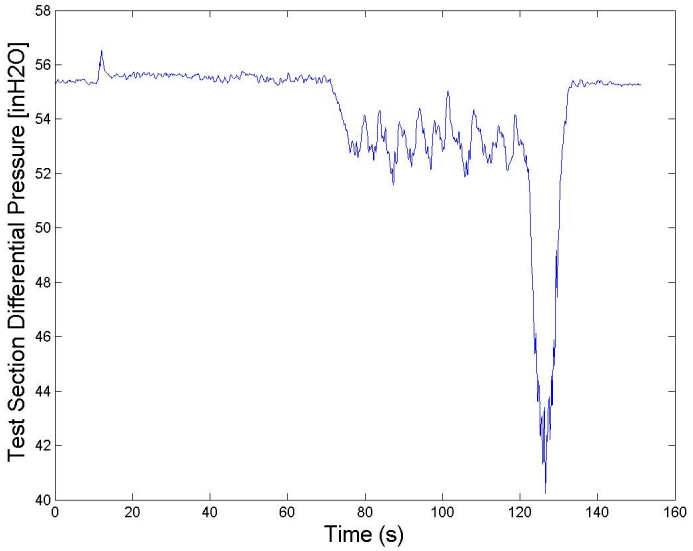

Figure E.125: Test Section Differential Pressure for Run #7, Test 18.

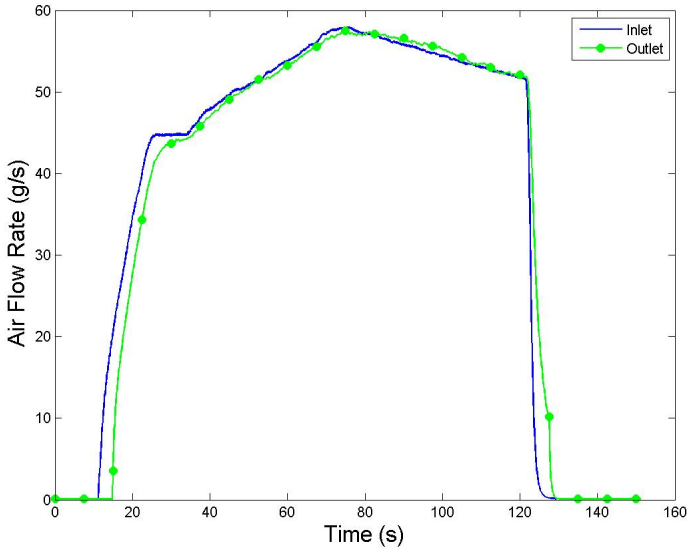

Figure E.126: Gas Mass Flow Rate for Run #7, Test 18.

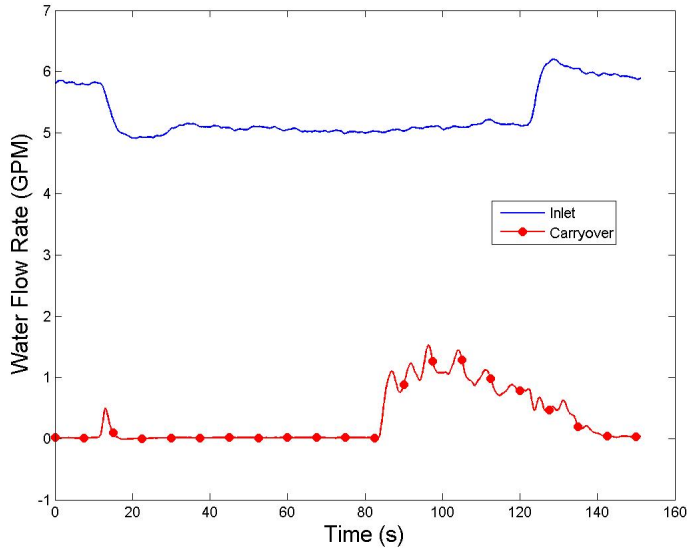

Figure E.127: Water Flow Rate for Run #7, Test 18.

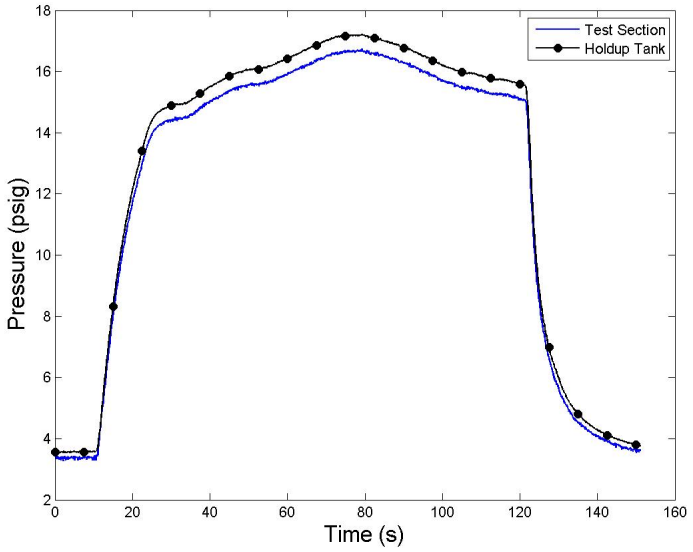

Figure E.128: System Pressure for Run #7, Test 18.

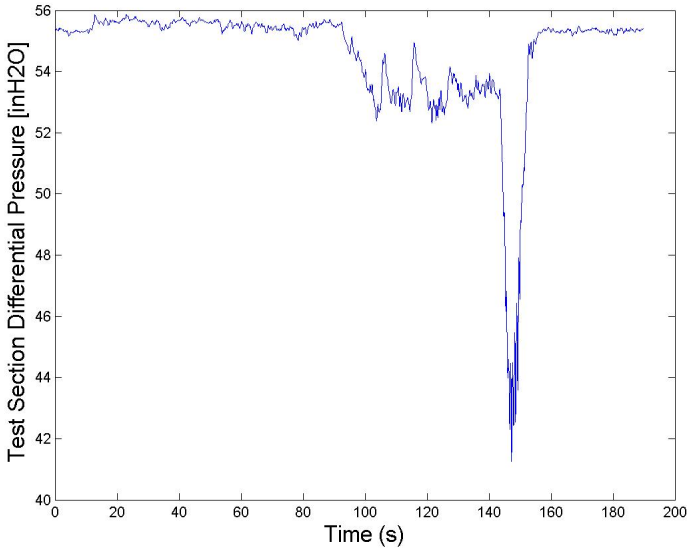

Figure E.129: Test Section Differential Pressure for Run #7, Test 19.

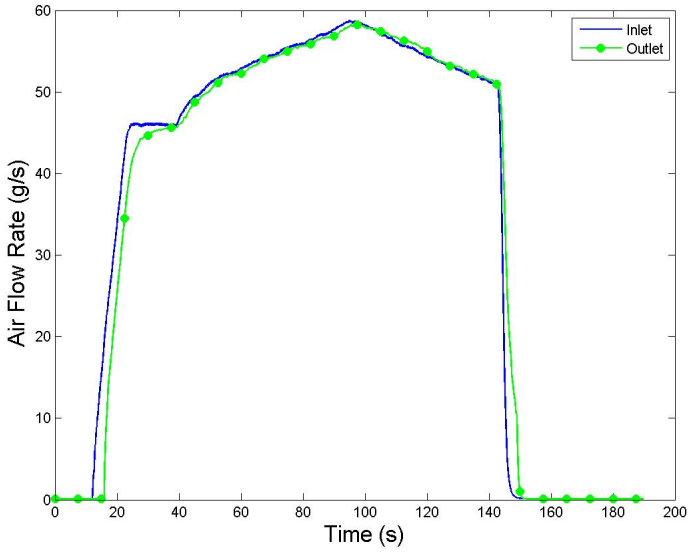

Figure E.130: Gas Mass Flow Rate for Run #7, Test 19.

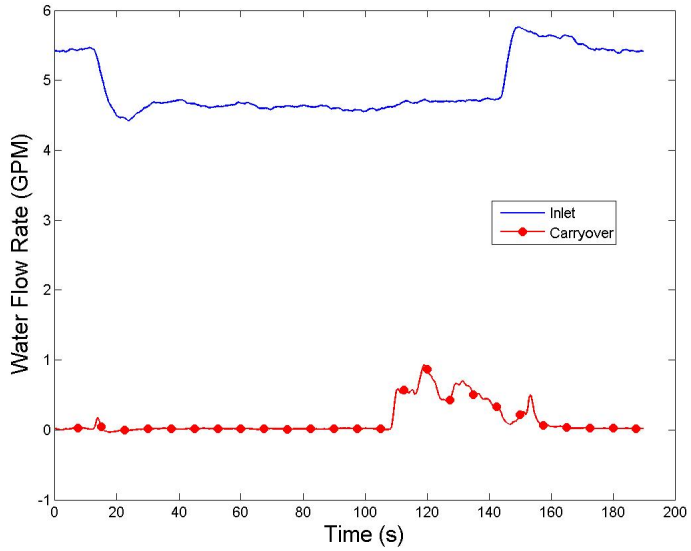

Figure E.131: Water Flow Rate for Run #7, Test 19.

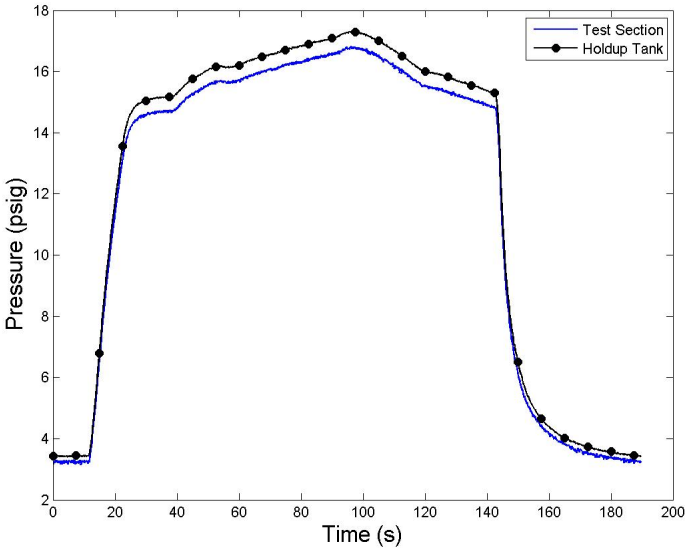

Figure E.132: System Pressure for Run #7, Test 19.

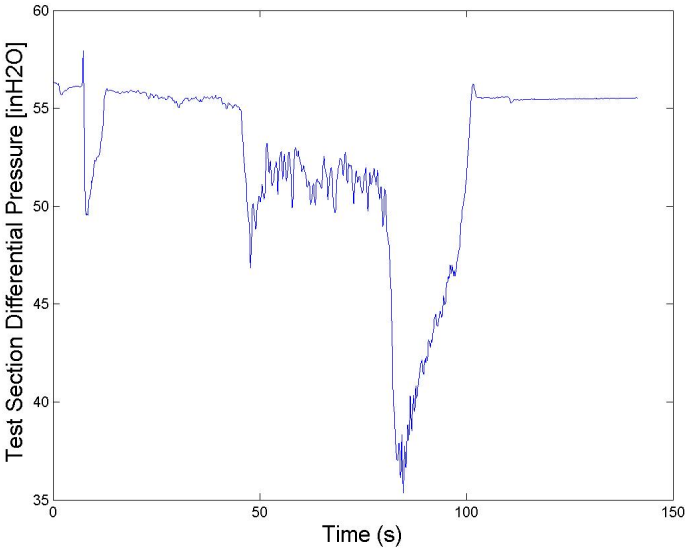

Figure E.133: Test Section Differential Pressure for Run #5, Test 3.

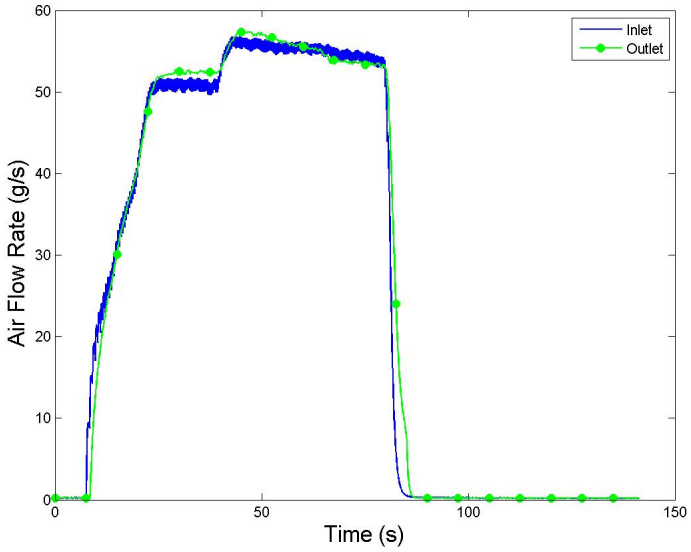

Figure E.134: Gas Mass Flow Rate for Run #5, Test 3.

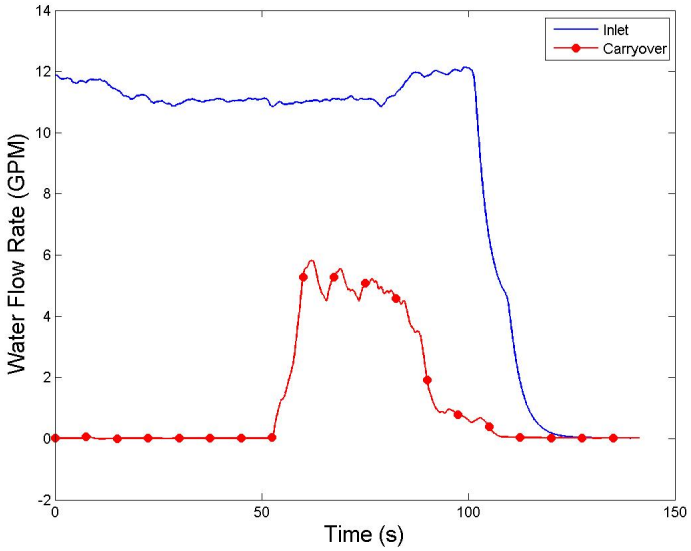

Figure E.135: Water Flow Rate for Run #5, Test 3.

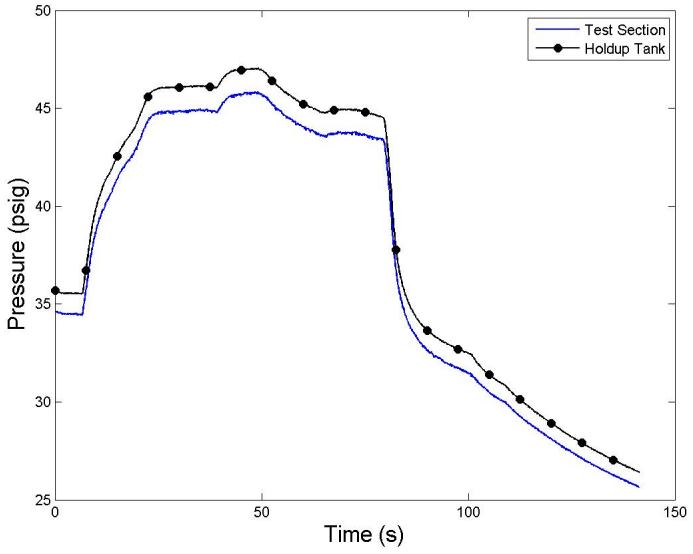

Figure E.136: System Pressure for Run #5, Test 3.

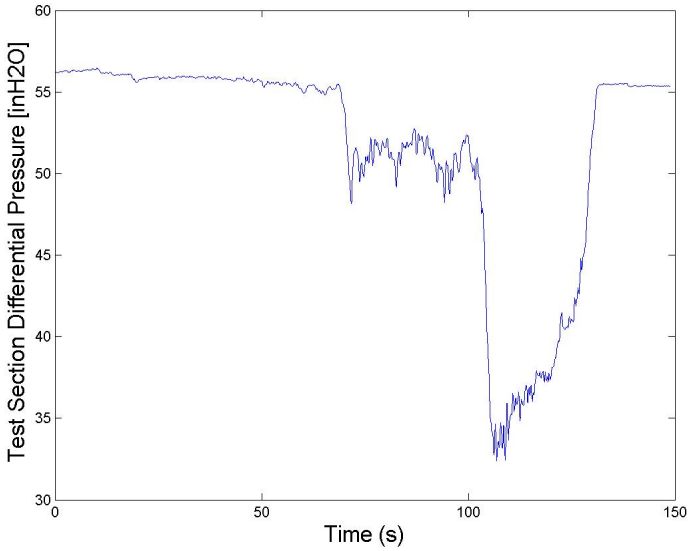

Figure E.137: Test Section Differential Pressure for Run #5, Test 4.

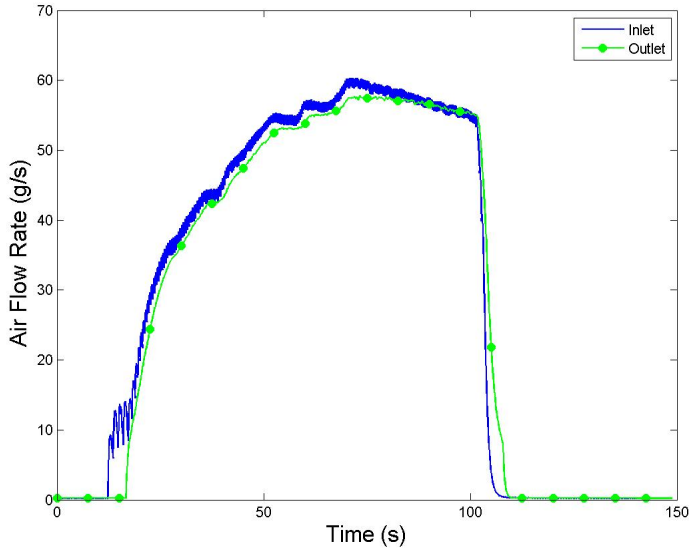

Figure E.138: Gas Mass Flow Rate for Run #5, Test 4.

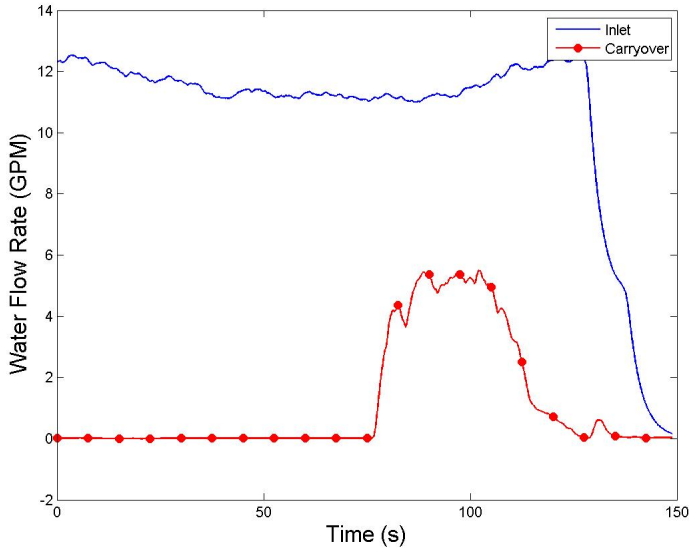

Figure E.139: Water Flow Rate for Run #5, Test 4.

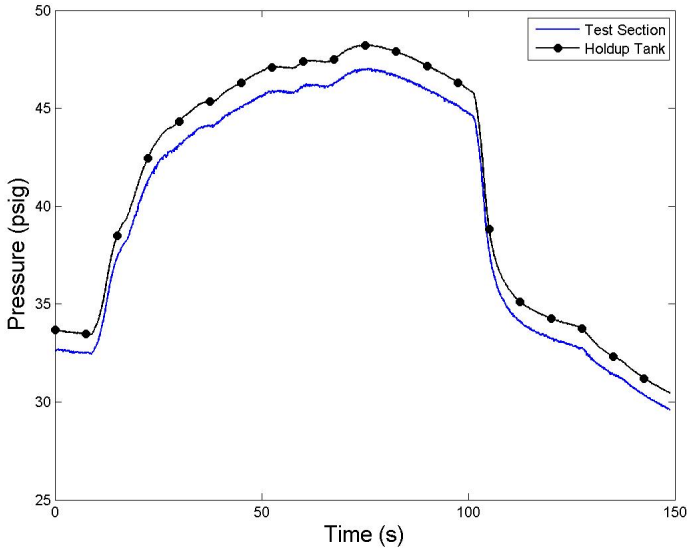

Figure E.140: System Pressure for Run #5, Test 4.

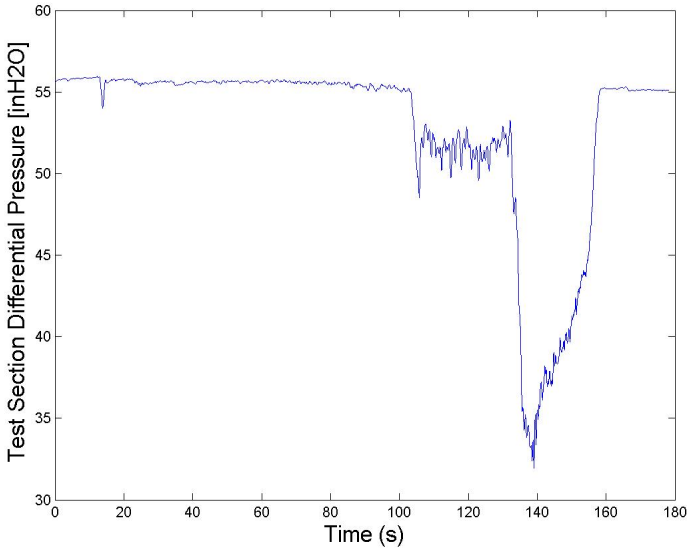

Figure E.141: Test Section Differential Pressure for Run #5, Test 6.

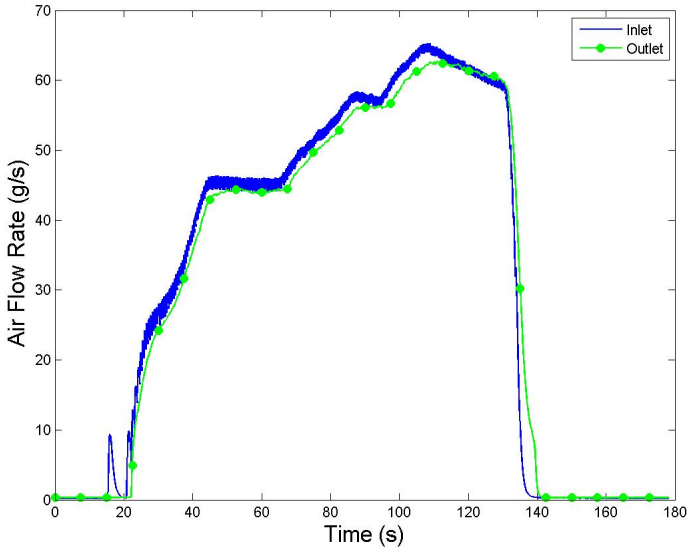

Figure E.142: Gas Mass Flow Rate for Run #5, Test 6.

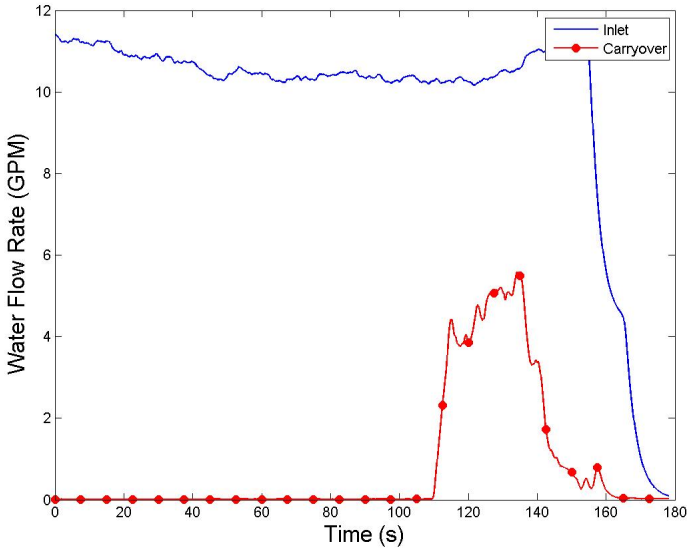

Figure E.143: Water Flow Rate for Run #5, Test 6.

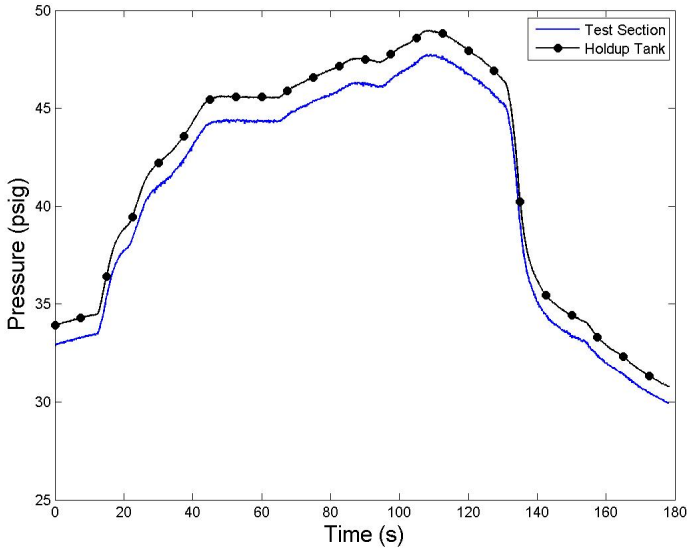

Figure E.144: System Pressure for Run #5, Test 6.

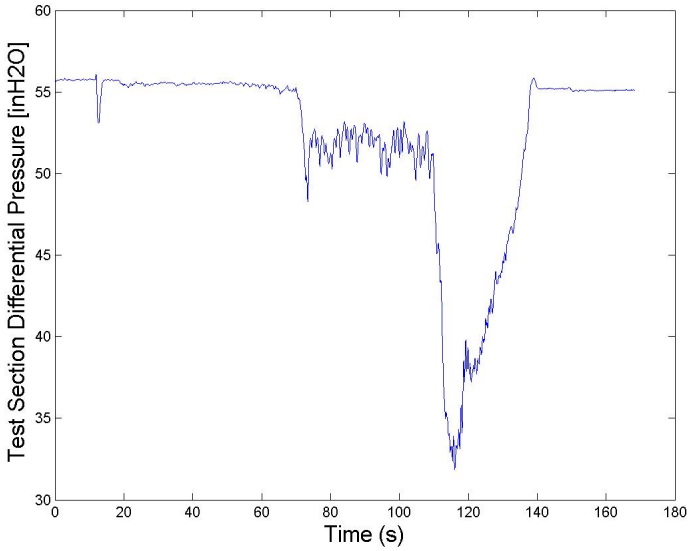

Figure E.145: Test Section Differential Pressure for Run #5, Test 7.

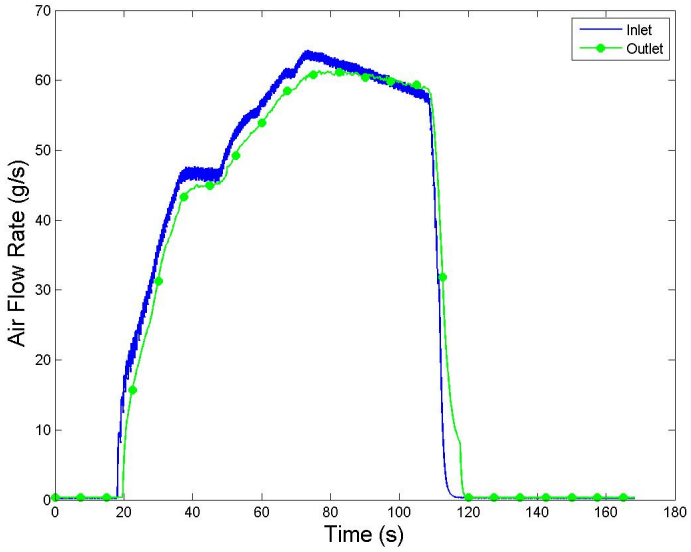

Figure E.146: Gas Mass Flow Rate for Run #5, Test 7.

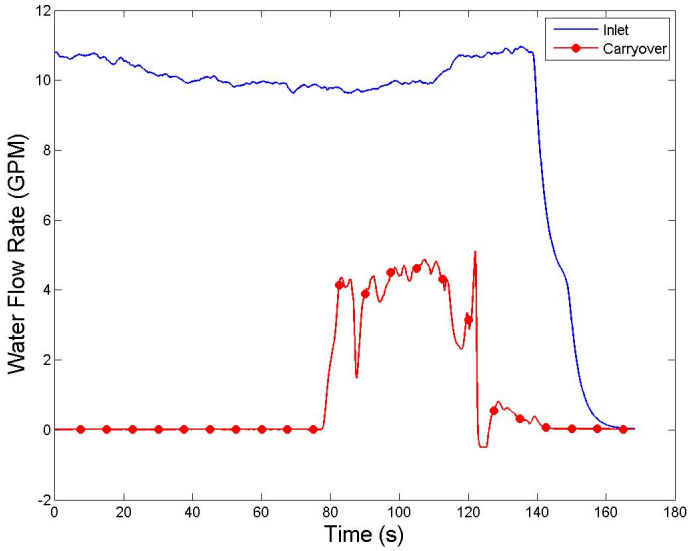

Figure E.147: Water Flow Rate for Run #5, Test 7.

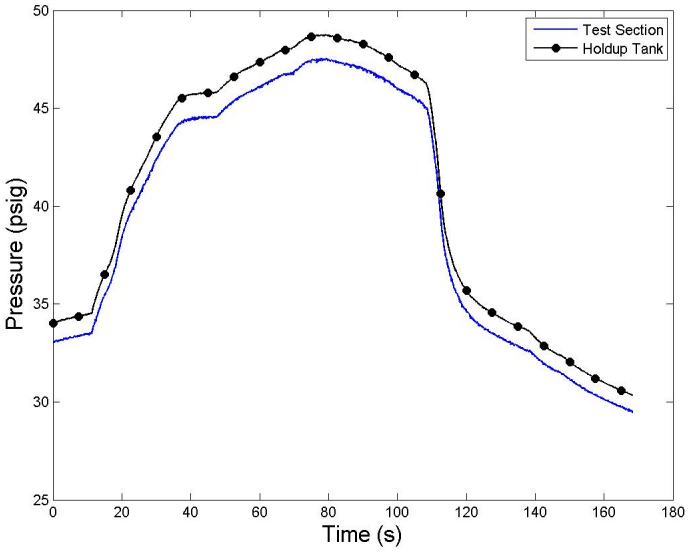

Figure E.148: System Pressure for Run #5, Test 7.

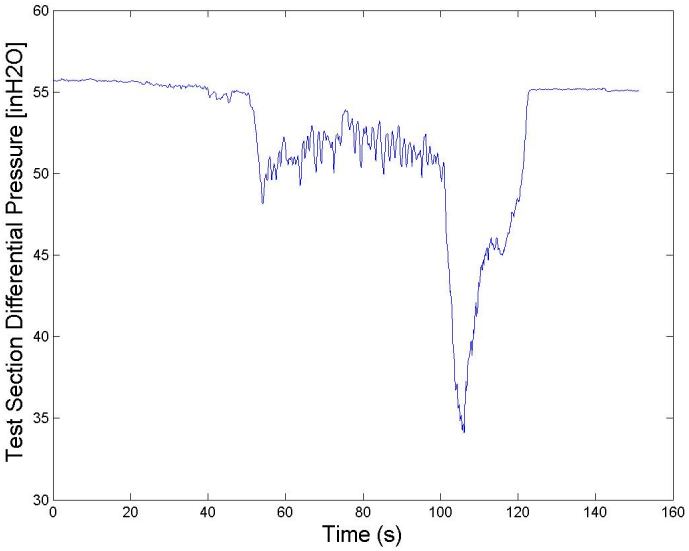

Figure E.149: Test Section Differential Pressure for Run #5, Test 8.

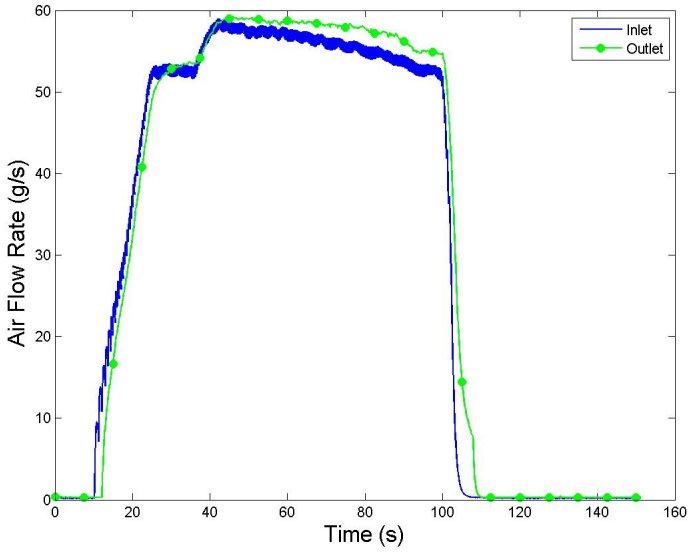

Figure E.150: Gas Mass Flow Rate for Run #5, Test 8.

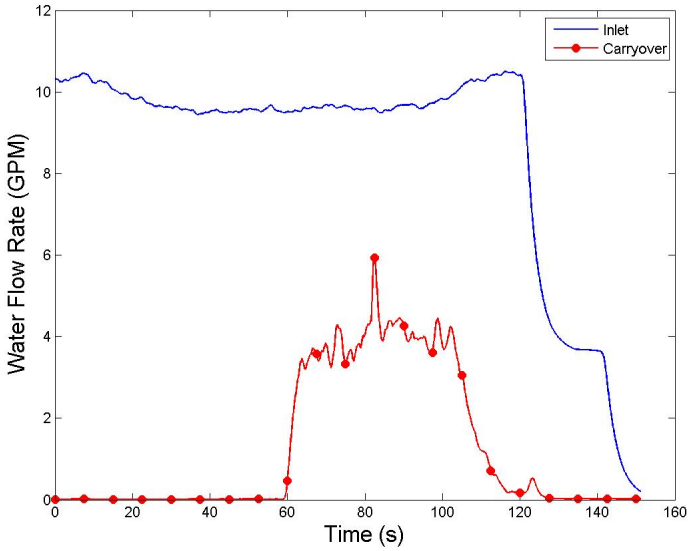

Figure E.151: Water Flow Rate for Run #5, Test 8.

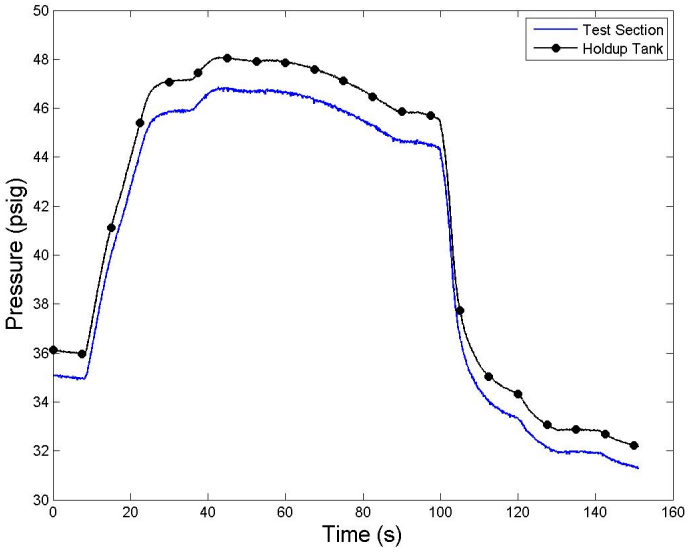

Figure E.152: System Pressure for Run #5, Test 8.

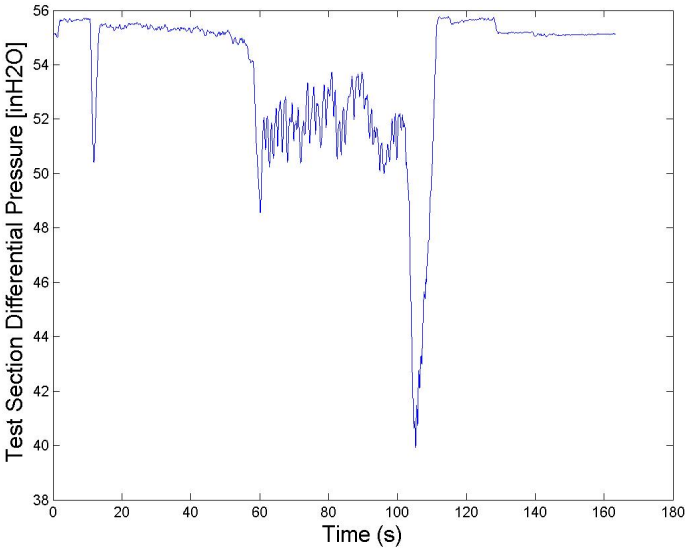

Figure E.153: Test Section Differential Pressure for Run #5, Test 9.

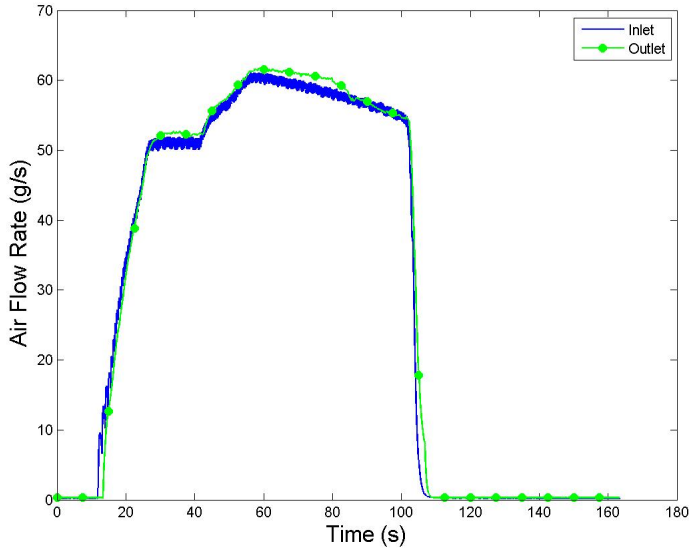

Figure E.154: Gas Mass Flow Rate for Run #5, Test 9.

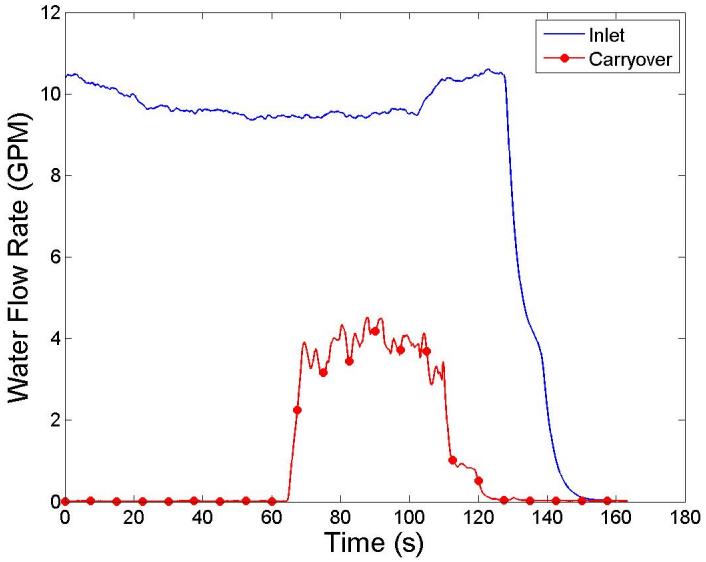

Figure E.155: Water Flow Rate for Run #5, Test 9.

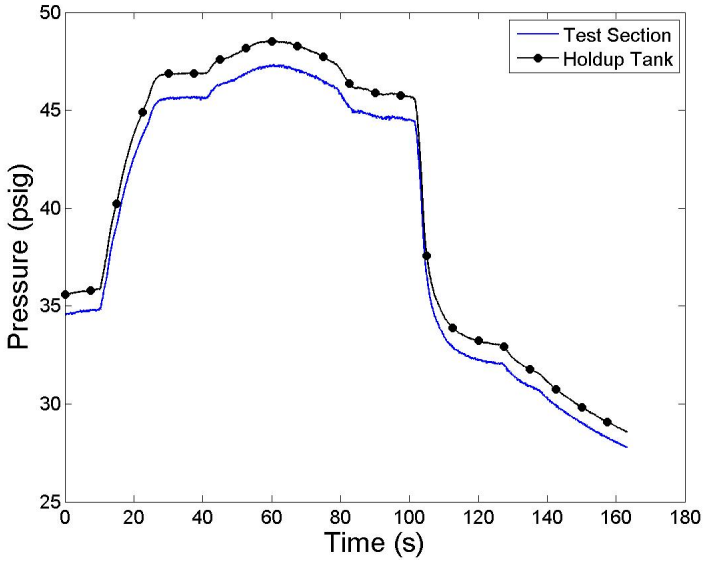

Figure E.156: System Pressure for Run #5, Test 9.

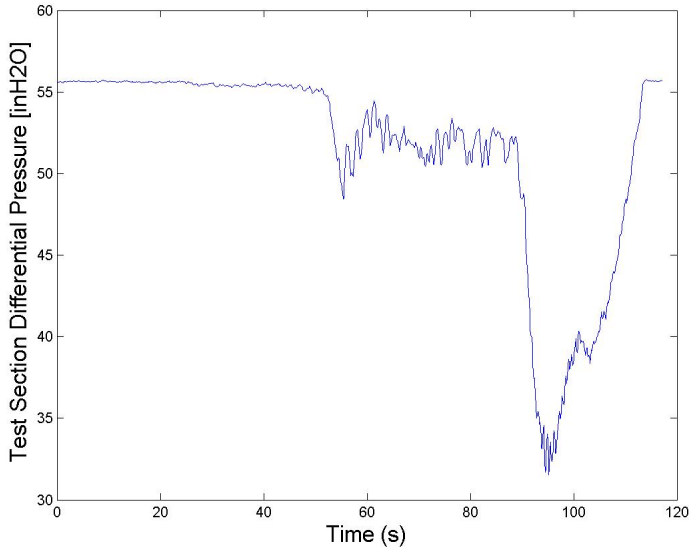

Figure E.157: Test Section Differential Pressure for Run #5, Test 10.

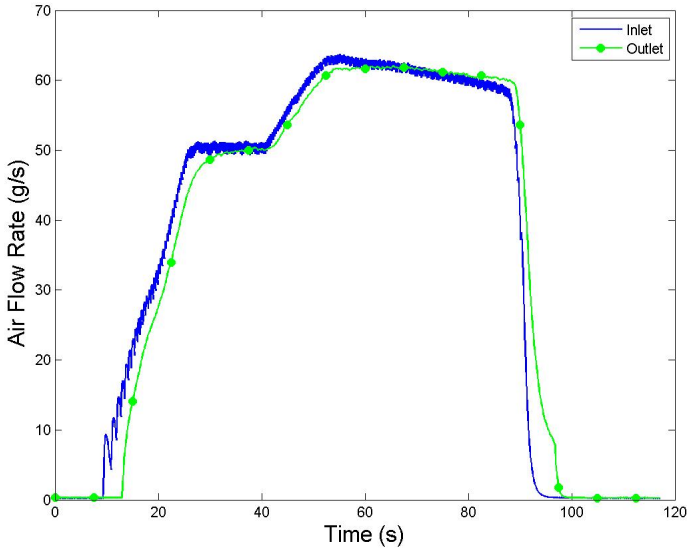

Figure E.158: Gas Mass Flow Rate for Run #5, Test 10.

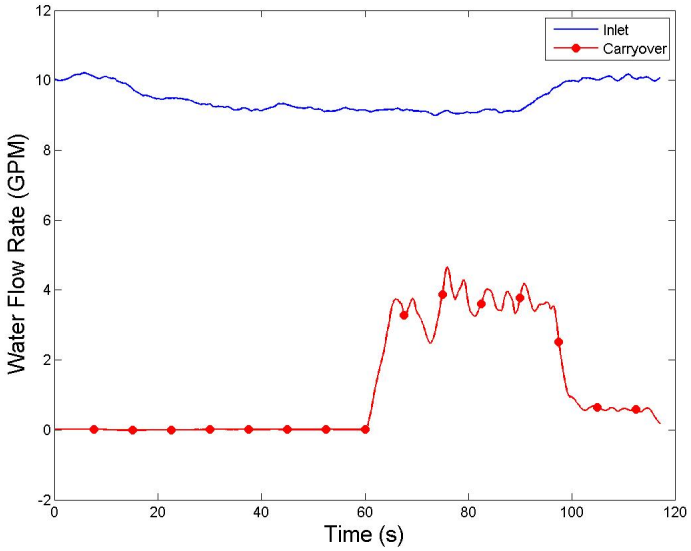

Figure E.159: Water Flow Rate for Run #5, Test 10.

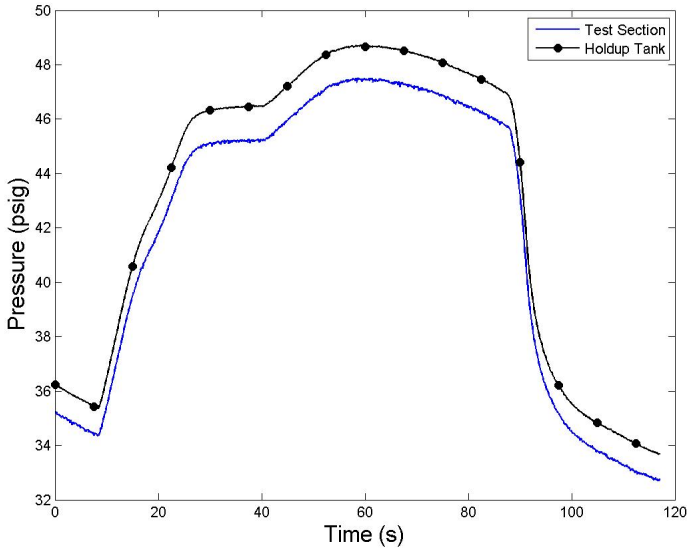

Figure E.160: System Pressure for Run #5, Test 10.

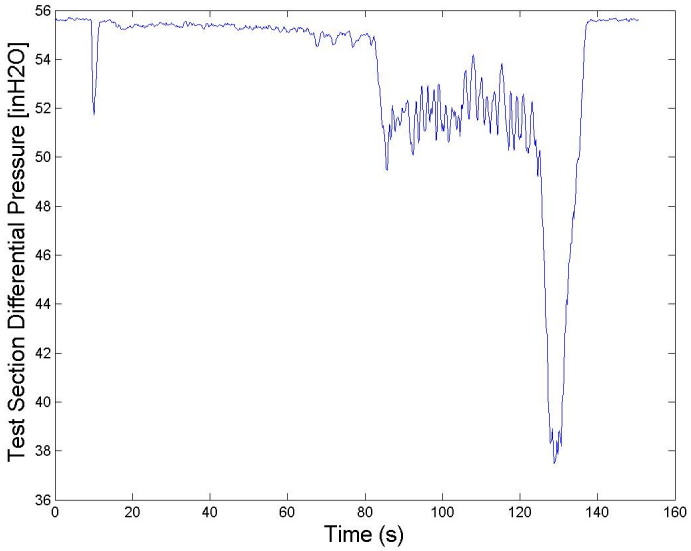

Figure E.161: Test Section Differential Pressure for Run #5, Test 11.

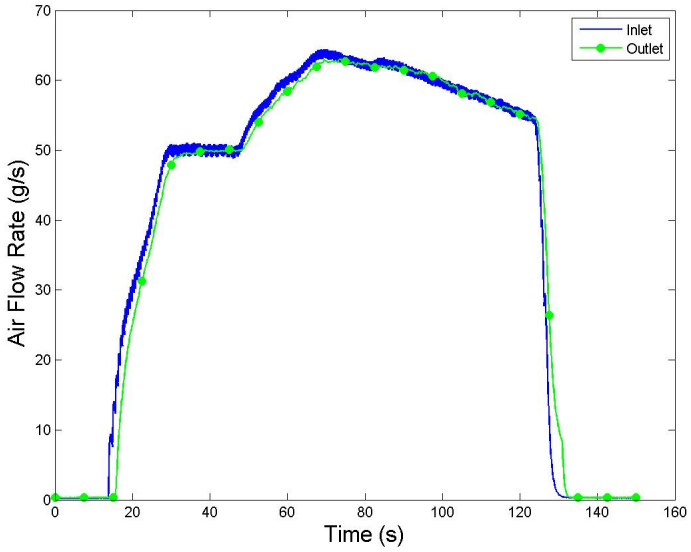

Figure E.162: Gas Mass Flow Rate for Run #5, Test 11.

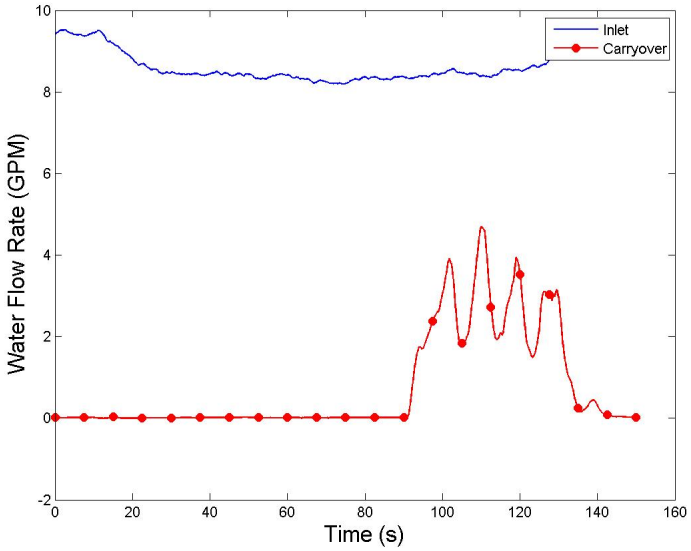

Figure E.163: Water Flow Rate for Run #5, Test 11.

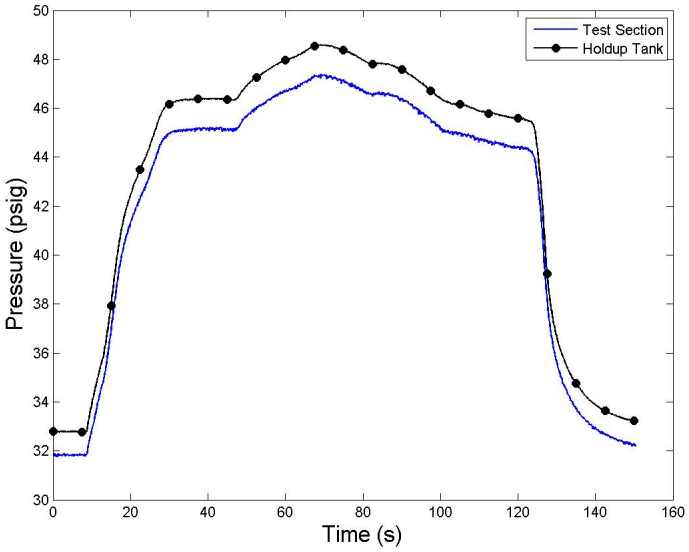

Figure E.164: System Pressure for Run #5, Test 11.

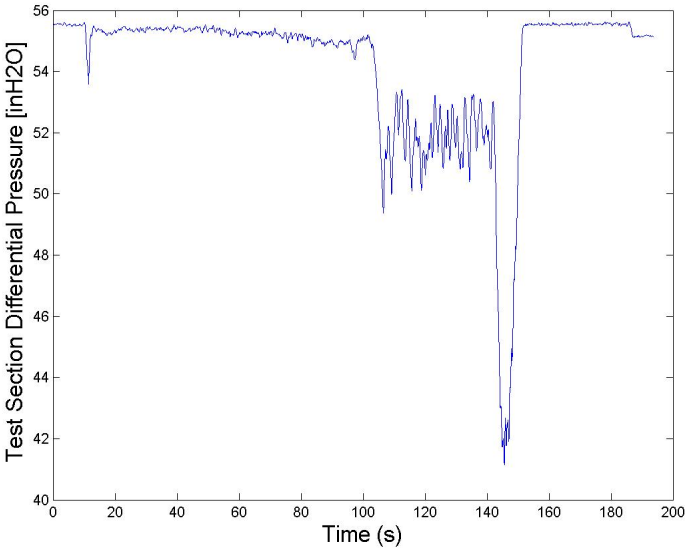

Figure E.165: Test Section Differential Pressure for Run #5, Test 12.

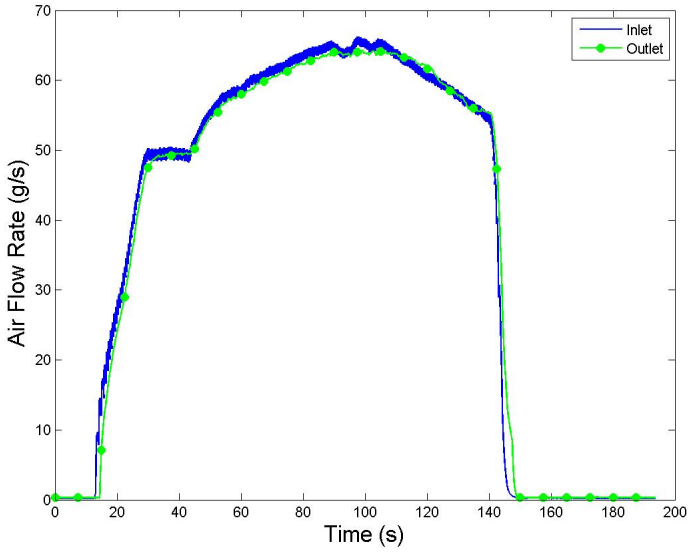

Figure E.166: Gas Mass Flow Rate for Run #5, Test 12.

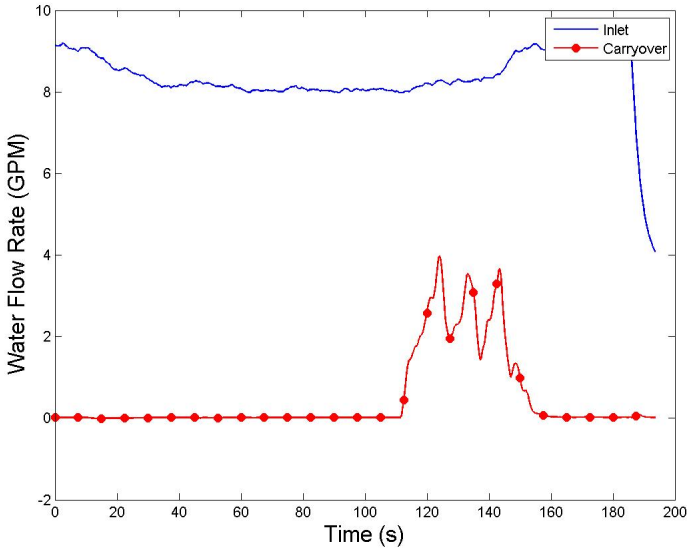

Figure E.167: Water Flow Rate for Run #5, Test 12.

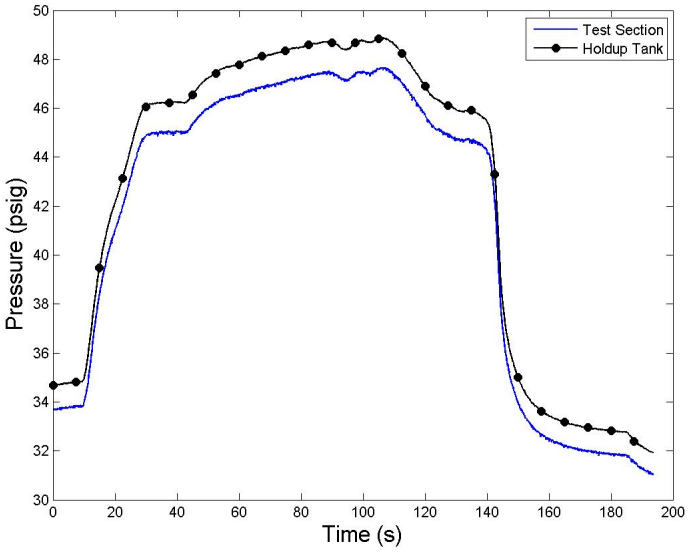

Figure E.168: System Pressure for Run #5, Test 12.

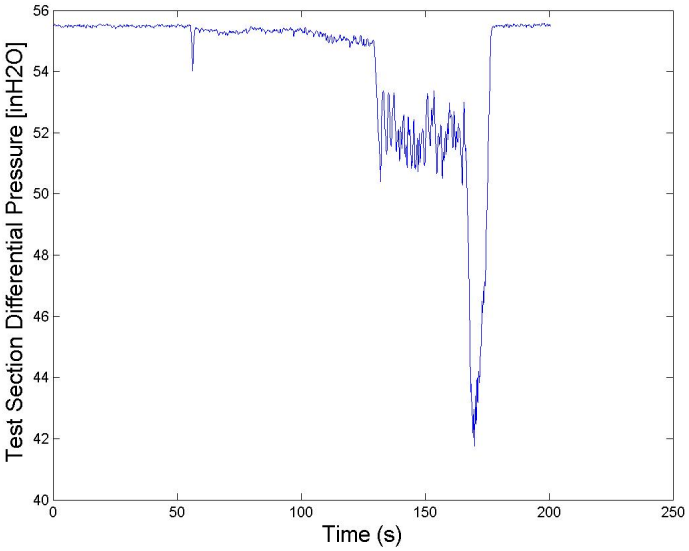

Figure E.169: Test Section Differential Pressure for Run #5, Test 13a.

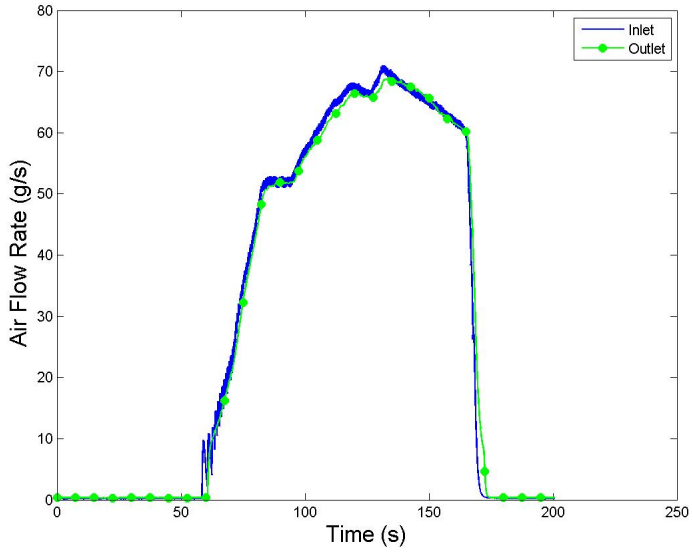

Figure E.170: Gas Mass Flow Rate for Run #5, Test 13a.

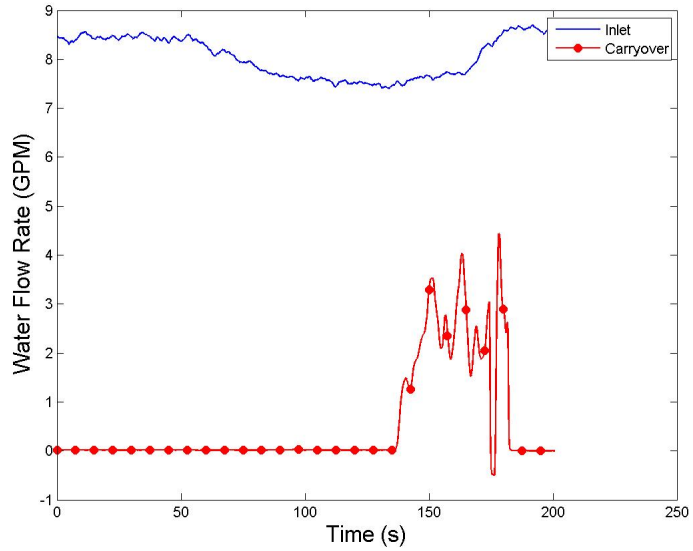

Figure E.171: Water Flow Rate for Run #5, Test 13a.

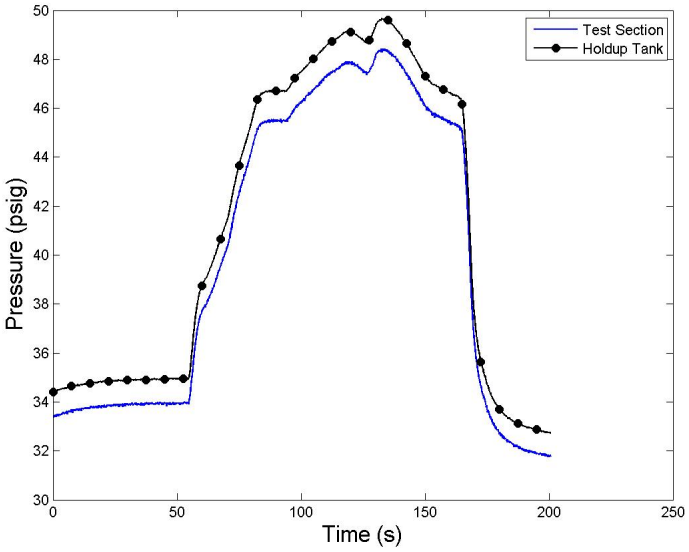

Figure E.172: System Pressure for Run #5, Test 13a.

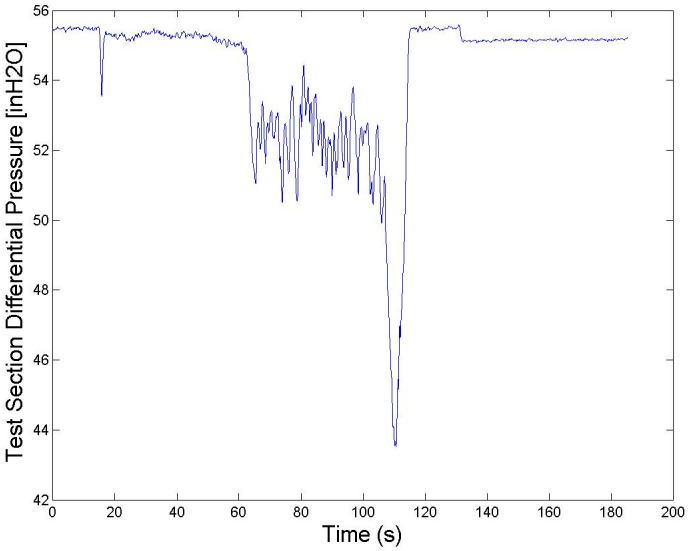

Figure E.173: Test Section Differential Pressure for Run #5, Test 13b.

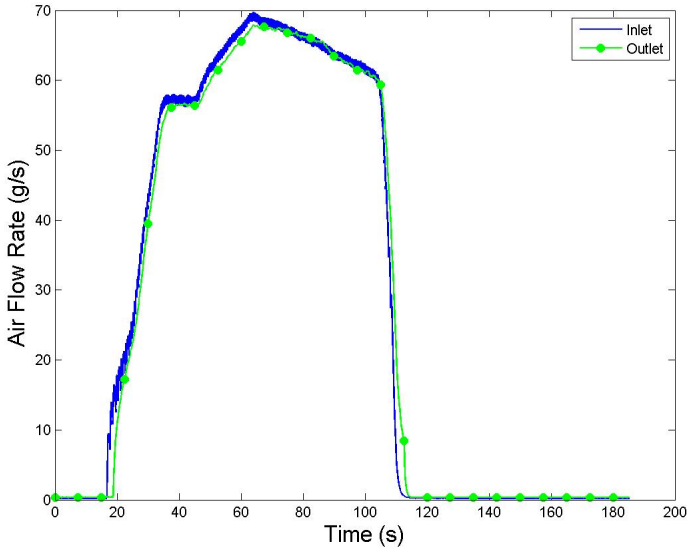

Figure E.174: Gas Mass Flow Rate for Run #5, Test 13b.

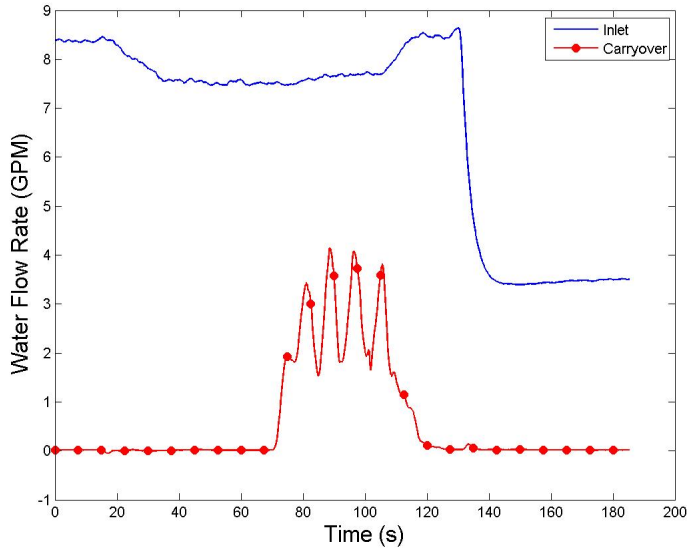

Figure E.175: Water Flow Rate for Run #5, Test 13b.

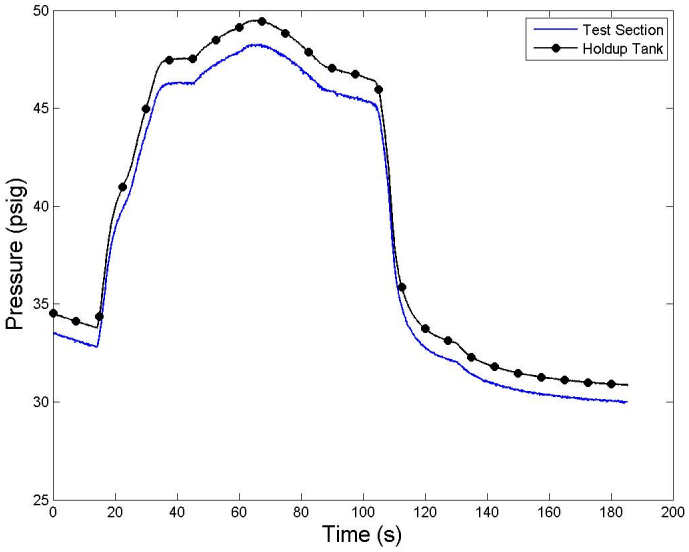

Figure E.176: System Pressure for Run #5, Test 13b.

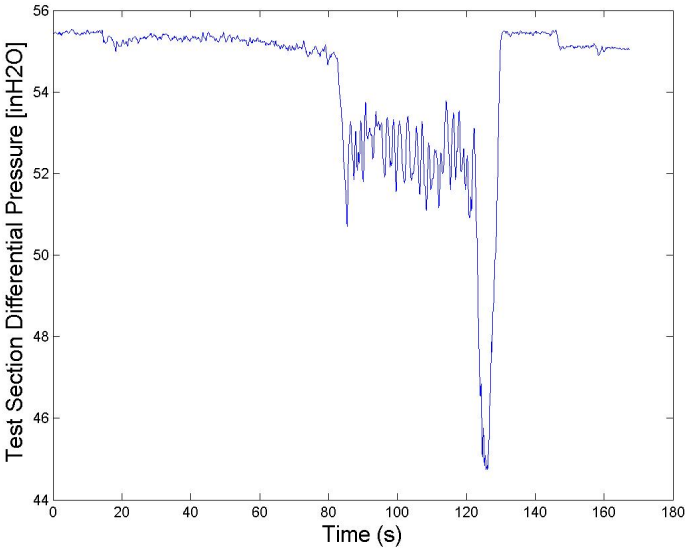

Figure E.177: Test Section Differential Pressure for Run #5, Test 14.

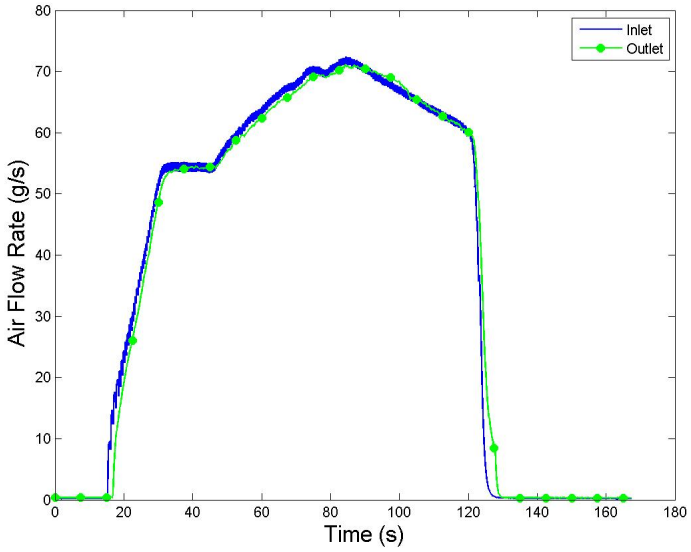

Figure E.178: Gas Mass Flow Rate for Run #5, Test 14.

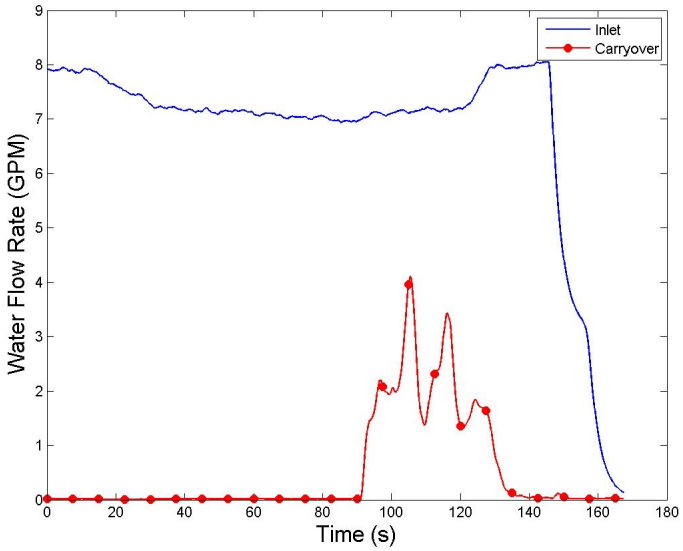

Figure E.179: Water Flow Rate for Run #5, Test 14.

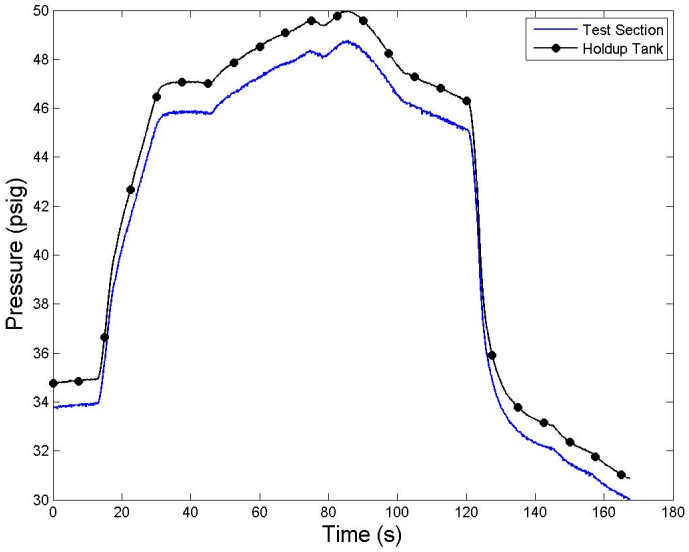

Figure E.180: System Pressure for Run #5, Test 14.

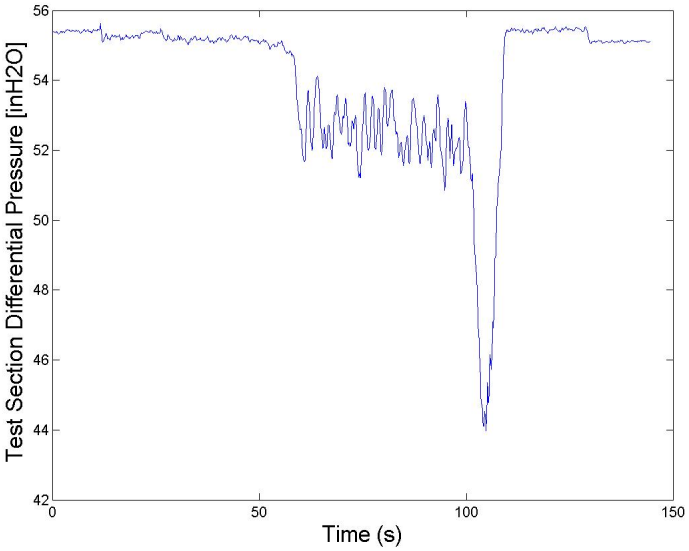

Figure E.181: Test Section Differential Pressure for Run #5, Test 15.

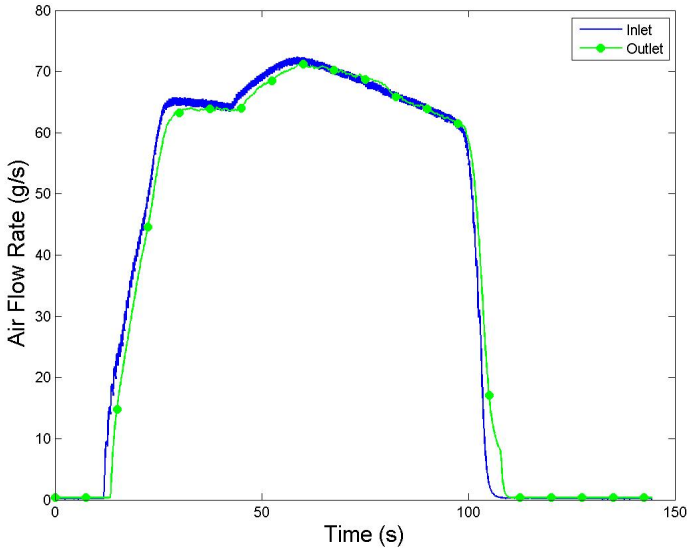

Figure E.182: Gas Mass Flow Rate for Run #5, Test 15.

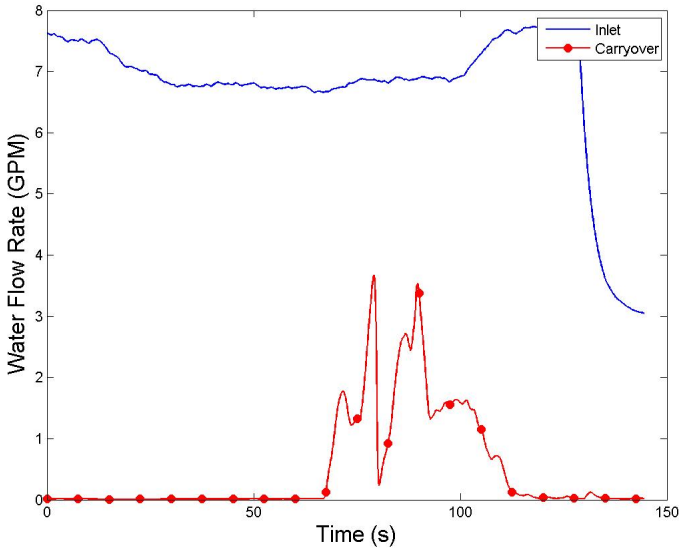

Figure E.183: Water Flow Rate for Run #5, Test 15.

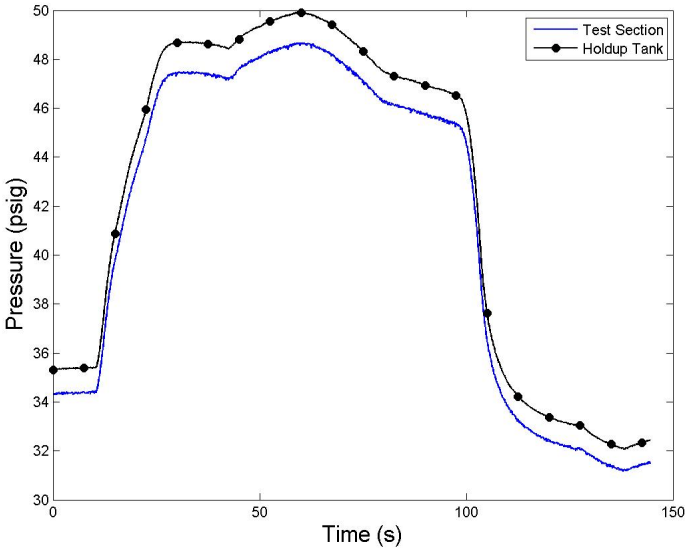

Figure E.184: System Pressure for Run #5, Test 15.

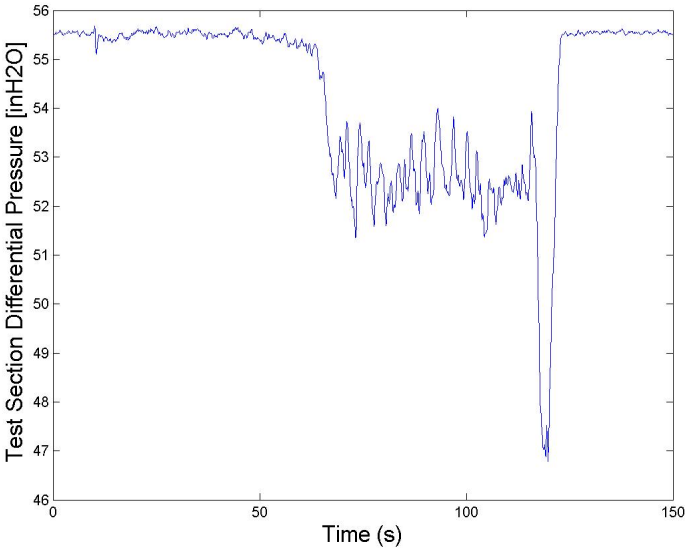

Figure E.185: Test Section Differential Pressure for Run #5, Test 16.

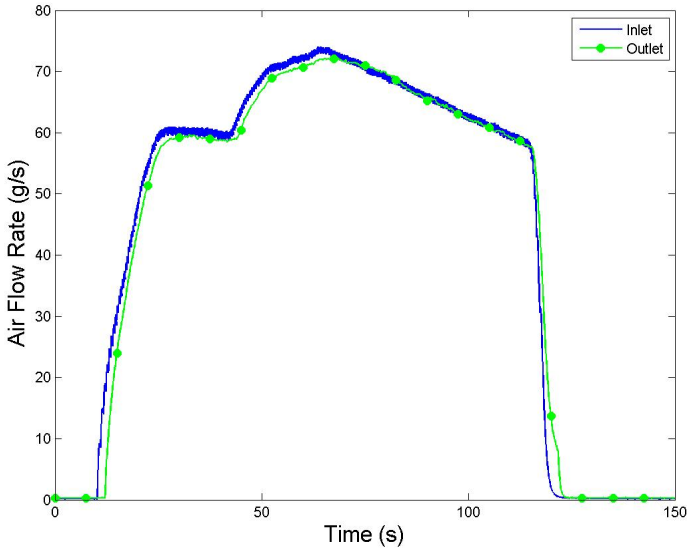

Figure E.186: Gas Mass Flow Rate for Run #5, Test 16.

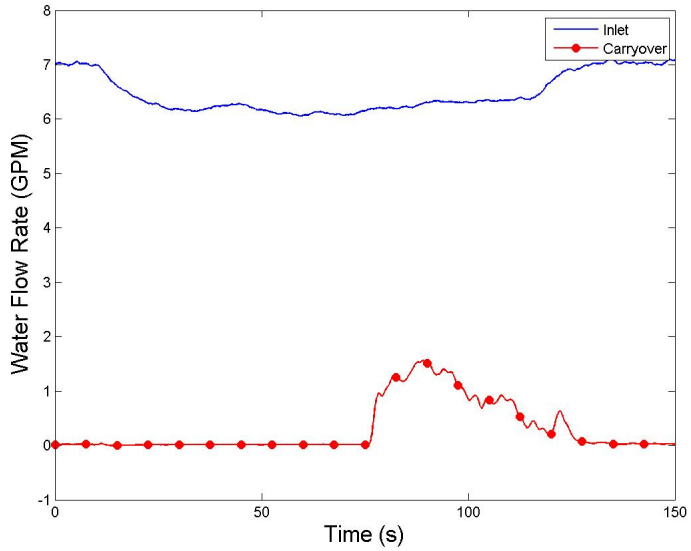

Figure E.187: Water Flow Rate for Run #5, Test 16.

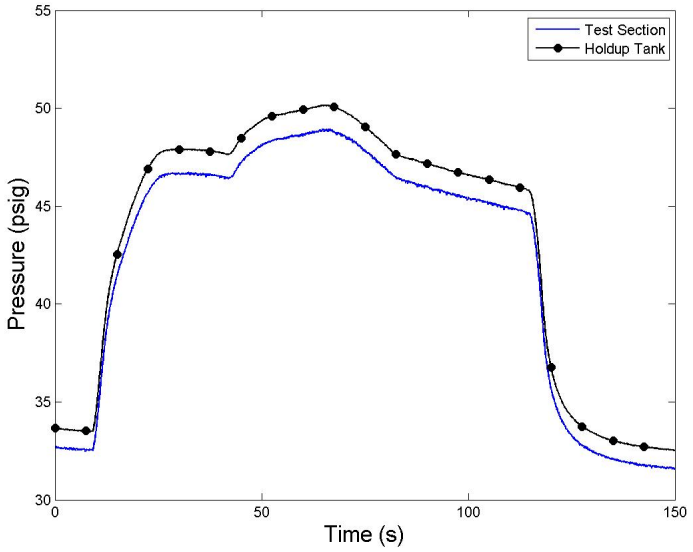

Figure E.188: System Pressure for Run #5, Test 16.

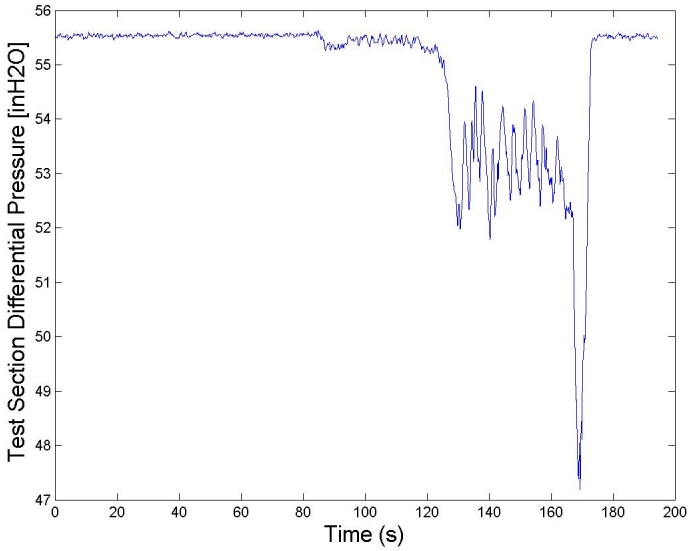

Figure E.189: Test Section Differential Pressure for Run #5, Test 17.

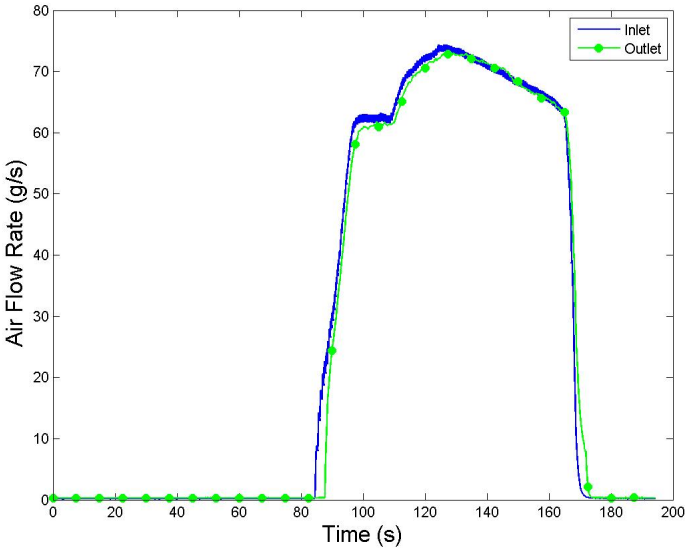

Figure E.190: Gas Mass Flow Rate for Run #5, Test 17.

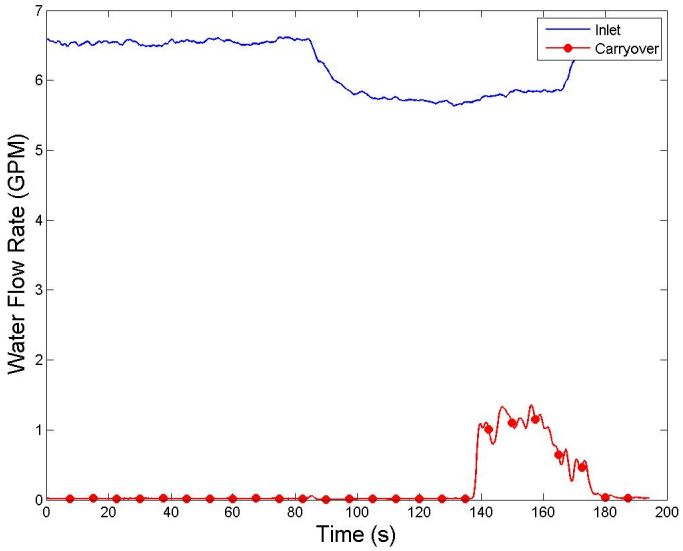

Figure E.191: Water Flow Rate for Run #5, Test 17.

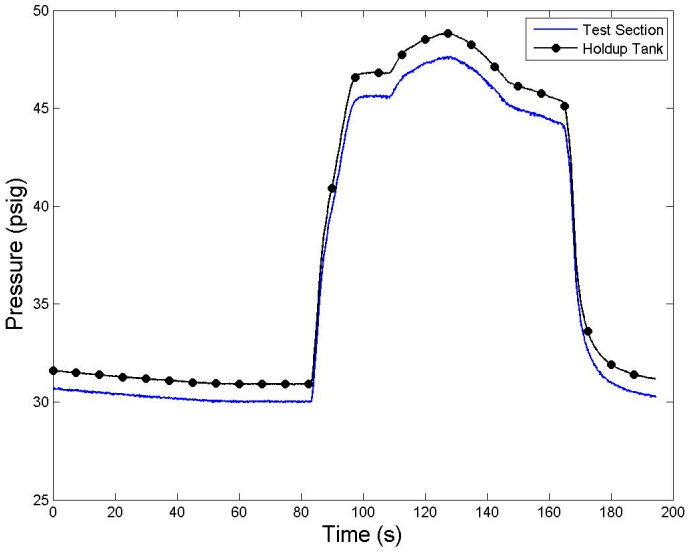

Figure E.192: System Pressure for Run #5, Test 17.

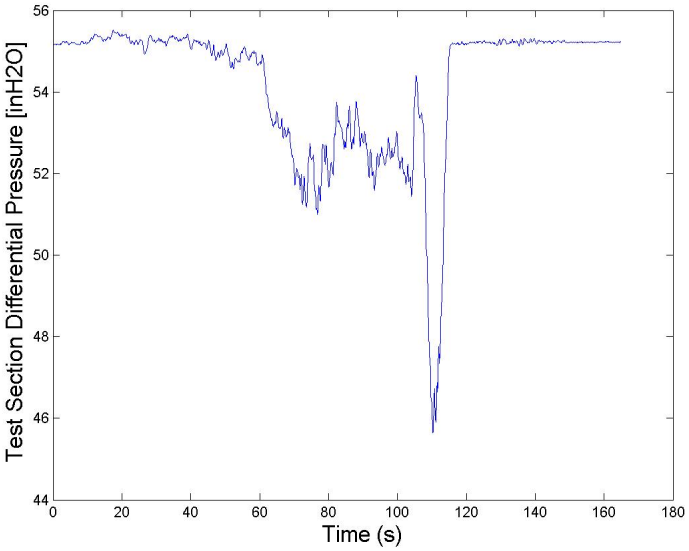

Figure E.193: Test Section Differential Pressure for Run #5, Test 18.

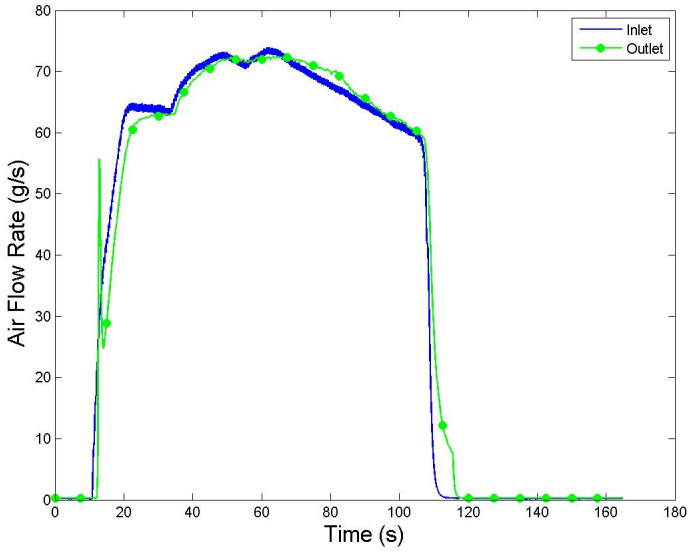

Figure E.194: Gas Mass Flow Rate for Run #5, Test 18.

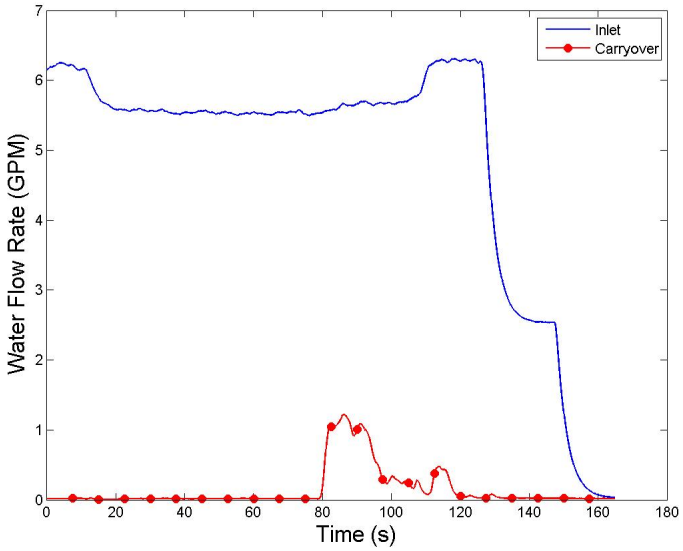

Figure E.195: Water Flow Rate for Run #5, Test 18.

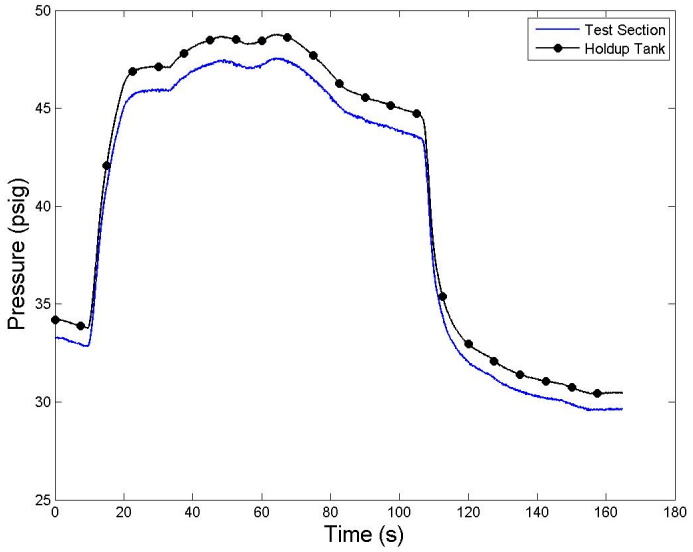

Figure E.196: System Pressure for Run #5, Test 18.

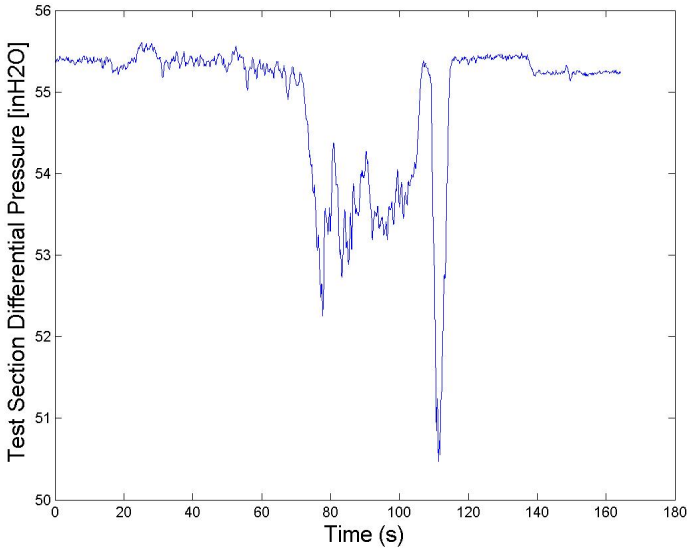

Figure E.197: Test Section Differential Pressure for Run #5, Test 19.

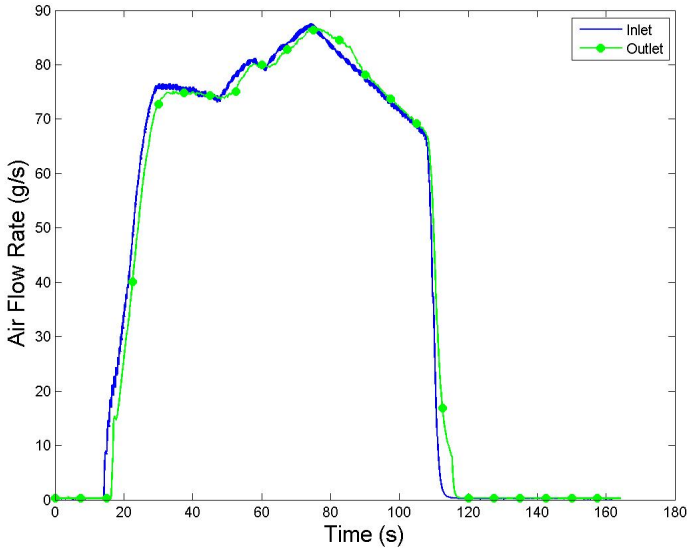

Figure E.198: Gas Mass Flow Rate for Run #5, Test 19.

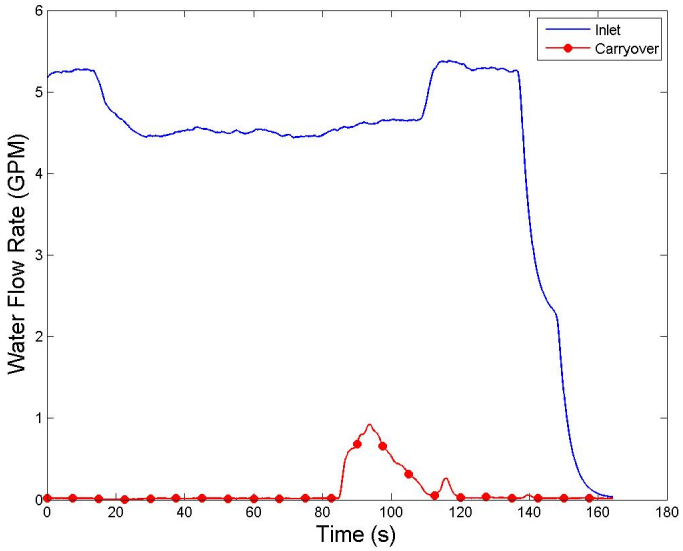

Figure E.199: Water Flow Rate for Run #5, Test 19.

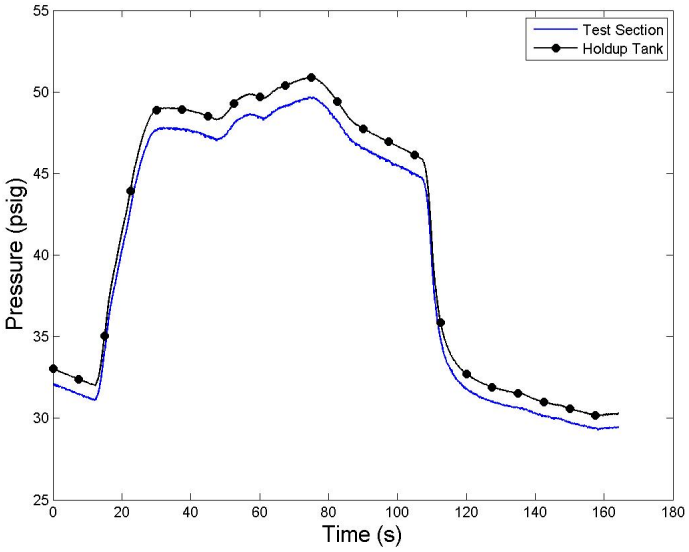

Figure E.200: System Pressure for Run #5, Test 19.

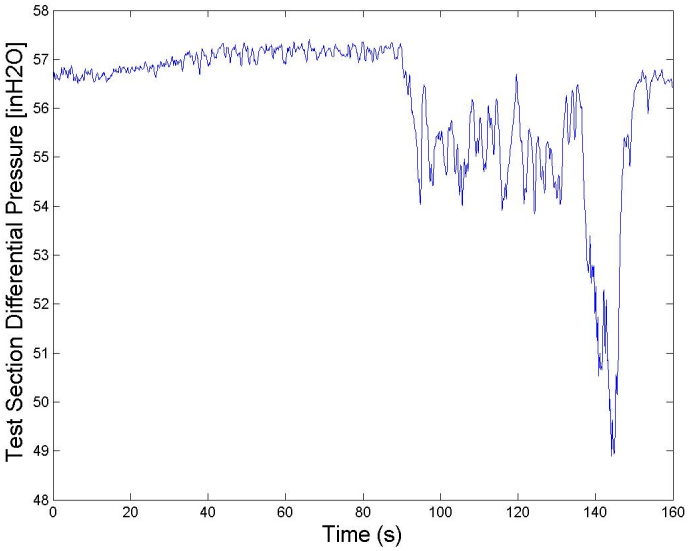

Figure E.201: Test Section Differential Pressure for Run #11, Test 5.

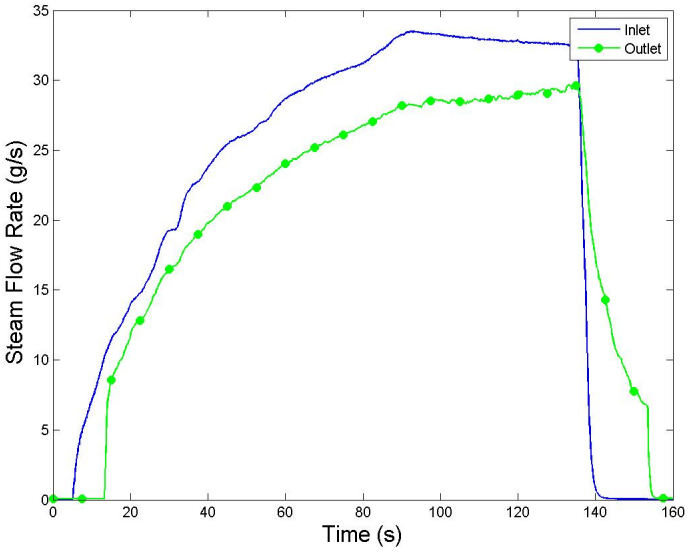

Figure E.202: Gas Mass Flow Rate for Run #11, Test 5.

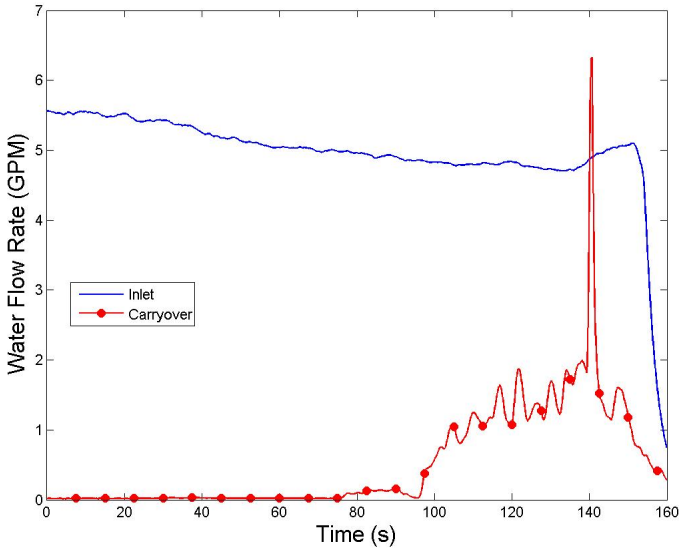

Figure E.203: Water Flow Rate for Run #11, Test 5.

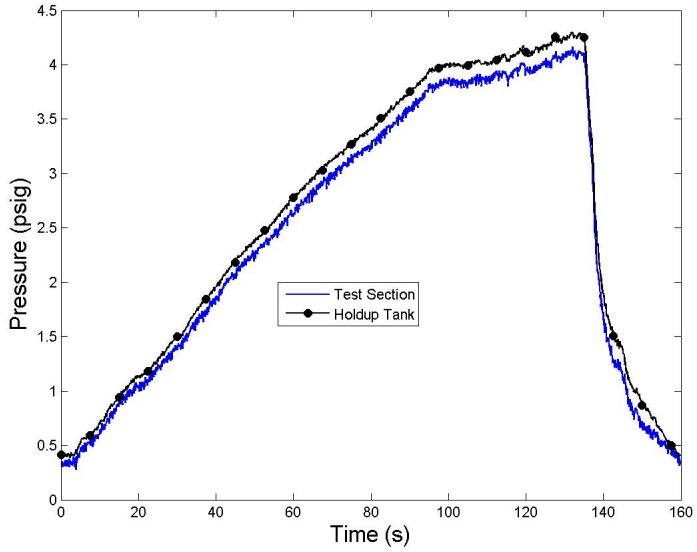

Figure E.204: System Pressure for Run #11, Test 5.

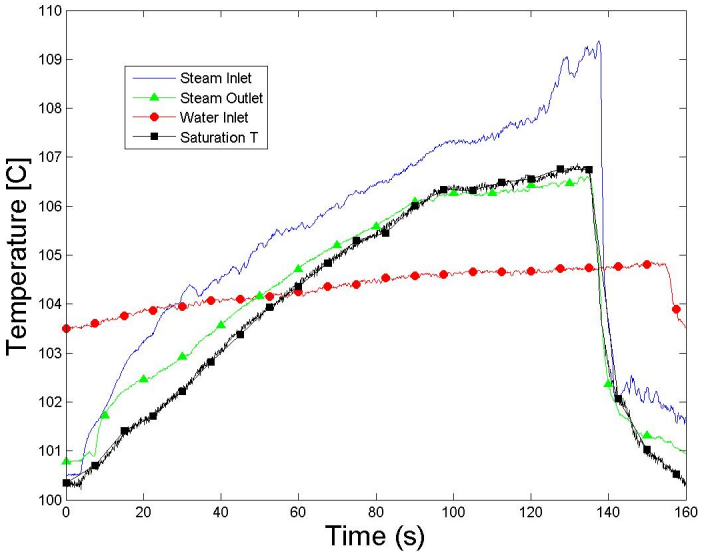

Figure E.205: Temperatures for Run #11, Test 5.

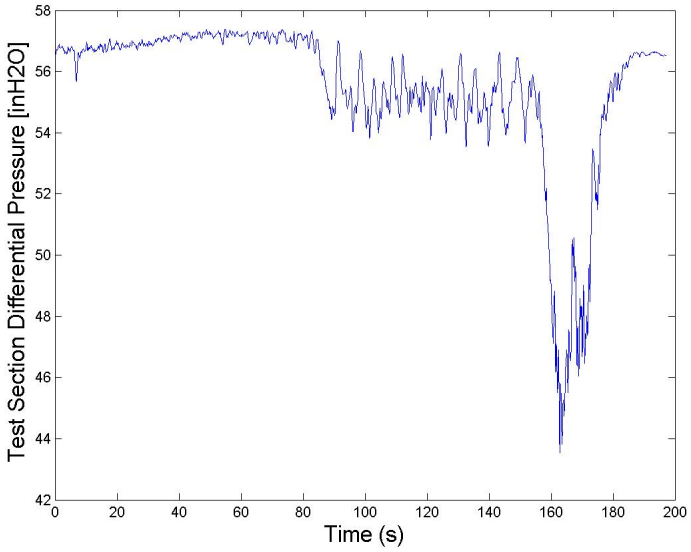

Figure E.206: Test Section Differential Pressure for Run #11, Test 6.

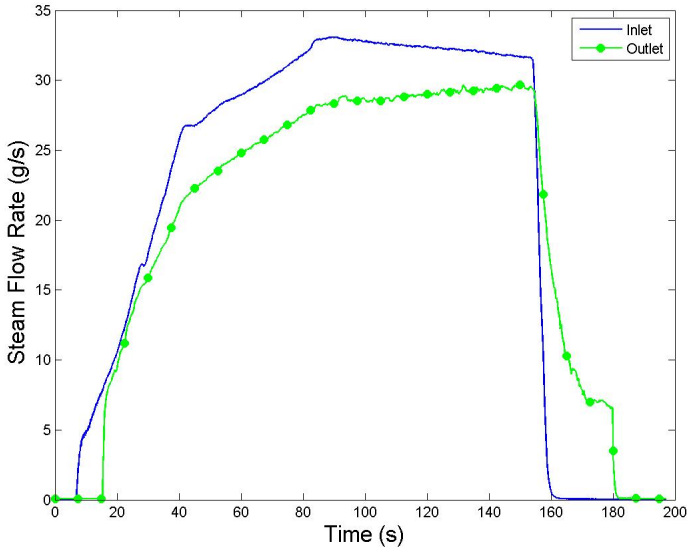

Figure E.207: Gas Mass Flow Rate for Run #11, Test 6.

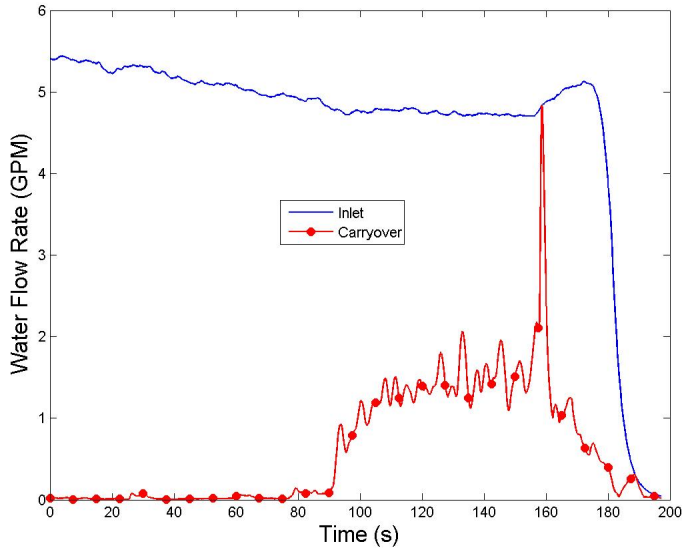

Figure E.208: Water Flow Rate for Run #11, Test 6.

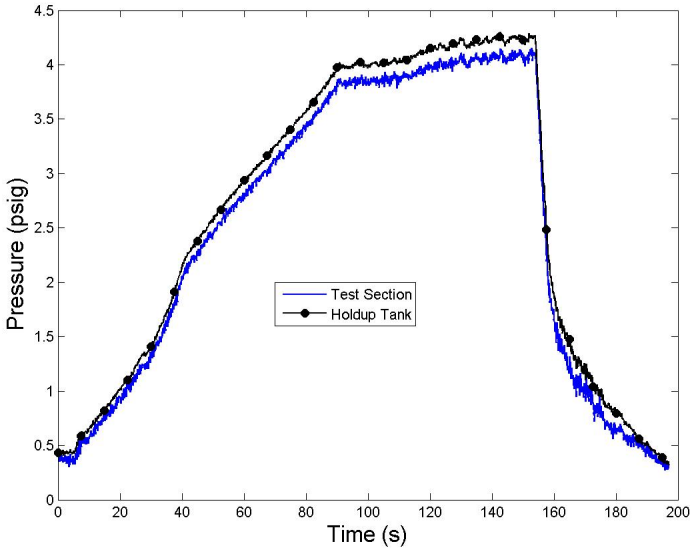

Figure E.209: System Pressure for Run #11, Test 6.

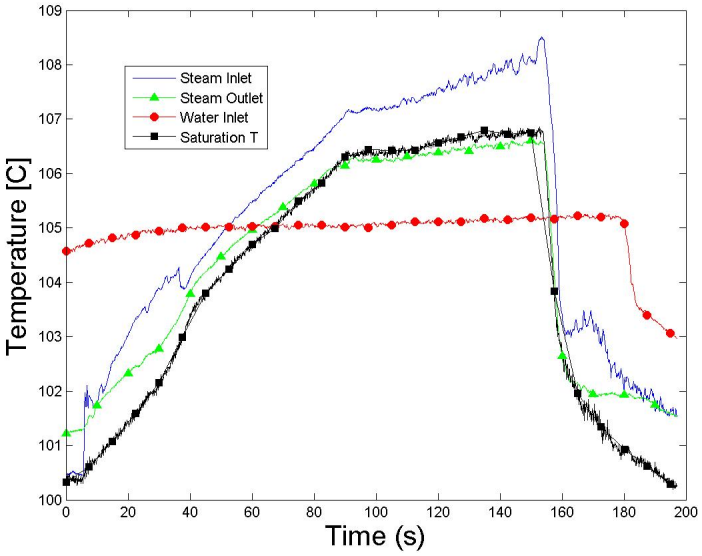

Figure E.210: Temperatures for Run #11, Test 6.

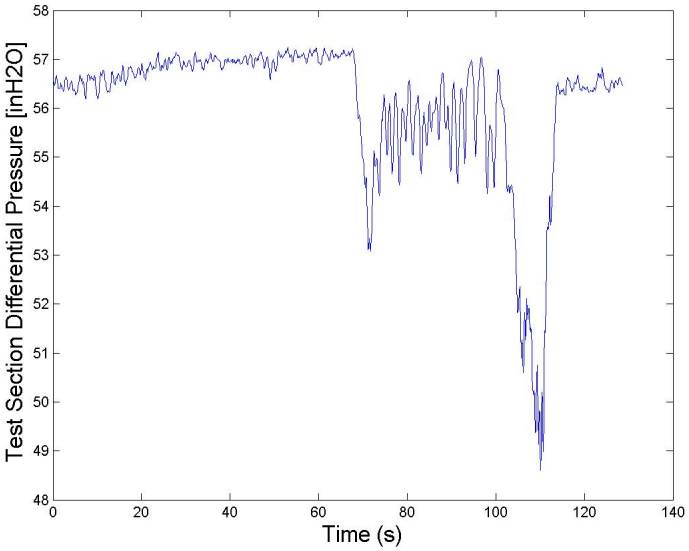

Figure E.211: Test Section Differential Pressure for Run #11, Test 4.

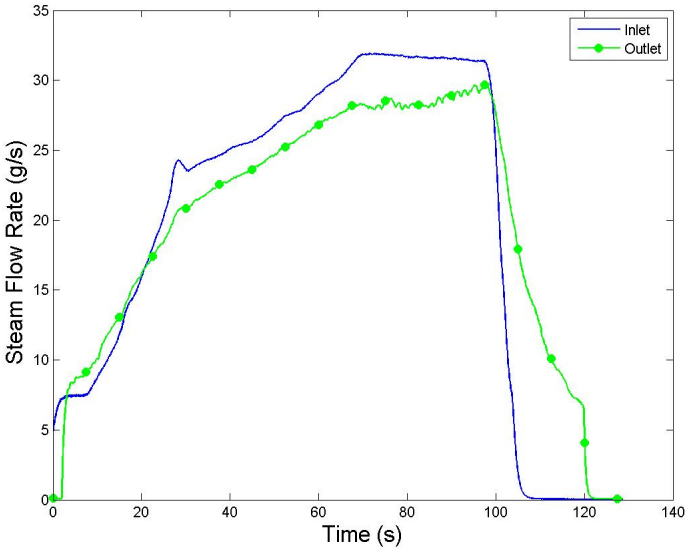

Figure E.212: Gas Mass Flow Rate for Run #11, Test 4.

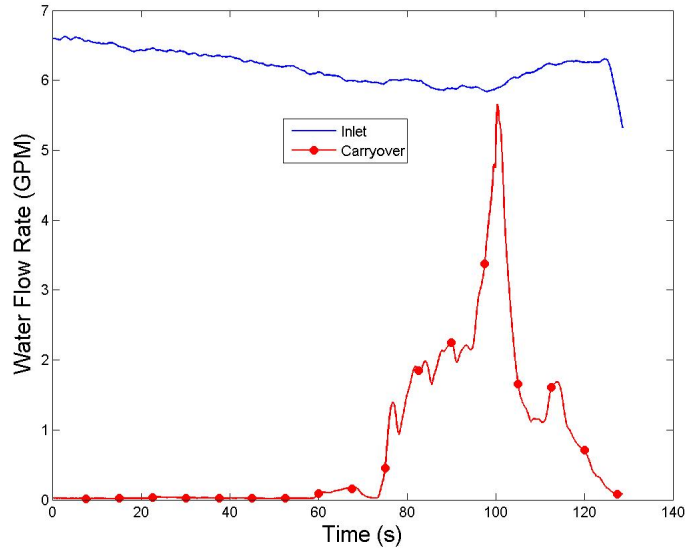

Figure E.213: Water Flow Rate for Run #11, Test 4.

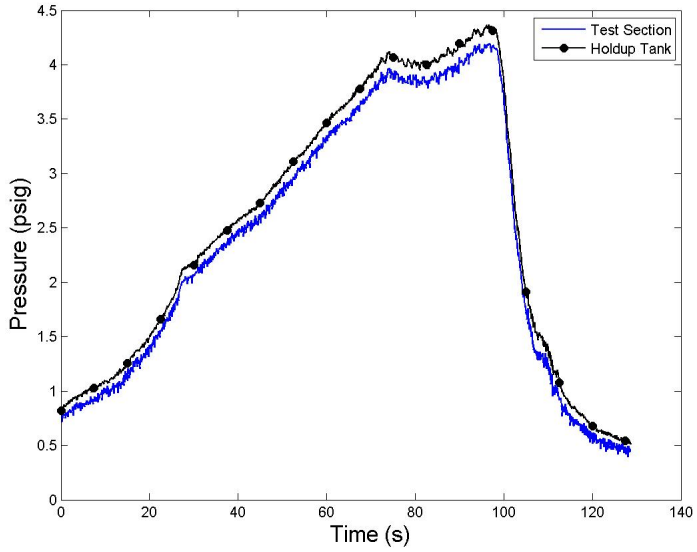

Figure E.214: System Pressure for Run #11, Test 4.

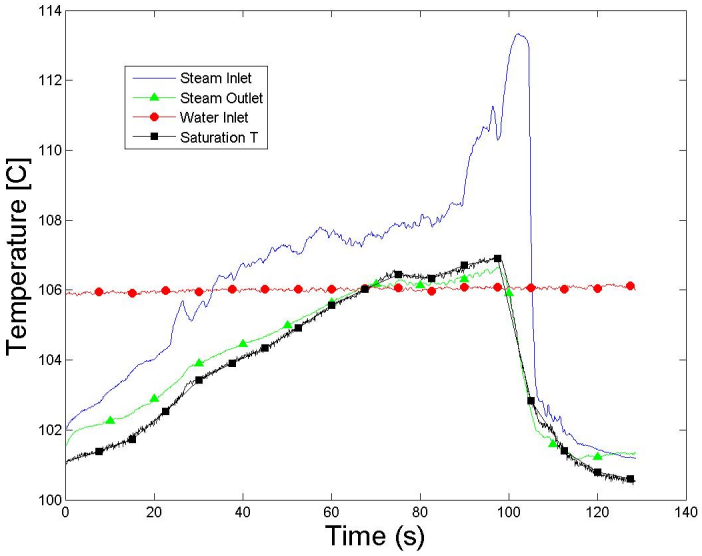

Figure E.215: Temperatures for Run #11, Test 4.

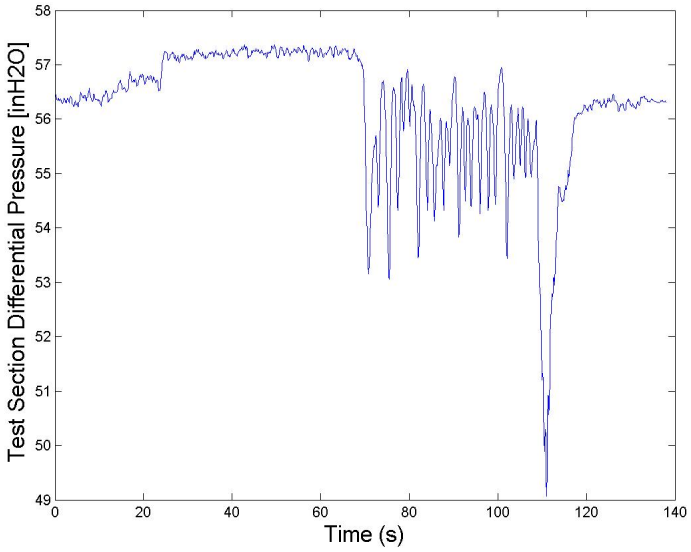

Figure E.216: Test Section Differential Pressure for Run #11, Test 3.

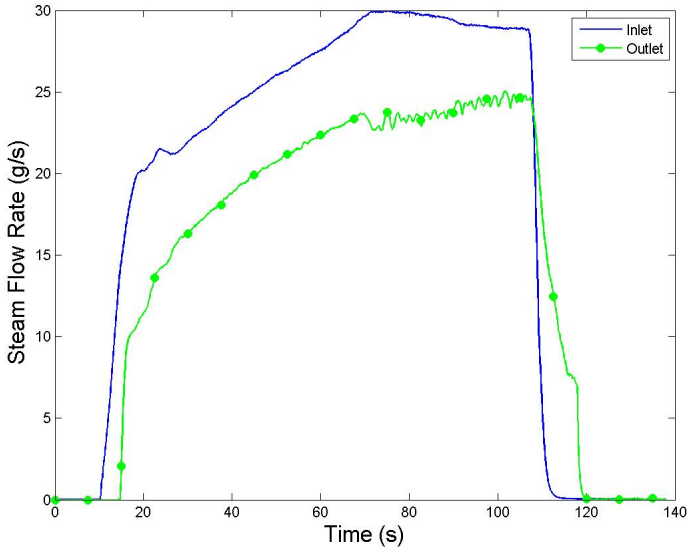

Figure E.217: Gas Mass Flow Rate for Run #11, Test 3.

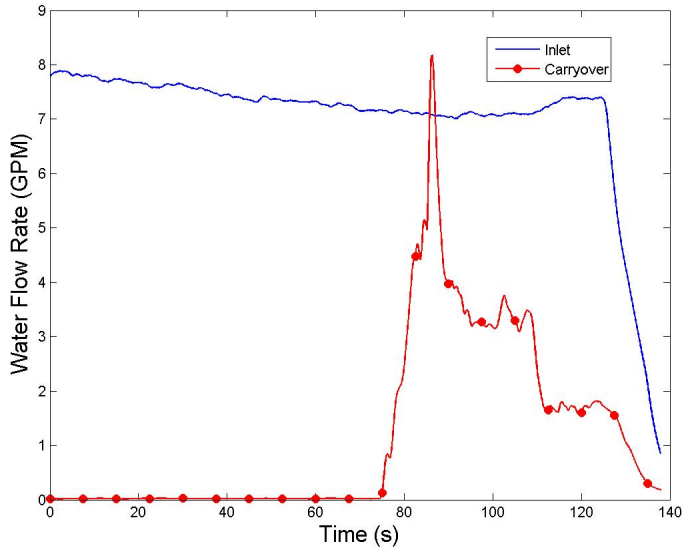

Figure E.218: Water Flow Rate for Run #11, Test 3.

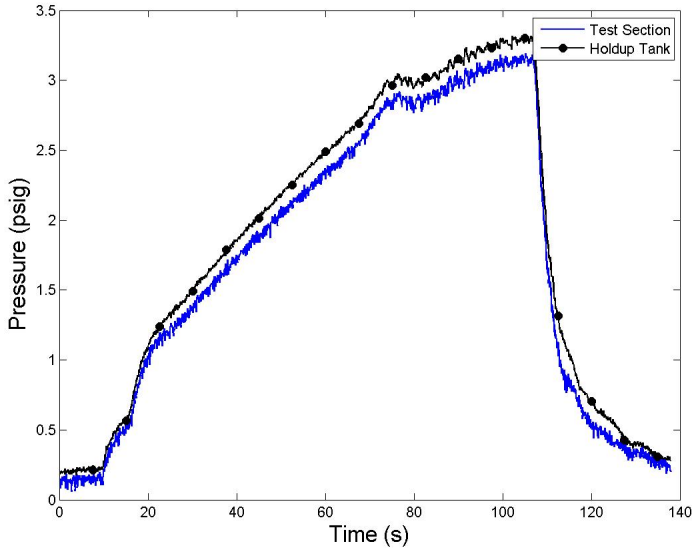

Figure E.219: System Pressure for Run #11, Test 3.

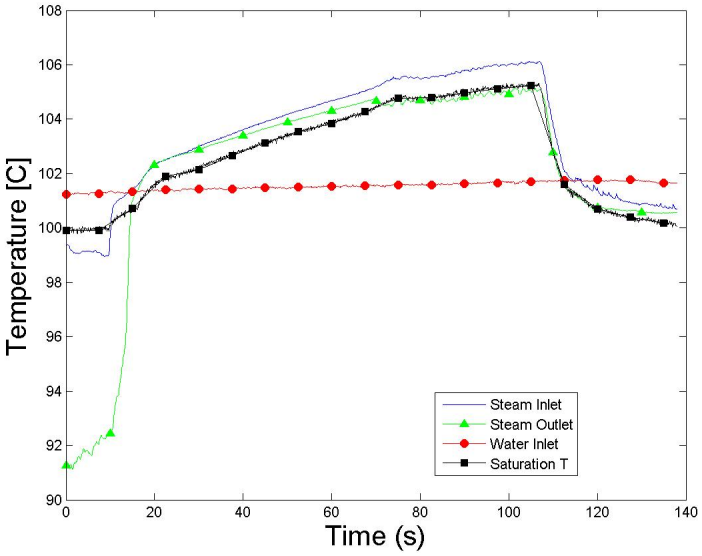

Figure E.220: Temperatures for Run #11, Test 3.

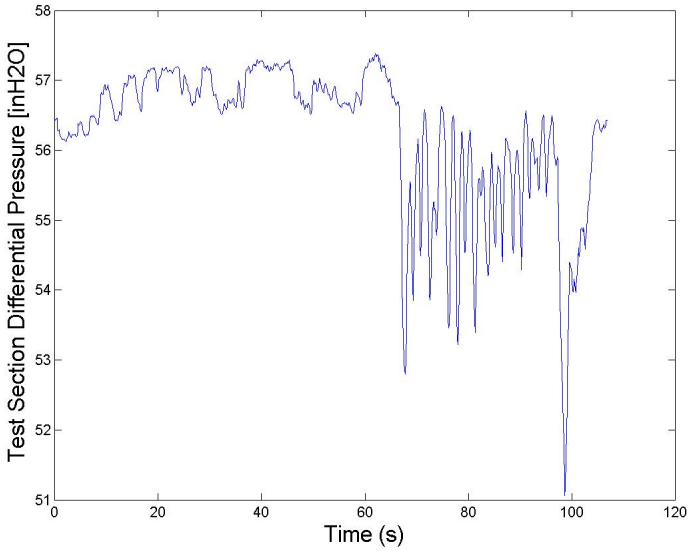

Figure E.221: Test Section Differential Pressure for Run #11, Test 2.

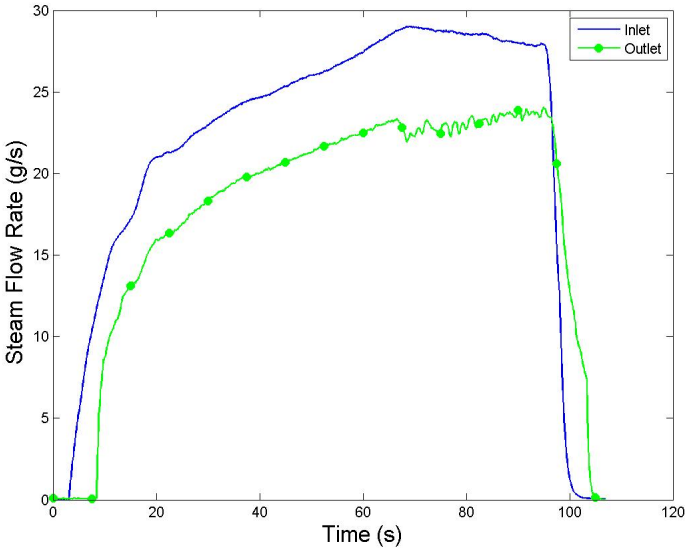

Figure E.222: Gas Mass Flow Rate for Run #11, Test 2.

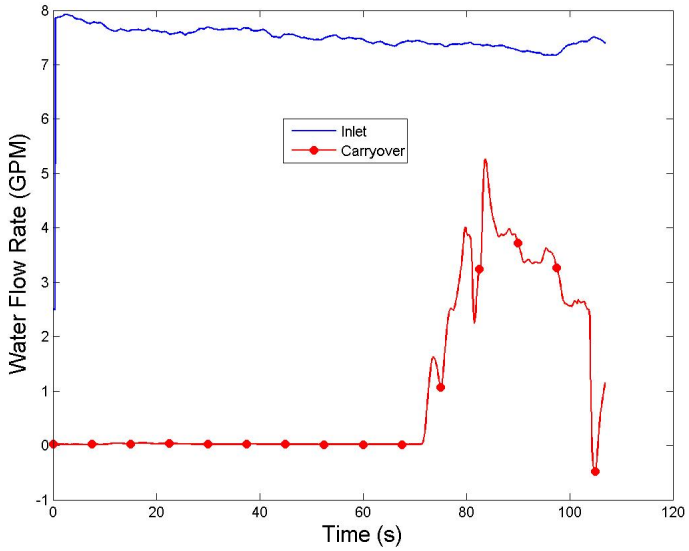

Figure E.223: Water Flow Rate for Run #11, Test 2.

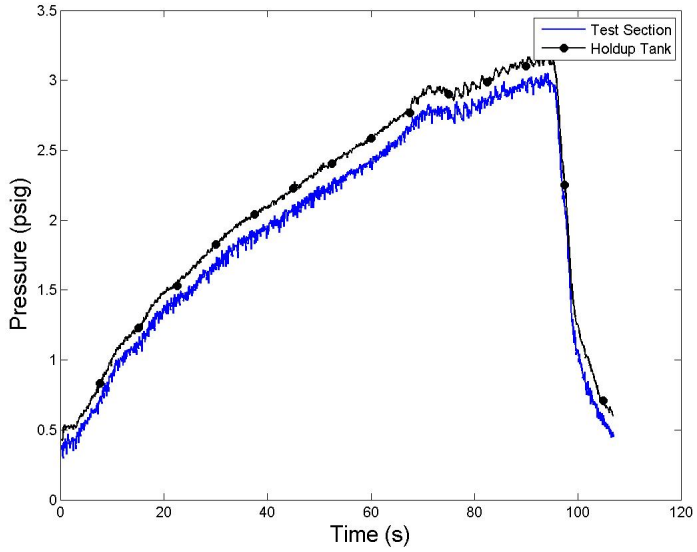

Figure E.224: System Pressure for Run #11, Test 2.

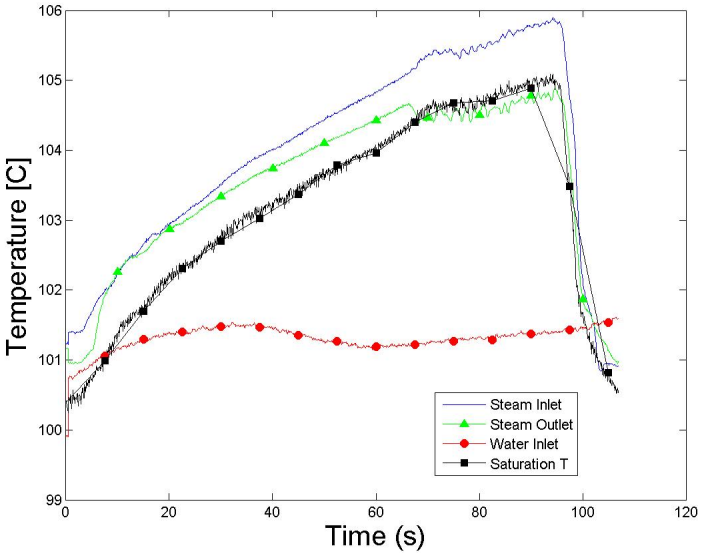

Figure E.225: Temperatures for Run #11, Test 2.

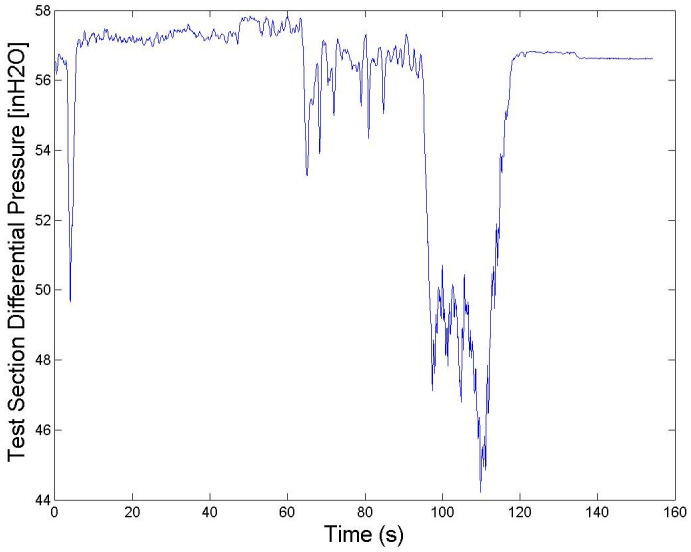

Figure E.226: Test Section Differential Pressure for Run #15, Test 7.

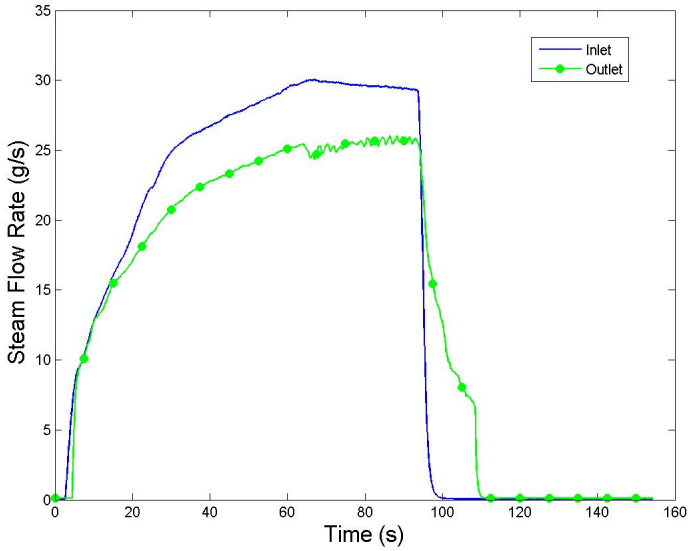

Figure E.227: Gas Mass Flow Rate for Run #15, Test 7.

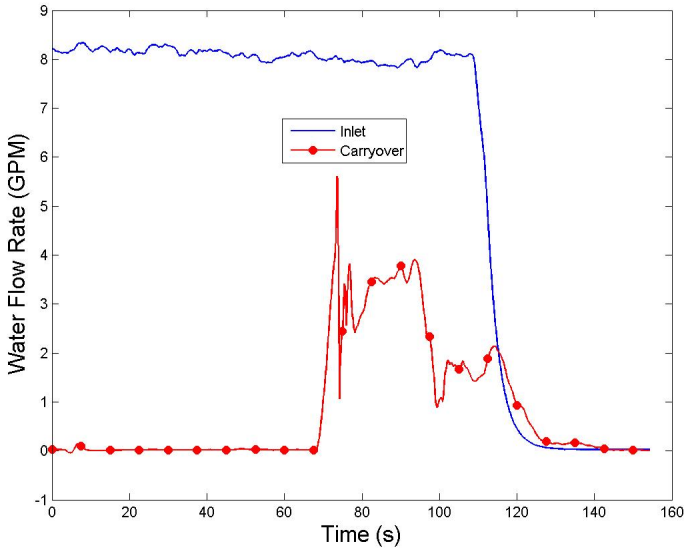

Figure E.228: Water Flow Rate for Run #15, Test 7.

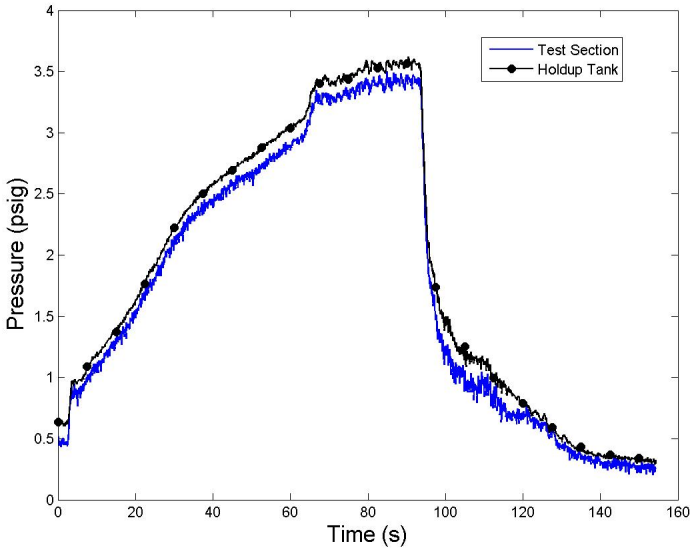

Figure E.229: System Pressure for Run #15, Test 7.

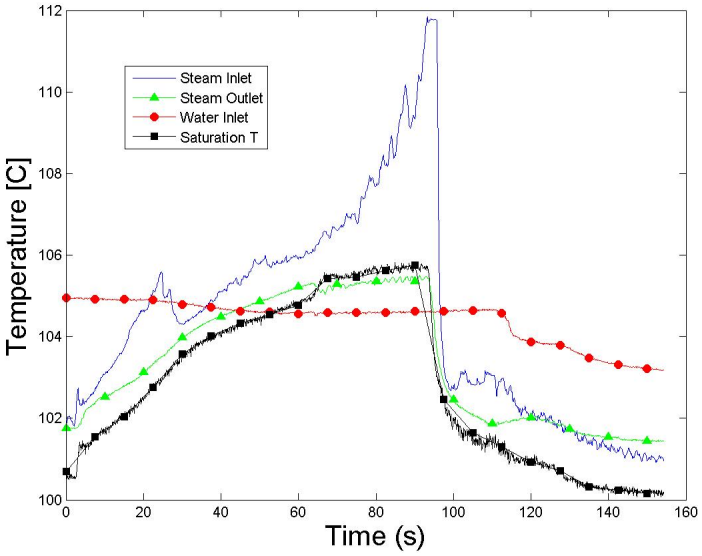

Figure E.230: Temperatures for Run #15, Test 7.

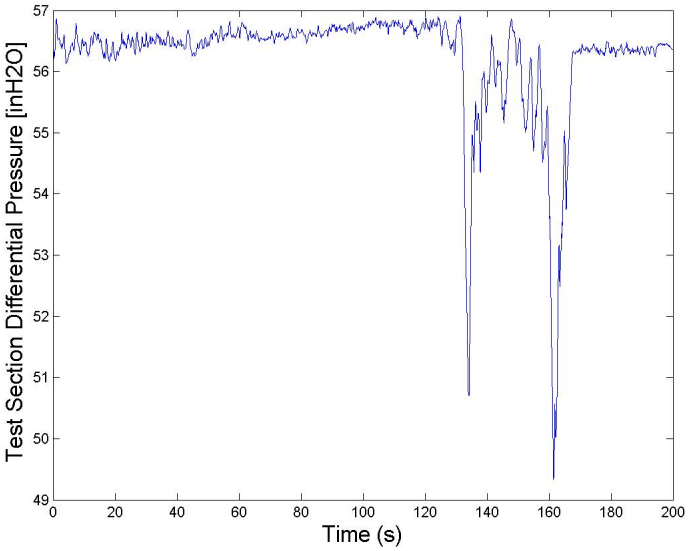

Figure E.231: Test Section Differential Pressure for Run #12, Test 1.

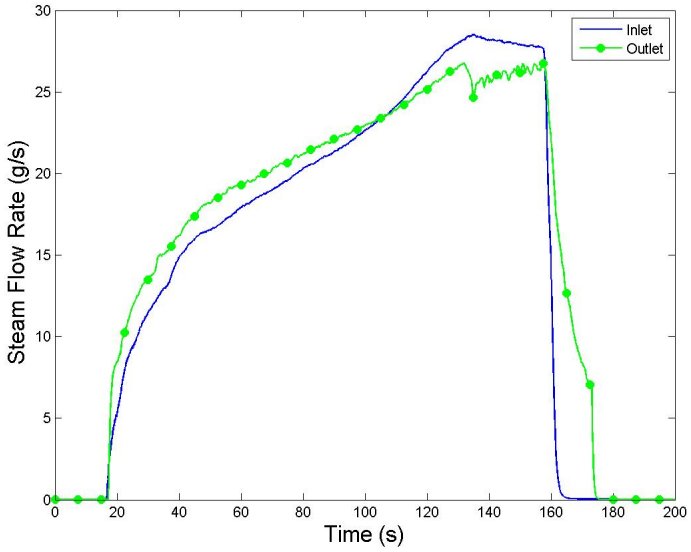

Figure E.232: Gas Mass Flow Rate for Run #12, Test 1.

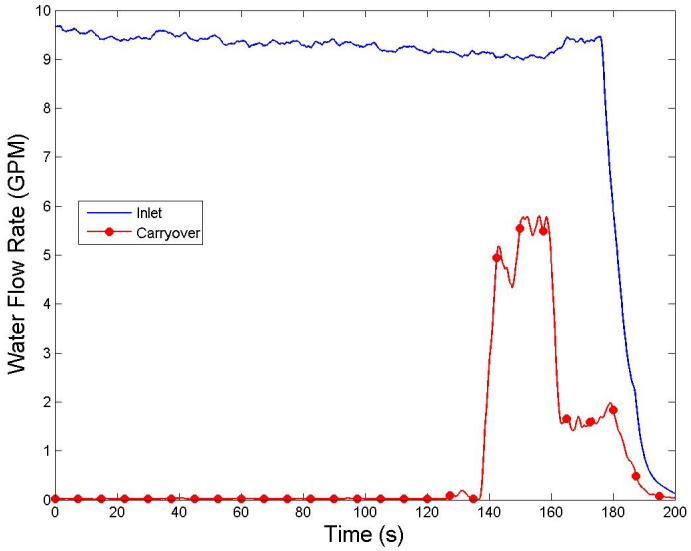

Figure E.233: Water Flow Rate for Run #12, Test 1.

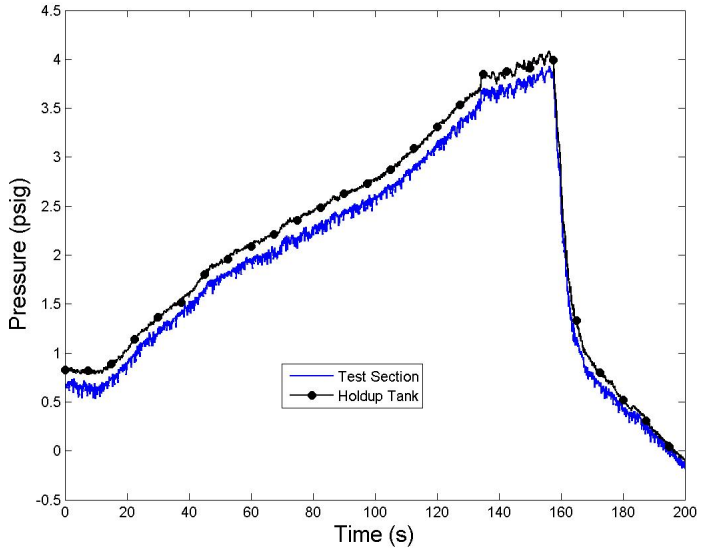

Figure E.234: System Pressure for Run #12, Test 1.

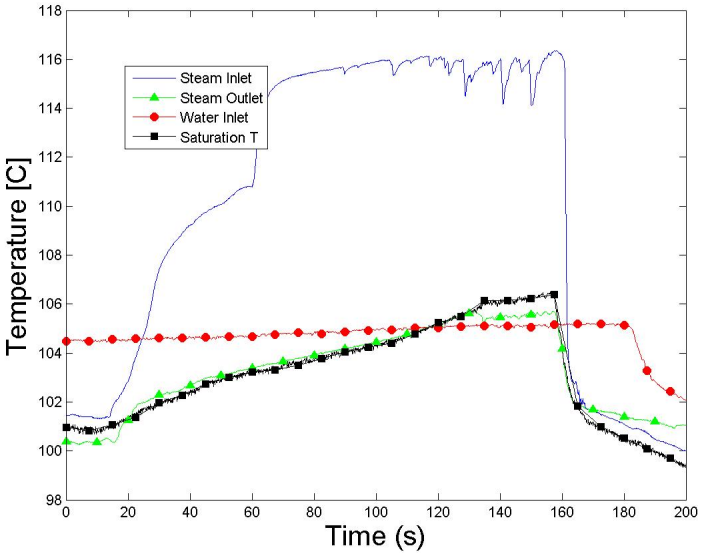

Figure E.235: Temperatures for Run #12, Test 1.

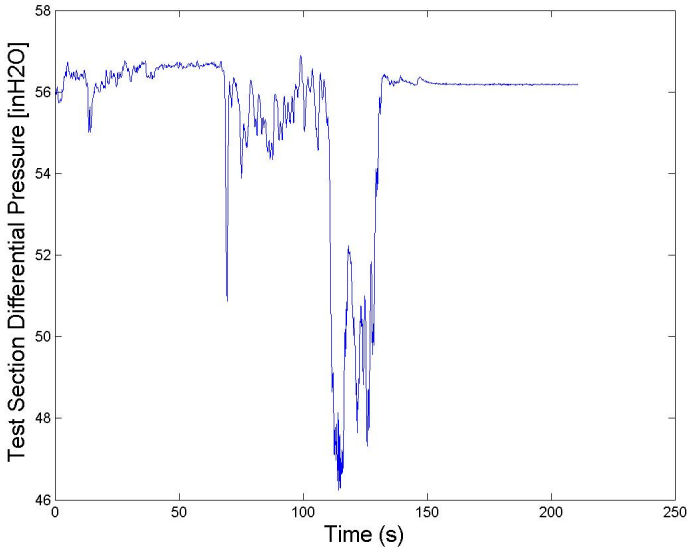

Figure E.236: Test Section Differential Pressure for Run #12, Test 6.

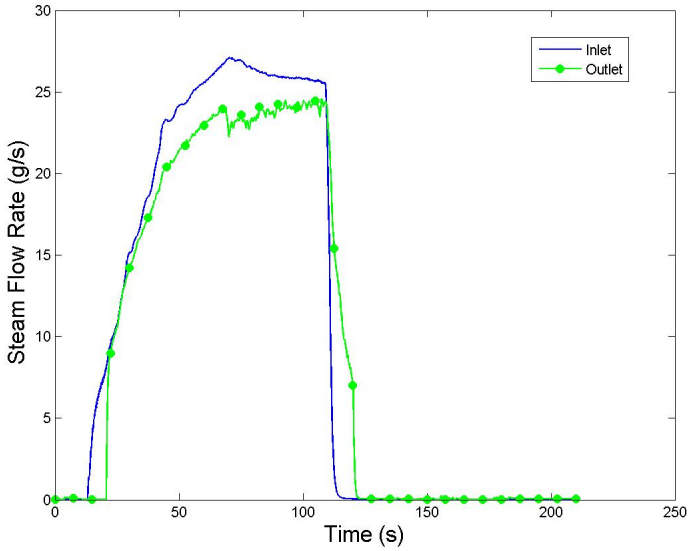

Figure E.237: Gas Mass Flow Rate for Run #12, Test 6.

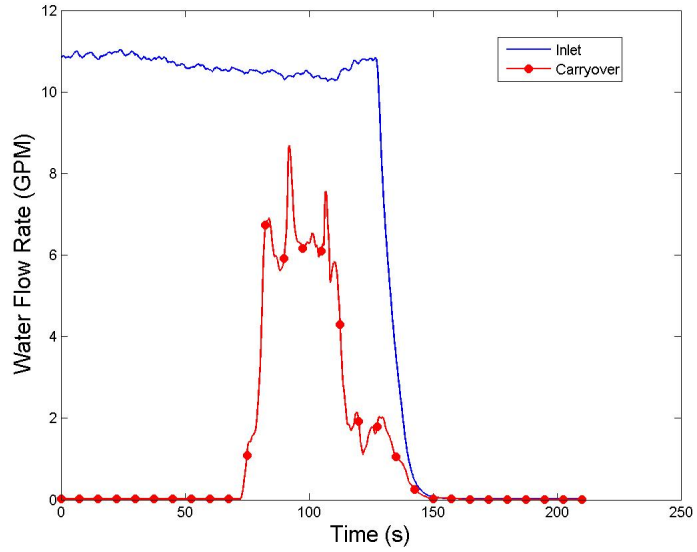

Figure E.238: Water Flow Rate for Run #12, Test 6.

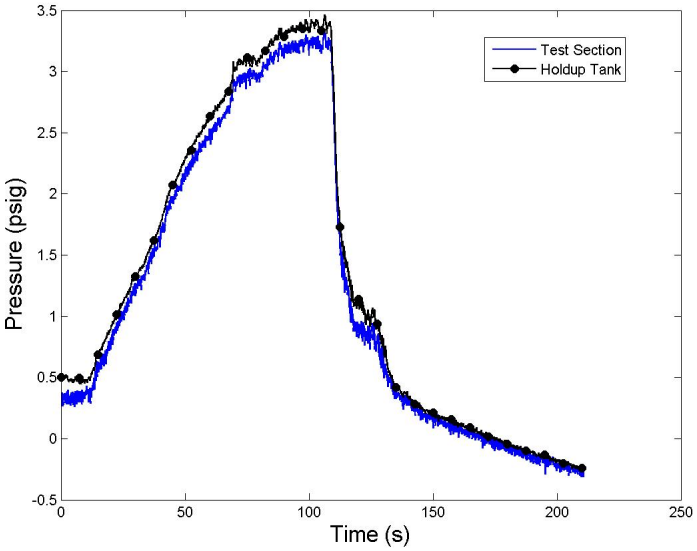

Figure E.239: System Pressure for Run #12, Test 6.

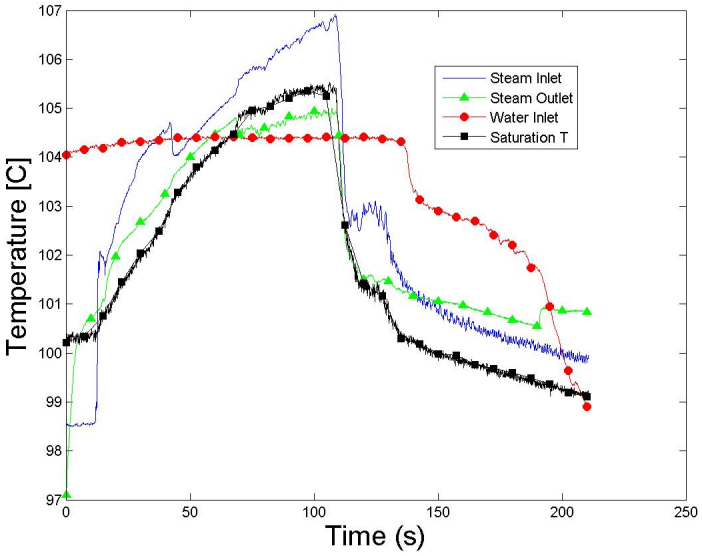

Figure E.240: Temperatures for Run #12, Test 6.

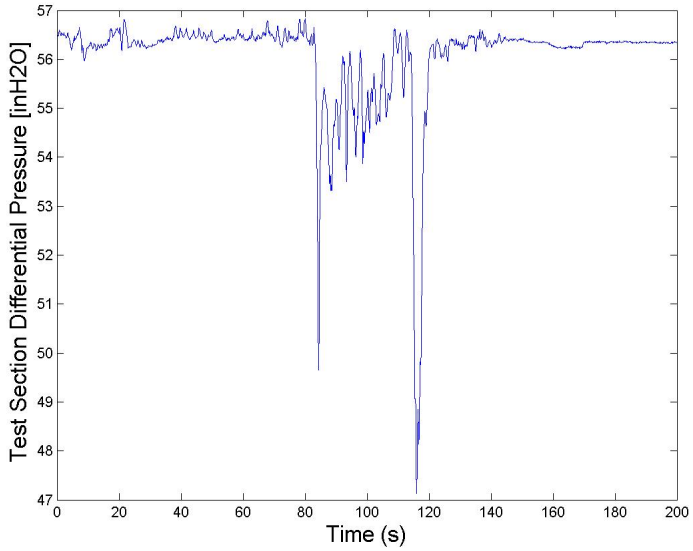

Figure E.241: Test Section Differential Pressure for Run #12, Test 2.

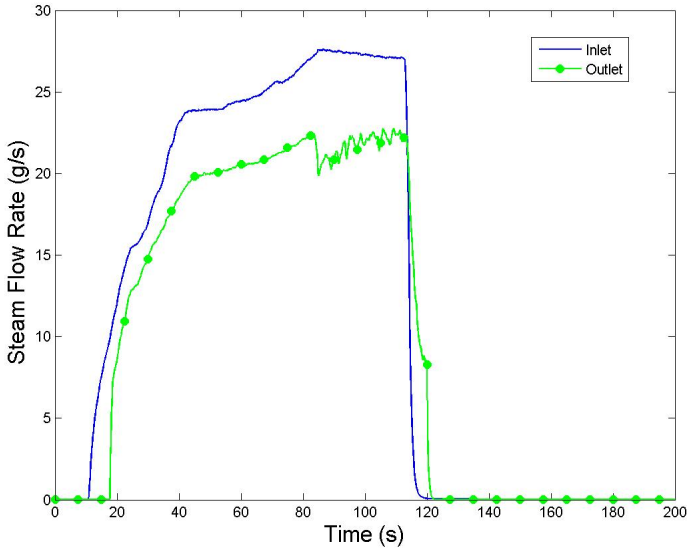

Figure E.242: Gas Mass Flow Rate for Run #12, Test 2.

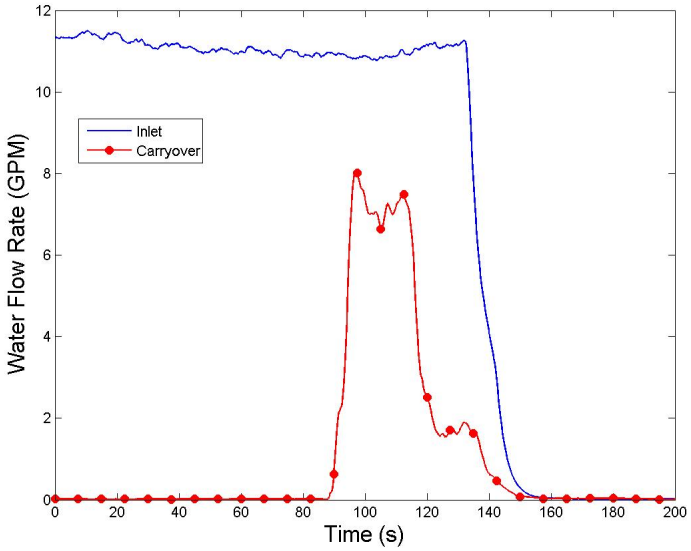

Figure E.243: Water Flow Rate for Run #12, Test 2.

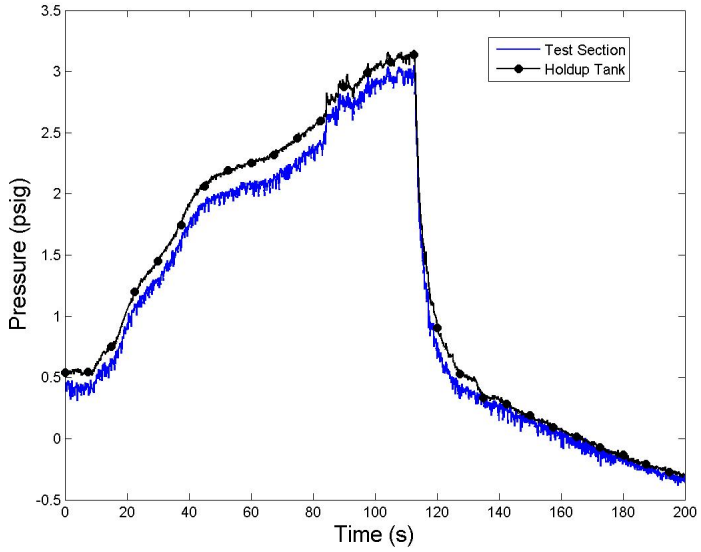

Figure E.244: System Pressure for Run #12, Test 2.

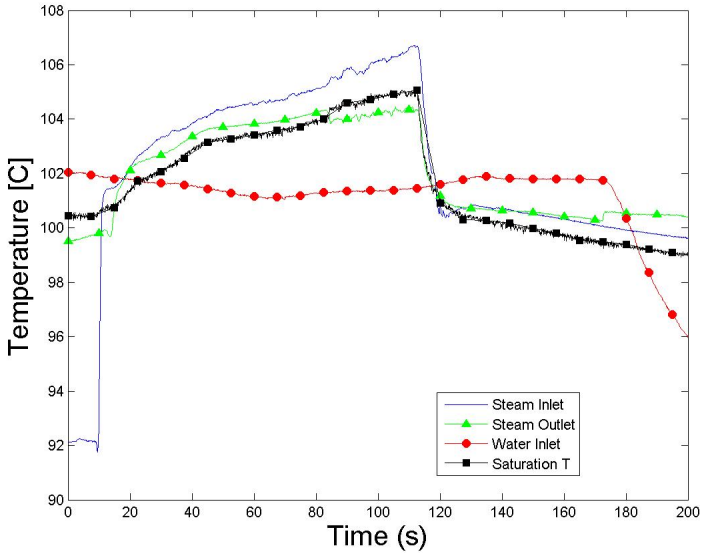

Figure E.245: Temperatures for Run #12, Test 2.

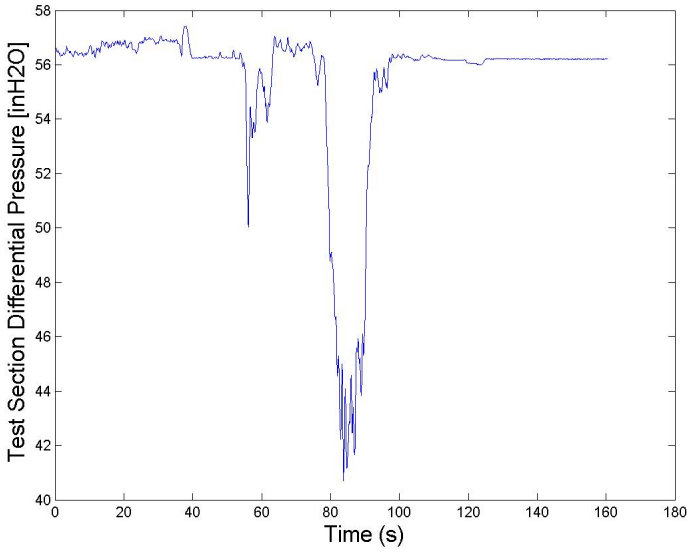

Figure E.246: Test Section Differential Pressure for Run #12, Test 4.

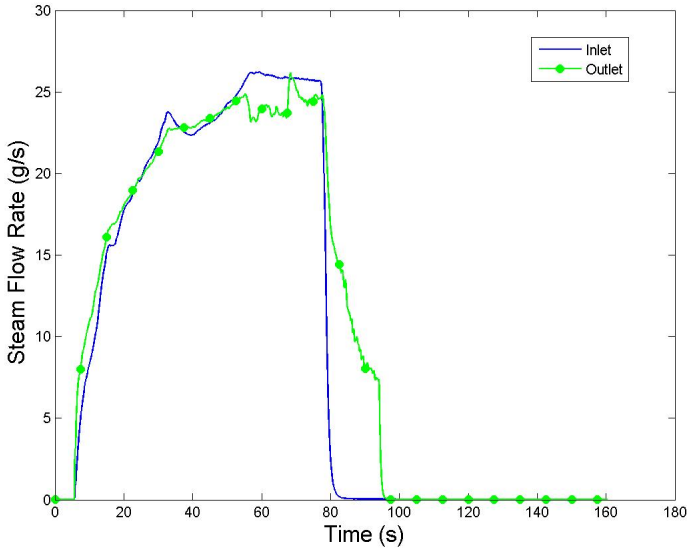

Figure E.247: Gas Mass Flow Rate for Run #12, Test 4.

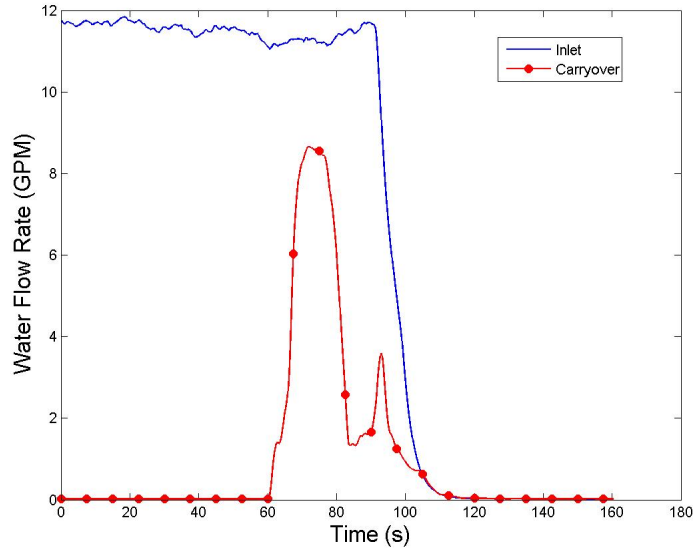

Figure E.248: Water Flow Rate for Run #12, Test 4.

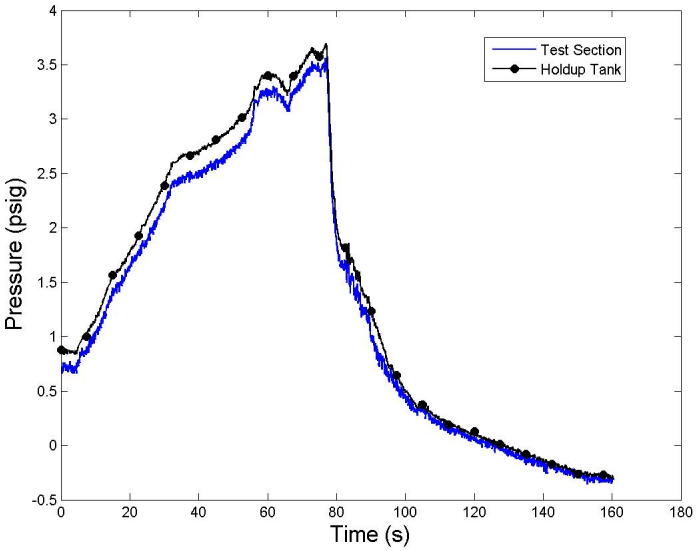

Figure E.249: System Pressure for Run #12, Test 4.

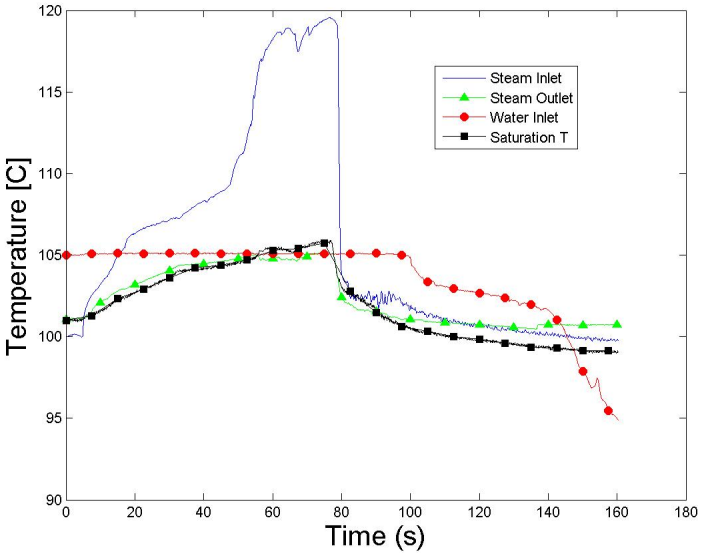

Figure E.250: Temperatures for Run #12, Test 4.

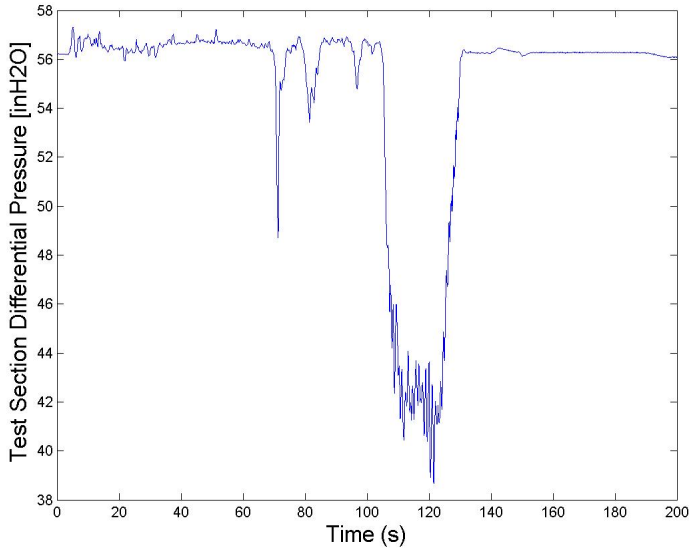

Figure E.251: Test Section Differential Pressure for Run #12, Test 5.

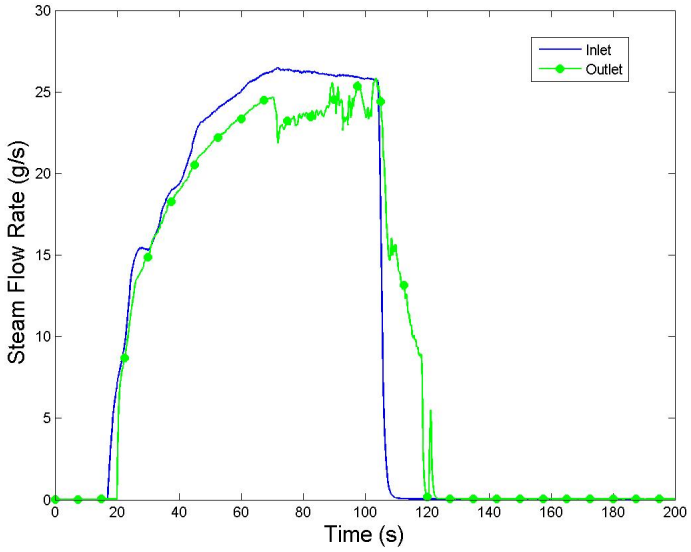

Figure E.252: Gas Mass Flow Rate for Run #12, Test 5.

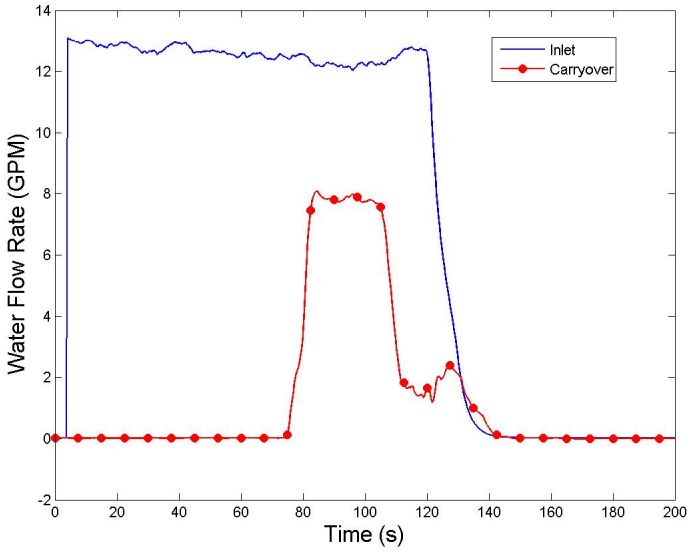

Figure E.253: Water Flow Rate for Run #12, Test 5.

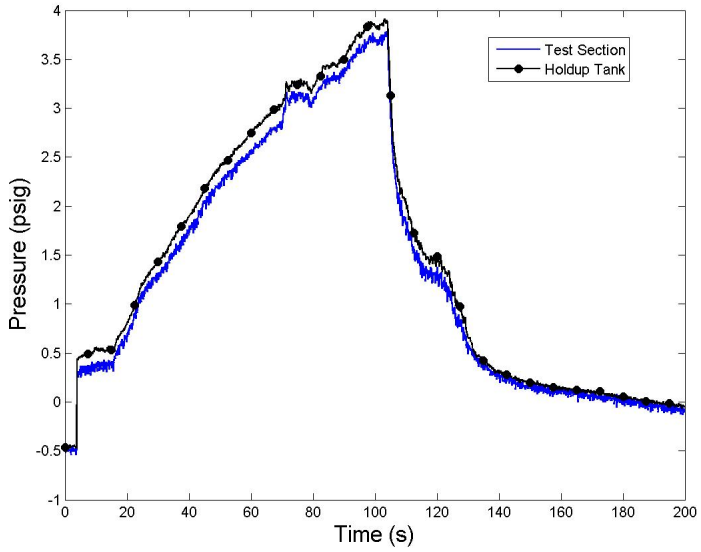

Figure E.254: System Pressure for Run #12, Test 5.

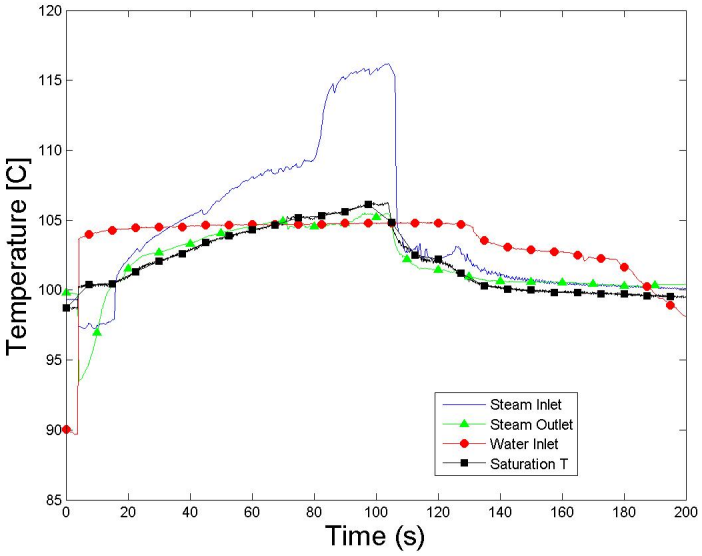

Figure E.255: Temperatures for Run #12, Test 5.

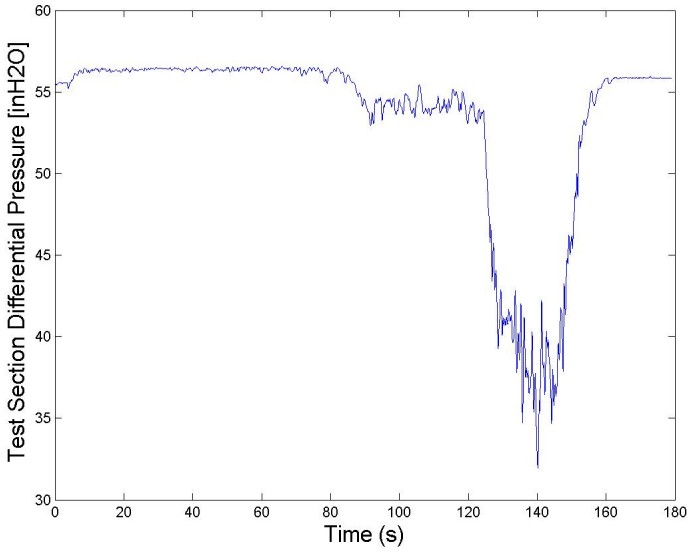

Figure E.256: Test Section Differential Pressure for Run #14, Test 6.

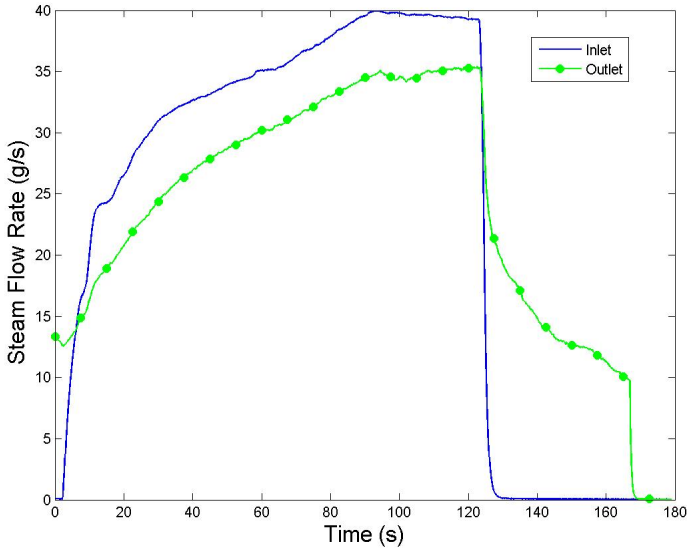

Figure E.257: Gas Mass Flow Rate for Run #14, Test 6.

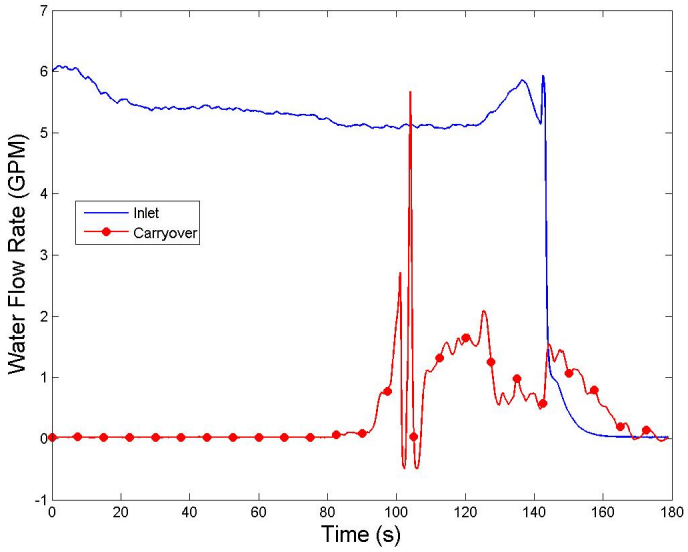

Figure E.258: Water Flow Rate for Run #14, Test 6.

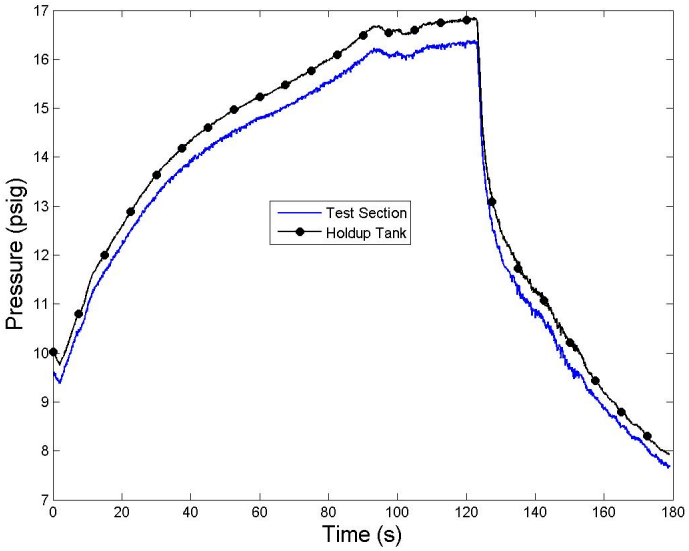

Figure E.259: System Pressure for Run #14, Test 6.

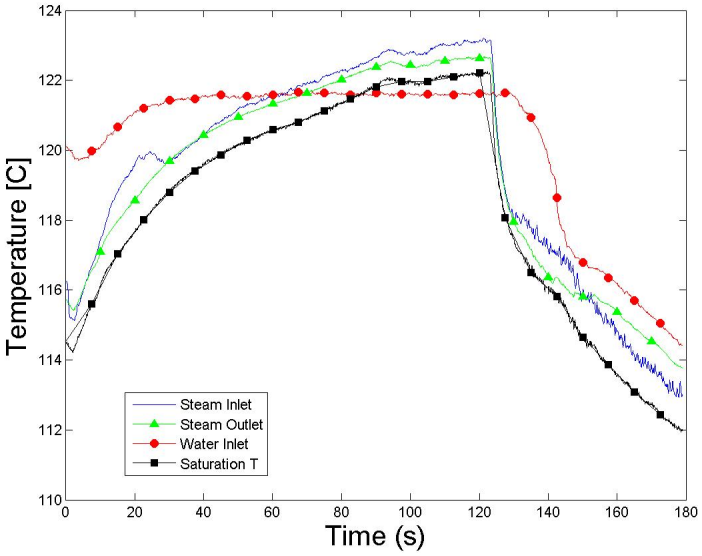

Figure E.260: Temperatures for Run #14, Test 6.

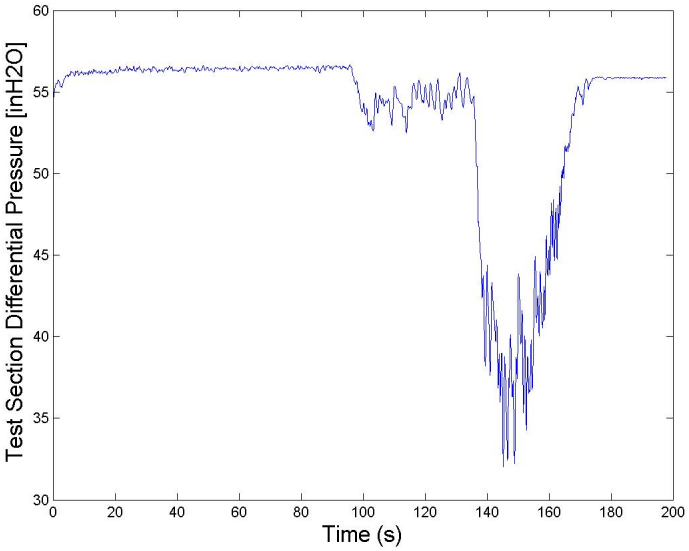

Figure E.261: Test Section Differential Pressure for Run #14, Test 5.

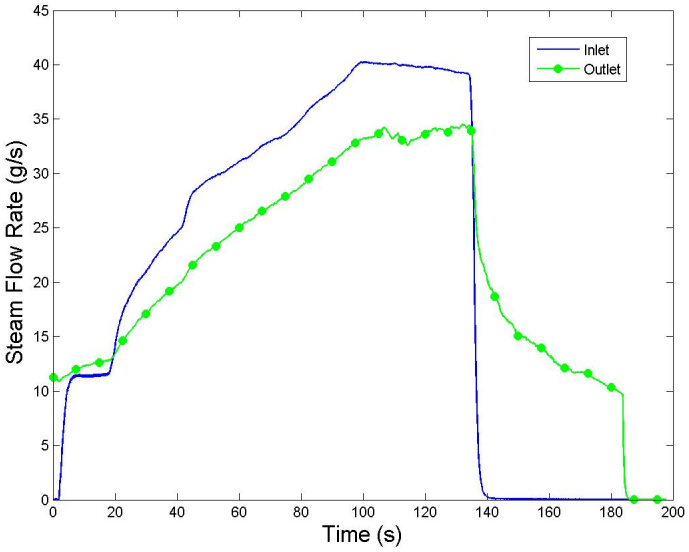

Figure E.262: Gas Mass Flow Rate for Run #14, Test 5.

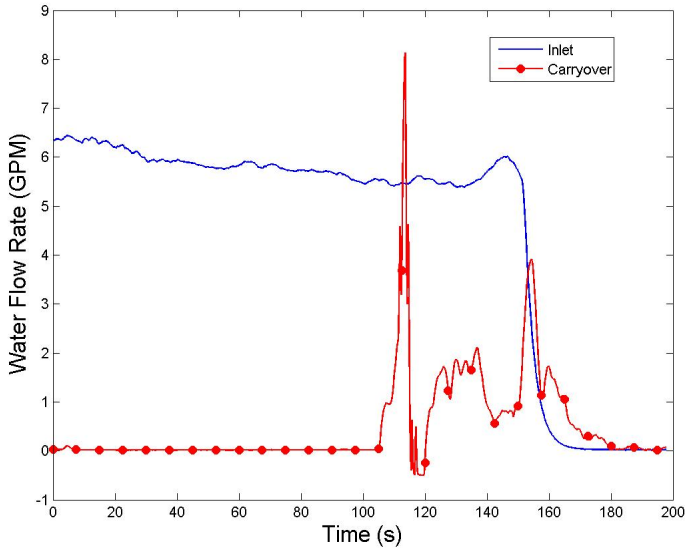

Figure E.263: Water Flow Rate for Run #14, Test 5.

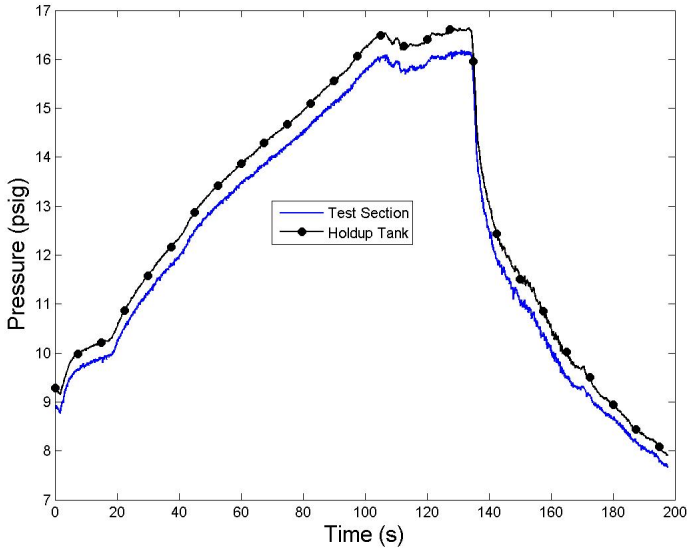

Figure E.264: System Pressure for Run #14, Test 5.

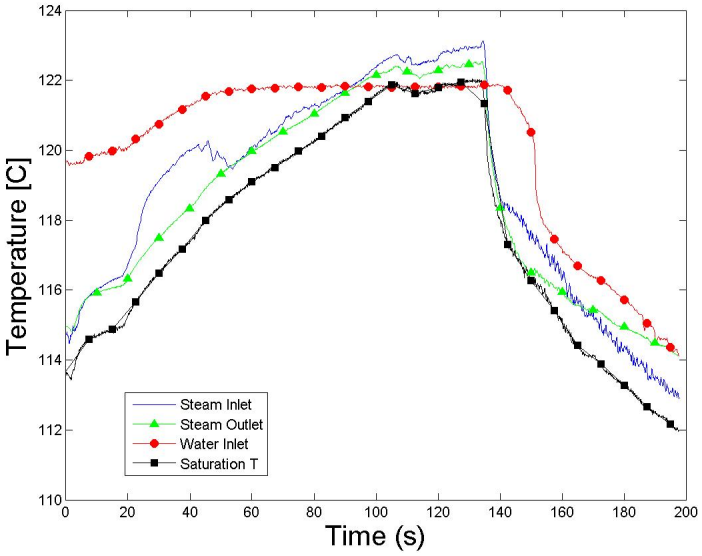

Figure E.265: Temperatures for Run #14, Test 5.

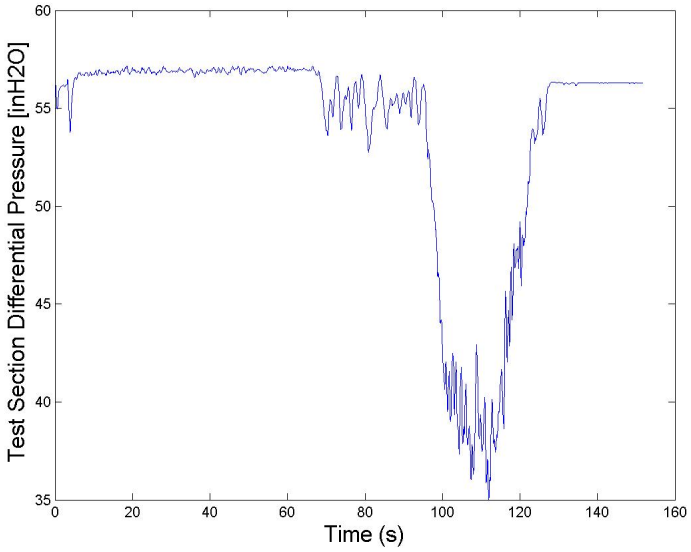

Figure E.266: Test Section Differential Pressure for Run #15, Test 3.

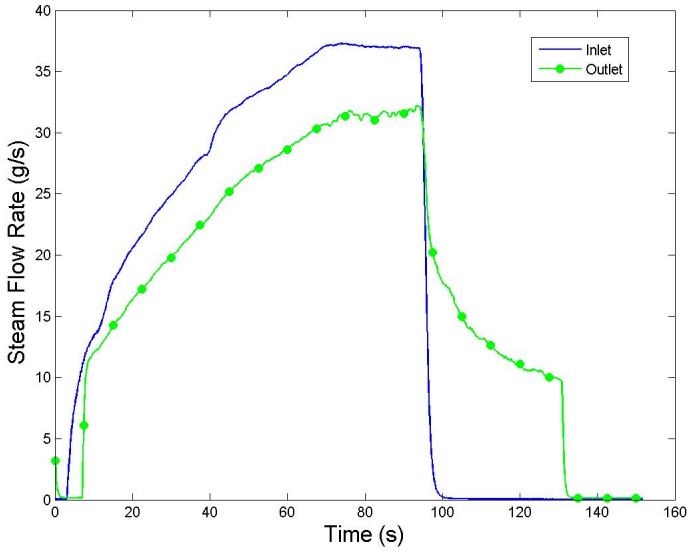

Figure E.267: Gas Mass Flow Rate for Run #15, Test 3.

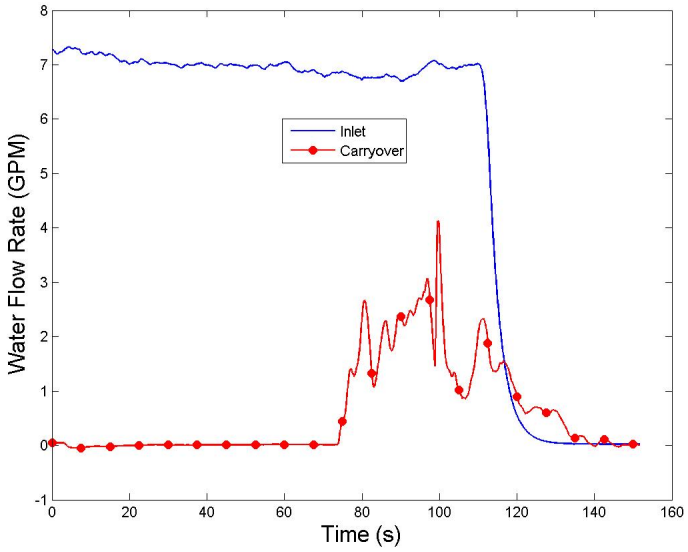

Figure E.268: Water Flow Rate for Run #15, Test 3.

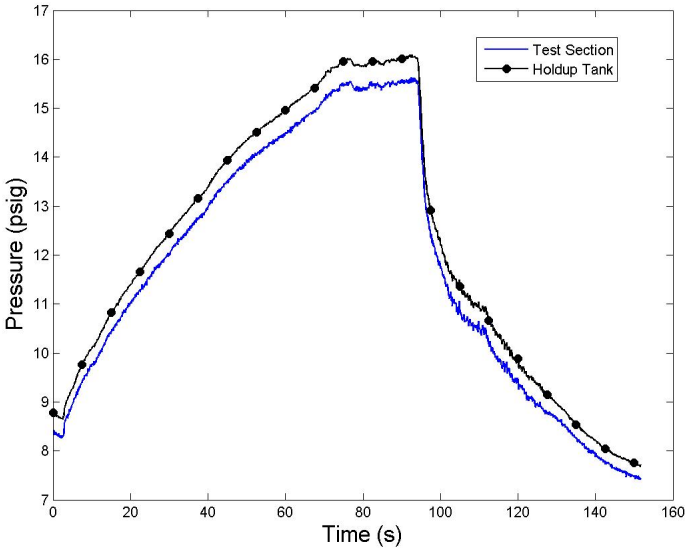

Figure E.269: System Pressure for Run #15, Test 3.

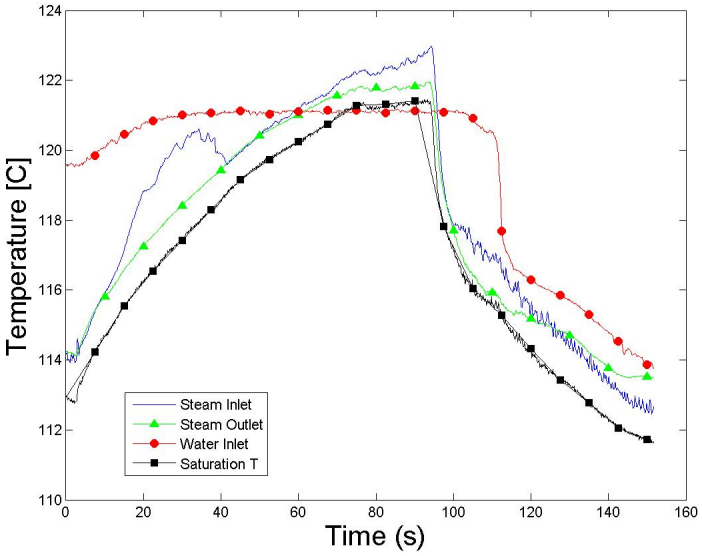

Figure E.270: Temperatures for Run #15, Test 3.

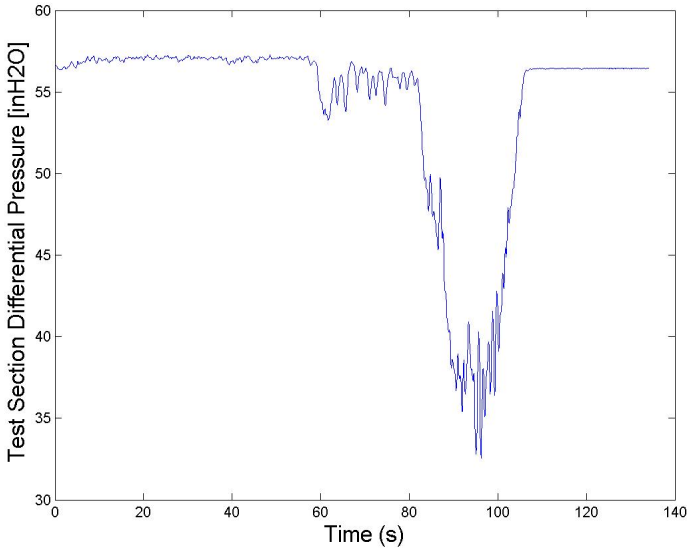

Figure E.271: Test Section Differential Pressure for Run #15, Test 2.

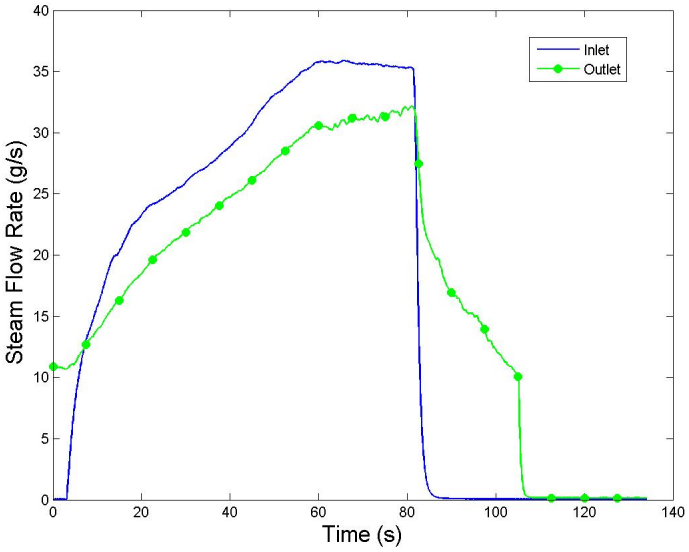

Figure E.272: Gas Mass Flow Rate for Run #15, Test 2.

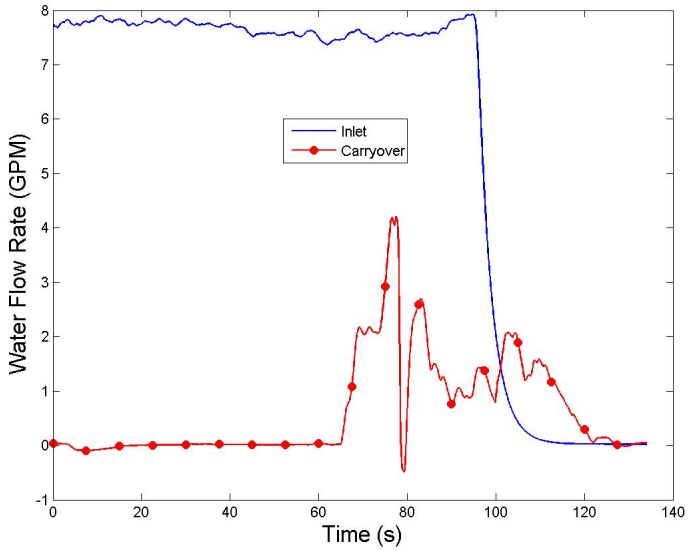

Figure E.273: Water Flow Rate for Run #15, Test 2.

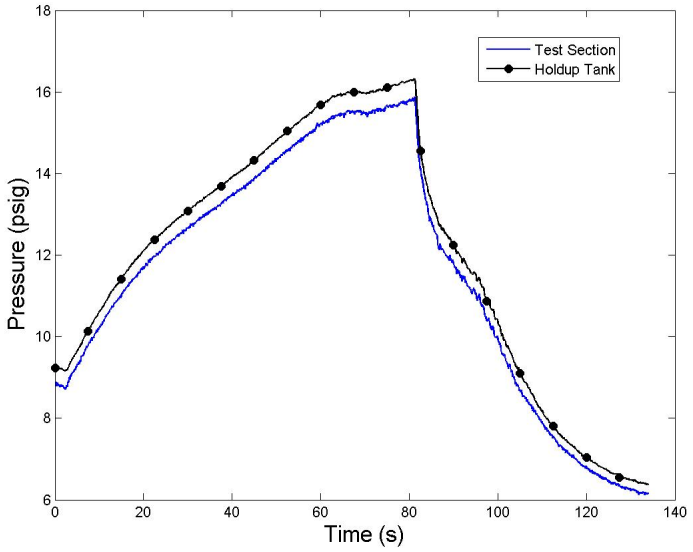

Figure E.274: System Pressure for Run #15, Test 2.

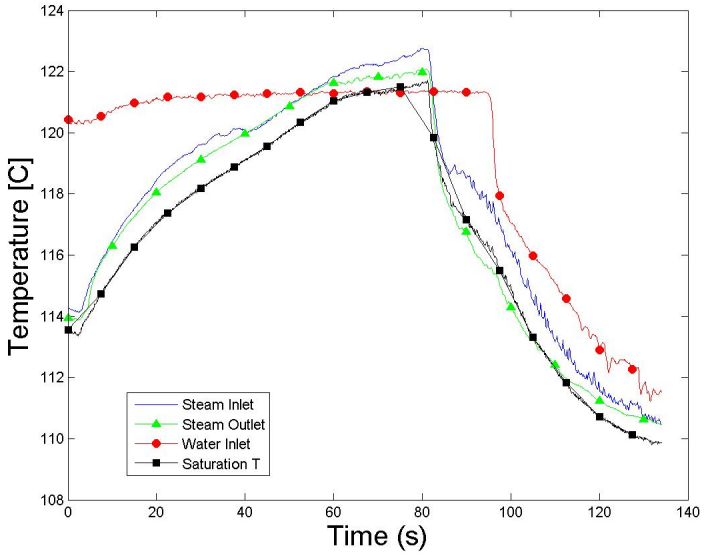

Figure E.275: Temperatures for Run #15, Test 2.

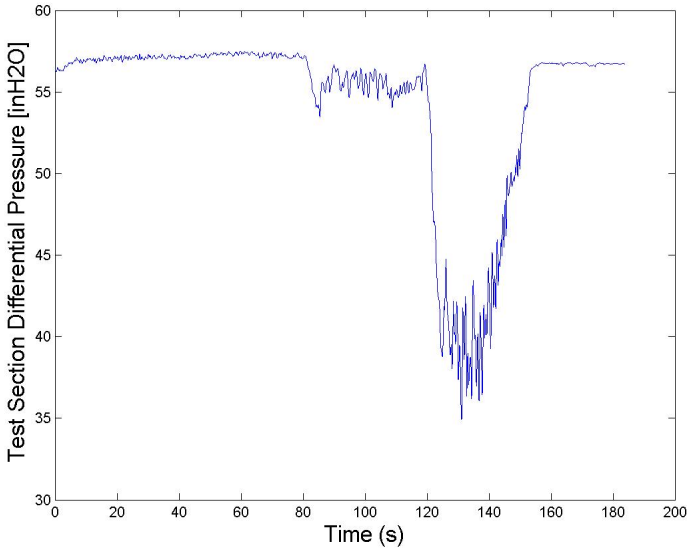

Figure E.276: Test Section Differential Pressure for Run #15, Test 4.

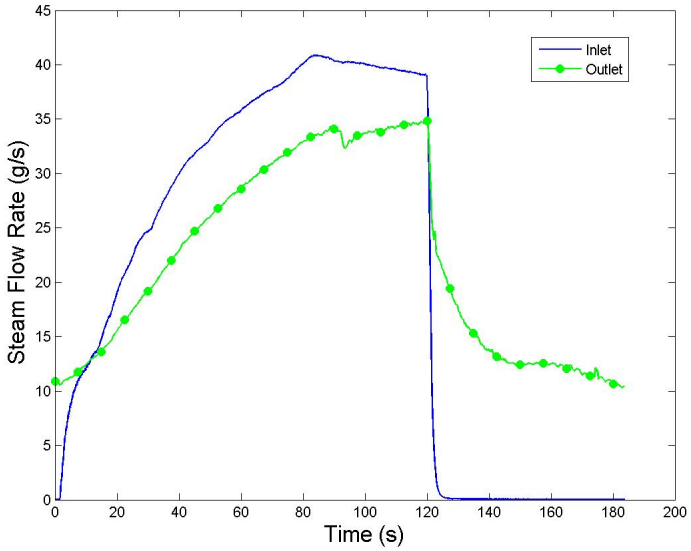

Figure E.277: Gas Mass Flow Rate for Run #15, Test 4.

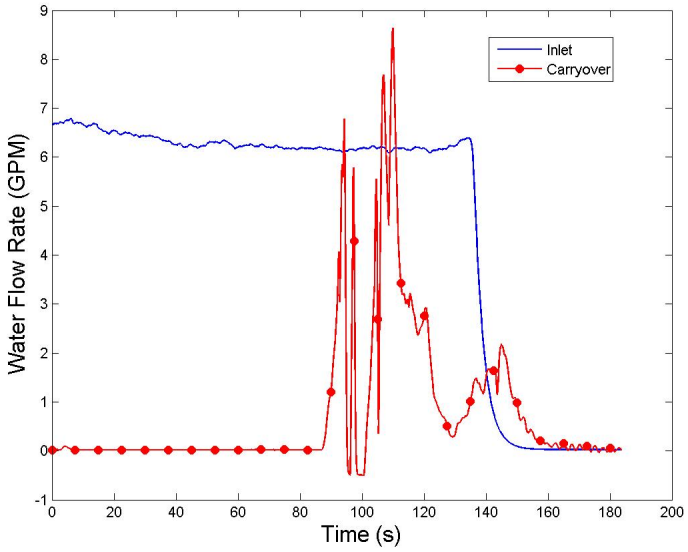

Figure E.278: Water Flow Rate for Run #15, Test 4.

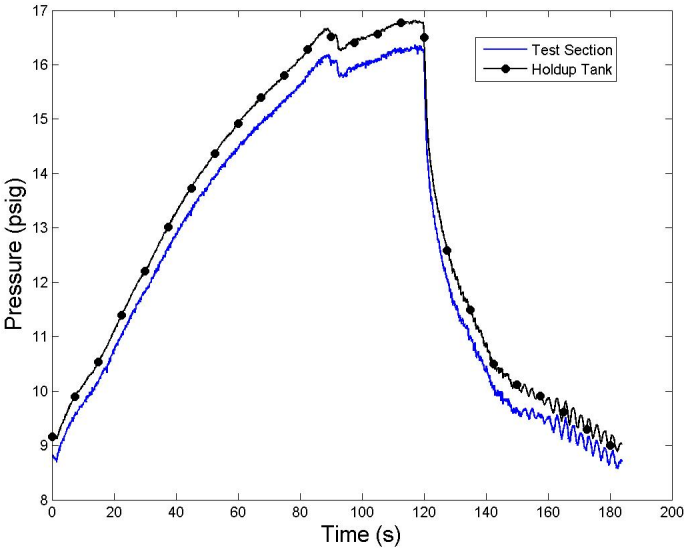

Figure E.279: System Pressure for Run #15, Test 4.

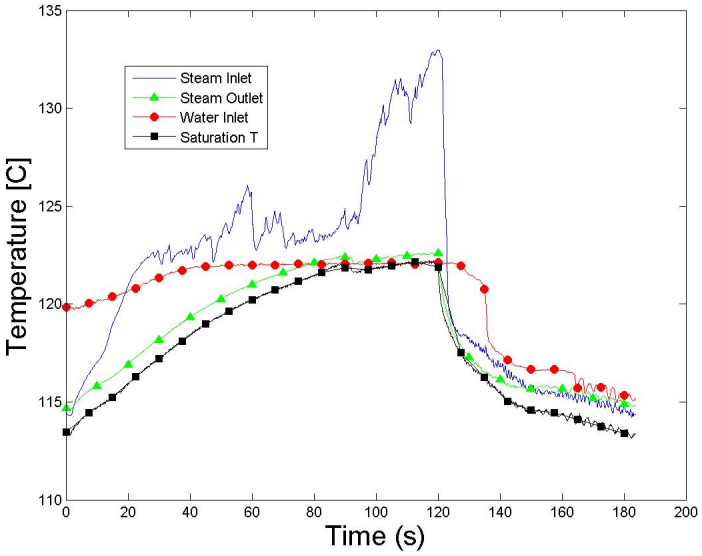

Figure E.280: Temperatures for Run #15, Test 4.

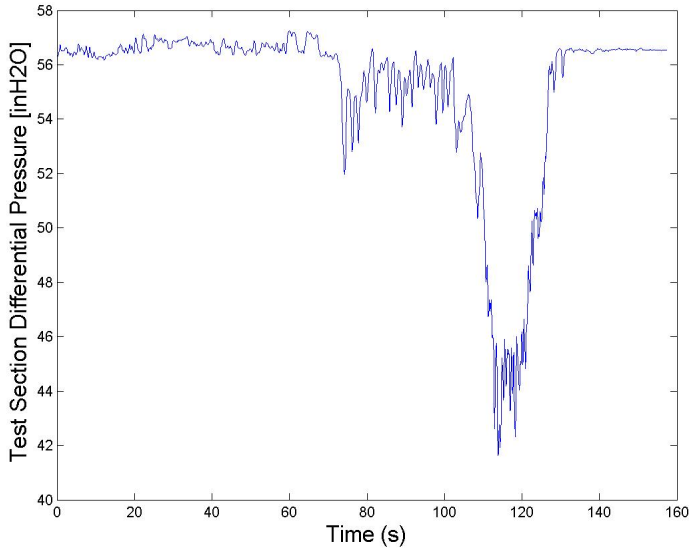

Figure E.281: Test Section Differential Pressure for Run #15, Test 1.

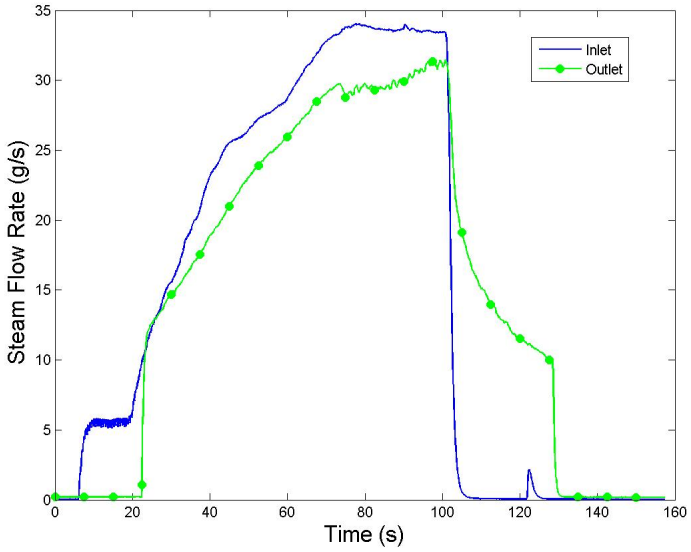

Figure E.282: Gas Mass Flow Rate for Run #15, Test 1.

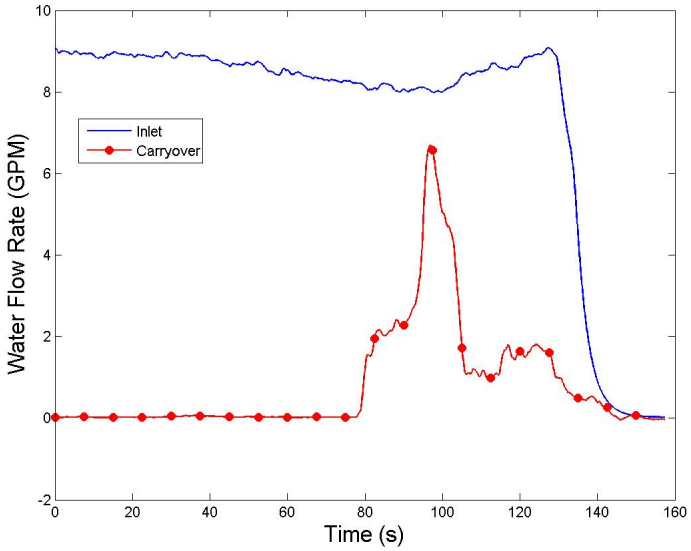

Figure E.283: Water Flow Rate for Run #15, Test 1.

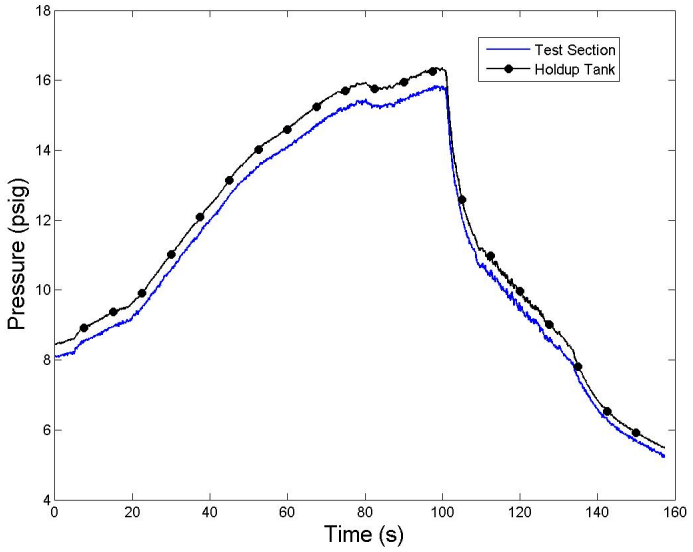

Figure E.284: System Pressure for Run #15, Test 1.

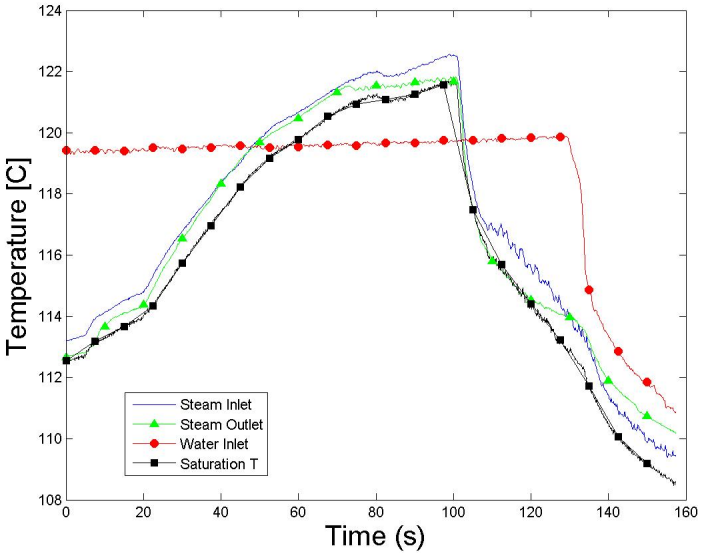

Figure E.285: Temperatures for Run #15, Test 1.

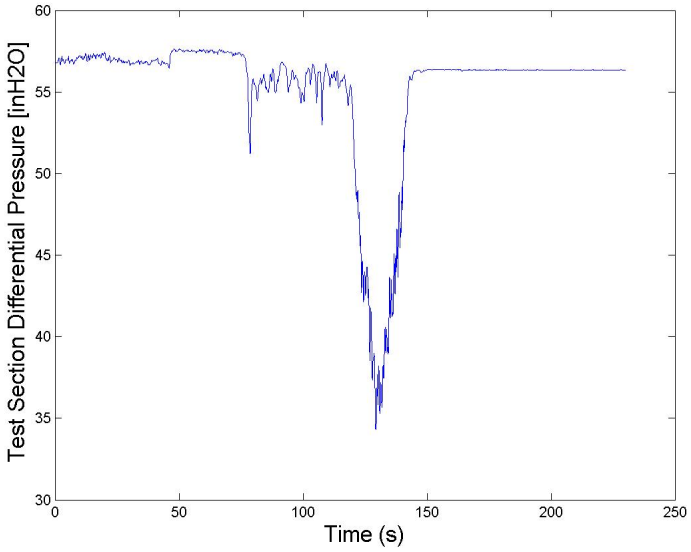

Figure E.286: Test Section Differential Pressure for Run #13, Test 8.

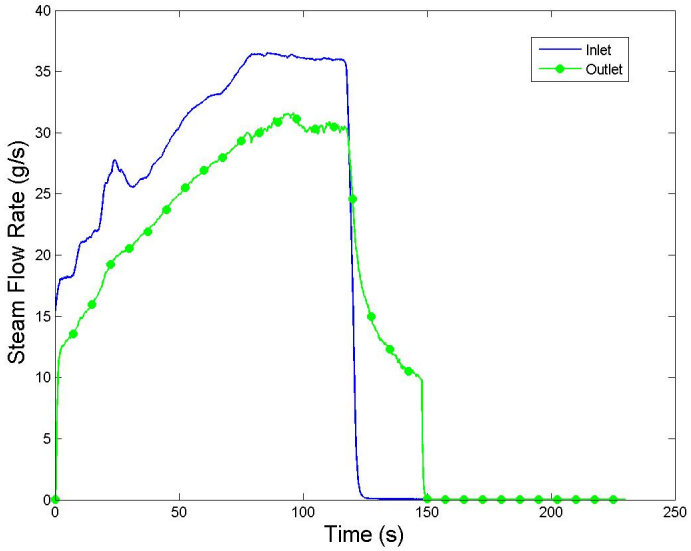

Figure E.287: Gas Mass Flow Rate for Run #13, Test 8.

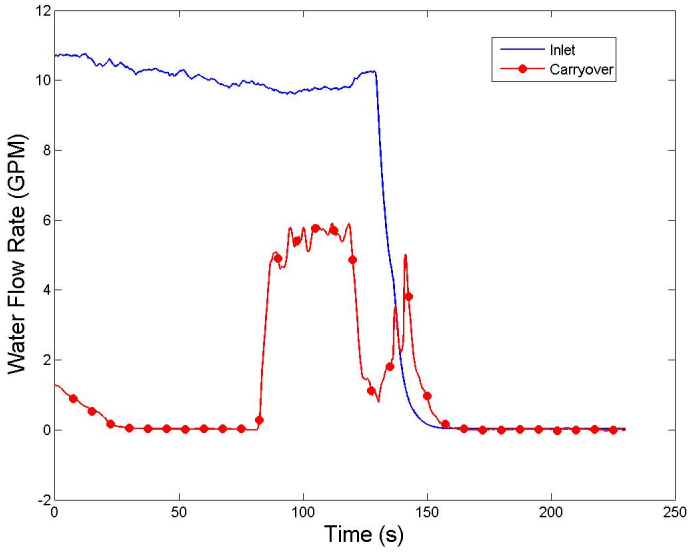

Figure E.288: Water Flow Rate for Run #13, Test 8.

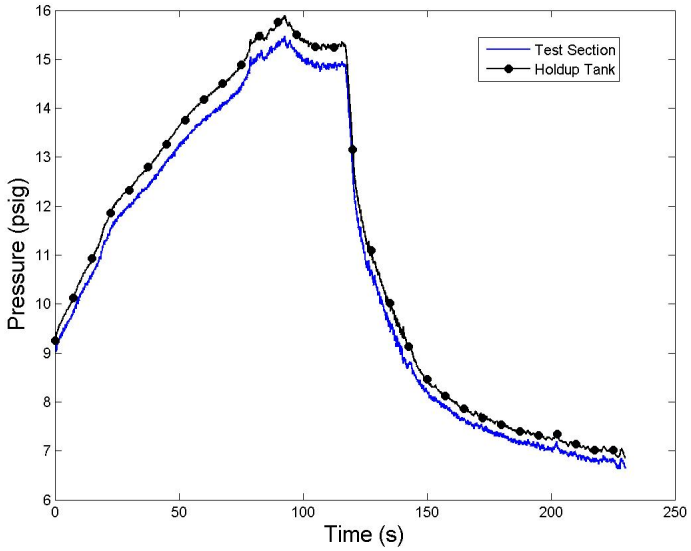

Figure E.289: System Pressure for Run #13, Test 8.

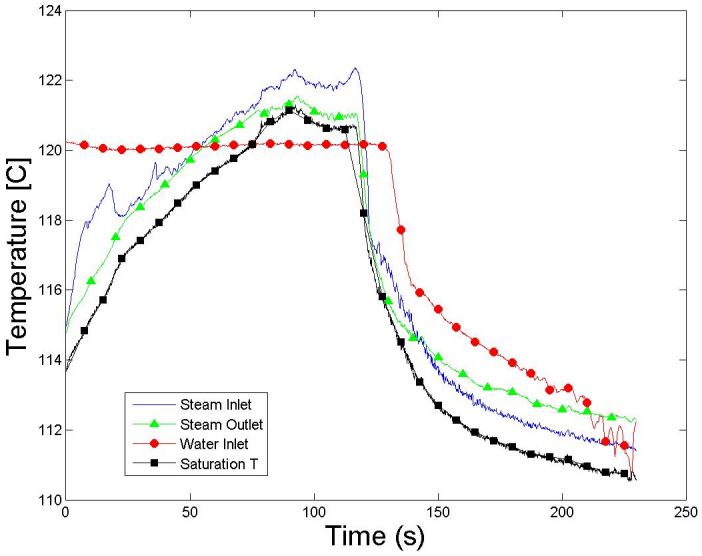

Figure E.290: Temperatures for Run #13, Test 8.

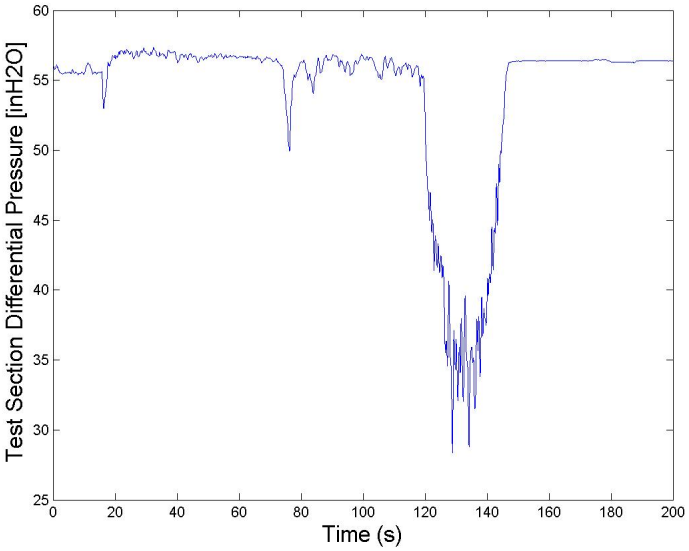

Figure E.291: Test Section Differential Pressure for Run #13, Test 7.

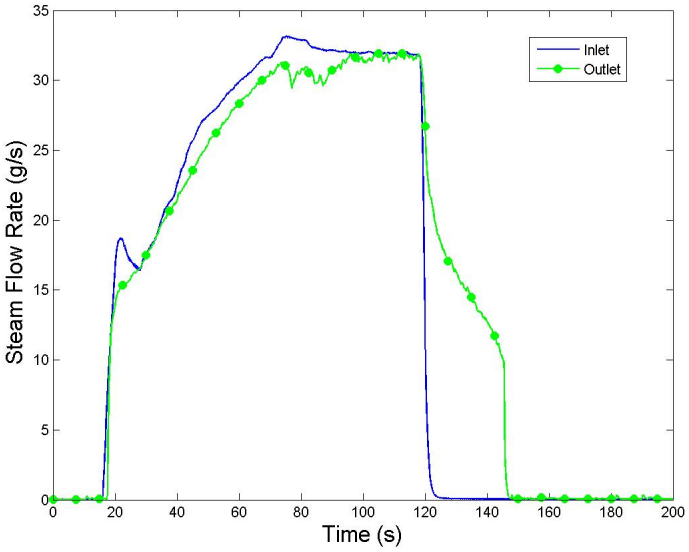

Figure E.292: Gas Mass Flow Rate for Run #13, Test 7.

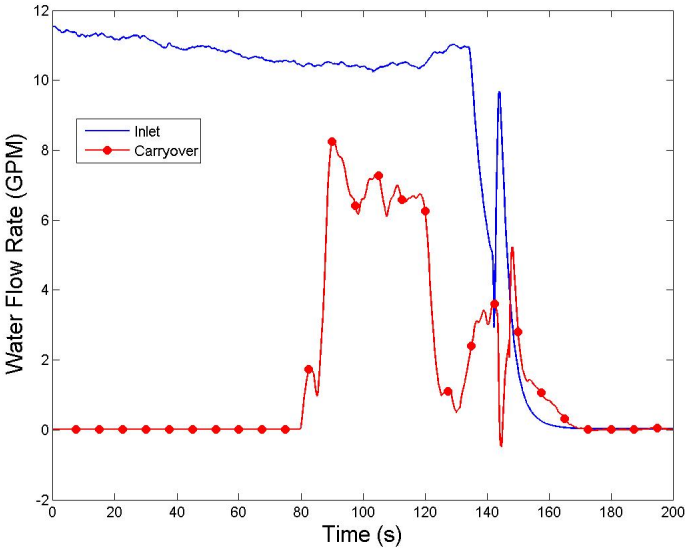

Figure E.293: Water Flow Rate for Run #13, Test 7.

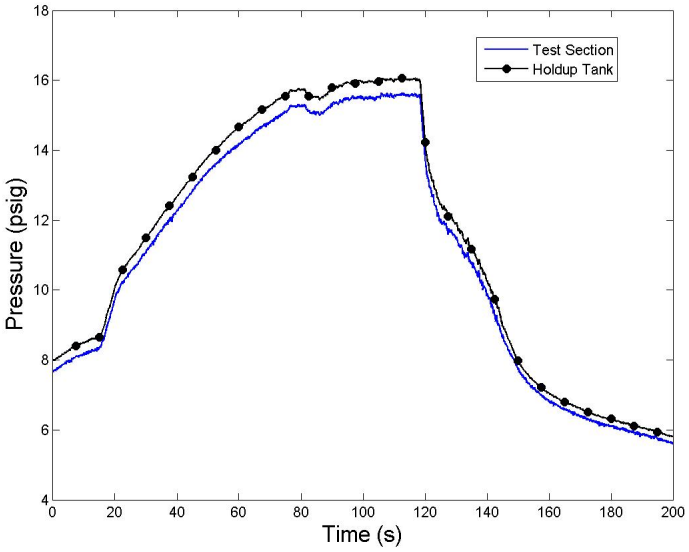

Figure E.294: System Pressure for Run #13, Test 7.

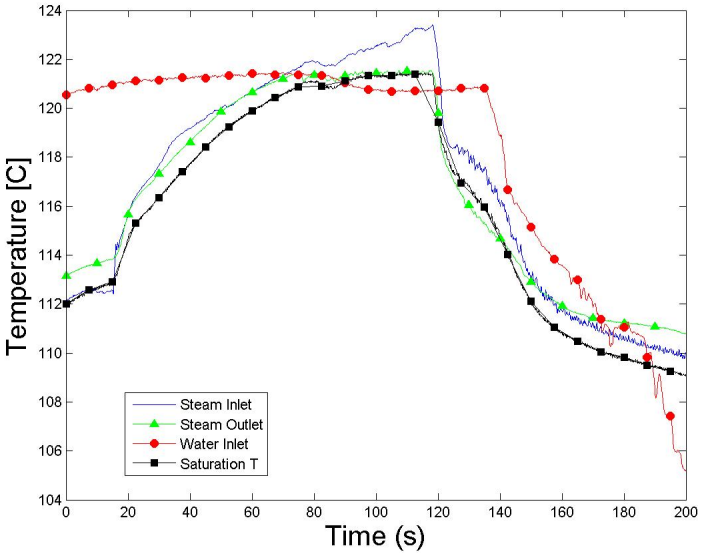

Figure E.295: Temperatures for Run #13, Test 7.

APPENDIX F

VITA

Nicholas Alan Wynne (née Mohammed), of Prairie Dell, Texas, received the degree of Bachelor of Science in Physics with a concentration in Nuclear and Radiation Engineering from The University of Texas at Austin in 2013. Nick has also worked part time as a Senior Reactor Operator at The University of Texas TRIGA reactor since 2011. In 2014, he began working as a graduate research assistant in the Nuclear Heat Transfer Systems Laboratory at Texas A&M University.

This thesis was typed by the author.

Address:
ATTN: Karen Vierow
Department of Nuclear Engineering
Texas A&M University
3133 TAMU
College Station, TX 77843

Email Address:
nicholaswynne@outlook.com